MODELLING, CHARACTERIZATION AND THERAPEUTIC TARGETING OF HUMAN BRAIN METASTASIS

MODELLING, CHARACTERIZATION, AND THERAPEUTIC TARGETING OF HUMAN BRAIN METASTASIS

MOHINI SINGH, BSc (Honours)

A Thesis Submitted to the School of Graduate Studies
In Partial Fulfillment of the Requirements
For the Degree of Doctor of Philosophy

Stem Cell and Cancer Research Institute & Department of Biochemistry
McMaster University

Descriptive Note

DOCTOR OF PHILOSOPHY (2018) McMaster University
(Biochemistry & Biomedical Sciences) Hamilton, Ontario

TITLE: Modelling, characterization, and therapeutic targeting of human brain metastasis

AUTHOR: Mohini Singh, Hon. B.Sc (McMaster University)

SUPERVISOR: Dr. Sheila K. Singh

NUMBER OF PAGES: 255

Abstract

Brain metastases (BM) are the most frequently diagnosed neoplasm to affect the adult central nervous system (CNS), occurring in 20-40% of all cancer patients throughout the course of the disease. The significant advancements to the treatment and control of primary cancers have unfortunately resulted in an increased incidence of BM, however, this complication of cancer progression continues to be met with a dismal outcome and limited therapeutic options. There remains a poor understanding of the several cellular hallmarks of BM, encompassing various molecular, genetic and epigenetic changes that underlay the stages of metastasis, which requires the development of clinically relevant models of metastasis. Our group has previously established the existence of a cancer stem cell/tumor initiating population with patient samples of BM, which established the foundation of this thesis. Thus, I postulate that there exists a subpopulation of cancer stem-like cells, termed brain metastasis initiating cells (BMICs), that is responsible for the initiation of BM and is identifiable by an exclusive subset of genes that regulate self-renewal and metastasis.

To support this hypothesis, I established novel experimental models of BM by inoculation of BMICs derived from patient samples of lung-to-brain metastases into intracranial (ICr), intracardiac (ICa), and intrathoracic (IT) routes into NOD/SCID mice. ICr injections validated the presence of a tumor initiating cell (TIC) capacity of BMICs in the secondary environment (brain). From ICa injections I was able to recapitulate macro-metastatic growth, whereas with IT injections I was able to capture the complete metastatic process, from primary lung tumor formation to micro-metastasis growth. Utilizing these models, I

determined that the STAT3 pathway and genes SPOCK1 and TWIST2 all contribute to the regulation of BM development, where SPOCK1 may pose as a potential BMIC marker. Further interrogation of the metastatic process utilizing the IT model of BM led to the characterization of "pre-metastasis", a stage where BMIC cells have crossed the blood-brain barrier and employ mechanisms to invade and seed the neural environment, while simultaneously repressing mechanisms of proliferation and cell growth that would indicate tissue colonization.

In summation, I propose a shift in the cancer research paradigm to target the metastatic process itself, to prevent the dissemination of primary tumor cells to the brain. I present models of clinically relevant models of human BM that have proved to be reliable as platforms to interrogate the process of BM, providing insight into the stage of pre-metastasis as a novel therapeutic window into BM prevention and possible extension of patient survival.

Acknowledgements

There have been many people that have had an impact on my life while at the SCC-RI. To Dr. Sheila K. Singh, my wonderful supervisor throughout this experience. Thank you for all of the opportunities you've granted me, allowing me to attend prestigious conferences and lectures, and guiding me throughout this arduous process of becoming a scientist. You've been an amazing mentor, not only for research but also for handling uncomfortable or undesirable situations, such as dealing with finicky collaborators or folk in general – you are always calm, collected, and more polite than I could understand, but in that you showed your unlimited degree of patience and it's a lesson I have tried to take to heart. Your first piece of advice to me when I started was that appearances will influence how others perceive you, and that when you look a certain way you have to work twice as hard to be successful. I know I've not made this an easy process for you, but I hope I have accomplished enough that you can proudly claim me as the FIRST doctoral graduate of your lab. To Dr. Michelle Ghert, thank you so much for taking a chance on me while I was trying to get into graduate school and starting me off on this path. To my committee members, oh boy. I know I've not made the best impression at our infrequent meetings, but you've guided me and allowed me to get this far and for that I'm forever thankful. To Dr. John A. Hassell, you initially terrified the bejesus me with your strong demeanor, however I believe it was acknowledgement of that fear of you that helped me see how such an emotion would hinder my quest for answers in this field. Conquering of that fear and being able to speak to you as a colleaque helped me to gain some much needed confidence.

Thank you to Dr. Chitra Venugopal. You have dealt with my constant stream of questions over these years with unflagging patience, helping me to learn concepts and providing an unlimited source of knowledge on every topic, and shaping my thinking process as a scientist. I hope I have also made you proud of my time in the lab, and to you I owe a debt of gratitude. Thank you to my *friends* in the Singh lab. I was privileged to be involved in many of your initial trainings and parts of your projects, and I'm really very proud to have worked alongside such amazing people. All of you have been so very supportive, working with me to better myself as both a researcher as well as an adult entering the workforce, and helping me learn to handle unsavoury individuals. I don't think my time here would have been as productive without you guys to turn to for jokes, laughter, and just overall relief from stresses and frustrations. To the friends and acquaintances I've made outside of the Singh lab, you have no idea how your kindness has helped get me through some bad times. A hug from you never failed to brighten my day. Thank you so much for all of the smiles and laughs, and timeouts for rants when things got too overwhelming. In my naiveté, I never thought that in such an altruistic and educated environment I would still encounter folk who are disrespectful and arrogant with their colleagues. I have definitely learned that not all who smile at you are friends, no one is obligated to be nice to you, and those who make no effort to be a decent human being at all don't believe in karma (but I do).

Most importantly, I cannot thank my family enough. Dad, who else but you understood what I was going through these last few years? The late nights and early mornings, the random emotional outbursts and petty mood swings and breakdowns from stress, you were

there to see me through it all. You pushed me to be *the* best, guided me at every step until I could finally see the end. You are my strength to succeed and I hope I always only ever give you reasons to keep your head held high. Mom, you made sure I had food even though I'd skip meals to get work done, and tried to get me to stay home and rest when I was about to crash. I only get one mother in life and I got the best, you are my heart. My siblings Omi and Giry, you guys are a pain in my well-maintained posterior half the time. But you've been there to keep me on my toes, to make me feel both smart and dumb whenever the situation arose (look I even rhymed), and helped me with stress (but not my liver Giry. After this PhD will stand for Pretty Hair Dresser or Permanent Head Damage, it alternates according to you guys). Look who's Dr. Doom now! Over these few years I've come home ecstatic or broken down with tears several times, caused by breakthrough results or ugly people and situations. My family has *always* been there to listen to me babble or rant, cheering or cursing along with me, and stood by me for every minute of the good and the bad. Especially near the end of my degree, plying me with edible enticements, commiseration and compliments to try to make me come back from the brink of breakdowns/depression. I would have given up if not for you all, I never could have survived this without all of you. Thank you will never be enough, and I love you.

During one of my overstressed moments, a good friend told me that "God never gives you more than you can handle", and this phrase has been at the forefront of my mind throughout the end of this process. For me, my faith in my religion, meditation, and prayers, has helped me greatly to remain grounded and thankful. I cannot take for granted the opportunities that have been bestowed on me and that have led me to this current state of success. I was chosen for an opportunity that few others will experience, placed in a position where I can do good in this world. At times I have buried myself in my studies to escape the negativity that seems to be flooding the world these days, hoping to generate some degree of positivity. With my work I've contributed in some way to helping others, hopefully helping to make some difference to the fight against cancer.

Graduate school is not easy, that's common knowledge. As students we can be easily disregarded and underestimated, and I have seen too many students stymied in phases of disillusionment and depression. I have been ridiculed of being overly possessive of this work, and I would be the first to agree. However I've spent every moment of my life for the last 6 years has been invested into this thesis project and to the lab. I've put my blood, sweat, and (too many) tears into my research, sacrificing health and sanity, family, and a social life. To blithely hand over this project to the next person, knowing what I have contributed and can still achieve but with no further thought of me continuing with it, breaks my heart. But to continue on in life one must focus on the positive. I have so much to appreciate with what I have accomplished, skills and knowledge that should make (or will lead to making) me an expert in the field of brain metastasis, all validated by this neat piece of paper with "Dr." beside my name.

I am Dr. Mohini Singh. I have come out of this a harder, stronger person, hopefully less naïve and more circumspect, and just a bit less of a doormat. I know I will succeed at anything after this.

"I have put my heart and soul into my work, and have lost my mind in the process" – Vincent Van Gogh

Table of Contents

List of Figures and Tables

Chapter 1

Chapter 2

Chapter 3

List of Abbreviations

ABC – ATP-binding cassette
BBB – blood brain barrier
BBM – breast to brain metastasis
BCSFB – bloodcerebrospinal fluid barrier
BM – brain metastasis
BMIC – brain metastasis initiating cell
BM^{IT} – brain metastasis from intrathoracic injection
BM^{IC} – brain metastasis from intracardiac injection
BM^{BM} – breast-to-brain metastasis
BM^{MB} – melanoma-to-brain metastasis
BT – brain tumor
BTIC – brain tumor initiation cell
cGAMP – cyclic guanosine adenosine monophosphate
CSC – cancer stem cell
CTC – circulating tumor cell
CNS – central nervous system
CX43 – connexin 43
DA – dopamine agonist
DRD2 – dopamine receptor D2
EGFR – epidermal growth factor receptor
EMT – epithelial – mesenchymal transition
FDA – federal drug agency
GEMM – genetically engineered mouse model
KIF16B – kinesin family member 16B
LT – lung tumor
MBM – melanoma to brain metastasis
NOD/SCID – non-obese diabetic/severe combined immunodeficiency
PCDH7 - protocadherin 7
PDGF – platelet-derived growth factor
PMN – pre-metastatic niche
SEPW1 – selenoprotein W
SLC – solute carrier
SPOCK1 - SPARC/Osteonectin, cwcv and kazal like domains proteoglycan 1
STAT3 - signal transducer and activator of transcription 3
TCIPA – tumor cell-induced platelet aggregation
TESK2 – testis specific kinase 2
TGFβ – transforming growth factor beta
TF – transcription factor
TIC – tumor initiating cell
TWIST2 - twist family BHLH transcription factor 2
uPAR – urokinase-type plasminogen activator receptor
VEGF – vascular endothelial growth factor

Preface

The body of work presented in this thesis was based on findings generated by Sara Nolte (Nolte 2014), and molded by the general limited state of knowledge within the field of brain metastasis (BM). This preliminary work was inspired by Dr. Sheila Singh's doctoral thesis, identifying a brain tumor initiating cell (BTIC) population within the primary brain cancer glioblastoma (Singh 2004). Nolte *et al*. (2014) applied similar cancer stem cell (CSC) assays, determining that BM from lung cancer possess a subpopulation of cells that retain CSC-like properties of sphere formation and tumor initiation, but cannot be isolated by typical BTIC markers CD133 and CD15. Furthermore, transcriptomic analysis comparing samples of lung-derived BM, glioblastomas and primary lung tumors let to the generation of the list of potential brain metastasis initiating cell (BMIC) markers. This gene list sets the foundation for the beginning of my doctoral project.

This thesis is preprared in the format of a "sandwich" thesis as outlined in the "guide for the preparation of Master's and Doctoral Theses" (v2016). Chapter 1 provides a general introduction into the present field of brain metastasis, highlighting the currently available treatment options for patients suffering from brain metastases, the biological concepts of the metastatic process, characterization of the cells capable of undergoing metastatic progression, the availability of preclinical *in vitro* and *in vivo* BM models, and lastly summarizing the hypothesis and overall aims of this thesis. This chapter contains excerpts from the following published reviews:

- **Singh M**, *et al*. *Brain metastasis-initiating cells: survival of the fittest.* Int J Mol Sci. 2014;15(5):9117-33. doi: 10.3390/ijms15059117. © <2014>. This manuscript version is made available under the CC-BY 3.0 license https://creativecommons.org/licenses/by/3.0/
- **Singh M**, Bakhshinyan D, Venugopal C, Singh SK. *Mechanisms and Therapy for Cancer Metastasis to the Central Nervous System*. Front Oncol. 2017;19(7)220. doi: 10.3389/fonc.2017.00220. © <2018>. This manuscript version is made available under the CC-BY 4.0 license https://creativecommons.org/licenses/by/4.0/
- **Singh M**, Yelle N, Venugopal C, Singh SK. *EMT: mechanisms and therapeutic implications*. (2017) Pharmacol Ther. 2017 Aug 20. pii: S0163-7258(17)30219-X. doi: 10.1016/j.pharmthera.2017.08.009. © <2018>. This manuscript version is made available under the CC-BY-NC-ND 4.0 license http://creativecommons.org/licenses/by-nc-nd/4.0/

Chapter 2 has been originally published as *STAT3 pathway regulates lung-derived brain metastasis initiating cell capacity through miR-21 activation.* Oncotarget 2015; 6(29):27461-77. Chapter 3 has been originally published as *RNAi screen identifies essential regulators of human brain metastasis initiating cells*. Acta Neuropathol. 2017 Dec;134(6):923-940. doi: 10.1007/s00401-017-1757-z. Chapter 4 is a manuscript submitted for publication at the time of this thesis submission, titled *Therapeutic targeting of the pre-metastatic stage in human brain metastasis.* Chapter 5 consists of the final discussion, summarized conclusion and overall future and implications of this thesis, containing excerpts from the reviews previously listed in Chapter 1, as well as unpublished

data (Figure 7, Figure 8) that will be included in a manuscript currently in preparation, and summarizes .

Chapter 1: Introduction

1.1 Brain metastasis

1.1.1 Epidemiology

Brain metastases (BM) are the most common neoplasm to affect the adult central nervous system, occurring 10 times more frequently than primary brain tumors (Patchell, 2003). ~90% of cancer-related deaths are associated directly or indirectly with metastatic progression, and 20-40% of patients diagnosed with cancer will develop BM throughout the course of the disease, dependent on the type of primary tumo (Gavrilovic & Posner, 2005; Patchell, 2003). The prevalence of BM has increased in recent years due to several factors: a) improved treatment of primary cancers, which in turn increases patient survival and subsequently prolongs the amount of time BM can develop, b) improved technologies to diagnose BM, and c) the inadequate efficacy of current treatment options for BM (Lu-Emerson & Eichler, 2012).

On average, BM are detected at 8.5 months after the initial diagnosis of the primary cancer. However, this range is dependent on the type of primary cancer, with detections as early as 3 months with lung carcinomas and as late as 37 months with melanomas (Lagerwaard *et al.*, 1999; Lu-Emerson & Eichler, 2012). Clinically, BMs may manifest in three distinct manners: metachronous, synchronous, and anachronous. The majority of patients are diagnosed with a BM following a known primary malignancy (metachronous presentation). Less commonly, patients are diagnosed simultaneously with the primary tumor and BM

(synchronous presentation), and rarely patients will be diagnosed with a BM prior to the detection of the primary cancer (anachronous presentation) (Soffietti *et al.*, 2002).

A significant controversy in metastasis research surrounds the timeline of metastatic spread; do metastases develop in a linear fashion after primary tumor formation, or in parallel to the primary tumor? The linear model of dissemination is intimated in cancers where there are close genetic similarities between the primary and secondary tumors, whereas the parallel model is suggested in cases of genetic diversity. A third theory suggests metastasis-to-metastasis seeding (Naxerova & Jain, 2015). Although the general consensus gathered from several studies leans towards parallel progression of metastatic dissemination, recent phylogenetic studies have shown multiple modes of dissemination (D. Brown *et al.*, 2017; Budczies *et al.*, 2015; Klein, 2009; Kroigard *et al.*, 2017; Sanborn *et al.*, 2015).

1.1.2 Clinical presentation and prognosis

Any cancer type can disseminate to the brain, however lung, breast and melanoma cancers account for the majority of BM cases (Figure 1). The type of primary tumor can also dictate the distribution and number of metastases within the brain.

Lung cancers account for the majority of BM cases. 10-25% of lung cancer patients are concurrently diagnosed with the primary cancer and BM, and approximately 40-50% of lung cancer patients will eventually develop BM (Langley & Fidler, 2011). Within the

histological divisions of lung cancer, non-small cell lung cancer (NSCLC) accounts for 20-40% of BM, arising primarily from the adenocarcinoma subtype, whereas the more aggressive small cell lung cancer (SCLC) accounts for ~20% of BM cases (Nayak *et al.*, 2012). In general, lung cancers typically result in multiple lesions within the occipital lobe and cerebellum (Barnholtz-Sloan *et al.*, 2004; D. Palmieri, 2012).

Breast cancer accounts for 15-25% of BM cases, resulting in single lesions within the brain parenchyma, leptomeninges, cerebellum, and brain stem (Barnholtz-Sloan *et al.*, 2004; D. Palmieri, 2012). BM development has been reported to be much higher in human epidermal growth factor receptor-2 (HER2) positive and triple negative breast cancer subtypes, accounting for ~35% of BM cases.

Melanomas have the highest propensity of all primary cancers to metastasize to the brain, likely due to the similar embryonic origin of neural tissues and melanocytes (Herlyn *et al.*, 1985; D. Palmieri, 2012). However, melanomas are only the third highest origin of BM, accounting for 6-11% of cases. Melanoma derived BM typically form within the cortex as opposed to the grey-white junctions as seen with other primary origins (Nayak *et al.*, 2012).

Renal cell, gastrointestinal and colorectal cancer have the lowest propensity to develop BM within the progression of the disease, and approximately 2-14% of BM cases present with no definable primary origin (Nayak *et al.*, 2012).

For most primary cancers, the size of the tumor correlates with prognosis and metastatic progression, *i.e.* the larger the primary tumor the higher likelihood that the patient will develop and succumb to metastases (Klein & Holzel, 2006). Mortality is then dependent on both the metastases and systemic disease. BM are associated with poor survival and high morbidity, but again prognosis varies with the primary cancer origin and number/size/location of metastatic lesions. The prognosis worsens as the number of lesions increases, or if the lesions are located in areas less accessible to surgery. Without treatment, the median life expectancy of patients from presentation of one lesion is 5 months, and 3 months for patients with multifocal disease. Treatment of single lesions are favorable for extended survival, whereas multifocal spread has no significant response to current treatment (Nussbaum *et al.*, 1996).

1.1.3 Treatment Strategies for BM

The typical treatment strategy for BM is palliative care or no treatment at all for poor risk patients, as treatment options offering any significant extension of survival are presently not available (Hardesty & Nakaji, 2016). Poor risk patients may receive radiation therapy, analgesics and corticosteroids for persistent pain and headaches, anti-depressants, anti-nauseants and anti-convulsants (DeAngelis & Boutros, 2005). Patients that have low systemic burden and good medical standing are considered good risk patients, and can receive aggressive treatments tailored to control the tumor. This includes surgical resection, stereotactic radiosurgery (Gamma Knife or CyberKnife), whole-brain radiotherapy, focused external beam radiotherapy, and systemic treatments (Ahluwalia *et al.*, 2014;

Hardesty & Nakaji, 2016). Systemic therapies include chemotherapies, small molecules and immunotherapies, and can be administered depending on various patient factors, such as tumor histology and the patient's prior treatment history to theoretically target both the active systemic disease as well as the BM (Groves, 2010).

1. Chemotherapy: A variety of chemotherapeutic agents have been employed to treat BM, often used in a combination of 2-3 along with whole-brain radiotherapy. For BM, standard chemotherapies are administered based on the primary cancer. Cisplatin, cyclophosphamide, etopside, prednisone and irinotecan have all been administered for BM of lung, breast and melanoma cancers (Ahluwalia 2014). Several other cytotoxic agents used in treating BM include capecitabine (Ekenel *et al.*, 2007) and temozolomide (Agarwala *et al.*, 2004; Antonadou *et al.*, 2002).
2. Small molecules: The mutational status of the primary tumor can determine the type of small molecule administered to BM. Tyrosine kinase inhibitors such as Gefitinib, Osimertinib and Erlotinib target EGFR mutations found in lung cancers, Lapatinib targets HER2 mutations of breast cancer, and Vemurafenib and Dabrafenib target BRAF mutations in melanoma, and Crizotinib, Ceritinib and Alectinib target ALK fusions in lung cancers (Ahluwalia *et al.*, 2014; Groves, 2010).
3. Immunotherapies: Recent studies have shown promising results with the administration of monoclonal antibodies and immune-modulating therapies, activating T-cell responses to target BM in a non-cytotoxic manner. Bevacizumab and Ranibizumab are monoclonal antibodies that target VEGF, a key factor implicated in angiogenesis (Ferrara & Kerbel, 2005). Checkpoint proteins in T-cells such as PD-

1/PD-L1 and CTLA-4 act as "off switches" that prevent self attacks and keep the immune system under control. Pembrolizumab, Atezolizumab, and Ipilimumab are a new class of checkpoint inhbitors that target these proteins, and currently show significant promise in clinical trials to boost the immune response against cancer cells (Leal *et al.*, 2011). A more extensive coverage of the ongoing research on immunotherapies directed at BM is comprehensively discussed in the review by Farber *et al*. (Farber *et al.*, 2016).

Unfortunately, few substantial advancements have been made in the therapeutic treatment of BM, and this lack of progress has added very little to the improvement upon the dismal survival rates for patients. Several methods have been employed when designing drugs and delivery systems to increase drug efficacy in crossing the blood-brain barrier (BBB) and blood-cerebrospinal fluid barrier (BCSFB) to target BM, either directly modulating the barriers, modifying the drug compositions, or bypassing the barriers entirely. Osmotic and chemical solutions, such as mannitol, alkylating agents, cytokines, and even high doses of ethanol or DMSO, can be administered to enhance drug delivery by shrinking capillary endothelial cells and forcing openings within the tight junctions. However, these methods are highly invasive, requiring intra-arterial catherization and general anaesthesia, and can cause seizures, bradycardia, and hypotension (Meairs, 2015; Pardridge, 2005). The evidence of exosome based communication in neural cells opened up a possibility of potentially developing therapies that deliver short interfering RNA (siRNA) against specific targets to the brain (Faure *et al.*, 2006). The introduction of microbubbles into the

blood stream and subsequent application of focused ultrasound can transiently open the BBB without significant neuronal damage (Hynynen *et al.*, 2001). The latter two methods are still in preclinical testing but show significant promise (Banks, 2009; Meairs, 2015).

Various methods can modify drug compositions to promote their entry into the brain, however the process can be expensive and result in delivery to the entire brain. Lipid groups can be added to water-soluble molecules to promote passive diffusion through the BBB, unfortunately once across the BBB the drug must then enter the surrounding aqueous interstitial fluid of the brain to be effective, resulting in drugs that are too lipid soluble being sequestered to the capillary bed and unable to reach areas beyond the BBB (Oldendorf, 1974). The addition of solute carrier proteins (SLC) to the endothelial surface can aid transcellular transport of polar and charged molecules. Coupling of drugs to a "trojan horse", a ligand that recognized by the BBB to promote endocytosis of the entire compound, which can improve the peripheral pharmacokinetics, yet results in a hybrid compound that may not be recognized by the transporter or is destroyed as a foreign body (Banks, 2009).

The BBB and BCSFB can be avoided altogether by changing the method of delivery. Drugs can be administered locally through a needle or catheter directly into the targeted site, but requires invasive surgery, is difficult to control drug distribution and carries risks of brain damage, bleeding and infection (Meairs, 2015). Intrathecal administration (direct injection into the spinal canal) of anticancer agents guarantees the treatment will enter the CSF and

distribute into the brain parenchyma *via* diffusion, however this route can have limited efficacy. An alternative intraventricular administration shows improved CSF drug levels, especially in bulky tumors, and less variability between patients (Groves, 2010). Transnasal delivery can reach the olfactory CSF through the submucus space, however this non-invasive method can allow delivery of only small amounts of drug and have significant inter-patient variability (Pires *et al.*, 2009).

Despite the advances in cancer research throughout the years, there still remains significant challenges in the treatment of cancer. Chemotherapy is a standard treatment that can be used alone as a monotherapy or in combination with surgery and/or radiotherapy (J. Wang, et al., 2016). The past decade has led to major advancements in targeted cancer therapies, as seen with monoclonal antibodies and small molecules, and over a hundred targeted therapies have been approved for usage with hundreds more under clinical investigation (Joosse & Pantel, 2013). Unfortunately, resistance developed from long-term usage has arisen in many patients, making drug resistance a major factor in drug discovery (Joosse & Pantel, 2013). A well known example of acquired resistence is with EGFR, a tyrosine kinase receptor commonly mutated in lung cancers. Erlotinib and Afatinib are first- and second-generation tyrosine kinase inhibitors (TKI) and are typically used as front-line treatments, however the gain of a secondary mutation at exon 20 of EGFR (T790M) results in patients becoming refractory these treatments and requires the additional used of third-generation TKIs such as Osimertinib (Nan *et al.*, 2017).

1.2 Basic Process of Metastasis

Metastatic progression requires a primary tumor cell to first escape from the primary tumor bulk into the circulation, travel throughout the body, arrest at a secondary location and subsequently colonize this new tissue (M. Singh *et al.*, 2014). In order to successfully complete this intricate process, the metastatic cell must undergo multiple genetic and molecular changes, shifting through several mechanisms to achieve each metastatic phase.

1.2.1 Steps of the metastatic cycle

Intravasation

The process of metastasis briefly requires a cell to undergo 1) loss of cell-cell adhesion, 2) acquisition of motility, 3) ability to digest through surrounding tissues to enter/exit the circulation. This process is termed intravasation, where the loss of intercellular junctions allows the cell to detach from the tumor bulk and invade the surrounding stroma. Cells can migrate as single entities or collectively (Friedl & Alexander, 2011). Single cells can adopt two main morphological types to promote their motility, amoeboid and mesenchymal (Figure 2). The amoeboid phenotype is achieved through activation of the Rho/ROCK pathway, causing the cell to adopt a rounded or abnormal shape, and produce "bleb"-like protrusions to aid movement (Rodriguez-Hernandez *et al.*, 2016). The mesenchymal phenotype is achieved by activation of RTK and Src pathways, resulting in an elongated, spindle-like cell body and production of plasma membrane protrusions like lamellipodia, filopodia, invadopodia, and podosomes that promote forward "crawling" (Voulgari & Pintzas, 2009). Cells can also migrate collectively as cohesive units with intact cell-cell

contacts, where either a single cell or multiple cells will serve as a leader to a line or sheet of follower cells. Collectively migrating cells can be of either epithelial or mesenchymal phenotypes, which may differ between the leader and follower cells (Clark & Vignjevic, 2015).

Invasion into the circulation and dissemination

These invasive cells can either secrete various matrix metalloproteinases (MMPs) and enzymes to remodel surrounding tissue or, in the case of amoeboid cells activate contractile actin:myosin core networks to squeeze between intercellular spaces, allowing them to intravasation into the surrounding tissue, and invading adjacent blood or lymphatic vessels (Friedl & Wolf, 2003). Once in the circulation, the majority of invasive cells, termed circulating tumor cells (CTC), will succumb to a myriad of lethal barriers. Shearing stress (aka fluid-shearing forces) encountered during circulation damage the majority of CTCs. In addition, the host's own immune response, *via* natural killer cells, further sequester and destroy CTCs (Luzzi *et al.*, 1998; Nieswandt *et al.*, 1999).

Extravasation and colonization

As the cell arrests at the new site, both through homing mechanisms as well as physical restraints (Ramakrishna & Rostomily, 2013), the cell will extravasate into the tissue. Depending on the received environmental cues the cell will either remain in a dormant state or colonize the tissue, where initial seeding of the brain will form micrometastases and subsequent development of tumor-associated vasculature (neoangiogenesis) will give rise

to macrometastases (M. Singh *et al.*, 2014). It is thought that the properties required to exit the circulation are the rate-limiting barrier; though millions of tumor cells can be shed into the circulation, only a very small percentage are able to survive and colonize the secondary environment (Luzzi *et al.*, 1998; Vanharanta & Massague, 2013), making this complex process very inefficient.

1.2.2 Theories of Organotrophic Mechanisms

Stephan Paget's "seed and soil hypothesis" aimed to explain the mechanisms that drive metastatic cells to their ultimate location. Briefly, metastases are not formed randomly (or stochastically) but may in fact be a consequence of the secondary nature of certain tumor cells—"seed"—that have a propensity for a specific secondary environment (Rahmathulla 2012, Ramakrishna 2013, fiddler 2003). Paget's theory comprised three main principles: (1) a tumor is composed of a heterogeneous population of cells with different characteristics; (2) only certain cells possess the specific traits that allow them to metastasize; (3) formation of a secondary neoplasm depends on the interactions between the tumor cell "seed" and secondary site microenvironment "soil". It is quite remarkable that even in the late 19th century, Paget was able to describe a model that attributes metastasis to a hierarchical cluster of cells with the metastatic-initiating cell at the apex of the hierarchy—the basis of the cancer stem cell (CSC) hypothesis (K. Chen *et al.*, 2013).

James Ewing's "mechanical hypothesis" was proposed in 1928, four decades following Paget's description of the seed and soil hypothesis (Ewing, 1928). The mechanical

hypothesis attributes the circulatory system for the homing capacity of metastatic cells to their secondary site. Due to the larger size of cancer cells (approximately 20 μm) compared to the lumen of an average vessel (3–5 μm) (Gavrilovic & Posner, 2005), CTCs would be restricted to arresting in the first capillary bed of the initial organ they encounter (Ewing, 1928; Fidler, 2003; Rahmathulla *et al.*, 2012). Although the circulatory pattern is adequate to explain the location of certain metastases, this is not enough to corroborate the incidence of metastases to most secondary sites (Fidler, 2003). A review of clinical data on metastatic site predilections established that mechanical factors could account for metastases to secondary sites within the vicinity of the primary malignancy. However, this finding could not be reproduced in metastases to distant organs, which were subsequently determined to be driven by site-specific factors as opposed to mechanical/circulatory factors (Sugarbaker, 1979; Weiss, 2000). Furthermore, despite comparable blood flow, the liver is a much more common site of metastasis compared to the spleen. Abdominal and pelvic primary cancers tend to form BMs that far exceed the proportion as estimated from the blood supply (Soffietti *et al.*, 2002). As such, the circulation can only explain approximately 66% of metastatic cases (Weiss, 1992), establishing a precedent for additional mechanisms of tumor seeding.

To date, research appears to confirm the seed-soil hypothesis (Hart & Fidler, 1980), where a primary tumor has even been shown to prime the predetermined secondary microenvironment to be more conducive for metastatic growth (Kaplan *et al.*, 2005). Briefly, a pre-metastatic niche (PMN) is initiated by tumor-shed extracellular vesicles and

factors (growth factors, chemokines/cytokines, proteases, etc.) secreted by primary tumor cells, myeloid cells and stromal cells, which collectively act to lure tumor-associated cells such as macrophages and bone marrow derived cells to the secondary site to alter the tissue and local milieu to be susceptible to invasion and engraftment (Psaila & Lyden, 2009). In turn, this PMN can generate "homing signals" to recruit metastatic cells. To date, six characteristics of the PMN have been suggested that determine the activity or dormancy of arriving metastatic cells: immunosuppression, inflammation, angiogenesis/vascular permeability, lymphangiogenesis, organotropism and reprogramming, and each stage heralded by specific factors (Y. Liu & Cao, 2016). The PMN represents abnormal, tumor-independent manipulation of secondary organs that could be perceived as preemptive indicators for metastasis initiation.

1.2.3 The Brain Microenvironment

Of all organs, the brain presents a distinctly unique environment for neoplastic development. The brain parenchyma is composed of neurons and subgroups of glial cells (astrocytes, oligodendrocytes, microglia, ependymal cells), that form separate regions of the brain to regulate specific processes and functions. The brain is the most vascularized organ of the human body, possessing a dense network of capillaries, different from the capillaries that reside throughout the body, to ensure every neuron is perfused in blood (D. Palmieri, 2012). Lastly, the brain is protected by the BBB and BCSFB. The BBB is a barrier formed by the endothelial cells of the brain capillaries, closely associated with pericytes, perivascular astrocytes, and microglia, and separates the circulating blood from the brain

interstitial fluid (Redzic, 2011). The BCSFB is composed of modified cuboidal epithelium of the choroid plexus, serving to secrete and separate CSF from circulating blood (Redzic, 2011). Both barriers express transporters, multi-specific carriers, receptors and enzymes that help to regulate diffusion and transport of polar molecules, essential nutrients, and wastes, and restrain the passage of anticancer compounds into the brain (Redzic, 2011). The brain microenvironment combined with the protective barriers of the leptomeninges and BBB collectively make the brain a welcome sanctuary for metastatic cells that can penetrate into the brain (Groves, 2010).

The flow of arterial blood largely determines the deposition of metastatic cells throughout the brain parenchyma, arresting at grey-white junctions and "watershed" areas where the vasculature narrows and has slower capillary flow (Lu-Emerson & Eichler, 2012; Pekmezci & Perry, 2013). Approximately 85% of BM arise within the cerebrum, 5-10% within the cerebellum, and 3-5% within the brainstem (Patchell, 2003).

1.3 Brain metastasis initiating cells

1.3.1 Theories of metastatic origin

Early theories of metastasis concerned a stochastic or clonal selection-based model of evolution, where metastasis was the culmination of accumulated genetic aberrations in any one cell (Liotta *et al.*, 1976a). Another proposition postulated that metastatic properties can be gained by horizontal transfer of circulating oncogenes or uptake of oncogenic DNA from apoptotic bodies (Garcia-Olmo *et al.*, 1999). Increasing evidence is suggestive of a

hierarchal model of metastasis, with CSCs as the initiating population (Fodde & Tomlinson, 2010). In general CSCs are immortal tumor-initiating cells (TICs), distinctly different from the general tumor bulk. They exhibit self-renewal and proliferative properties enabling initiation and maintenance of tumor growth, and can undergo asymmetric division and differentiation to give rise to all the other cell phenotypes within the heterogenous tumor (Lobo, Shimono, Qian, & Clarke, 2007). CSCs can be identified, isolated, and most recently targeted, by specific biomarkers in most human cancers (Chen, Huang, & Chen, 2013). Despite the current lack of prospective identification of metastatic initiating cells (MICs), evidence suggests that this population is related to or comes from CSCs. The first indicator of this theory is the tumor initiating capacity (TIC) seen with both populations. The increased exhibition of metastasis-associated mechanisms found at the leading edge of primary or metastatic tumors suggests the existence of at least two different forms of CSCs within the primary tumor, an inner progression-stationary subset and an outer motile subset (Liao, *et al*., 2014). The stationary CSCs are active throughout primary tumor progression but are unable to escape the primary tumor borders. The metastasis-initiating CSCs, or MICs, are selected and primed for dissemination by receiving signals from the stroma resembling the environment of a distant organ (Baccelli & Trumpp, 2012; T. Brabletz, *et al*., 2005; Oskarsson, Batlle, & Massague, 2014). Induction of certain metastatic traits appears to result in cells acquiring both mesenchymal and stem-like properties (Mani *et al.*, 2008). Lastly, certain CSC populations and subpopulations were found to have enhanced metastatic tendencies (Al-Hajj *et al.*, 2003; Hermann *et al.*, 2007; Lawson *et al.*, 2015; H. Liu *et al.*, 2010; Pang *et al.*, 2010).

1.3.2 Properties of MICs

MICs have adapted several mechanisms that support their survival throughout the metastatic cascade as well as ability to serve as the TIC pool in a distinctly different secondary organ environment (Celia-Terrassa & Kang, 2016).

The plasticity of MICs enables them to adapt different migratory phenotypes, allowing cells to be motile even when one form is pharmacologically inhibited (Wolf *et al.*, 2003). A widely accepted mechanism to achieve a mesenchymal phenotype is through the epithelial-mesenchymal transition (EMT), a process initiated by external and internal factors (environmental cues, transcription factors, etc.) (Heerboth *et al.*, 2015; Thiery *et al.*, 2009). Conversely, recent studies have addressed the necessity of EMT in metastasis where, due to the transient, nonlinear nature of the process, tumor cells may not require full completion of EMT to become metastatic. Studies have shown that forced induction of EMT through overexpression of EMT-regulating transcription factors causes a loss of tumor-initiating properties in the mesenchymal tumor cell (Celia-Terrassa *et al.*, 2012; Ocana *et al.*, 2012; Tsai *et al.*, 2012). As such, EMT has been proposed to be more of a spectrum of phenotypes, where a tumor cell will undergo partial phase shifts to promote migration as well as maintain their tumor-initiation capacity (Lambert *et al.*, 2017). In some cases, such as collective cell migration, EMT may not be required at all to achieve migration (Fischer *et al.*, 2015; X. Zheng *et al.*, 2015).

A characteristic feature of tumor cells is their anchorage-dependent growth; cell release from a substratum often results in anoikis, a detachment-induced apoptosis. This feature has been hypothesized to be a major contributor to metastatic inefficiency of tumor cells within the circulatory system, and successful MICs are capable of resisting anoikis by expressing multiple RTKs, invasion signaling components, and anti-apoptotic molecules (Grossmann, 2002; Steeg, 2006). Another feature of MICs that promote their survival is their aggregation with other cellular elements such as fibrinogen, fibrin, and thrombin (Langley & Fidler, 2013; Steeg, 2006).

MICs have adopted successful defensive strategies to survive within the circulation. One such method employed by single MICs involves tumor cell-induced platelet aggregation (TCIPA), where the MIC will express thrombin to collect platelets and form protective layer from immune-surveillance and hemodynamic shearing forces (Palumbo *et al.*, 2007). This MIC-platelet association in turn stimulates the platelets to produce α-granules containing TGF-β and PDGF, which in turn stimulates the SMAD and NOTCH pathway, respectively, in the MIC to ultimately help maintain their mesenchymal/stem properties (M. Singh *et al.*, 2018). Rarely metastasizing cells that have invaded the circulation as collective groups can form clusters of MICs or microemboli, arising from oligoclonal tumor cells, and appear to have a higher metastatic potential than single MICs (Aceto *et al.*, 2014). These clusters provide protection similar to platelet shields but also an added benefit of avoiding anchorage-dependent apoptosis (Liotta *et al.*, 1976b).

As previously stated, the largest barrier to metastatic development is extravasation, where most cells succumb to apoptosis within the first 24 hours (Sahai, 2007). At this secondary site, the surviving MICs will either enter a dormant state to delay colonization until a more favorable time/condition or eventually die, or they immediately initiate colonization. Dormancy can occur if the MIC does not receive favourable growth signals from the new microenviroment. For instance, transient adhesion of the MIC to the microenvironment can induce stress response signalling, such as activation of urokinase-type plasminogen activator receptor (uPAR) deactivation. Low or downregulated uPAR signalling can prevent MIC adherence through β1integrins and reduce MIC proliferation (Aguirre Ghiso *et al.*, 1999). The ratio of ERK *vs* p38 activity can dictate MIC entrance into a proliferative or dormant state, respectively, and in tumor cells can be predictive of early or late reocurrence. Activation of the MAPK pathway results in increased levels of p38 and in turn activates p53 and p16, causing subsequent arrest of the tumor cell in the G_0 cell cycle phase. Activation of the WNT and ERK signalling pathways can inhibit p38 and promote progression into MIC invasion and proliferation (Gomis & Gawrzak, 2016).

Brain-specific MICs (BMICs) retain particular features that allow them to circumvent apoptosis as well as self-protective strategies of the brain to colonize the tissue. Astrocytes, the first cells encountered by extravasating BMICs, can play both a BM-suppressive and BM-promotion role. They initially secrete plasminogen activators, where plasmin will prevent BM by 1) inducing a paracrine death signal for BMICs through conversion of FasL, and 2) inactivating L1CAM, a pathfinding molecule utilized by BMICs to spread along

capillaries. To circumvent this defense, BMICs secrete plasminogen activator inhibitory serpins, such as neuroserpins and serpin B2 (Valiente *et al.*, 2014). BMICs express PCDH7, a protocadherin that promotes BMIC-astrocyte gap junction formation through connexin 43 (CX43). This gives BMICs access to transfer the secondary messenger cGAMP to astrocytes, activating paracrine signals for the release of cytokines that promote BM growth (Q. Chen *et al.*, 2017). The high glucose and oxygen content within the neural tissue promotes successful colonization of BMICs that utilize aerobic glycolysis (DeBerardinis *et al.*, 2008). BMICs possess an adaptive metabolic mechanism that utilizes the citric acid cycle to co-oxidize acetate and glucose into fuel sources to support the high demand of proliferating cells (Mashimo *et al.*, 2014). Expression of αVβ3 integrin can mediate upregulation of VEGF to promote vascular recruitment and promote tumor growth, an effect seen only within the neural microenvironment (Lorger *et al.*, 2009).

Chemoresistance is another major survival tactic bestowed upon MICs, enabling them to evade therapy and contribute to recurrent tumor growth post-treatment (Hay, 2005). Drug resistance can be either intrinsic, such as the expression of ATP-binding cassette (ABC) transport proteins that regulate drug efflux, and extrinsic, as seen by the gain of resistance to apoptosis-inducing agents. Several EMT regulating transcription factors (TFs) (ex. SNAIL1, SNAIL2, TWIST, FOXC2) have been shown to induce these mechanisms in metastatic cells (Abdullah & Chow, 2013; Gottesman *et al.*, 2002).

1.3.3 BMIC genes and signatures

Several studies have undertaken the effort to identify genes and metastastic gene signatures essential to BMICs, where neurotrophism-predicting factors would help develop treatments to prevent BM development. Genomic profiling has led to the identification of different metastatic gene sets predictive of BM. Ramaswamy *et al.* compared metastatic adenocarcinomas to non-metastatic cancers of the same type to yield the best descriptor set of 128 metastasis-associated genes (64 overexpressed and 64 underexpressed) and derived a core gene signature of 17 metastasis markers, but didn't provide an obvious set of genes with related function (Ramaswamy *et al.*, 2003). Kikuchi *et al*. compared lung adenocarcinomas with their matched BM, identifying 244 genes to be overexpressed in BM (Kikuchi *et al.*, 2006). Similar work conducted by Zohrabian *et al*. identified 1561 genes dysregulated in lung-derived BM (Zohrabian *et al.*, 2007). Nolte *et al*. identified 30 candidate genes as being significantly over-expressed in a stem cell population for BM, primary brain and lung tumors, 11 of which were found to be significant predictors of patient outcome (Nolte *et al.*, 2013).

Other studies have functionally validated genes that mediate metastasis to the brain. Bos *et al*. utilized genomic sequencing to determine α-2,6-sialyltransferase (ST6GALNAC5) mediates breast cancer metastasis to the brain by enhancing tumor cell adhesion to neural endothelial cell walls, and inhibition of COX2 and EGFR prevented breast tumor cells from crossing the BBB *in vitro(Bos et al., 2009)*. Okuda *et al.* identified high expression of Kruppel-like factor 4 (KLF4) in CSCs of breast cancer, and upregulation of miR-7 was able to attenuate brain metastases (Okuda *et al.*, 2013). Wu *et al*. showed a COX2-MMP1-

CCL7 axis to promote BM from breast cancer, whereby upregulated expression of COX2 in BMICs induced prostaglandins, which in turn promoted both MMP1 expression and subsequent modification the BBB as well as upregulation of CCL7 in astrocytes to promote BM initiation (K. Wu *et al.*, 2015). Valiente *et al*. determined breast- and lung-derived BMICs secrete serpins, inhibitors of plasminogen activators secreted by the reactive brain stroma in response to invasion, which protects BMICs from death signals and promotes vascular co-option to initiate BM (Valiente *et al.*, 2014). Massague *et al*. found breast- and lung-derived BMICs express PCDH7, which aids recruitment of connexin 43 and promotes tumor-astrocyte gap junction formation and subsequent invasion into the brain parenchyma (Q. Chen *et al.*, 2017).

1.4 Modelling Brain Metastasis

1.4.1 In vitro methods

Several 2D *in vitro* models have been generated to quickly assess fundamental properties of metastatic cells. Basic cell migration, an integral component of metastatic cells, can be assessed with variations of scratch/wound or zone exclusion assays, where cells are first seeded in an adherent monolayer and then a "cell-free" zone is created either by making a scratch or removing a barrier, and monitoring the cells moving into the empty space. These assays are very common as they are simple, economical, offer real-time observation and can be high throughput. Microfluid devices assess migration of cells along channels following a chemoattractant, however these assays are currently expensive and time consuming (Katt *et al.*, 2016). Transwells and Boyden chambers offer the most flexibility

when assessing cell migration, where cells are plated in an upper well and migrate through a porous membrane to a lower well following a chemoattractant. The addition of a basement membrane extract layer (Matrigel, collagen) over the porous membrane can then model cellular invasion (Kramer *et al.*, 2013). Transwells can be further modified to mimic cell passage through the blood-brain barrier (BBB) by plating pericytes, astrocytes, and endothelial cells (commonly derived from cells of the human umbilical cord) in layers across the membrane to mimic those that comprise the BBB. Unfortunately, transwells are time consuming and cells cannot be viewed in real time (Kramer *et al.*, 2013).

Technological advances into the development of 3D assay systems that better represent the microenvironment, allow to interrogation of cellular architecture and cellular interactions more similar to what is experienced *in vivo*. Tumor cells cultured as spheroids are considered to represent avascular tumor nodules or micro-metastases, and despite expense and time-consuming preparation, they allow investigation of several metastatic properties including invasion, matrix remodelling, and immune cell interactions (Friedrich *et al.*, 2009; Katt *et al.*, 2016). Co-culturing systems are used to investigate the synergism between tumor and stromal cells (Sasser *et al.*, 2007; Sieh *et al.*, 2010). Angiogenesis or neovascularization, the process of forming new blood vessels branching from existing vasculature, can be recognised through a tube formation assay, where cells plated on an extracellular matrix layer that mimics the *in vivo* environment and will form tubule-like structures that resemble vessels (DeCicco-Skinner *et al.*, 2014).

These *in vitro* assays have been invaluable as tools to not only delineate the mechanistic regulation of metastasis but also serve as screening platforms for therapeutic targets, unfortunately they also face several limitations in that they cannot reproduce the entire metastatic cycle and they lack proper live host interactions.

1.4.2 In vivo methods

Animal models represent a vital tool in a scientist's repertoire for translational research, allowing examination of anatomical barriers (BBB and BCSFB), stromal/environmental determinants, immune signalling and response, and cytokines/growth factors (Huszthy, et al., 2012). A clinically relevant *in vivo* model can enable researchers to identify the genetic events that contribute to metastatic development within the CNS, and provide a platform to identify and screen novel therapeutics (Huszthy, *et al*., 2012).

Although, the genetic mouse models have become an important tool in studying the functional significance of a defined mutations in the development of BM, such models lack the ability to recapitulate the genetic heterogeneity of primary human tumors. Furthermore, the genetically engineered mouse models (GEMMs) are limited by complex breeding schemes, incomplete tumor penetrance and variable tumor onset (Sanden *et al.*, 2017). In contrast, patient-derived xenograft (PDX) models for many cancer subtypes (Joo *et al.*, 2013; Q. Shu *et al.*, 2008; S. K. Singh *et al.*, 2004; Wakimoto *et al.*, 2012; L. Yu *et al.*, 2010; Zhao *et al.*, 2012) have been generated through injection of patient tumor cells into an appropriate microenvironment. Tumors generated through PDX models have been

shown to retain the molecular identity and recapitulate the complex heterogeneity of the original patient tumor. In addition, PDX models allow for a more accurate evaluation of tumor growth patterns, metastatic properties and their changes in response to therapeutic intervention (Hoffman, 2015; Talmadge *et al.*, 2007). Currently a variety of xenograft models have been developed that are capable of reproducing specific individual stages of metastasis, providing a more detailed understanding of the intricacies involved in the process. For instance, the avian embryo provides a unique model support system for many metastatic features, including growth, invasion, and angiogenesis. The chorioallantoic membrane (CAM), a vascularized embryonic tissue, shows easy engraftment of human cells, and the embryo itself provides an immunodeficient environment (Lokman *et al.*, 2012; Palmer *et al.*, 2011; Wilson & Chambers, 2004). The use of zebrafish xenograft models has also risen over the last few years, providing a novel high throughput and inexpensive platform for drug discovery and *in vivo* imaging (H. K. Brown *et al.*, 2017; C. F. Liu *et al.*, 2017). Despite the novelty of these unique models, the use of mice and rats (murine) have remained a standby host species in modelling metastasis, providing high reproducibility in disease development and easy to manipulate/inject due to size (Schabet & Herrlinger, 1998). The advent of transgenic and immunodeficient strains significantly increased the success rate of tumor transplantation and human-mouse xenograft model development (Shultz *et al.*, 2007).

When developing an appropriate *in* vivo model for LM and BM, several biological and technical factors must be considered.

1. The number of cells delivered: a property easily controlled by the researcher, can also play a large role in the time it takes for engraftment. A larger cell number injected may permit for a shorter incubation period, however this may not accurately represent the slower growth observed with the clinical presentation of metastatic progression. Conversely, a low cell number may not be engrafted easily, reducing the success rate of engraftment or cell collection (Francia *et al.*, 2011).
2. Host selection: The choice of host when establishing a metastasis model can be key to successful engraftment rates. Murine models can be divided into 2 broad categories: 1) syngeneic and 2) xenogeneic. Syngeneic models utilize cancer cell lines of the same genetic background as the host, and are typically generated through chemical or experimental induction. These models offer researchers the ability to study oncogenesis and metastatic progression in the presence of a functioning immune response and potential to identify therapeutics that can target the immune system. Unfortunately, this model is solely mouse-related, which can have difficulties with correlations to human disease. On the contrary, xenograft models are developed from the administration of human cancer cells into an immunocompromised host. The lack of an immune response, which would otherwise attack the foreign cells injected and limit engraftment, permits a high rate of human tumor transplantation and study of human cancer cell behaviour in a live host but lacks information on the interaction between the immune system and tumor cells. However, this drawback can be somewhat circumvented through the use of humanized mouse models.

3. The route of injection (Figure 4): The location of cell delivery and subsequent tumor engraftment and metastatic progression is another decision critical to model development. Due to circulation patterns, some locations for metastatic spread are more likely to select for metastatic growth over others, such as tail vein injections resulting in primary lung metastases (Francia *et al.*, 2011). Certain hosts do not possess the proper/compatible physiology to represent clinical disease progression, whereas injections in some areas may not even be feasible for a particular host due to anatomical differences. Another criteria is host size, where a larger animal may allow for easy and safe repeated access to the injection route (Schabet & Herrlinger, 1998).

When modelling metastasis, the best route of inoculation would replicate tumor formation at the primary site first and subsequent metastatic development. Several such models have been established with commercial mouse and human cell lines, unfortunately this method can be laden with difficulties in capturing the metastatic cells at the desired secondary site. To overcome this, successive rounds of *in vivo* selection are performed with cells harvested from the secondary site and re-injected, selecting for cells that are aggressively metastatic with each round (Bos *et al.*, 2009; Fidler, 1970).

1. Intracardiac/intracarotid: A common method for BM development is direct injection of tumor cells into the circulation. This method is more of an assessment of brain colonization and not full metastasis, as it selectively ignores the ability of cells to undergo EMT and intravasate into the circulation, and often times several

folds higher numbers of cells are injected into the circulation than the number of cells that would typically escape from the primary tumor. Nonetheless, this method allows for selection of highly metastatic populations that are able to cross the BBB and BCSF to engraft into the brain. Intracardiac injections (*via* the left ventricle), allows cells to freely enter the circulation and have indiscriminate access to all organs of the body, allowing cells to seed metastases in different areas (Song *et al.*, 2009). Injection of cells into the intracarotid artery allows cells to travel directly to the brain, and primarily produces BM and LM (Daphu *et al.*, 2013; Kircher *et al.*, 2016; Martinez-Aranda *et al.*, 2013; Z. Zhang *et al.*, 2008).

2. Orthotopic: Orthotopic injections places cells directly into the originating environment of the primary tumor. For BM development, the most common route of inoculation of tumor cells derived from a BM or primary brain tumor is directly into the brain parenchyma (intracranial). This surpasses all barriers encountered in the initial and mid stages of metastasis, allowing the cells to begin colonization, but creating a significant selection bias by giving cells that may not be capable of surviving the metastatic cascade an opportunity to engraft. When utilizing tumor cells from other primary cancers, the injection site will follow accordingly to best represent the metastatic cascade. For instance, melanoma cells can be injected subcutaneously, lung cancer cells injected intrathoracically, and breast cancer cells injected into the 4^{th} fatpad (Cruz-Munoz *et al.*, 2008; Marsden *et al.*, 2012; Sakamoto *et al.*, 2015).

Tumor models provide platforms to interrogate intricacies of molecular interactions, allowing researchers to gain much insight into cancer progression as well as develop and screen novel treatments. Despite technological advancements (tumor cell biology, tissue engineering, biomaterials, microfluidics, etc.), the complexities of the metastatic cascade limit the degree to which current models can represent progression of the disease as seen in patients.

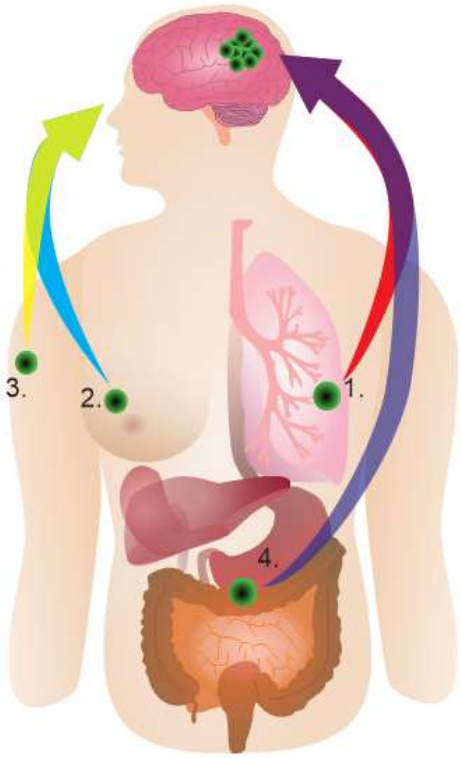

Figure 1. Primary sources of brain metastasis.
Brain metastases can arise from various primary sources. 1. Lung cancers are the primary source of 40-60% brain metastasis, followed by 2. Breast cancer with 15-25% of cases, 3. Melanoma with 6-11% of cases, and 4. Renal, colorectal and gastrointestinal cancers with 2-14% cases.

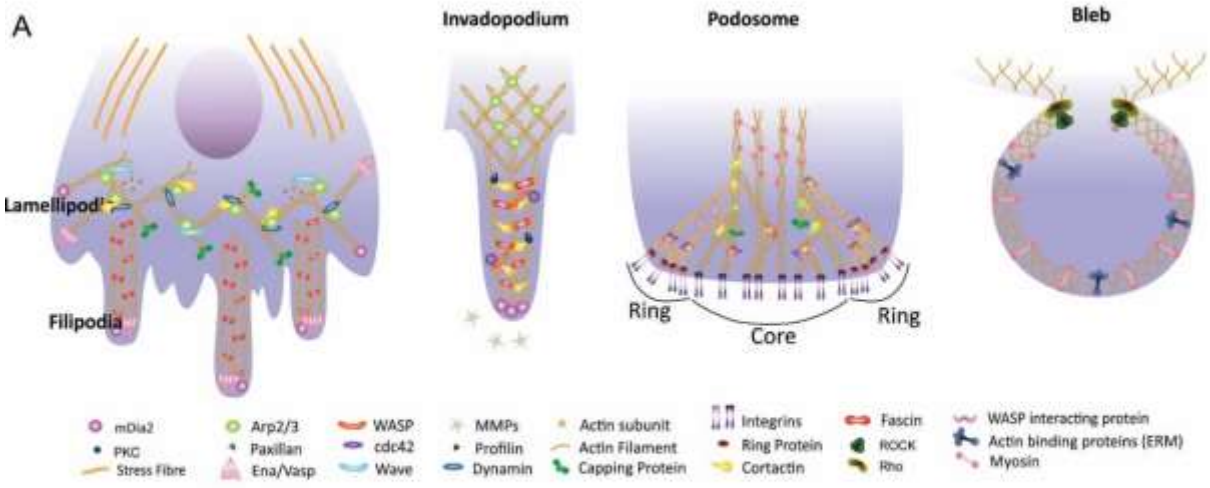
A
Invadopodium
Podosome
Bleb
Lamellipodia
Filipodia
Ring
Core
Ring
mDia2
PKC
Stress Fibre
Arp2/3
Paxillan
Ena/Vasp
WASP
cdc42
Wave
MMPs
Profilin
Dynamin
Actin subunit
Actin Filament
Capping Protein
Integrins
Ring Protein
Cortactin
Fascin
ROCK
Rho
WASP interacting protein
Actin binding proteins (ERM)
Myosin

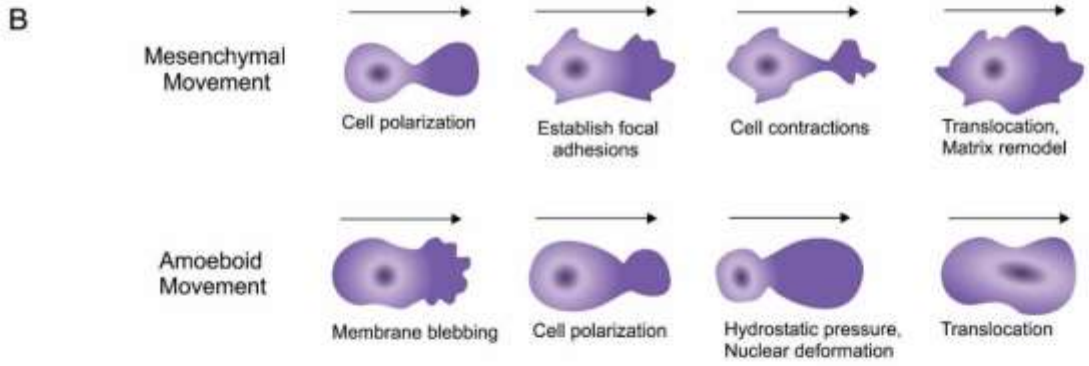
B
Mesenchymal Movement
Cell polarization
Establish focal adhesions
Cell contractions
Translocation, Matrix remodel
Amoeboid Movement
Membrane blebbing
Cell polarization
Hydrostatic pressure, Nuclear deformation
Translocation

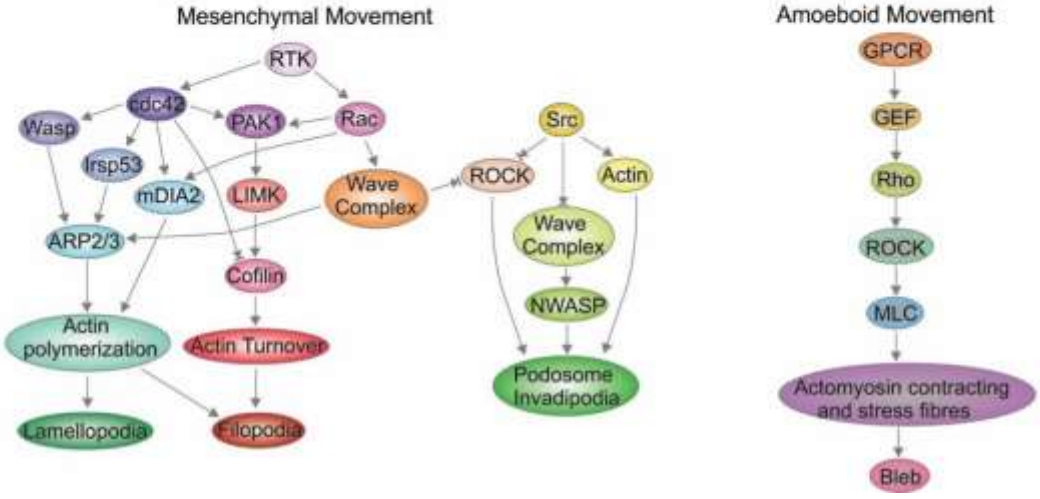
Mesenchymal Movement
RTK
cdc42
Rac
PAK1
Wasp
Irsp53
mDIA2
LIMK
Wave Complex
ARP2/3
Cofilin
Actin polymerization
Actin Turnover
Lamellipodia
Filopodia
Src
ROCK
Actin
Wave Complex
NWASP
Podosome Invadipodia
Amoeboid Movement
GPCR
GEF
Rho
ROCK
MLC
Actomyosin contracting and stress fibres
Bleb

Figure 2. Cellular structures that aid cell migration and invasion (M. Singh *et al.*, 2018).

Actin filaments are a primary component of the cytoskeleton, residing under the plasma membrane to provide structural support and maintain tissue integrity. (A) Tumor cell invasion is assisted by several protrusive structures such as lamellopodia, filopodia, invadopodia or membrane blebs, which are formed through the nucleation, rapid assembly and disassembly of these actin filaments. (B) During active migration, cells will undergo mesenchymal-type movement, where the cell will first polarize and establish points of focal adhesion with the ECM fibres, then the cell will translocate through contractions of the cell body, leaving behind the remodeled EMC. For this process, CDC42 is activated and binds to the N-WASP and IRSp53, which will bind the actin-nucleating ARP2/3 complex to promote actin polymerization and formation of the leading edge and wave-like lamellopodia. CDC42 binding to mDIA2 also activates nucleation of unbranched actin. CDC42 activation of PAK will activate LIMK to inhibit cofilin and increase actin turnover, inducing the formation of sensory filopodia. Activation of Rac induces actin polymerization and the formation of lamellopodia similarly to CDC42 but operates through the WAVE complex. The Src pathway inhibits ROCK and N-WASP to promote invadopodia and podosome formation, which are actin-rich protrusions tailored for ECM degradation (Friedl & Wolf, 2003; Heasman & Ridley, 2008). Non-apoptotic blebs are structures utilized in amoeboid movement in passive migration. Blebs are formed by intracellular hydrostatic pressure resulting compression of the cytoskeletal network as it separates from the plasma membrane, which pushes out on areas of weak cortical actin in the plasma membrane. This protrusion is initially devoid of actin as it expands, and is reformed as the bleb retracts. As blebs are formed they polarize, and hydrostatic pressure will deform the nucleus and force the cell to move forward through these blebs (Friedl & Wolf, 2003; Nurnberg *et al.*, 2011). This process is initiated by GEF activation of RHO, which works through ROCK and MLC to produce actomyosin contractions (de Lucas *et al.*, 2016; Morley *et al.*, 2014). N-WASP, Wiscott-Aldrich syndrome protein; IRSp53, insulin receptor substrate p53; mDIA2, mammalian diaphanous 2; WAVE, WASP-family verprolin-homologous protein; RHO, Ras homolog gene family member; ROCK, Rho-associated protein kinases; GEF, guanine nucleotide exchange factors; MLC, myosin light chain.

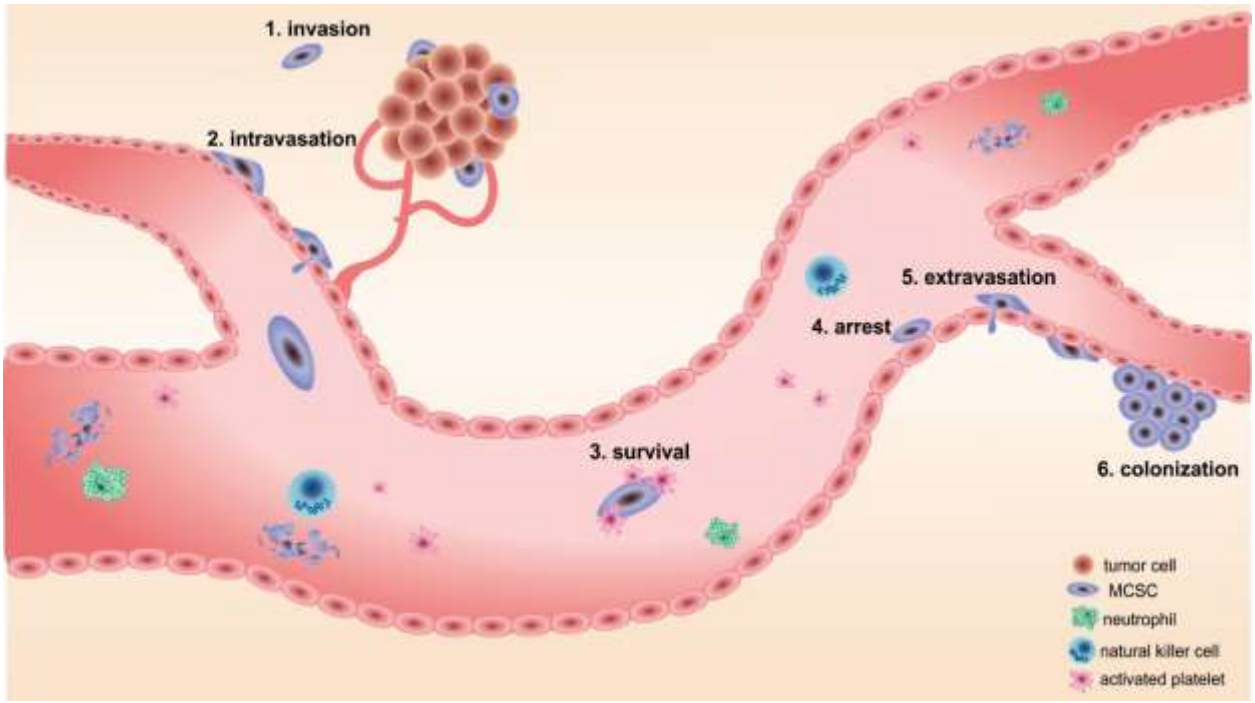

Figure 3. Stages of the metastatic cascade (M. Singh *et al.*, 2018).
MICs will initiate the metastatic cascade. 1) The MIC will lose adhesion to neighbouring cells and the ECM, allowing them to break away from the tumor bulk and 2) invade the surrounding tissue. 3) To intravasate into adjacent blood or lymphatic vessels, metastatic cells initiate local neoangiogenesis, allowing the formation of vessels possessing weak endothelial cell junctions that the cells can easily pass through as they undergo TEM. 4) Upon entering the circulation, metastatic cells will circumvent lethal barriers such as shearing forces and host immune responses before arresting at a new secondary site. 5) The metastatic cells will undergo TEM again to extravasate and invade the BM surrounding the vessel, where they will undergo 6) MET and enter either a dormancy state or initiate colonize the tissue (Cavallaro, 2013; Reymond *et al.*, 2013; M. Singh *et al.*, 2014). EMT, epithelial mesenchymal transition, MCSC, metastatic cancer stem cell; ECM, extracellular matrix; TEM, transendothelial migration; BM, basement membrane; MET, mesenchymal epithelial transition.

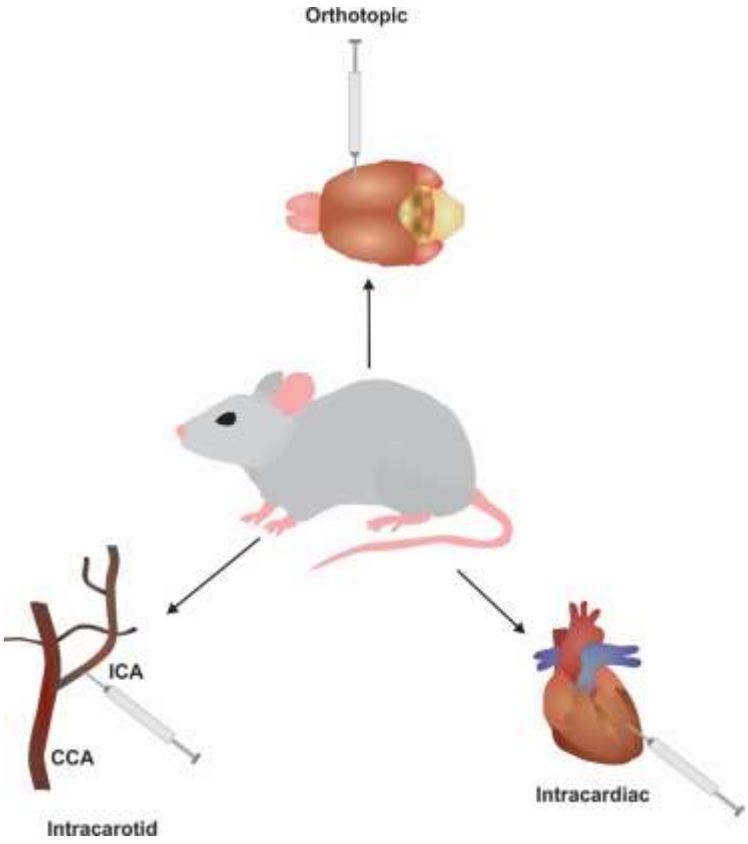

Figure 4. Routes of injection to develop brain metastasis in vivo.
Common injection routes used in murine models to develop BM, typically involving injection of cells of directly into the circulation or CSF to bypass the initial stages of metastasis. ICA, intracarotid artery; CCA, common carotid artery.

1.5 Summary of Intent

Metastases arise from the dissemination of cancer cells from a primary tumor, and 90% of all cancer-related deaths are due to metastases (Sleeman & Steeg, 2010). Metastasis to the brain (BM) are the most frequently diagnosed of all adult brain tumors, arising in 20-40% of cancer patients throughout the course of the disease (Gavrilovic & Posner, 2005). The invasive nature of BM and their ability to escape aggressive treatments predicts uniformly poor patient outcome, with a median survival time of only months (Stelzer, 2013). Advances in screening, detection and therapeutics for systemic cancers have led to an increase in cancer patient survival, yet leave cancer survivors vulnerable to an increased prevalence of BM (Langley & Fidler, 2013). A lack of new therapeutic options for BM and the inefficiency of current therapies implies a severely limited knowledge of this process and proper translation into novel therapeutic avenues. In fact, on average, as little as 5% of total cancer research funding is typically assigned to the study of metastasis (Steeg *et al.*, 2009). Effective studying of BM is hindered by the inability to properly represent the metastatic intricacies as experienced by the patient. As such, there still remains a dearth of models that are able to capture every molecular, genetic and epigenetic change a tumor cell undergoes to achieve BM. Thus, **I hypothesize that there exists a rare subfraction of BM cells termed BMICs will survive the metastatic process as well as initiate a tumor in a secondary neural niche**. These cells can be identified, enriched and characterized through a clinically relevant human-mouse xenograft model, and will provide novel therapeutic avenues into the prevention of BM. The goals of this thesis were to:

i. *Development of a patient-derived xenograft (PDX) model of BM that properly represents the metastatic stages.*
ii. *Identification and functional characterization of BMIC regulatory genes.*
iii. *Identification and preclinical validation of BM-targeting therapeutics.*

The ability to isolate the cells that have already undergone all stages required to form BM provides us with a better opportunity to characterize the mechanisms involved. To address these aims, I first generated cell lines enriched in BMICs from primary patient samples of lung-derived BM. I then optimized 3 xenograft models that could properly recapitulate the various stages of metastasis. Briefly, I injected BMICs in NOD/SCID mice through the following routes (Figure 5):

a) Intracranial (ICr): to assess for reformation of tumors within the secondary neural environment
b) Intracardiac (ICa): to assess for a homing capacity of BMICs for either the originating tissue (lung) or the secondary tissue (brain)
c) Intrathoracic (IT): To recapitulate the entire metastatic process, from primary (lung) tumor formation progressing to BM formation.

A limiting dilution assay was initially performed to determine the optimal and lowest number of BMICs that were required to be injected to result in tumor or BM formation in an appropriate span of time. From this work I was able to model clinically different stages within metastasis. BMICs injected into the ICa model were able to generate macro-metastasis, whereas the BMICs injected into the IT model managed only initial seeding of the brain before mice succumbed to gross lung tumor burden (**Chapter 3**).

Utilizing these models, I screened potential BMIC regulatory and metastatic genes, identifying STAT3 (**Chapter 2**), SPOCK1 and TWIST2 (**Chapter 3**) genes to be essential regulators of BM. Further characterization of the seeding stage using my IT model was performed by transgenomic analysis, showing several mechanisms employed in BMICs undergoing this state that promote their invasion and adaption to the neural tissue and concurrently prevent their proliferation and colonization. With this data I determined that the IT model captured BMICs undergoing "pre-metastasis", a stage impossible to capture in human patients due to the current limitations of diagnostic technology. *In silico* interrogation of the BM^{IT} genes and *in vivo* validation identified Apomorphine, a repurposed Parkinson's drug, to prevent BM development by targeting premetastatic genes KIF16B, SEPW1, and TESK2. Lastly, low expression of these 3 genes was associated with poor patient survival in a cohort of lung adenocarcinoma patients, suggesting that these particular genes have the potential to predict patient response to therapeutic intervention and prevention of BM (**Chapter 4**).

Collectively, the work of this thesis gives much needed insight into the progression of BM. Our clinically relevant models question the usage of macro-metastases in current *in vivo* models for therapeutic development, and identify a novel therapeutic window in the pre-metastatic stage in the prevention of BM and ultimately to extend patient survival.

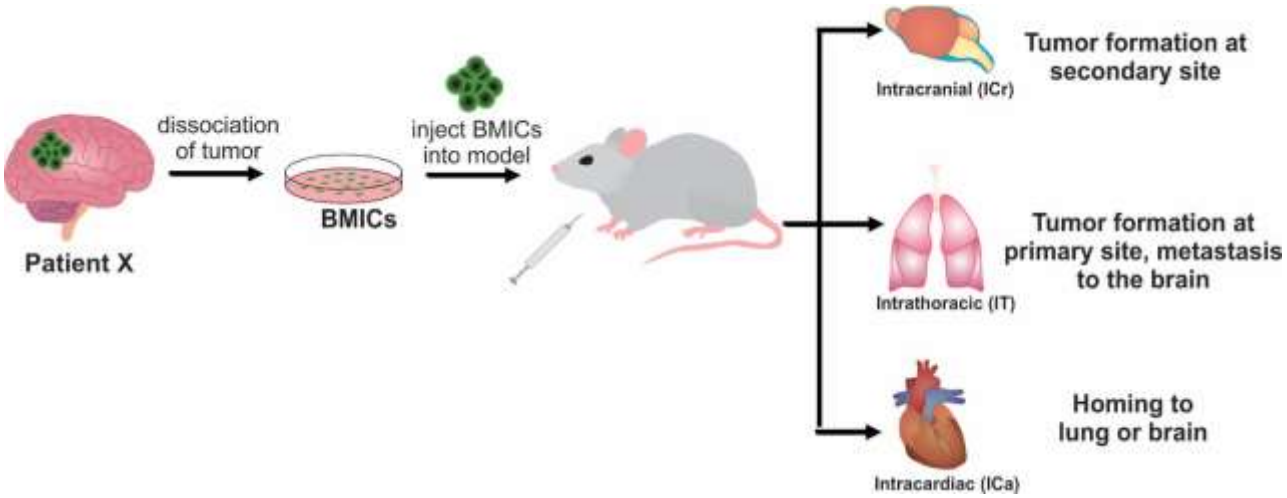

Figure 5. Schematic representation of BM modelling routes.
Planned routes of injection to interrogate the tumor/metastasis initiating capacity of BMICs.

Chapter 2: STAT3 pathway regulates lung-derived brain metastasis initiating cell capacity through miR-21 activation

Preamble

This chapter is an original published article presented in its published format in *Oncotarget*, available online at https://doi.org/10.18632/oncotarget.4742.

Singh M, Garg N, Venugopal C, Hallett R, Tokar T, McFarlane N, Mahendram S, Bakhshinyan D, Manoranjan B, Vora P, Qazi M, Arpin CC, Page B, Haftchenary S, Rosa DA, Lai PS, Gómez-Biagi RF, Ali AM, Lewis A, Geletu M, Murty NK, Hassell JA, Jurisica I, Gunning PT, Singh SK. *STAT3 pathway regulates lung-derived brain metastasis initiating cell capacity through miR-21 activation.* Oncotarget. 2015 Sep 29;6(29):27461-77. doi: 10.18632/oncotarget.4742.

Experimental concept and study design were developed by myself C. Venugopal, N. Garg and S. Singh. Intellectual guidance was provided by S. Singh and C. Venugopal, and supervision by S. Singh. BM samples were provided by N. Murty. The putative BMIC regulatory gene list was generated in previous work by S. Nolte (Nolte *et al.*, 2013). I performed all *in vitro* BMIC line generation, maintenance and characterization. I performed all STAT3 knockdown experiments with the exception of western blots, which were generated with the aid of S. Mahendram. Flow cytometric analyses were performed by N. McFarlane. All *In vivo* experiments were led and performed by myself, with aid from D. Bakhshinyan and M. Qazi. Generation of the STAT3 compound library was achieved by C.C. Arpin, B. Page, S. *Haftchenary, D.A. Rosa, P.S.* Lai, R.F. Gómez-Biagi, A.M. Ali, A. Lewis and M. Geletu under the supervision of P.T. Gunning. *In vitro* screening of the

STAT3 library was performed by myself. *In vitro* miRNA-21 experiments were conducted by N. Garg with assistance from myself. *In silico* analyses (protein connectivity mapping and network mapping) were performed by R. Hallett under the supervision of J.A. Hassell and by T. Tokar under the supervision of I. Jurisica. The manuscript was prepared myself, N.Garg, C. Venugopal and S. Singh, with input and edits provided by P. Vora, B. Manoranjan, I. Jurisica, and P.T. Gunning.

The main goal of this body of work was to validate the list of potential BMIC regulators previously generated by Nolte. *et al*. (Nolte *et al.*, 2013). Annotation of this list led to STAT3 as a novel protein interactor. I found that inhibition of STAT3 through shRNA knockdown and drug interference reduced BMIC sphere formation, proliferation and migration *in vitro*, and decreased tumor growth *in vivo*. Previous literature implied a possible relationship between miR-21 and STAT3, so I further elucidated this relationship to find miR-21 was a downstream target of STAT3.

STAT3 pathway regulates lung-derived brain metastasis initiating cell capacity through miR-21 activation

Mohini Singh[1,4], Neha Garg[1,6], Chitra Venugopal[1,6], Robin Hallett[2], Tomas Tokar[7], Nicole McFarlane[1,6], Sujeivan Mahendram[1,6], David Bakhshinyan[1,4], Branavan Manoranjan[1,3,4], Parvez Vora[1,6], Maleeha Qazi[1,4], Carolynn C. Arpin[10], Brent Page[10], Sina Haftchenary[10], Aleksandra Todic[10], David A. Rosa[10], Ping-Shan Lai[10], Rodolfo Gómez-Biagi[10], Ahmed M. Ali[11], Andrew Lewis[10], Mulu Geletu[10], Naresh K. Murty[6] , John A. Hassell[1,2,4,5], Igor Jurisica[7,8,9], Patrick T. Gunning[10], Sheila K. Singh[1,4,6,a]

[1]McMaster Stem Cell and Cancer Research Institute, [2]McMaster Centre for Functional Genomics, McMaster University, Hamilton, Ontario, L8S 4K1, Canada

[3]Michael G. DeGroote School of Medicine, McMaster University, Hamilton, Ontario, L8S 4K1, Canada

Departments of [4]Biochemistry and Biomedical Sciences and [5]Pathology & Molecular Medicine, [6]Surgery, Faculty of Health Sciences, McMaster University, 1200 Main Street West, Hamilton, Ontario, L8N 3Z5, Canada

[7] Princess Margaret Cancer Centre, University Health Network, IBM Life Sciences Discovery Centre, Toronto Medical Discovery Tower, Toronto, Ontario M5G 1L7, [8]TECHNA Institute for the Advancement of Technology for Health, UHN and

[9]Departments of Medical Biophysics and Computer Science, University of Toronto, Canada.

[10]Department of Chemistry, University of Toronto, Mississauga, ON L5L 1C6, Canada

[11]Department of Medicinal Chemistry, Faculty of Pharmacy, Assiut University, Assiut, Egypt

[a]**Corresponding Author Contact Information:**

Sheila K. Singh MD PhD FRCS(C), MDCL 5027, McMaster University Stem Cell and Cancer Research Institute, 1280 Main Street West, Hamilton, ON, L8S 4K1, CANADA.

T: 905 521 2100 x75237 F: 905 521 9992 Email: ssingh@mcmaster.ca

Abstract

Brain metastases (BM) represent the most common tumor to affect the adult central nervous system. Despite the increasing incidence of BM, likely due to consistently improving treatment of primary cancers, BM remain severely understudied. In this study, we utilized patient-derived stem cell lines from lung-to-brain metastases to examine the regulatory role of STAT3 in brain metastasis initiating cells (BMICs). Annotation of our previously described BMIC regulatory genes with protein-protein interaction network mapping identified STAT3 as a novel protein interactor. STAT3 knockdown showed a reduction in BMIC self-renewal and migration, and decreased tumor size *in vivo*. Screening of BMIC lines with a library of STAT3 inhibitors identified one inhibitor to significantly reduce tumor formation. Meta-analysis identified the oncomir microRNA-21 (miR-21) as a target of STAT3 activity. Inhibition of miR-21 displayed similar reductions in BMIC self-renewal and migration as STAT3 knockdown. Knockdown of STAT3 also reduced expression of known downstream targets of miR-21. Our studies have thus identified STAT3 and miR-21 as cooperative regulators of stemness, migration and tumor initiation in lung-derived BM. Therefore, STAT3 represents a potential therapeutic target in the treatment of lung-to-brain metastases.

Keywords: brain metastases, brain metastasis initiating cell; STAT3; miR-21

Introduction

Metastases are the most common neoplasm to affect the adult central nervous system, occurring at a rate ten times greater than that of primary neural cancers(Lu-Emerson & Eichler, 2012). Brain metastases (BM) occur late in the progression of the primary cancer, and are typically associated with poor patient prognosis and survival; even with multimodal treatment, survival is only 4-12 months(Eichler & Loeffler, 2007; Soffietti *et al.*, 2002). Lung cancer is the primary source for BM and accounts for 40-50% of cases, followed by breast cancer with 15-25% of cases, and melanoma with 5-20% of cases(Wilhelm *et al.*, 2014). An increase in the incidence of BM has been recently noted, the reasons for which remain unclear but may be associated with the constantly improving treatment of the primary cancer that allows resistant cells to escape to the brain as a sanctuary site(C. Palmieri *et al.*, 2012). The role of a subpopulation of cells capable of tumor formation, also known as tumor initiating cells or TICs, has been extensively studied and reported in several solid primary cancers including those of the brain(S. K. Singh *et al.*, 2004), breast(Al-Hajj *et al.*, 2003), colon(O'Brien *et al.*, 2007), and prostate(Collins *et al.*, 2005; Patrawala *et al.*, 2006). Our previous work(Nolte *et al.*, 2013) established the identification of TICs specifically in BM through intracranial xenotransplantation of BM from lung primary cancers. These cells exhibited properties similar to BTICs, and are indicative of a brain metastasis initiating cell (BMIC) population.

The metastatic progression of cancer involves several extremely complex but poorly understood stages. Identification and characterization of the pathways and molecules that regulate this process will thus be crucial to our understanding and subsequent treatment of

BM. Several genes have been implicated in the regulation of metastases. We have identified a list of candidate genes as being significantly overexpressed in BM, as compared to primary brain and lung tumors(Nolte *et al.*, 2013). A protein interaction network mapping of metastasis regulatory genes identified Signal Transducers and Activators of Transcription 3 (STAT3) as one of the key interactors of BM candidate genes.

The STAT family of transcription factors mediates cell communication and prompts a wide range of biological responses. Persistent activation of STAT3 has been observed in approximately 70% of cancers(Hodge *et al.*, 2005; Resemann *et al.*, 2014; H. Yu *et al.*, 2007) and is believed to regulate TIC activity(Sherry *et al.*, 2009). Inhibition of STAT3 has been validated *in vitro* and *in vivo* as a promising therapeutic avenue for cancer treatment, and several molecules have been identified to block STAT3 activation(Haftchenary *et al.*, 2013; Kamran *et al.*, 2013). Recent studies have implicated STAT3 as a vital regulator of microRNA (miRNA) expression, and subsequently the STAT3 signaling pathway is controlled by several specific miRNAs(Iliopoulos *et al.*, 2010; Loffler *et al.*, 2007; Rozovski *et al.*, 2013). miRNAs are a class of evolutionarily conserved non-coding RNA molecules(Bartel, 2004). miRNAs bind to the 3' UTR regions of target genes and suppress their expression at a post-transcriptional level, ultimately resulting in mRNA degradation or translational inhibition(Bartel, 2009). Iliopoulos *et al*.(Iliopoulos *et al.*, 2010) identified transcription of miR-21 and miR-181b to be activated by STAT3, which subsequently led to the induction of a stable transformed state in cancer cell lines. Rozovski *et al*. (Rozovski *et al.*, 2013) found the gene expression of several miRNAs, including miR-21, to be regulated by STAT3 in chronic lymphocytic leukemia cells. It was

Loffler and colleagues (Loffler *et al.*, 2007) who discovered two phylogenetically conserved STAT3 binding sites in miR-21 that regulate its oncogenic activity.

Though lung cancer is the most common source of BM, there is very little data supporting the role of STAT3 and miR-21 in BM progression. In this study we identify STAT3 as a key regulator of lung-to-brain metastases through interaction with miR-21. We demonstrate that STAT3 knockdown can reduce self-renewal, migration, and tumor formation of a TIC population in BM. Further studies reveal that STAT3 potentially exerts its activity through miR-21, possibly through regulation of downstream tumor suppressor genes. Our studies confirm the role of STAT3 in BM development, and suggest that STAT3 may be a therapeutic target in the treatment of the lung-to-brain metastatic process.

Results

BMIC lines exhibit stem cell properties

Brain metastasis initiating cells (BMICs) isolated from human primary lung-derived brain metastasis samples BT478 and BT530 were propagated as tumorspheres in tumor sphere medium (TSM). Both the cell lines were shown to possess self-renewal capacity and migratory potential as assessed by secondary sphere formation (Figure 1A) and zone exclusion assays, respectively. Both BMIC lines showed differential expression of surface markers such as CD133 and EpCAM, as analyzed by flow cytometry (Figure 1B). CD133 has been used to prospectively identify brain tumor initiating cells (BTICs)(S. K. Singh *et al.*, 2004) as well as cancer stem cell populations in other primary tumors(Tirino *et al.*, 2009; K. Zhang & Waxman, 2010). EpCAM is an epithelial cell marker overexpressed in carcinomas of various origins(Went *et al.*, 2004). The tumor-initiating capacity of both BMIC lines used in this study was assessed through intracranial injections into NOD-SCID mice (Figure 1C), where both BMIC lines were capable of tumor formation. Together these data confirm the presence of a TIC population in both BMIC lines tested.

STAT3 is a putative BMIC regulatory gene

BMIC regulatory genes identified from our previous work(Nolte *et al.*, 2013) were annotated with known and predicted physical protein interactions using I2D V2.3(Brown & Jurisica, 2007) and FpClass V1.0(Kotlyar *et al.*, 2014). We found that Activators of Transcription 3 (STAT3) was a novel and direct interactor in the BMIC regulatory network (Figure 2). STAT3 has already been shown to be persistently activated in a variety of

cancers, and is believed to regulate multiple cancer stem cell populations including those that may drive primary brain tumors such as glioblastoma. STAT3 is required for proliferation and maintenance of multi-potency in glioblastoma stem cells(Sherry *et al.*, 2009).

STAT3 functions to regulate self-renewal and tumorigenicity of BMICs

To interrogate the functional significance of STAT3 in lung-derived brain metastasis, we performed lentiviral-mediated shRNA vector knockdown (KD) of STAT3 in BMIC lines. Scrambled shRNA (shControl) served as a control. The efficiency of STAT3 KD was validated at transcript (Figure 3A) and protein levels including the active phosphoform (Figure 3B) by RT-PCR and Western blotting respectively. shSTAT3-1 showed the most efficient KD and was chosen for further study. Knockdown of STAT3 corresponded with a reduction of BMIC self-renewal and migration, as seen with a decrease in sphere formation capacity (Figure 3C) and zone closure (Figure 3D). Furthermore, we also implemented *in vivo* studies in order to investigate the tumorigenic potential of STAT3 KD BMICs. We performed intracranial injections of BT478 into NODSCID mice brains and found that STAT3 KD formed tumors approximately 60% smaller than control tumors , which generated much larger and infiltrative tumors (Figure 4). Our data thus implicates STAT3 as an important regulator of self-renewal, migration and tumorigenicity in BMIC populations.

STAT3 inhibitors impede tumor formation in NOD-SCID xenograft model

BMIC line BT478 showed varied sensitivity to the STAT3 inhibitor library (Figure 5A), amongst which PG-S3-002 showed enhanced potency. To assess the clinical utility of STAT3 inhibitor PG-S3-002, BT478 was treated with PG-S3-002 at IC_{90} or DMSO after which $1x10^5$ viable cells, representing treatment-refractory BMICs, were injected intracranially into NOD-SCID mice. After 4 weeks, mice were sacrificed. PG-S3-002-treated cells reduced tumor formation by approximately 60% as compared to control tumors, which is similar to tumors formed by STAT3 KD (Figure 5B).

miR-21 as the target of STAT3

As previously described, miR 21 promoter has two putative STAT3 binding sites(Loffler *et al.*, 2007). Additionally, it has also been demonstrated that STAT3 directly binds to the miR21 promoter and modulates its expression(Iliopoulos *et al.*, 2010). Hence we wanted to explore the STAT3 and hsa-mir-21 regulatory network and identify its potential targets by collating data from four different TF databases and miRDip as described in the methods. We found that both molecules are strongly interrelated (Figure 6). The regulatory potential of both molecules exists through transcriptional regulatory relationships between their targets.

Inhibition of miR -21 reduces BMIC self-renewal and proliferation

To evaluate the functional significance of miR-21 in BMIC populations, cells were transfected with a miR-21 inhibitor (LNA miR-21) and scrambled LNA control. Knockdown of miR-21 as confirmed by RT-PCR (Figure 7A) resulted in reduced BMIC proliferation (Figure 7B), self-renewal (Figure 7C) and cell migration (Figure 7D).

miR-21 is overexpressed in lung cancer patients and predicts poor survival

Our observations suggesting that miR-21 regulated key biological characteristics of aggressive lung cancer samples prompted us to examine the expression of miR-21 in a large cohort of lung cancer patients. Briefly, we obtained gene expression profiling from 420-lung adenocarcinoma, and 18 normal lung samples, from the caner genome atlas (TCGA) lung project. Relative to normal lung, miR-21 was dramatically upregulated in lung adenocarcinoma (Figure 8A, *$p<0.0001$). Given that 214 of the tumor samples had clinically annotated outcome data, we also examined whether miR-21 expression was associated with patient survival. Using the mean expression level of miR-21 to stratify patients into miR-21 high and low expression groups, we observed that patients whose tumors had high miR-21 expression experienced substantially poorer overall survival than those whose tumors expressed low levels of miR-21 (Figure 8B, HR: 1.8, *$p=0.02$). Although the 5-year survival of the low expression group was 55%, the 5-year survival of the mir-21 high expression group was a dismal 25%. Additionally, we also validated the upregulation of mir-21 in lung cancer with 12 other miRNA profiling studies (Supplementary Table 5) and found that it is significantly upregulated compared to normal tissue. Overall, these data support our observations that miR-21 expression is associated with hyper-aggressive lung tumors, likely due to enhanced metastatic propensity.

STAT3 exerts its activity *via* miR-21 in BMIC cells

We observed that miR-21 transcript levels were downregulated in BMICs when STAT3 was knocked down (Figure 7E and F). Using results of meta-analysis of gene expression

profiles in NSCLC, we examined the expression status of STAT3/hsa-mir-21 targets. We found that the majority (232 out of 451) of transcriptional targets of STAT3 are consistently downregulated, despite expression of STAT3 itself remaining stable. At the same time, only 37 out of 289 targets of hsa-mir-21 are downregulated, despite the fact that hsa-mir-21 itself is consistently reported as highly upregulated in NSCLC (Supplementary Table 5). This allows us to hypothesize that elevated expression of hsa-mir-21, rather than causing detectable expression changes of its direct targets, decreases expression of certain transcription factors by disrupting their translation.

Therefore, to better understand the role of the STAT3-miR-21 network, we tested the potential downstream targets of miR-21 using a list of published genes in the literature (Supplementary Table 6) for various malignancies. We evaluated their transcript expression levels in shSTAT3 or shControl BMIC lines (Figure 8C and D). Genes significantly upregulated upon STAT3 knockdown were *SPRY2*, *TIMP3*, *PTEN* and *CDKN1A*. Intriguingly, we also found an inverse correlation of miR-21 with *SPRY2* and *TIMP3* (Figure 8E) in gene expression profiles of lung adenocarcinoma samples from TCGA, emphasizing the importance of studying STAT3-miR-21 interactions in BM.

Discussion

Metastases are the cause of 90% of all deaths from cancer(Yilmaz *et al.*, 2007), with metastasis to the brain occurring in approximately 20-40% of patients with systemic cancer(Nathoo *et al.*, 2005; Schouten *et al.*, 2002). Despite the known complexity of the metastatic process, there remains a lack of knowledge concerning the molecular mechanisms that govern BM formation. In the present study, we have implicated a regulatory pathway involving STAT3 control of miR-21 in the development of lung-to-brain metastasis (Figure 9). Several members of the family of STAT transcription factors regulate the expression of oncogenes and subsequently are key factors in the progression of many cancers(Klampfer, 2006).

Previous work in our lab has identified a TIC population in lung-to-brain metastases(Nolte *et al.*, 2013) and suggests the presence of a subgroup of cells capable of BM formation, termed BMICs. In this study we show that the STAT3 pathway is upregulated in these BMICs. To the best of our knowledge this is the first reported study that discovered the role of STAT3 in lung-to-brain metastasis using patient-derived BMICs and both *in vitro* and *in vivo* experimental approaches.

STAT3 regulates transcriptional activity in inflammation, cell proliferation, and stem cell maintenance(Darnell, 1997; Resemann *et al.*, 2014). Binding of cytokines to cell surface receptors initiates the activation of the Janus Kinase (JAK) pathway, which results in the downstream recruitment, phosphorylation, dimerization and translocation of STAT3 into the nucleus, whereupon STAT3 will go on to regulate the transcription of target protein-coding genes(Resemann *et al.*, 2014). STAT3 has been implicated in each step of the

metastatic process(Kamran *et al.*, 2013), in particular BM progression in melanoma(Xie *et al.*, 2006) and breast cancers(Chiu *et al.*, 2011).

The oncogenic potential of miR-21 has also been extensively studied in a variety of hematological malignancies and primary solid tumors (!!! INVALID CITATION !!!; Yan *et al.*, 2008) and it may represent a promising therapeutic target for patients with advanced-stage cancers. Although some studies show that miR-21 regulates metastasis in breast cancer (Schramedei *et al.*, 2011; Yan *et al.*, 2008), prostate cancer (Schramedei *et al.*, 2011), colorectal cancer(Asangani *et al.*, 2008) and melanoma(Yang *et al.*, 2011), the role of miR-21 in lung metastasis is still unclear. STAT3 directly activates transcription of miR-21, as previously shown in breast cancer studies(Iliopoulos *et al.*, 2010), and newly shown in BM in the current study.

Therapies affecting both self-renewal and migration would likely succeed in blocking the metastatic process. Knocking down miR-21 leads to decreased migration potential of BMICs (Figure 7), suggesting that miR21 promotes brain metastatic potential. Additionally, we propose that miR-21 protects BMICs from apoptosis, regulates invasion by controlling matrix metalloproteinase inhibition and promotes cell proliferation by regulating genes such as *SPRY2*, *TIMP3*, *CDKN1A*, *SERPINB5* and *PTEN*. These, together with other analyzed genes, have already been demonstrated as targets of miR-21 in a variety of cancers(Asangani *et al.*, 2008; Buscaglia & Li, 2011; Orvis *et al.*, 2014; Schramedei *et al.*, 2011; Yan *et al.*, 2008; Zhu *et al.*, 2008). Although *HNRPK*, *SPRY1*, *RHOB*, *RECK* and *BTG2* are reported to be regulated by miR-21, we did not observe any significant effect on these genes in BMICs. These findings are suggestive of many

additional molecular mechanisms downstream of miR-21 and STAT3 that operate at different stages of the metastatic process, in keeping with the nature of miRNAs to target over 100 genes in different cellular systems(Brennecke *et al.*, 2005). These mechanisms support miR-21 targeting as a potentially effective strategy to block tumor metastasis.

As shown in Figure 6, STAT3 was found to be a direct target of hsa-mir-21. At the same time, the hsa-mir-21 precursor gene is targeted by TFAP2C, which is a target of transcriptional control of STAT3. TFAP2C also targets the closely related gene *VMP1*, downstream of which this precursor gene is located(Ribas *et al.*, 2012). Although targets of STAT3-mediated transcriptional control overlap only slightly with those of hsa-mir-21, STAT3 and hsa-mir-21 form an interesting negative feedback loop. In addition, PG-S3-002 appears to be a most effective STAT3 inhibitor, likely due to greater cell penetrating properties, metabolic resistance, and resultant availability to interact with the target.

Conclusion

Our study suggests that STAT3 and miR-21 coordinately regulate the metastatic behavior of BMICs by promoting migration and self-renewal of tumor stem cell populations, tumor cell proliferation, survival and migration. Blocking the STAT3-miR-21 pathway could form a strong rationale for a novel therapeutic approach in patients with lung-to-brain metastasis.

Materials and Methods

Primary Tumorsphere Culture

Lung derived brain metastasis samples were obtained from consenting patients, as approved by the Research Ethics Board at Hamilton Health Sciences. Tumors were washed, acutely dissociated in artificial cerebrospinal fluid and subject to enzymatic dissociation as described previously(Venugopal *et al.*, 2012). BMICs were then resuspended TSM consisting of DMEM F-12 (Life Technologies), human recombinant EGF (20 ng/mL; Sigma), bFGF (20 ng/ml; Upstate), leukemia inhibitor factor (10 ng/mL; Chemicon), Neuronal Survival Factor (NSF) (1x; Clonetics), N-acetylcysteine (60 µg/mL; Sigma; and antibiotic antimycotic solution (Wisent). BMICs were maintained in TSM at 37 °C with a humidified atmosphere of 5% CO2. Of the two BMIC lines developed only BT478 was used to continue in depth *in vivo* experiments due to its high rate of engraftment.

Flow Cytometric Analysis

BMICs were dissociated to single cell suspension and adjusted to 1 million single cells/mL in PBS+2mM EDTA, labelled with anti-CD133, EpCAM, or a matched isotype control, and incubated for 30 min on ice (see Supplementary Table 1). Samples were analyzed using a MoFlo XDP Cell Sorter and Kaluza software (Beckman Coulter). Dead cells were excluded with 7-AAD viability dye. Compensation was performed by using mouse IgG CompBeads

Protein-protein interaction network

BMIC regulatory genes were mapped to proteins and their direct physical interactions were identified using I2D V2.3(Brown & Jurisica, 2005, 2007) and FpClass V1.0 (http://ophid.utoronto.ca/fpclass; (Kotlyar *et al.*, 2014). Protein-protein interaction network was visualized using NAViGaTOR version 2.3.1(Brown *et al.*, 2009; Pastrello *et al.*, 2013).

Lentivirus preparation and Transduction

shSTAT3 lentiviral vectors shSTAT3-1 and shSTAT3-2 with mature antisense sequence TGCATGTCTCCTTGACTCT and TACCTAAGGCCATGAACTT respectively, and a control scrambled shRNA vector were purchased from Thermo Scientific. Replication-incompetent lentivirus was produced by cotransfection of the expression vector and virapower packaging mix (Invitrogen) in HEK 293FT cells. Viral supernatant was harvested 48 hours post-transfection and filtered through a 0.45 μm cellulose acetate filter and precipitated by PEGit as recommended by the manufacturer (System Biosciences). The viral pellet was resuspended in 1.0 mL of DMEM F-12 media (Life Technologies) and stored at -80°C. BMIC lines were transduced with lentiviral vectors and treated with puromycin after 48 hours of transduction to develop stable shSTAT-3 lines.

Reverse transcription and quantitative PCR of mRNA and mature miRNA

For both mRNA and miRNA quantification, total RNA was isolated using Norgen RNA extraction kit (Norgen Biotek). For mRNA analysis, total RNA was reverse transcribed using qScript cDNA Super Mix (Quanta Biosciences) and a C1000 Thermo Cycler (Bio-Rad). qRT-PCR was performed using the Cfx96 (Bio-Rad) with SsoAdvanced SYBR

Green (Bio-Rad) using gene specific primers (Supplementary Table 2). Data is presented as the ratio of the gene of interest to GAPDH as control.

For miRNA analysis, total RNA was reverse transcribed using Taqman MicroRNA Reverse Transcription kit (Applied Biosytems) as described previously(Garg *et al.*, 2013). qRT–PCR analysis was performed using TaqMan probes of miR-21-5p (Assay ID:000397), U6snRNA (Assay ID:001973) and Taqman Universal Master Mix II, (Catalog No. 4440040) according to manufacturer's instructions (Applied Biosystems/LifeTech). miRNA quantification was expressed, in arbitrary units, as the ratio of the sample quantity to the calibrator. U6snRNA was used as an internal control.

Western Immunoblotting

30μg of denatured protein per sample was loaded and resolved on SDS polyacrylamide gel, followed by electrotransfer onto PVDF membrane. Membranes were blocked with 3% BSA in 1xTBS (for phosphorylated proteins) and 3% non-fat dry milk in 1xTBS (for normal proteins), incubated with primary antibody at 4^{o}C overnight, then washed and hybridized with peroxidase-conjugated secondary antibodies for 1 hour at room temperature. Protein was detected using Chemidoc. Primary antibodies used were as follows: anti-STAT3 (1:1000; mouse IgG2a; Cell Signaling#9139), anti-phosphorylated STAT3 (mouse IgG1; 1:1000; Cell Signaling#4113), anti-GAPDH (mouse; 1:40,000; Abcam#ab8245). The secondary antibodies were horseradish peroxidase-conjugated goat anti-mouse IgG (Bio-Rad) or goat anti-rabbit IgG (Sigma).

Secondary Sphere formation Assay

After primary sphere formation was noted, spheres were dissociated to single cells and replated in TSM as previously described(S. K. Singh *et al.*, 2003). Stem cell frequency was quantified by calculating the rate of secondary sphere formation from 200 dissociated single cells.

Zone Exclusion Migration Assay

BMIC spheres were dissociated to single cells and replated at a density of 30,000 cells per well in a 96 well plate TSM containing 1% FBS and a 1% agar drop in the center of the well. After 24 hours to allow cell adherence, the agar drop was removed, the wells washed gently with PBS to remove floating cells, and media replaced with TSM. Migration into the empty zone was monitored over 3 days, with time points taken at day 0 and day 3.

Cell proliferation assay

Single cells were plated in a 96-well plate at a density of 1,000 cells/200 µL per well in quadruplicate and incubated for five days. 20 µL of Presto Blue (Invitrogen), a fluorescent cell metabolism indicator, was added to each well approximately 4h prior to the readout time point. Fluorescence was measured using a FLUOstar Omega Fluorescence 556 Microplate reader (BMG LABTECH) at excitation and emission wavelengths of 535 nm and 600 nm respectively. Readings were analyzed using Omega analysis software.

***In vivo* BMIC intracranial injections and H&E staining of xenograft tumors**

All experimental procedures involving animals were reviewed and approved by the Animal Research Ethics Board (AREB). Intracranial injections were performed as previously

described(S. K. Singh *et al.*, 2004). Briefly, 10μL of cell suspension was injected into the right frontal lobe of 8-10 week old NOD/SCID mice (n=3). Mice were monitored weekly for signs of illness, and upon reaching endpoint, brains were harvested and embedded in paraffin for hematoxylin and eosin (H&E) staining. Images were scanned using an Aperio Slide Scanner and analyzed by ImageScope v11.1.2.760 software (Aperio).

Screening and *Ex Vivo* treatment of BMICs with STAT3 inhibitors

A library of known direct-binding STAT3 inhibitors (BP-1-102(Page *et al.*, 2011), BP-5-087(Eiring *et al.*, 2014), PG-S3-002, and PG-S3-004; Supplementary Figure 1) was provided by Dr. Patrick Gunning (University of Toronto, Mississauga campus). BMIC line BT478 was treated with log dilutions of the inhibitors and IC_{50} values determined by assessing cell proliferation. Compounds with IC_{50} values of <2μM, specifically PG-S3-002 were further assessed for inhibition of BT478 tumor formation. BMIC cells were dissociated to singles cells and 1,000,000 cells replated in TSM. Cells were treated with either PG-S3-002 IC_{90} or DMSO for 4 days, harvested, and injected intracranially into NOD/SCID mice (n=3). Mice were sacrificed at 4 weeks and the brains harvested and embedded in paraffin for H&E staining.

Meta-analysis of gene-expression profiles in NSCLC

We analyzed 12 publicly available NSCLC gene expression datasets (Supplementary Table 3), originally from studies on tissue samples obtained from surgically resected human lung tumors and containing at least one sample of noncancerous normal tissue for comparison. To enable uniform processing and analysis of all the datasets and thus to improve

comparability of results, we chose only datasets that were produced by using Affymetrix platforms. Each of the datasets was first separately normalized and summarized using Bioconductor project's package gcrma (GeneChip Robust Multiarray Averaging)(Z. Wu & Irizarry, 2004). For the each individual dataset, we then evaluated differential expression of the genes using Bioconductor's limma package(GK, 2005). Based on expression fold change, genes were classified as either up- or downregulated, and then ranked according to statistical significance, which was evaluated by q-value (adjusted p-value). Analyzing 12 datasets we thus obtained 22 different rankings, 11 rankings for upregulated genes and 11 for downregulated ones. To identify consistently deregulated genes obtained rankings were subjected to robust rank aggregation analysis implemented as an R package RobustRankAggreg(Kolde *et al.*, 2012). This analysis detects genes which are ranked consistently better than expected under a null hypothesis of uncorrelated inputs and assigns a p-value as a significance score for each gene. The stability of resulting significance scores was then assessed by the leave-one-out validation, in which the same analysis was repeated 11 times, each time excluding one of the rankings. Acquired p-values from each round were finally averaged into corrected p-value. Genes whose significance score was greater than chosen threshold ($p < 0.05$) were further considered as consistently deregulated genes.

Assembly of the STAT3- hsa-mir-21 regulatory network

Both STAT3 and hsa-mir-21 are very potent regulators of expression targeting wide range of genes. To identify their targets and relationships among them, we collated data from multiple independent sources. Knowledge of human transcription factors (TF) and their respective targets was obtained from four different databases, namely: ChEA (ChIP

Enrichment Analysis) database(Lachmann *et al.*, 2010), ITFP(G. Zheng *et al.*, 2008) (Integrated Transcription Factor Platform), PAZAR (Portales-Casamar *et al.*, 2009), TRED(Jiang *et al.*, 2007) (Transcriptional Regulatory Element Database). These data were either downloaded as a flat file (ITFP, PAZAR), manually collected (ITFP), or acquired from the web-based interactive application (ChEA). Additional data were obtained from lists of TF:target pairs from human fetal lung provided by Neph *et al*. (Neph *et al.*, 2012). Names of TFs and their respective targets as obtained from these databases were first standardized according to HGNC symbol checker [http://www.genenames.org/cgi-bin/symbol_checker] and then concatenated into the single list comprising all the unique TF:target pairs. We used mirDIP(Shirdel *et al.*, 2011) (microRNA Data Integration Portal, version 2.0) to acquire a list of targets of hsa-mir-21. In our search we considered only miRNA–target relationships which fall among the top third of the most plausible predictions from at least three different databases. HGNC symbol checker then standardized names of the targeted genes. As a result we obtained a network comprising STAT3- hsa-mir-21 and their targets represented by nodes, and regulatory relationships between these as edges.

In silico analysis of miR 21 in lung adenocarcinoma

Patients and Samples: All TCGA data was obtained through the TCGA data portal (https://tcga-data.nci.nih.gov/tcga/) on September 15th 2014. Level 3 gene or miRNA expression data, as well as de-identified patient clinical data, was used for our analysis.

miR-21 co-expression data: We calculated Pearson distance between miR-21 and all the Genes/miRNAs to identify features that were inversely co-expressed with miRNA-21 in lung adenocarcinoma samples. The top 250 inversely co-expressed genes/miRNAs are included as Supplementary table 4.

Survival analysis: Survival analysis was completed in R and survival curves were graphed using Graphpad Prism 5.

miR-21 knockdown

Antagomir mediated miRNA knockdown was carried out using LNA oligonucleotides (Life technologies, Applied Biosytems) as described previously(Garg *et al.*, 2013). Hsa-miR-21-5p (Assay ID: MH10206) or scrambled miRVana miRNA inhibitor negative control #1 (Catalog# 4464076) was transfected into BMIC line BT478 at a final concentration of 50nM using Lipofectamine 2000. After 48 hours, miR-21 expression levels were determined by qRT-PCR, relative to a U6 internal control.

Statistical analysis

Replicates from at least three samples were compiled for each experiment, unless otherwise specified in figure legends. Respective data represent mean±SD with n values listed in figure legends. Student's *t-test* analyses and 2-way *ANOVA* analysis were performed using GraphPad Prism 5. $P<0.05$ was considered significant.

Author Contributions

Mohini Singh, Neha Garg: Conception and design, Collection and/or assembly of data, Data analysis and interpretation, Manuscript writing, Final approval of manuscript

Chitra Venugopal, Robin Hallett, Tomas Tokar: Design, Collection and/or assembly of data, manuscript writing, Final approval of manuscript

Nicole McFarlane, Carolynn Arpin, Brent Page, Sina Haftchenary, David Rosa, Ping-Shan Lai, Rodolfo Gómez-Biagi, Ahmed Ali Andrew Lewis, Mulu Geletu:Sujeivan Mahendram, David Bakhshinyan, Branavan Manoranjan, Parvez Vora, Maleeha Qazi: Collection and/or assembly of data, Final approval of manuscript

Naresh Murty: Provision of study material, Final approval of manuscript

John A. Hassell, Igor Jurisica, and Patrick T. Gunning: Conception and design, Data analysis and interpretation, Final approval of manuscript

Sheila K. Singh: Conception and design, Data analysis and interpretation, Manuscript writing, Final approval of manuscript

Funding: This work was supported by funds from the Department of Surgery at McMaster University, Stem Cell Network Drug Discovery Grant, Ontario Institute for Cancer Research Cancer Stem Cell Program, a Canadian Cancer Society Research Institute Innovation Grant for Dr. Sheila Singh; Brain Canada PhD Studentship for Mohini Singh; Ontario Research Fund (GL2-01-030), McLaughlin Centre Accelerator grant (#MC-2013-05) and Canada Foundation for Innovation (CFI #12301, #203373, #29272, #225404, #30865) supported Dr. Igor Jurisica. Dr. Patrick T. Gunning research was funded by the Alberta Innovates, Stem Cell Network, and CIHR and CFI.

Conflict of interest: The authors declare no conflict of interest.

[a]**Corresponding Authors:**

Sheila K. Singh MD PhD FRCS(C), MDCL 5027, McMaster University Stem Cell and Cancer Research Institute, 1280 Main Street West, Hamilton, ON, L8S 4K1, CANADA.

T: 905 521 2100 x75237 F: 905 521 9992 Email: ssingh@mcmaster.ca

References

1. Lu-Emerson C and Eichler AF. Brain metastases. Continuum (Minneap Minn). 2012; 18(2):295-311.

2. Eichler AF and Loeffler JS. Multidisciplinary management of brain metastases. Oncologist. 2007; 12(7):884-898.

3. Soffietti R, Ruda R and Mutani R. Management of brain metastases. J Neurol. 2002; 249(10):1357-1369.

4. Wilhelm I, Fazakas C, Molnar J, Hasko J, Vegh AG, Cervenak L, Nagyoszi P, Nyul-Toth A, Farkas AE, Bauer H, Guillemin GJ, Bauer HC, Varo G and Krizbai IA. Role of Rho/ROCK signaling in the interaction of melanoma cells with the blood-brain barrier. Pigment Cell Melanoma Res. 2014; 27(1):113-123.

5. Palmieri C, Monteverde M, Lattanzio L, Gojis O, Rudraraju B, Fortunato M, Syed N, Thompson A, Garrone O, Merlano M, Lo Nigro C and Crook T. Site-specific CpG methylation in the CCAAT/enhancer binding protein delta (CEBPdelta) CpG island in breast cancer is associated with metastatic relapse. Br J Cancer. 2012; 107(4):732-738.

6. Singh SK, Hawkins C, Clarke ID, Squire JA, Bayani J, Hide T, Henkelman RM, Cusimano MD and Dirks PB. Identification of human brain tumor initiating cells. Nature. 2004; 432(7015):396-401.

7. Al-Hajj M, Wicha MS, Benito-Hernandez A, Morrison SJ and Clarke MF. Prospective identification of tumorigenic breast cancer cells. Proceedings of the National Academy of Sciences of the United States of America. 2003; 100(7):3983-3988.

8. O'Brien CA, Pollett A, Gallinger S and Dick JE. A human colon cancer cell capable of initiating tumor growth in immunodeficient mice. Nature. 2007; 445(7123):106-110.

9. Patrawala L, Calhoun T, Schneider-Broussard R, Li H, Bhatia B, Tang S, Reilly JG, Chandra D, Zhou J, Claypool K, Coghlan L and Tang DG. Highly purified CD44+ prostate cancer cells from xenograft human tumors are enriched in tumorigenic and metastatic progenitor cells. Oncogene. 2006; 25(12):1696-1708.

10. Collins AT, Berry PA, Hyde C, Stower MJ and Maitland NJ. Prospective identification of tumorigenic prostate cancer stem cells. Cancer research. 2005; 65(23):10946-10951.

11. Nolte SM, Venugopal C, McFarlane N, Morozova O, Hallett RM, O'Farrell E, Manoranjan B, Murty NK, Klurfan P, Kachur E, Provias JP, Farrokhyar F, Hassell JA, Marra M and Singh SK. A cancer stem cell model for studying brain metastases from primary lung cancer. J Natl Cancer Inst. 2013; 105(8):551-562.

12. Resemann HK, Watson CJ and Lloyd-Lewis B. The Stat3 paradox: a killer and an oncogene. Mol Cell Endocrinol. 2014; 382(1):603-611.

13. Yu H, Kortylewski M and Pardoll D. Crosstalk between cancer and immune cells: role of STAT3 in the tumor microenvironment. Nature reviews Immunology. 2007; 7(1):41-51.

14. Hodge DR, Hurt EM and Farrar WL. The role of IL-6 and STAT3 in inflammation and cancer. European journal of cancer. 2005; 41(16):2502-2512.

15. Sherry MM, Reeves A, Wu JK and Cochran BH. STAT3 is required for proliferation and maintenance of multipotency in glioblastoma stem cells. Stem cells. 2009; 27(10):2383-2392.

16. Kamran MZ, Patil P and Gude RP. Role of STAT3 in cancer metastasis and translational advances. Biomed Res Int. 2013; 2013:421821.

17. Haftchenary S, Luchman HA, Jouk AO, Veloso AJ, Page BD, Cheng XR, Dawson SS, Grinshtein N, Shahani VM, Kerman K, Kaplan DR, Griffin C, Aman AM, Al-Awar R, Weiss S and Gunning PT. Potent Targeting of the STAT3 Protein in Brain Cancer Stem Cells: A Promising Route for Treating Glioblastoma. ACS Med Chem Lett. 2013; 4(11):1102-1107.

18. Iliopoulos D, Jaeger SA, Hirsch HA, Bulyk ML and Struhl K. STAT3 activation of miR-21 and miR-181b-1 via PTEN and CYLD are part of the epigenetic switch linking inflammation to cancer. Molecular cell. 2010; 39(4):493-506.

19. Rozovski U, Calin GA, Setoyama T, D'Abundo L, Harris DM, Li P, Liu Z, Grgurevic S, Ferrajoli A, Faderl S, Burger JA, O'Brien S, Wierda WG, Keating MJ and Estrov Z. Signal transducer and activator of transcription (STAT)-3 regulates microRNA gene expression in chronic lymphocytic leukemia cells. Molecular cancer. 2013; 12:50.

20. Loffler D, Brocke-Heidrich K, Pfeifer G, Stocsits C, Hackermuller J, Kretzschmar AK, Burger R, Gramatzki M, Blumert C, Bauer K, Cvijic H, Ullmann AK, Stadler PF and Horn F. Interleukin-6 dependent survival of multiple myeloma cells involves the Stat3-mediated induction of microRNA-21 through a highly conserved enhancer. Blood. 2007; 110(4):1330-1333.

21. Bartel DP. MicroRNAs: genomics, biogenesis, mechanism, and function. Cell. 2004; 116(2):281-297.

22. Bartel DP. MicroRNAs: target recognition and regulatory functions. Cell. 2009; 136(2):215-233.

23. . !!! INVALID CITATION !!!

24. Tirino V, Camerlingo R, Franco R, Malanga D, La Rocca A, Viglietto G, Rocco G and Pirozzi G. The role of CD133 in the identification and characterisation of tumor-initiating cells in non-small-cell lung cancer. European journal of cardio-thoracic surgery : official journal of the European Association for Cardio-thoracic Surgery. 2009; 36(3):446-453.

25. Zhang K and Waxman DJ. PC3 prostate tumor-initiating cells with molecular profile FAM65Bhigh/MFI2low/LEF1low increase tumor angiogenesis. Molecular cancer. 2010; 9:319.

26. Went PTH, Lugli A, Meier S, Bundi M, Mirlacher M, Sauter G and Dirnhofer S. Frequent EpCam protein expression in human carcinomas. Human Pathology. 2004; 35(1):122-128.

27. Brown KR and Jurisica I. Unequal evolutionary conservation of human protein interactions in interologous networks. Genome biology. 2007; 8(5):R95.

28. Kotlyar M, Pastrello C, Pivetta F, Lo Sardo A, Cumbaa C, Li H, Naranian T, Niu Y, Ding Z, Vafaee F, Broackes-Carter F, Petschnigg J, Mills GB, Jurisicova A, Stagljar I, Mills GB, et al. In silico prediction of physical protein interactions and characterization of interactome orphans. Nature methods. 2014.

29. Yilmaz M, Christofori G and Lehembre F. Distinct mechanisms of tumor invasion and metastasis. Trends Mol Med. 2007; 13(12):535-541.

30. Nathoo N, Chahlavi A, Barnett GH and Toms SA. Pathobiology of brain metastases. J Clin Pathol. 2005; 58(3):237-242.

31. Schouten LJ, Rutten J, Huveneers HA and Twijnstra A. Incidence of brain metastases in a cohort of patients with carcinoma of the breast, colon, kidney, and lung and melanoma. Cancer. 2002; 94(10):2698-2705.

32. Klampfer L. Signal transducers and activators of transcription (STATs): Novel targets of chemopreventive and chemotherapeutic drugs. Curr Cancer Drug Targets. 2006; 6(2):107-121.

33. Darnell JE, Jr. STATs and gene regulation. Science. 1997; 277(5332):1630-1635.

34. Xie TX, Huang FJ, Aldape KD, Kang SH, Liu M, Gershenwald JE, Xie K, Sawaya R and Huang S. Activation of stat3 in human melanoma promotes brain metastasis. Cancer research. 2006; 66(6):3188-3196.

35. Chiu WT, Lee HT, Huang FJ, Aldape KD, Yao J, Steeg PS, Chou CY, Lu Z, Xie K and Huang S. Caveolin-1 upregulation mediates suppression of primary breast tumor growth and brain metastases by stat3 inhibition. Cancer research. 2011; 71(14):4932-4943.

36. Yan LX, Huang XF, Shao Q, Huang MY, Deng L, Wu QL, Zeng YX and Shao JY. MicroRNA miR-21 overexpression in human breast cancer is associated with advanced clinical stage, lymph node metastasis and patient poor prognosis. RNA. 2008; 14(11):2348-2360.

37. Schramedei K, Morbt N, Pfeifer G, Lauter J, Rosolowski M, Tomm JM, von Bergen M, Horn F and Brocke-Heidrich K. MicroRNA-21 targets tumor suppressor genes ANP32A and SMARCA4. Oncogene. 2011; 30(26):2975-2985.

38. Asangani IA, Rasheed SA, Nikolova DA, Leupold JH, Colburn NH, Post S and Allgayer H. MicroRNA-21 (miR-21) post-transcriptionally downregulates tumor suppressor Pdcd4 and stimulates invasion, intravasation and metastasis in colorectal cancer. Oncogene. 2008; 27(15):2128-2136.

39. Yang CH, Yue J, Pfeffer SR, Handorf CR and Pfeffer LM. MicroRNA miR-21 regulates the metastatic behavior of B16 melanoma cells. J Biol Chem. 2011; 286(45):39172-39178.

40. Zhu S, Wu H, Wu F, Nie D, Sheng S and Mo YY. MicroRNA-21 targets tumor suppressor genes in invasion and metastasis. Cell Res. 2008; 18(3):350-359.

41. Orvis T, Hepperla A, Walter V, Song S, Simon J, Parker J, Wilkerson MD, Desai N, Major MB, Hayes DN, Davis IJ and Weissman B. BRG1/SMARCA4 Inactivation Promotes Non-Small Cell Lung Cancer Aggressiveness by Altering Chromatin Organization. Cancer research. 2014; 74(22):6486-6498.

42. Buscaglia LE and Li Y. Apoptosis and the target genes of microRNA-21. Chin J Cancer. 2011; 30(6):371-380.

43. Brennecke J, Stark A, Russell RB and Cohen SM. Principles of microRNA-target recognition. PLoS Biol. 2005; 3(3):e85.

44. Ribas J, Ni X, Castanares M, Liu MM, Esopi D, Yegnasubramanian S, Rodriguez R, Mendell JT and Lupold SE. A novel source for miR-21 expression through the alternative polyadenylation of VMP1 gene transcripts. Nucleic acids research. 2012; 40(14):6821-6833.

45. Venugopal C, McFarlane NM, Nolte S, Manoranjan B and Singh SK. Processing of primary brain tumor tissue for stem cell assays and flow sorting. J Vis Exp. 2012; (67).

46. Brown KR and Jurisica I. Online predicted human interaction database. Bioinformatics. 2005; 21(9):2076-2082.

47. Brown KR, Otasek D, Ali M, McGuffin MJ, Xie W, Devani B, Toch IL and Jurisica I. NAViGaTOR: Network Analysis, Visualization and Graphing Toronto. Bioinformatics. 2009; 25(24):3327-3329.

48. Pastrello C, Otasek D, Fortney K, Agapito G, Cannataro M, Shirdel E and Jurisica I. Visual data mining of biological networks: one size does not fit all. PLoS Comput Biol. 2013; 9(1):e1002833.

49. Garg N, Po A, Miele E, Campese AF, Begalli F, Silvano M, Infante P, Capalbo C, De Smaele E, Canettieri G, Di Marcotullio L, Screpanti I, Ferretti E and Gulino A. microRNA-17-92 cluster is a direct Nanog target and controls neural stem cell through Trp53inp1. EMBO J. 2013; 32(21):2819-2832.

50. Singh SK, Clarke ID, Terasaki M, Bonn VE, Hawkins C, Squire J and Dirks PB. Identification of a cancer stem cell in human brain tumors. Cancer research. 2003; 63(18):5821-5828.

51. Page BD, Fletcher S, Yue P, Li Z, Zhang X, Sharmeen S, Datti A, Wrana JL, Trudel S, Schimmer AD, Turkson J and Gunning PT. Identification of a non-phosphorylated, cell permeable, small molecule ligand for the Stat3 SH2 domain. Bioorganic & medicinal chemistry letters. 2011; 21(18):5605-5609.

52. Eiring AM, Page BD, Kraft IL, Mason CC, Vellore NA, Resetca D, Zabriskie MS, Zhang TY, Khorashad JS, Engar AJ, Reynolds KR, Anderson DJ, Senina A, Pomicter AD, Arpin CC, Ahmad S, et al. Combined STAT3 and BCR-ABL1 inhibition induces synthetic lethality in therapy-resistant chronic myeloid leukemia. Leukemia. 2014.

53. Wu Z and Irizarry RA. Preprocessing of oligonucleotide array data. Nat Biotechnol. 2004; 22(6):656-658; author reply 658.

54. GK S. (2005). Limma: linear models for microarray data. In: Gentleman R CV, Huber W, Irizarry R, Dudoit S, ed. Bioinformatics and Computational Biology Solutions Using R and Bioconductor. (Mew York: Springer), pp. 397-420.

55. Kolde R, Laur S, Adler P and Vilo J. Robust rank aggregation for gene list integration and meta-analysis. Bioinformatics. 2012; 28(4):573-580.

56. Lachmann A, Xu H, Krishnan J, Berger SI, Mazloom AR and Ma'ayan A. ChEA: transcription factor regulation inferred from integrating genome-wide ChIP-X experiments. Bioinformatics. 2010; 26(19):2438-2444.

57. Zheng G, Tu K, Yang Q, Xiong Y, Wei C, Xie L, Zhu Y and Li Y. ITFP: an integrated platform of mammalian transcription factors. Bioinformatics. 2008; 24(20):2416-2417.

58. Portales-Casamar E, Arenillas D, Lim J, Swanson MI, Jiang S, McCallum A, Kirov S and Wasserman WW. The PAZAR database of gene regulatory information coupled to the ORCA toolkit for the study of regulatory sequences. Nucleic acids research. 2009; 37(Database issue):D54-60.

59. Jiang C, Xuan Z, Zhao F and Zhang MQ. TRED: a transcriptional regulatory element database, new entries and other development. Nucleic acids research. 2007; 35(Database issue):D137-140.

60. Neph S, Stergachis AB, Reynolds A, Sandstrom R, Borenstein E and Stamatoyannopoulos JA. Circuitry and dynamics of human transcription factor regulatory networks. Cell. 2012; 150(6):1274-1286.

61. Shirdel EA, Xie W, Mak TW and Jurisica I. NAViGaTing the micronome--using multiple microRNA prediction databases to identify signalling pathway-associated microRNAs. PLoS One. 2011; 6(2):e17429.

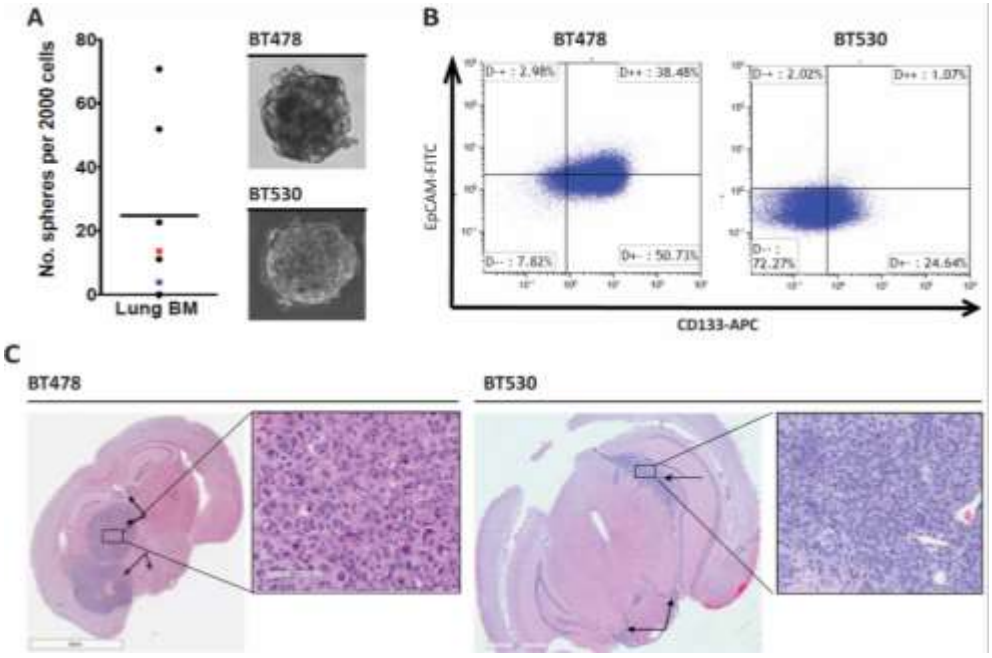

Figure 1. Brain metastases (BM) from the lung possess a cancer stem cell (CSC) population in vitro and possess tumor-initiating cell (TIC) populations in vivo. Patient-derived BM samples were grown as tumorspheres in tumor sphere media (TSM). A) Self-renewal, a hallmark of CSCs, was determined though assessment of secondary sphere-forming capacity. Each dot represents a single patient sample, coloured dots indicate samples which have developed into sustainable patient-derived cell lines (red, BT478; blue, BT530); bar indicates mean; insets are representative bright field images of spheres of BT478 and BT530. B) CSC marker CD133 and epithelial marker EpCAM expression was assessed by flow cytometry. C) NOD-SCID mice were used in all experiments; injected

cells were cultured as tumorspheres. TIC capacity is demonstrated through tumor growth in the brain, when injected intracranially (100,000 cells, n=5 for BT478, n=4 for BT530).

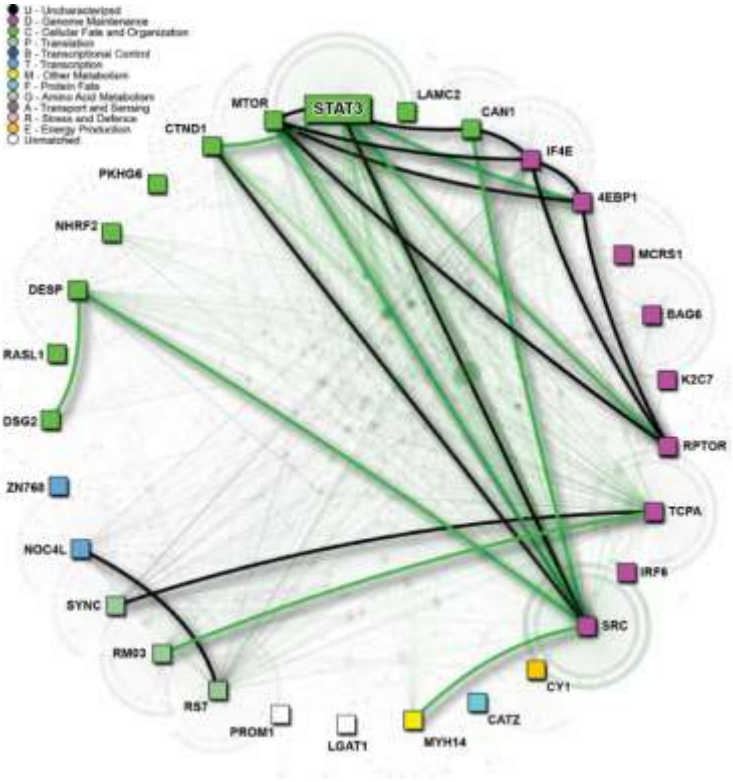

Figure 2. Protein connectivity mapping implicates STAT3 as a putative BMIC regulatory gene. Protein-protein interaction network of putative BMIC regulatory genes. Black lines represent known interactions; green lines signify predicted, and thus novel

interactions. Direct interactions among BMIC genes is highlighted by thicker edges. Gene Ontology (GO) biological function is represented by node color, as per legend.

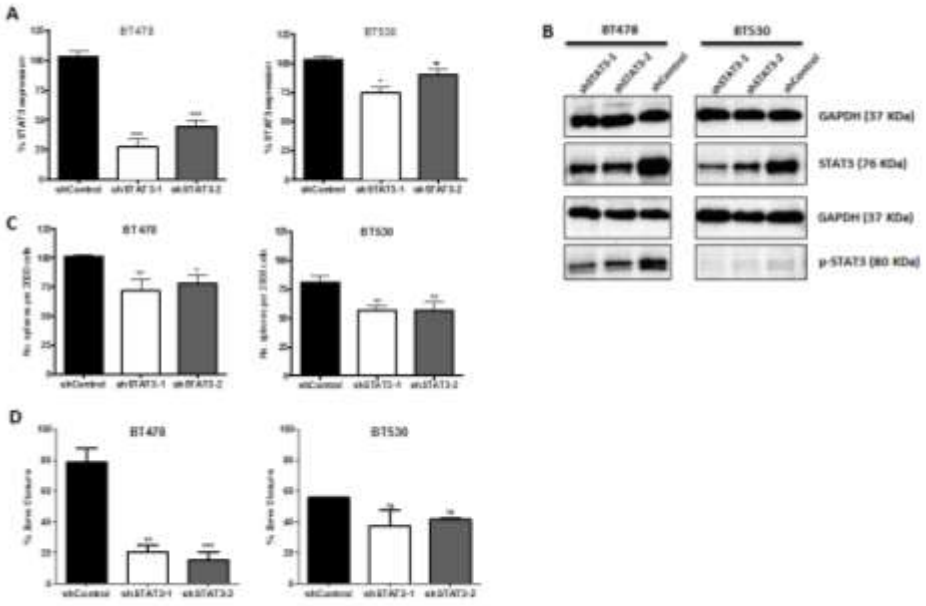

Figure 3. Knockdown of STAT3 demonstrates potential regulatory role in self-renewal and metastasis. Tumorspheres were transduced with short-hairpin lentiviral vectors against candidate BMIC regulatory gene STAT3. A) STAT3 transcript levels by qRT-PCR reveal significant knockdown in brain metastases achieved by two different shSTAT3 vectors as compared to the shControl. B) Protein levels of STAT3 and phosphorylated STAT3 in control and knockdown samples by Western blot, relative to a GAPDH control. C) Self-renewal was assessed through sphere formation per 2000 cells; knockdown of STAT3 corresponded with decreased sphere formation. D) Zone-exclusion assays showed decreased migratory capability with STAT3 knockdown. ns non-significant; *p<0.05; **p<0.01; ***p<0.001 (1-way ANOVA).

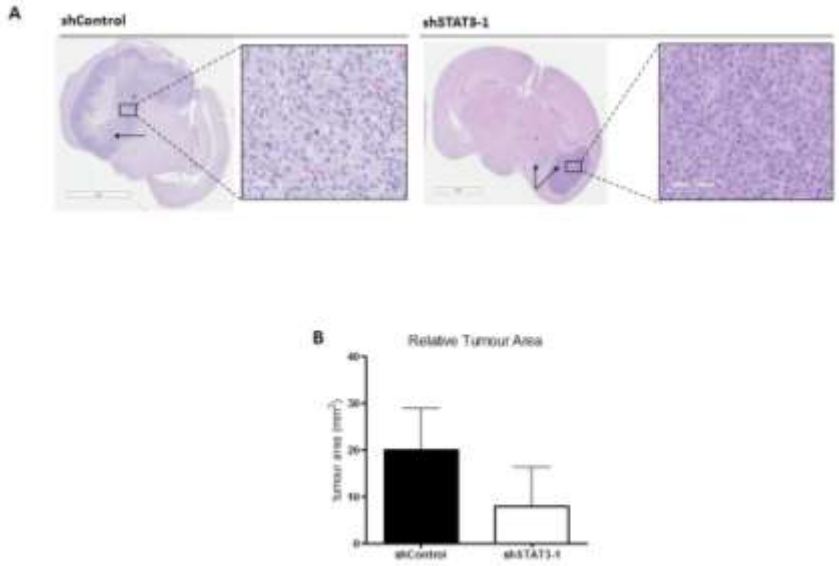

Figure 4. Knockdown of STAT3 demonstrates potential regulatory role in self-renewal and tumor formation. A) 100,000 cells of shSTAT3-1 or shControl were injected into the frontal lobes of NOD-SCID mice (n=3 in each group). Mice were sacrificed upon reaching endpoint. H&E sections of the brains are shown. shSTAT3 cells formed smaller tumors than shControls (arrows indicat tumors). B) shSTAT3-1 cells formed tumors approximately 60% smaller as compared to shControl mice. *$p<0.05$ (t test).

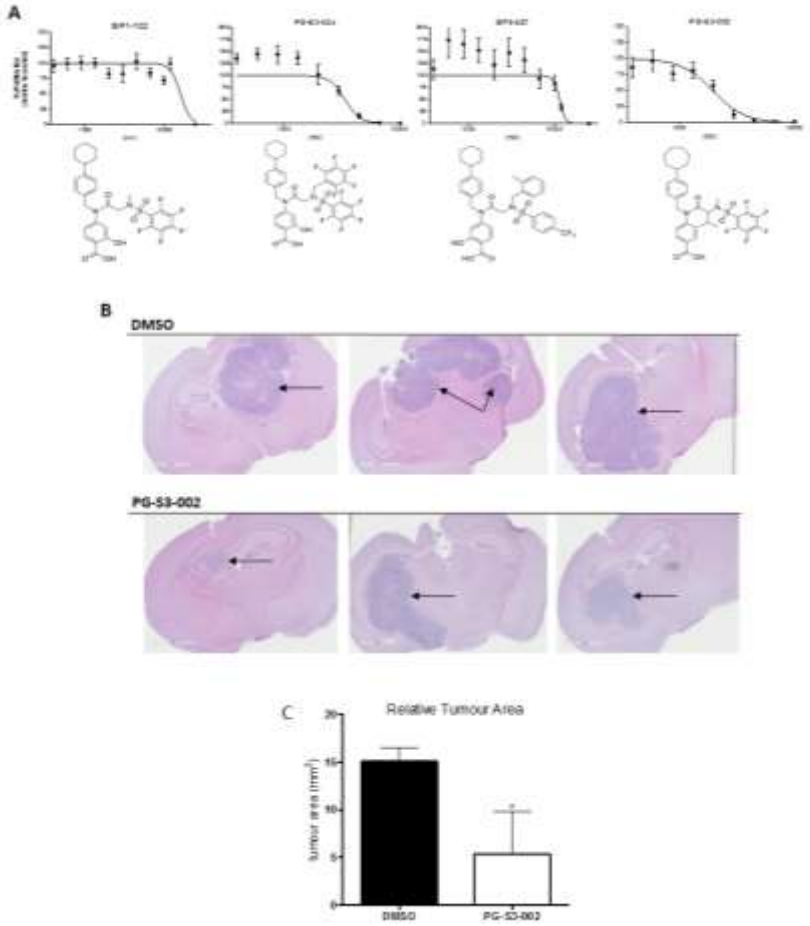

Figure 5. STAT3 inhibitors as candidate drugs for targeting tumor formation in brain metastases. A) IC50 curves of several STAT3 inhibitors, with associated structures, were generated using BT478 tumorsphere cells. B) BT478 tumorspheres were treated ex vivo with 6μM (IC90) PG-S3-002 or DMSO control for 4 days. 100,000 cells were injected into the frontal lobes of NOD-SCID mice (n=3 in each group). After 4 weeks, mice were sacrificed. H&E sections of the brains are shown PG-S3-002 treated cells formed smaller tumors than controls. C) Cells treated with PG-S3-002 showed approximately 60% reduction in tumor size as compared to tumors from DMSO treated cells *$p<0.05$ (t test).

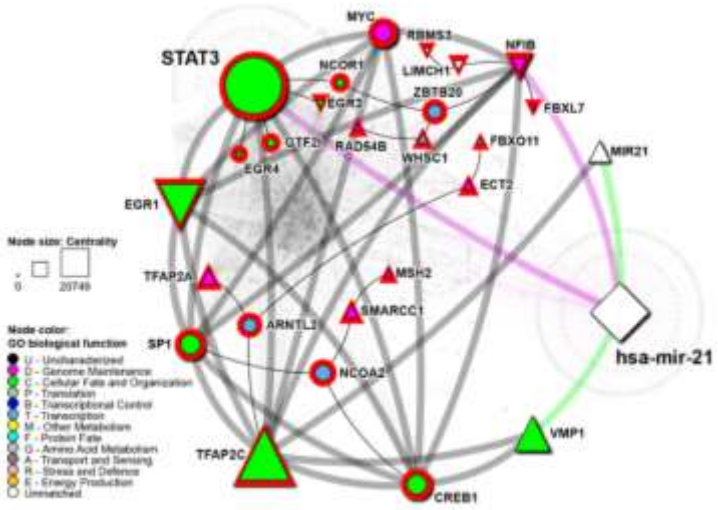

Figure 6. Network of STAT3 and hsa-mir-21 regulatory targets. STAT3, hsa-mir-21 and their regulatory targets are represented by nodes, while regulatory relationships among these are represented by edges. hsa-mir-21 is represented by white diamond. Genes are coloured according to their biological function. Green edges link hsa-mir-21 to its precursor mIR21 and related gene VMP1. Grey edges represent TF: target relationships, magenta edges represent hsa-mir-21:target relationships. Shape of the nodes denotes expression status of genes as comes from the meta-analysis of gene expression profiles in NSCLC. Downward oriented triangles denote downregulation, while those pointing up denote upregulation. Cycles denote no significant differential expression. Size of the nodes corresponds to its centrality, measured by network betweenness.

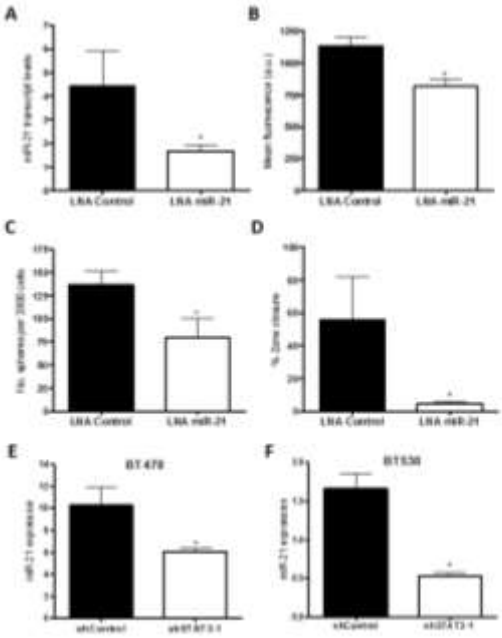

Figure 7. Knockdown of miR-21 produces similar reduction in self-renewal and migration in vitro. miR-21 was knocked down using a locked nucleic acid (LNA) oligonucleotide in the BMIC line BT478. A) miR-21 transcript levels by qRT-PCR were moderately reduced, relative to the U6snRNA control. B) Self-renewal was assessed through sphere formation per 2000 cells; miR-21 knockdown corresponded with decreased sphere formation. C) miR-21 knockdown resulted in decreased proliferation (PrestoBlue assay). D) Zone-exclusion assays showed decreased migratory capability with inhibited miR-21. E) miR-21 transcript levels in STAT3 knockdown cells were assessed by qRT-PCR, where miR-21 transcript levels relative to the U6snRNA control were significantly lower in shSTAT3 cells as compared to the shControl. *$p<0.05$.

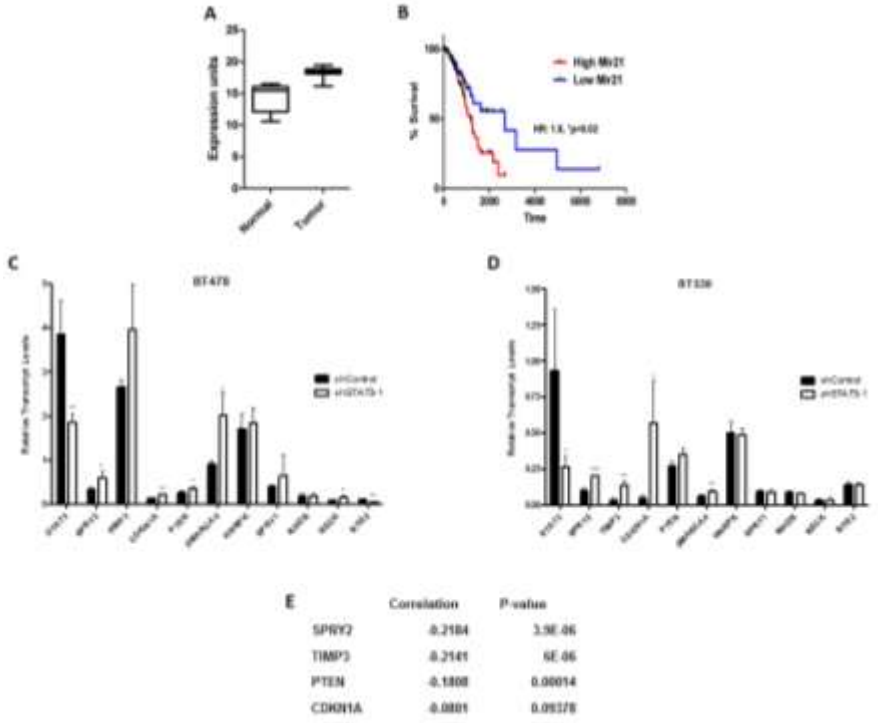

Figure 8. miR-21 expression in lung adenocarcinoma patients and its association with STAT3. A) Examination of gene expression profiling obtained from TCGA identified a significant upregulation of miR-21 in lung adenocarcinoma samples as compared to normal lung. ($p<0.0001$). B) Patients with high miR-21 expressing tumors had poorer overall survival. ($p=0.02$). qRT-PCR analysis of target genes downstream of miR-21 in STAT3 KD in BMIC lines C) BT478 and D) BT530. E) The calculated Pearson distance between miR-21 and genes identified those that were inversely co-expressed with miRNA-21 by gene expression analysis in lung adenocarcinoma samples (TCGA). These genes showed significant upregulation in the STAT3 KD as compared to the control. ns non significant; *$p<0.05$; **$p<0.01$; ***$p<0.001$ (multiple T tests).

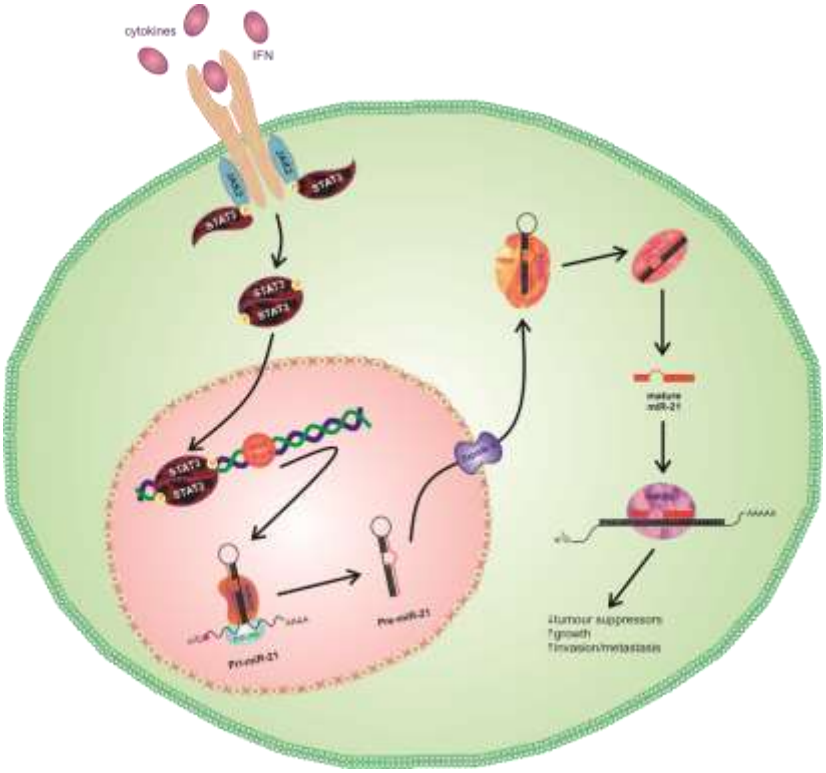

Figure 9. Representative schematic of STAT3 activation of miR-21. Binding of appropriate cytokines or interferons to the cell surface receptor triggers activation of Janus Kinases (JAKs), which in turn phosphorylates the tyrosine residue of bound STAT3 proteins. The phosphotyrosines mediate the dimerization of STAT3, where activated dimers will translocate to the nucleus to activate transcription of pri-miR-21. Cleavage of pri-miR-21 by Drosha will generate a precursor miR-21, or pre-miR-21, which is translocated to the cytoplasm and further processed by a Dicer complex to produce mature miR-21. miR-21 will be integrated into the RNA-induced silencing complex (RISC) and interact with target mRNA to reduce expression of tumor suppression genes such as PTEN and CYLD.

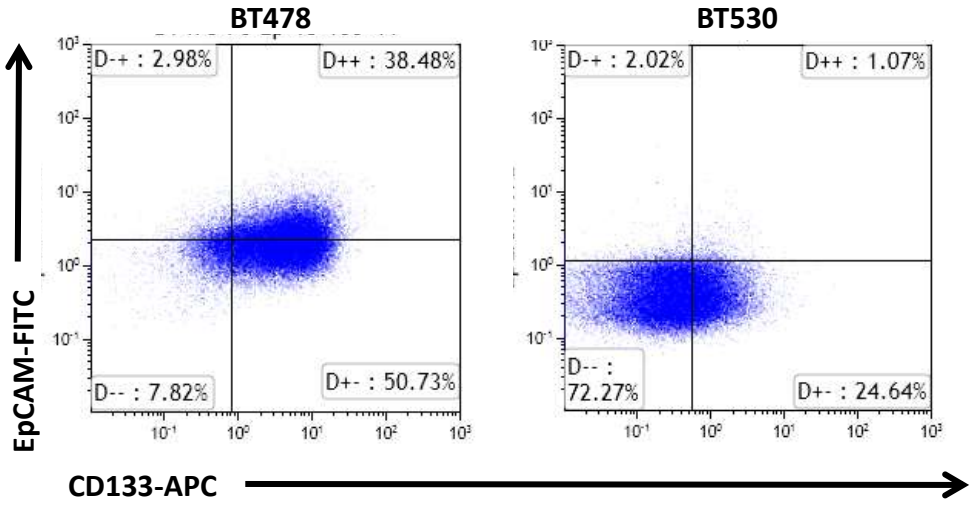

Supplementary Figure 1. CSC marker CD133 and epithelial marker EpCAM expressionfor BT478 and BT530 was assessed by flow cytometry.

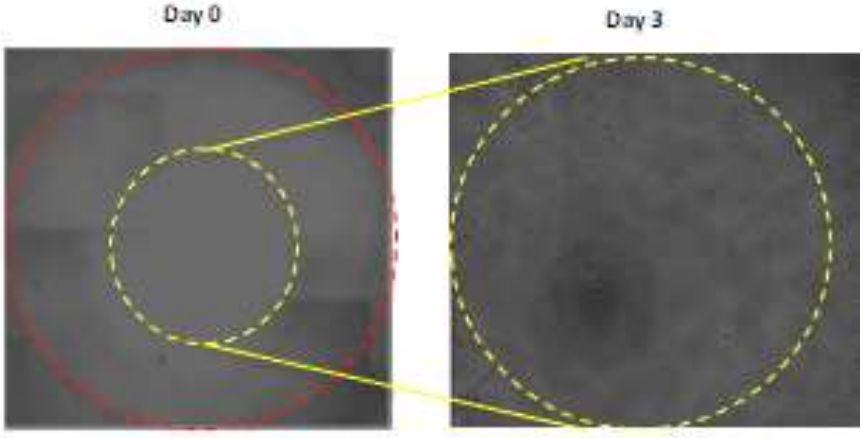

Supplementary Figure 2. Representative phase contrast images of zone exclusion assay. Red line is outline of cell border at day 0, yellow line is cell border at day 3.

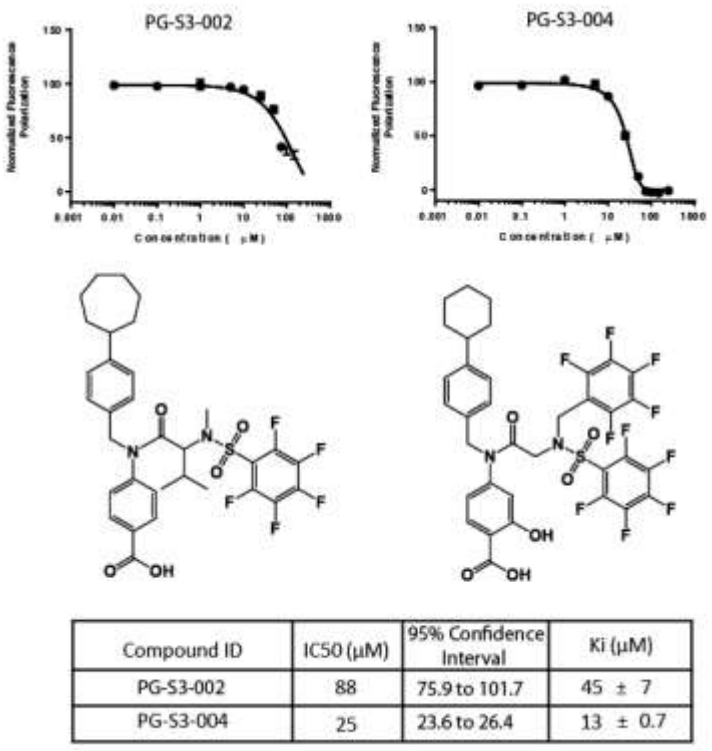

Compound ID	IC50 (μM)	95% Confidence Interval	Ki (μM)
PG-S3-002	88	75.9 to 101.7	45 ± 7
PG-S3-004	25	23.6 to 26.4	13 ± 0.7

Supplementary Figure 3. Determination of inhibitory constants for lead molecules using Fluorescence Polarization (FP) assay. Competitive binding FP assays were carried out for PG-S3-002 and PG-S3-004 (BP-5-087 FP previously determined by Gunning et al.)[74,75] employing STAT3 and fluoresceinated-phosphopeptide 5-FAM-GpYLPQTV. Respective K_i's and IC_{50} values were derived from the appended competitive displacement curves and consolidated in the inset table. The assay results indicate that this family of molecules exhibits high affinity for the STAT3 protein.

Antibody or Dye	Company	Amt/test (μL)	Isotype Control	Ex. (nm)	Em. (nm)
7-AAD Viability Dye	Beckman Coulter	10	N/A	546	647
Human CD133/2 APC	Miltenyi Biotec	10	IgG2b APC	650	660
EpCAM FITC	Miltenyi Biotec	10	IgG2a FITC	480	578
Mouse IgG2a FITC	R&D Systems	10	N/A	495	519
Mouse IgG2b APC	Miltenyi Biotec	10	N/A	650	660

Supplementary Table 1. List of antibodies and dyes used for flow cytometry and sorting. Ex = excitation wavelength; Em = emission wavelength.

Gene	Forward Primer	Reverse Primer
GAPDH	TGCACCACCAACTGCTTAGC	GGCATGGACTGTGGTCATGAG
Stat3	AGGGTACATCATGGGCTTTATC	CTCCTTCTTTGCTGCTTTCAC
BTG2	CGTGAGCGAGCAGAGGCT TAAG	TGGACGGCTTTTCGGGAA
CDKN1A	GGCAGACCAGCATGACAGATT TC	CGGATTAGGGCTTCCTCTTGG
SMARCA4	GGGTAGCAGCAGATGTAGTTT C	CCAGTCACAAACAGTCCTACA G
ANP32A	TCCCTGTAAATGCGATAGCTA AG	GGGAAATACCAGGAAACGTAA GA
RECK	GCTCGGTTTGTTGCAGTTATG	ATCTGAGATGGACCAGGAGAA
PDCD4	GAGTACCAGTGTTGGCAGTATC	GTCCCACAAAGGTCAGAAAGA
RHOB	GGAGCTTGATATCCCTTGTCTG	CACCCATCACCACCCTTAAATA
TIMP3	TTTGCCCTTCTCCTCCAATAC	TCTTTCACACACCTTGAGTCT ATC
HNRPK	GGTGATCTTGGTGGACCTATTATT	TAATCCGCTGACCACCTTTG
SPRY2	TGTGGCAAGTGCAAATGTAAG	CAGCATACACAAGTCCCATAGT
SPRY1	GCCATCCACTTGAGGGTATT	GTAGTCTGGATGTGGGTGTATG

Supplementary Table 2. List of qRT-PCR primers and their corresponding reverse and forward sequences

Fold Change	P-value	Histology	No. of samples (total/normal)	Author	Year	Ref.
2.9	< 0.001	SCC, ADC	52/24	Boeri et al.	2011	Boeri, Mattia, et al. "MicroRNA signatures in tissues and plasma predict development and prognosis of computed tomography detected lung cancer." Proceedings of the National Academy of Sciences 108.9 (2011): 3713-3718.
4.7	1.08E-005	ADC	20/10	Cho et al.	2009	Cho, William, Andrew SC Chow, and Joseph SK Au. "Restoration of tumor suppressor hsa-miR-145 inhibits cancer cell growth in lung adenocarcinoma

						patients with epidermal growth factor receptor mutation." European Journal of Cancer 45.12 (2009): 2197-2206.
3.5	6.13E-005	ADC	20/8	Crawford et al.	2009	Crawford, Melissa, et al. "MicroRNA 133B targets pro-survival molecules MCL-1 and BCL2L2 in lung cancer." Biochemical and biophysical research communications 388.3 (2009): 483-489.
3.2	2.00E-004	SCC, ADC	12/6	Gao et al.	2010	Gao, Wen, et al. "Deregulated expression of miR-21, miR-143 and miR-181a in non small cell lung cancer is related to clinicopathologic characteristics or patient prognosis." Biomedicine & Pharmacotherapy 64.6 (2010): 399-408.
2.4	2.30E-009	ADC	112/56	Jang et al.	2012	Jang, Jin Sung, et al. "Increased miR-708 expression in NSCLC and its association with poor survival in lung adenocarcinoma from never smokers." Clinical Cancer Research 18.13 (2012): 3658-3667.
-	<0.01	SCC, ADC	40/20	Puissegur et al.	2011	Puissegur, M. P., et al. "miR-210 is overexpressed in late stages of lung cancer and mediates mitochondrial alterations associated with modulation of HIF-1 activity." Cell Death & Differentiation 18.3 (2010): 465-478.
2.4	3.00E-004	SCC, ADC	56/28	Seike et al.	2009	Seike, Masahiro, et al. "MiR-21 is an EGFR-regulated anti-apoptotic factor in lung cancer in never-smokers." Proceedings of the National Academy of Sciences 106.29 (2009): 12085-12090.
2.3	4.11E-003	SCC, ADC	65/27	Vosa et al.	2011	Võsa, Urmo, et al. "Identification of miR-374a as a prognostic marker for survival in patients with early-stage nonsmall cell lung cancer." Genes, Chromosomes and Cancer 50.10 (2011): 812-822.
2.6	<0.01	SCC, ADC	46/23	Wang et al.	2011	Wang, R., et al. "MicroRNA-451 functions as a tumor suppressor in human non-small cell lung cancer by targeting ras-related protein 14 (RAB14)." Oncogene 30.23 (2011): 2644-2658.
1.7	<0.01	SCC, ADC	30/15	Xing et al.	2010	Xing, Lingxiao, et al. "Early detection of squamous cell lung cancer in sputum by a

						panel of microRNA markers." Modern Pathology 23.8 (2010): 1157-1164.
-	1.00E-007	SCC, ADC	208/104	Yanaihara et al.	2006	Yanaihara, Nozomu, et al. "Unique microRNA molecular profiles in lung cancer diagnosis and prognosis." Cancer cell 9.3 (2006): 189-198.
2.6	<0.01	ADC	40/20	Yu et al.	2010	Yu, Lei, et al. "Early detection of lung adenocarcinoma in sputum by a panel of microRNA markers." International Journal of Cancer 127.12 (2010): 2870-2878.

Supplementary Table 3: gene expression datasets**.** Summary of gene expression datasets which were subjected to gene-expression meta-analysis described in material & methods gene expression meta-analysis.

Inverse Correlation with miR-21	Correlation Co-efficient	P-value
FGR	-0.2137634	6.231E-06
C2orf39	-0.2137697	6.227E-06
CSRP2BP	-0.2137713	6.226E-06
LIPA	-0.2138031	6.206E-06
LEPR	-0.2138322	6.187E-06
RIMKLA	-0.2139388	6.12E-06
RP1-177G6.2	-0.2139501	6.113E-06
TGFBRAP1	-0.213967	6.102E-06
MEOX1	-0.2140475	6.052E-06
MAN1A1	-0.2140548	6.048E-06
ZDHHC3	-0.2140701	6.038E-06
TIMP3	-0.2140774	6.034E-06
USP8	-0.2141791	5.971E-06
GPBAR1	-0.2142519	5.927E-06
SYNE1	-0.2142598	5.922E-06
C6orf72	-0.2143394	5.874E-06
NIPSNAP3A	-0.2143462	5.87E-06
GIMAP1	-0.2144321	5.819E-06
DYX1C1	-0.2144417	5.813E-06
TYRP1	-0.2145129	5.771E-06
C4orf19	-0.2146031	5.717E-06
SPATA1	-0.2146151	5.71E-06
HELQ	-0.2146483	5.691E-06
ZNF620	-0.2146789	5.673E-06
TMEM107	-0.2147763	5.617E-06
DCTN1	-0.2148942	5.549E-06
DMD	-0.2149165	5.536E-06
GATA5	-0.214938	5.524E-06
CRTC3	-0.21499	5.495E-06
FAM183A	-0.2150234	5.476E-06
RAB4A	-0.2151681	5.395E-06
SNCAIP	-0.2152695	5.339E-06
DTHD1	-0.2152724	5.338E-06
C11orf66	-0.2153902	5.273E-06
GIMAP4	-0.2153957	5.27E-06
RNF152	-0.2155458	5.189E-06
GORASP1	-0.2156193	5.15E-06
GP5	-0.2156493	5.134E-06
TSPYL4	-0.2156529	5.132E-06
IHH	-0.2157948	5.058E-06
CDS2	-0.2158304	5.039E-06
PCDHB1	-0.2158562	5.026E-06
HNRNPH2	-0.2159212	4.992E-06
GKAP1	-0.2159392	4.983E-06
ISOC1	-0.2159428	4.981E-06
AR	-0.2159433	4.981E-06
KNCN	-0.2159556	4.975E-06
SH3BGRL2	-0.2161892	4.856E-06
DNAH10	-0.2162708	4.815E-06
hsa-mir-29c	-0.2162953	4.803E-06
CRTAP	-0.2163165	4.792E-06
HSF2	-0.2163317	4.785E-06
CTAGE1	-0.2164685	4.718E-06
C6orf165	-0.2165042	4.7E-06
FLJ10357	-0.2165216	4.692E-06
WDR19	-0.2165717	4.668E-06
MYO1C	-0.2165918	4.658E-06
MIPEP	-0.2166741	4.618E-06
TPRG1L	-0.2166744	4.618E-06
hsa-mir-3619	-0.2166798	4.616E-06
RCBTB1	-0.2166806	4.615E-06
DIRC2	-0.2167577	4.578E-06
ITPR1	-0.2167633	4.576E-06
GAS7	-0.2169031	4.51E-06
FIG4	-0.2169034	4.51E-06
SENP8	-0.2169084	4.507E-06
EFCAB6	-0.2169473	4.489E-06
MAP9	-0.2170261	4.453E-06
IFT172	-0.2170481	4.443E-06
SEC23B	-0.2170689	4.433E-06
FAM134B	-0.2171249	4.407E-06
LIN52	-0.2171234	4.408E-06
CNR1	-0.217155	4.394E-06
SIN3A	-0.2172971	4.329E-06
ACADM	-0.2173316	4.314E-06
TMSB15A	-0.217397	4.284E-06
hsa-mir-501	-0.2174483	4.262E-06
RNF185	-0.2175804	4.204E-06
FBLN1	-0.2176092	4.191E-06
SETX	-0.2176477	4.174E-06
PRRG3	-0.2176794	4.16E-06
FAM105A	-0.217759	4.126E-06
RNF122	-0.2177864	4.114E-06
GPRASP1	-0.2178293	4.096E-06
C1orf150	-0.2178439	4.09E-06
FAM188A	-0.2178562	4.085E-06
CCL24	-0.2179691	4.037E-06
ACR	-0.2180029	4.023E-06
CRMP1	-0.2180225	4.014E-06
OSR1	-0.2180289	4.012E-06
SHH	-0.218051	4.003E-06
CCDC65	-0.2181219	3.973E-06
ZFP1	-0.2181635	3.956E-06
AXIN2	-0.2182355	3.926E-06
STAG1	-0.2182684	3.913E-06
CACHD1	-0.2182727	3.911E-06
ZNF192	-0.218289	3.904E-06
SPRY2	-0.2183687	3.872E-06
MTMR9	-0.2184087	3.856E-06
CHST10	-0.2184182	3.852E-06
LPPR5	-0.218443	3.842E-06
CDHR3	-0.2184675	3.832E-06
MAP1LC3B2	-0.218763	3.716E-06
WBP4	-0.2187828	3.708E-06
C9orf171	-0.2188375	3.687E-06
ID3	-0.2188646	3.676E-06
hsa-mir-3940	-0.2189321	3.65E-06
ALDH2	-0.2189918	3.628E-06
CYB5A	-0.2190779	3.595E-06
AADAC	-0.2190835	3.593E-06
EFCAB1	-0.2190903	3.59E-06
DTWD2	-0.2192643	3.526E-06
C11orf58	-0.2193356	3.499E-06
NFYB	-0.2193862	3.481E-06
SAMHD1	-0.2194152	3.47E-06
CD68	-0.2194246	3.467E-06
PRMT8	-0.2194607	3.454E-06
CHST9	-0.2194863	3.444E-06
KIF26A	-0.2194889	3.443E-06
NMBR	-0.2195201	3.432E-06
FBXL7	-0.2195265	3.43E-06
STK33	-0.2195314	3.428E-06
C9orf153	-0.219538	3.426E-06
FRMPD1	-0.2195508	3.421E-06
FAM110B	-0.2195653	3.416E-06
ZMYND10	-0.2195903	3.407E-06
ZNF441	-0.2196303	3.393E-06
hsa-mir-92a-1	-0.2196761	3.376E-06
DYNC1LI1	-0.2196993	3.368E-06
DNAH9	-0.2197759	3.341E-06
TPT1	-0.2198786	3.305E-06
PLEKHA2	-0.2198789	3.305E-06
SLC4A1	-0.2198968	3.299E-06
GPD1L	-0.2199198	3.291E-06
C1orf88	-0.2200335	3.252E-06
ZNF20	-0.2200835	3.235E-06
FBXW2	-0.2201312	3.219E-06
SLC5A9	-0.2201332	3.218E-06
ATP8A2	-0.2201434	3.215E-06
KIF19	-0.2201704	3.205E-06
WDR16	-0.2202321	3.185E-06
TUBB1	-0.2202427	3.181E-06
RASSF5	-0.2230249	2.368E-06
hsa-mir-320c-1	-0.2230523	2.362E-06
ZBTB7C	-0.2232174	2.32E-06
KIAA1958	-0.2232485	2.313E-06
PPPDE1	-0.2233126	2.297E-06
SCD5	-0.2233911	2.278E-06
ARHGEF2	-0.2234129	2.272E-06
C4orf3	-0.2235013	2.251E-06
MT1M	-0.2235185	2.247E-06
ICAM2	-0.2235228	2.246E-06
ANKRD1	-0.2237605	2.189E-06
DENND5A	-0.2238421	2.17E-06
CLEC4M	-0.2238968	2.158E-06
SYNPO2L	-0.2239025	2.156E-06
TNFSF12	-0.2239337	2.149E-06
SEMA6D	-0.2241106	2.109E-06
MITF	-0.224142	2.102E-06
FAM124A	-0.2242278	2.082E-06
C2orf67	-0.2242396	2.08E-06
KIAA0564	-0.2242519	2.077E-06
JDP2	-0.2244195	2.04E-06
GJA4	-0.2244906	2.024E-06
CCDC152	-0.2245314	2.016E-06
SLC24A3	-0.2247037	1.979E-06
C11orf88	-0.2247349	1.972E-06
PHF17	-0.2247447	1.97E-06
FXR2	-0.2249092	1.935E-06
LOC285796	-0.2249177	1.934E-06
SLC35A1	-0.2249266	1.932E-06
FAM188B	-0.2249584	1.925E-06
ST7L	-0.2250667	1.903E-06
TMEM125	-0.2251253	1.891E-06
LRRC48	-0.2251545	1.885E-06
BIVM	-0.2252641	1.863E-06
CYGB	-0.2252953	1.857E-06
CAMP	-0.2252963	1.856E-06
PPP2R5A	-0.2253875	1.838E-06
PCDHGA9	-0.2255059	1.815E-06
C6orf97	-0.2255288	1.81E-06
USP54	-0.2255463	1.807E-06
hsa-mir-92b	-0.2255781	1.801E-06
SLC22A3	-0.225594	1.798E-06
FAM82A1	-0.2255948	1.798E-06
PPP1R14A	-0.225642	1.788E-06
UACA	-0.2257861	1.761E-06
RNF11	-0.2258238	1.754E-06
LCORL	-0.2259605	1.728E-06
KIF3B	-0.2259775	1.725E-06
SWAP70	-0.2260871	1.704E-06
ATF7	-0.2261481	1.693E-06
TNFRSF19	-0.2261629	1.69E-06
GSTA4	-0.2261774	1.688E-06
FAM43A	-0.2262422	1.676E-06
hsa-mir-200c	-0.2262697	1.671E-06
KIAA0427	-0.2263043	1.665E-06
C1orf194	-0.2263314	1.66E-06
C6orf225	-0.2264753	1.634E-06
NHLRC4	-0.2266156	1.609E-06
UNC13B	-0.2267202	1.591E-06
DLL1	-0.2267784	1.581E-06
ZNF295	-0.2202431	3.181E-06
FRAT1	-0.220355	3.144E-06
KIAA0513	-0.2203605	3.142E-06
IRX1	-0.2204367	3.117E-06
ARHGAP28	-0.2204605	3.109E-06
KIDINS220	-0.2204624	3.108E-06
SPAG6	-0.2205465	3.081E-06
hsa-mir-607	-0.2205482	3.08E-06
SERGEF	-0.2207014	3.031E-06
SLC25A38	-0.220726	3.023E-06
RAB36	-0.2209666	2.947E-06
C1orf129	-0.2210794	2.912E-06
MBNL3	-0.2211417	2.893E-06
TOP2B	-0.2212776	2.852E-06
B3GALNT1	-0.2213013	2.845E-06
EIF3F	-0.2213536	2.829E-06
NUCB1	-0.2213637	2.826E-06
LOC144571	-0.2213992	2.815E-06
ACP5	-0.2214151	2.811E-06
KCNJ11	-0.2214198	2.809E-06
ROCK1	-0.2214327	2.805E-06
ENG	-0.2214741	2.793E-06
ALOX15	-0.2214765	2.792E-06
RAB39B	-0.2214969	2.786E-06
SEC14L4	-0.2217393	2.716E-06
GRINL1A	-0.2218065	2.696E-06
RNF6	-0.2218022	2.698E-06
KCNRG	-0.2218342	2.688E-06
GALC	-0.2218923	2.672E-06
SECISBP2L	-0.2219035	2.669E-06
CYP4V2	-0.2219426	2.658E-06
C8orf84	-0.2219631	2.652E-06
PCDH20	-0.2219737	2.649E-06
OSCAR	-0.2220473	2.628E-06
KBTBD11	-0.2220564	2.626E-06
TTC19	-0.2220586	2.625E-06
CDH23	-0.2222177	2.581E-06
FHDC1	-0.222297	2.559E-06
B9D2	-0.2223257	2.552E-06
C17orf108	-0.2223365	2.549E-06
CTR9	-0.2223921	2.534E-06
MECOM	-0.2224532	2.517E-06
ZBTB44	-0.2227983	2.426E-06
C10orf105	-0.22289	2.403E-06
RGS22	-0.2229588	2.385E-06
ZBTB3	-0.2229643	2.384E-06
hsa-mir-769	-0.223015	2.371E-06
KLF2	-0.223015	2.371E-06

Supplementary Table 4. Top 250 inversely co-expressed genes/miRNAs in lung adenocarcinoma samples

Fold Change	P-value	Cancer Type	No. of samples (total/normal)	Author	Year	Ref.
2.9	< 0.001	SCC, ADC	52/24	Boeri et al.	2011	Boeri, Mattia, et al. "MicroRNA signatures in tissues and plasma predict development and prognosis of computed tomography detected lung cancer."

						Proceedings of the National Academy of Sciences 108.9 (2011): 3713-3718.
4.7	1.08E-005	ADC	20/10	Cho et al.	2009	Cho, William, Andrew SC Chow, and Joseph SK Au. "Restoration of tumor suppressor hsa-miR-145 inhibits cancer cell growth in lung adenocarcinoma patients with epidermal growth factor receptor mutation." European Journal of Cancer 45.12 (2009): 2197-2206.
3.5	6.13E-005	ADC	20/8	Crawford et al.	2009	Crawford, Melissa, et al. "MicroRNA 133B targets pro-survival molecules MCL-1 and BCL2L2 in lung cancer." Biochemical and biophysical research communications 388.3 (2009): 483-489.
3.2	2.00E-004	SCC, ADC	12/6	Gao et al.	2010	Gao, Wen, et al. "Deregulated expression of miR-21, miR-143 and miR-181a in non small cell lung cancer is related to clinicopathologic characteristics or patient prognosis." Biomedicine & Pharmacotherapy 64.6 (2010): 399-408.
2.4	2.30E-009	ADC	112/56	Jang et al.	2012	Jang, Jin Sung, et al. "Increased miR-708 expression in NSCLC and its association with poor survival in lung adenocarcinoma from never smokers." Clinical Cancer Research 18.13 (2012): 3658-3667.
-	<0.01	SCC, ADC	40/20	Puissegur et al.	2011	Puissegur, M. P., et al. "miR-210 is overexpressed in late stages of lung cancer and mediates mitochondrial alterations associated with modulation of HIF-1 activity." Cell Death & Differentiation 18.3 (2010): 465-478.
2.4	3.00E-004	SCC, ADC	56/28	Seike et al.	2009	Seike, Masahiro, et al. "MiR-21 is an EGFR-regulated anti-apoptotic factor in lung cancer in never-smokers." Proceedings of the National Academy of Sciences 106.29 (2009): 12085-12090.
2.3	4.11E-003	SCC, ADC	65/27	Vosa et al.	2011	Võsa, Urmo, et al. "Identification of miR-374a as a prognostic marker for survival in patients with early-stage nonsmall cell lung cancer." Genes, Chromosomes and Cancer 50.10 (2011): 812-822.
2.6	<0.01	SCC, ADC	46/23	Wang et al.	2011	Wang, R., et al. "MicroRNA-451 functions as a tumor suppressor in human non-small cell lung cancer by targeting ras-related protein 14 (RAB14)." Oncogene 30.23 (2011): 2644-2658.
1.7	<0.01	SCC, ADC	30/15	Xing et al.	2010	Xing, Lingxiao, et al. "Early detection of squamous cell lung cancer in sputum by a panel of microRNA markers." Modern Pathology 23.8 (2010): 1157-1164.
-	1.00E-007	SCC, ADC	208/104	Yanaihara et al.	2006	Yanaihara, Nozomu, et al. "Unique microRNA molecular profiles in lung cancer diagnosis and prognosis." Cancer cell 9.3 (2006): 189-198.
2.6	<0.01	ADC	40/20	Yu et al.	2010	Yu, Lei, et al. "Early detection of lung adenocarcinoma in sputum by a panel of microRNA markers." International Journal of Cancer 127.12 (2010): 2870-2878.

Supplementary Table 5. mir-21 upregulation across various miRNA profiling studies **.** Expression of mir-21 in tumors has been found significantly upregulated compared to normal tissue by 12 miRNA profiling studies. Table summarizes reported fold-change (if available) of mir-21 expression, together with its level of significance, as well as histology and number of samples that have been used.

Genes	Functional Role	Reference
TPM1	Tumor suppressor gene	Zhu S, Si ML, Wu H, Mo YY. MicroRNA-21 targets the tumor suppressor gene tropomyosin 1 (TPM1). The Journal of biological chemistry 2007; 282: 14328-14336
PDCD4	Reduce invasion and metastasis	Asangani IA, Rasheed SA, Nikolova DA, Leupold JH, Colburn NH, Post S et al. MicroRNA-21 (miR-21) post-transcriptionally downregulates tumor suppressor Pdcd4 and stimulates invasion, intravasation and metastasis in colorectal cancer. Oncogene 2008; 27: 2128-2136. Lu Z, Liu M, Stribinskis V, Klinge CM, Ramos KS, Colburn NH et al. MicroRNA-21 promotes cell transformation by targeting the programmed cell death 4 gene. Oncogene 2008; 27: 4373-4379.
PTEN	Reduces Growth and Invasion	Meng F, Henson R, Wehbe-Janek H, Ghoshal K, Jacob ST, Patel T. MicroRNA-21 regulates expression of the PTEN tumor suppressor gene in human hepatocellular cancer. Gastroenterology 2007; 133: 647-658
RHOB	Tumor suppressor gene	Liu M, Tang Q, Qiu M, Lang N, Li M, Zheng Y et al. miR-21 targets the tumor suppressor RhoB and regulates proliferation, invasion and apoptosis in colorectal cancer cells. FEBS letters 2011; 585: 2998-3005. Luis-Ravelo D, Anton I, Zandueta C, Valencia K, Pajares MJ, Agorreta J et al. RHOB influences lung adenocarcinoma metastasis and resistance in a host-sensitive manner. Molecular oncology 2014; 8: 196-206.
TIMP-3	Matrix metalloproteinase inhibitor	Gabriely G, Wurdinger T, Kesari S, Esau CC, Burchard J, Linsley PS et al. MicroRNA 21 promotes glioma invasion by targeting matrix metalloproteinase regulators. Molecular and cellular biology 2008; 28: 5369-5380.
RECK	Matrix metalloproteinase inhibitor	Gabriely G, Wurdinger T, Kesari S, Esau CC, Burchard J, Linsley PS et al. MicroRNA 21 promotes glioma invasion by targeting matrix metalloproteinase regulators. Molecular and cellular biology 2008; 28: 5369-5380.
HNRPK	Player in p53/TP53 response	Papagiannakopoulos T, Shapiro A, Kosik KS. MicroRNA-21 targets a network of key tumor-suppressive pathways in glioblastoma cells. Cancer research 2008; 68: 8164-8172.
SPRY1	Inhibit DNA damage response pathways	Gastwirt RF, Slavin DA, McAndrew CW, Donoghue DJ. Spy1 expression prevents normal cellular responses to DNA damage: inhibition of apoptosis and checkpoint activation. The Journal of biological chemistry 2006; 281: 35425-35435. McAndrew CW, Gastwirt RF, Meyer AN, Porter LA, Donoghue DJ. Spy1 enhances phosphorylation and degradation of the cell cycle inhibitor p27. Cell cycle 2007; 6: 1937-1945.

SPRY2	Inhibits cell migration	Sayed D, Rane S, Lypowy J, He M, Chen IY, Vashistha H et al. MicroRNA-21 targets Sprouty2 and promotes cellular outgrowths. Molecular biology of the cell 2008; 19: 3272-3282.
CDKN1A	Cell cycle regulator	de Oliveira PE, Zhang L, Wang Z, Lazo JS. Hypoxia-mediated regulation of Cdc25A phosphatase by p21 and miR-21. Cell cycle 2009; 8: 3157-3164.
ANP32A	Modulator of Apoptosis	Schramedei K, Morbt N, Pfeifer G, Lauter J, Rosolowski M, Tomm JM et al. MicroRNA-21 targets tumor suppressor genes ANP32A and SMARCA4. Oncogene 2011; 30: 2975-2985.
SMARCA4	Tumor suppressor	Schramedei K, Morbt N, Pfeifer G, Lauter J, Rosolowski M, Tomm JM et al. MicroRNA-21 targets tumor suppressor genes ANP32A and SMARCA4. Oncogene 2011; 30: 2975-2985. Watanabe T, Semba S, Yokozaki H. Regulation of PTEN expression by the SWI/SNF chromatin-remodelling protein BRG1 in human colorectal carcinoma cells. British journal of cancer 2011; 104: 146-154.
BTG2	Anti-proliferative	Liu M, Wu H, Liu T, Li Y, Wang F, Wan H et al. Regulation of the cell cycle gene, BTG2, by miR-21 in human laryngeal carcinoma. Cell research 2009; 19: 828-837.

Supplementary Table 6. downstream targets of miR-21

Chapter 3: RNAi screen identifies essential regulators of human brain metastasis-initiating cells.

Preamble

This chapter is an original published article presented in its published format in *Acta Neuropathologica* available at http://rdcu.be/FYNi.

Singh M, Venugopal C, Tokar T, Brown KR, McFarlane N, Bakhshinyan D, Vijayakumar T, Manoranjan B, Mahendram S, Vora P, Qazi M, Dhillon M, Tong A, Durrer K, Murty N, Hallet R, Hassell JA, Kaplan DR, Cutz JC, Jurisica I, Moffat J, Singh SK. *RNAi screen identifies essential regulators of human brain metastasis-initiating cells.* Acta Neuropathol. 2017 Dec;134(6):923-940. doi: 10.1007/s00401-017-1757-z.

Experimental concept and study design was developed by myself C. Venugopal, R. Hallett and S.K. Singh, and the work was supervised by S.K. Singh. BM samples were provided by N. Murty. I performed all *in vitro* BMIC line generation, maintenance and characterization. All flow cytometric analyses were performed by N. McFarlane. Generation of the *in vivo* models was conducted by myself, with surgical assistance (suturing) by D. Bakhshinyan, M. Qazi, T. Vijayakumar and M. Dhillon. The shRNA lentiviral library was generated by C. Venugopal, and the *in vitro* and *in vivo* screens and sample collection performed by myself. Compiling of the shRNA library and sample preparation was performed by A. Tong and K. Durrer under the supervision of J, Moffit. Analysis of the shRNA screen results was performed by K.R Brown under the supervision

of J. Moffit. *In vitro* validation of SPOCK1 and TWIST2 was performed by myself, with assistance from M. Dhillon. *In vivo* validation of SPOCK1 and TWIST2 was performed by myself, with assistance from D. Bakhshinyan, M. Qazi and M. Dhillon, and sample collection was performed by myself. Patient biopsy samples of lung adenocarcinoma and brain metastases were compiled by J.C. Cutz. *In silico* analyses (COX modelling, protein-protein mapping, *etc*.) were performed by R. Hallett under the supervision of J.A. Hassell and by T. Tokar under the supervision of I. Jurisica. The manuscript was prepared myself, with input and edits provided by S.K. Singh, C. Venugopal, P. Vora, B. Manoranjan, S. Mahendram, I. Jurisica, D.R. Kaplan, J.C. Cutz and J.A. Hassell.

This study was originally designed to develop clinically relevant models of BM. The route of injection was vital to our models, as different routes would garner information about different aspects of the metastatic cycle. I chose an intracranial route to validate the TIC capacity of BMICs within the brain, intracardiac route as this route is commonly used in metastatic studies and I wanted to determine if the BMICs had any homing capacity for either the lung or the brain, and I chose the intrathoracic route as this would theoretically provide us with the best replication of the metastatic cycle. Having successfully accomplished all three models, I then set out to validate their usefulness as platforms to screen novel BMIC regulators. For this I initially performed a RNA interference screen, providing us with a list of potential BMIC regulators. Further *in vitro* and *in vivo* validation determined SPOCK1 and TWIST2 to be essential BMIC regulators.

RNAi screen identifies essential regulators of human brain metastasis initiating cells

Mohini Singh[1,2], Chitra Venugopal[1,3], Tomas Tokar[6], Kevin R. Brown[4], Nicole McFarlane[1,3], David Bakhshinyan[1,2], Thusyanth Vijayakumar[1,2], Branavan Manoranjan[1,2], Sujeivan Mahendram[1,3], Parvez Vora[1,3], Maleeha Qazi[1,2], Manvir Dhillon[1,3], Amy Tong[4], Kathrin Durrer[4], Naresh Murty[3], Robin Hallett[2], John A. Hassell[2], David Kaplan[7], Jean-Claude Cutz[8], Igor Jurisica[5,6], Jason Moffat[4], and Sheila K. Singh[1,2,3]

[1]Stem Cell and Cancer Research Institute, McMaster University, Hamilton, ON, Canada

[2]Department of Biochemistry and Biomedical Sciences, McMaster University, Hamilton, ON, Canada

[3]Department of Surgery, McMaster University, Hamilton, ON, Canada

[4]Donnelly Centre and Department of Molecular Genetics, University of Toronto, ON, Canada [5]Princess Margaret Cancer Centre, IBM Life Sciences Discovery Centre, University Health Network, Toronto, ON, Canada

[6] Departments of Medical Biophysics and Computer Science, University of Toronto, Toronto, ON, Canada

[7]Cell Biology Program, The Hospital for Sick Children; Department of Molecular Genetics, University of Toronto, ON, Canada

[8]Anatomic Pathology, St. Joseph's Healthcare, Hamilton, ON, Canada

Corresponding Author Contact Information:

Sheila K. Singh MD PhD FRCS(C), MDCL 5027, McMaster University Stem Cell and Cancer Research Institute, 1280 Main Street West, Hamilton, ON, L8S 4K1, CANADA.

T: 905 521 2100 x75237 F: 905 521 9992 Email: ssingh@mcmaster.ca

Abstract

Brain metastases (BM) are the most common brain tumor in adults and are a leading cause of cancer mortality. Metastatic lesions contain subclones derived from their primary lesion, yet their functional characterization is limited by a paucity of preclinical models accurately recapitulating the metastatic cascade, emphasizing the need for a novel approach to BM and their treatment. We identified a unique subset of stem-like cells from primary human patient brain metastases, termed brain metastasis initiating cells (BMICs). We now establish a BMIC patient-derived xenotransplantation (PDXT) model as an investigative tool to comprehensively interrogate human BM. Using both *in vitro* and *in vivo* RNA interference screens of these BMIC models, we identified SPOCK1 and TWIST2 as essential BMIC regulators. SPOCK1 in particular is a novel regulator of BMIC self-renewal, modulating tumor initiation and metastasis from the lung to the brain. A prospective cohort of primary lung cancer specimens showed SPOCK1 was over-expressed only in patients who ultimately developed BM. Protein-protein interaction network mapping between SPOCK1 and TWIST2 identified novel pathway interactors with significant prognostic value in lung cancer patients. Of these genes, INHBA, a TGF-β ligand found mutated in lung adenocarcinoma, showed reduced expression in BMICs with knockdown of SPOCK1. In conclusion, we have developed a useful preclinical model of BM, which has served to identify novel putative BMIC regulators, presenting potential therapeutic targets that block the metastatic process, and transform a uniformly fatal systemic disease into a locally controlled and eminently more treatable one.

Keywords: brain metastasis, brain metastasis-initiating cell, BMIC, BMIC regulators, TWIST2, SPOCK1, patient-derived xenotransplant, non-small cell lung cancer

Introduction

Brain metastases (BM) are the most common tumor to affect the adult central nervous system, occurring at a rate ten times greater than that of primary brain tumors[37]. With a median survival calculated in weeks in untreated patients, extended to only 3-18 months following multimodal therapy, BM represent a leading cause of cancer mortality[14]. Although BM pose a significant clinical burden, the metastatic process is highly inefficient as individual tumor cells maintain a variable capacity for invasion, dissemination, therapeutic resistance, and other "hallmarks of metastasis"[44]. While it is apparent that metastatic lesions are genetically divergent from their primary tumors[4,55], determining the subclonal architecture of primary and metastatic lesions may lead to novel therapeutic opportunities, the identification of predictive biomarkers and subsequent prophylactic treatment of those patients most likely to develop metastases.

The use of primary patient samples to study metastasis is limited by several factors[49], from initial procurement of specimens to gathering a sufficient number of cells for experiments. Additionally, models utilizing primary human cells have yet to be successful in recapitulating each stage of the metastatic cascade[44]. Instead, current frameworks investigate each metastatic stage in isolation, limiting the translational efficacy of putative therapeutic targets[40]. In the current study, we have established in-

house early-passage brain metastasis cell lines termed as brain metastasis initiating cells (BMICs) from primary patient samples of lung-to-brain metastases. We demonstrate that BMIC lines are enriched for stem cell properties as well as the ability to recapitulate the metastatic process both *in vitro* and *in vivo*. We also established a BMIC patient-derived xenotransplantation (PDXT) model to interrogate human lung-derived BM. We performed *in vitro* and *in vivo* RNA interference screens to identify SPOCK1, a TGF β target gene [29] and TWIST2 as important BMIC regulators. SPOCK1 in particular is a potent regulator of BMIC self- renewal, tumor initiation, and metastasis. Moreover, our results were translatable to clinical samples, where in a prospective cohort of primary non-small cell lung cancer patient slides, both targets were exclusively expressed in only those patients who developed BM. We then examined whether an indirect relationship exists between SPOCK1 and TWIST2 using protein-protein interaction networks, through which we identified a unique set of BMIC interactors that have significant prognostic value in lung cancer patient survival. One such marker, INHBA, a TGF-β ligand found mutated in lung adenocarcinoma [41], showed reduced expression in BMICs with knockdown of SPOCK1, further implicating a role for the TGF β pathway in BM development as well as identifying novel therapeutic targets in the pathway. With this work, we present a unique method of modelling human BM using patient-derived BMICs. Using this model, we have successfully identified and functionally validated novel regulators of primary and metastatic tumor growth, and clinically validated our targets as predictive biomarkers for BM. In blocking the metastatic process we aim to transform a uniformly fatal systemic disease into one that is locally controlled and eminently more treatable.

Materials and Methods

Patient Sample Processing and Cell Culture

Brain metastases (BM) originating from non-small cell lung carcinoma (NSCLC) primary samples were obtained from consenting patients, as approved by the Research Ethics Board at Hamilton Health Sciences. BMs were processed and maintained in Tumor Sphere Media (TSM) as previously described [54]. BMICs were grown as tumorspheres that were maintained at 37°C with a humidified atmosphere of 5% CO_2. Each BMIC line was characterized by performing limiting dilution assays (LDA) as previously described [45]. The most aggressive BMIC line with an enhanced engraftment capacity, BT478, was the primary BMIC line used for *in vivo* and RNAi experiments.

Cell Proliferation Assay

Single cells were plated in a 96-well plate at a density of 1,000 cells/200 µL per well in quadruplicate and incubated for four days. 20 µL of Presto Blue (Invitrogen) was added to each well approximately 2h prior to the readout time point. Fluorescence was measured using a FLUOstar Omega Fluorescence 556 Microplate reader (BMG LABTECH) at excitation and emission wavelengths of 535 nm and 600 nm, respectively. Readings were analyzed using Omega analysis software.

Zone Exclusion Migration Assay

A zone exclusion assay was utilized to assess cell migration over three 3 days, a timepoint determined to be most appropriate for the slow doubling times associated with GBM and BMIC populations. BMIC and glioblastoma (GBM) spheres were dissociated to single cells and plated at a density of 30,000 cells per well in a 96-well

plate containing TSM+1% FBS, and a 1% agar drop in the center of the well. Following cell adherence (24 hours), the agar drop was removed to create a cell-free zone, then wells washed gently with PBS and media replaced with TSM. Migration into the empty zone was monitored over 3 days, with time point images taken at day 0 and day 3. The percentage of migration was calculated as shown below:

$$\% \text{ migration} = \frac{\text{area of empty space at endpoint}}{\text{area of emtpy space at T=0}} \times 100$$

Flow cytometric characterization

BMIC tumorspheres were dissociated and single cells resuspended in PBS+2mM EDTA. Cell suspensions were stained with anti-CD133, anti-CD44, anti-CD15, anti-EpCAM or matched isotype controls (Miltenyi) and incubated for 30 minutes on ice. For TWIST2 and SPOCK1 co-expression analysis, single cell suspensions of BMIC lines BT478 and BT530 were stained with primary SPOCK1 antibody (Mouse monoclonal IgG, Abcam) followed by goat anti-mouse alexafluor 647 secondary antibody (1:1000, Invitrogen), and TWIST2 (Sheep Polyclonal IgG, R&D Systems) followed by donkey anti-sheep FITC secondary antibody (1:1000, Life Technologies), with 30 min incubations on ice for each antibody.

Samples were run on a MoFlo XDP Cell Sorter (Beckman Coulter). Dead cells were excluded using the viability dye 7AAD (1:10; Beckman Coulter). Compensation was performed using mouse IgG CompBeads (BD). Surface marker expression was defined as positive or negative based on the analysis regions established using the isotype control.

Immunofluorescence Staining of BMIC lines for SPOCK1 and TWIST2

50,000 cells from BMIC lines BT478, BT530, and BT751 were cultured on Matrigel coated- coverslips in 24 well plates for 72 hours. Wells were washed with PBS and cells fixed with 4% paraformaldehyde for 20 minutes at room temperature (RT), permeabilized with 0.1% Triton X-100 for 5 min, then blocked with 1% BSA at RT for 20 min. Cells were stained with primary Anti-human SPOCK1 antibody (10 µg, Mouse monoclonal IgG, Abcam) followed by donkey anti-mouse alexafluor 647 secondary antibody (1:1000, Invitrogen), or Anti-human TWIST2 (10 µg, Sheep polyclonal IgG, R&D Systems) followed by donkey anti-sheep FITC secondary antibody (1:1000, Life Technologies), for 2 hours at RT then followed by secondary antibodies for 1 hour at RT. Slides were then mounted with mounting medium and analyzed using Volocity imaging software.

***In vivo* Modelling of Metastasis**

All experimental procedures involving animals were reviewed and approved by McMaster University Animal Research Ethics Board (AREB). NOD-SCID mice were used for all experiments. Mice were anaesthesized using gas anaesthesia (Isoflurane: 5% induction, 2.5% maintenance) before minimally invasive surgery.

a) Intracranial injections (ICr)

   Intracranial injections were performed as previously described[53]. Briefly, 10µL of cell suspension (Online Resource 1 Table 2) was injected into the right frontal lobe of 8-10 week old mice.

b) Intrathoracic injections (IT)

30uL cell suspension ($5x10^5$ cells) mixed with 30µL of growth factor reduced matrigel (BD Bioscience) was injected into the right upper chest of 8-10 week old mice.

c) Intracardiac injections (ICa)

100µL cell suspension ($2.5x10^5$ cells) was injected into the left ventricle over 15 seconds in 8- 12 week old mice.

Mice were monitored weekly, and upon reaching endpoint brains and lungs (for IT and ICa injections) were harvested, sectioned, and paraffin-embedded for hematoxylin and eosin (H&E) and Anti-human COXIV immunohistochemistry. Images were scanned using an Aperio Slide Scanner and analyzed by ImageScope v11.1.2.760 software (Aperio).

Reverse transcription and quantitative PCR of mRNA

Total RNA was isolated using Norgen RNA extraction kit (Biotek) and reverse transcribed using qScript cDNA Super Mix (Quanta Biosciences) and a C1000 Thermo Cycler (Bio-Rad). qRT-PCR was performed using the Cfx96 (Bio-Rad) with SsoAdvanced SYBR Green (Bio-Rad) using gene specific primers (Online Resource 1 Table 7) and 28SrRNA as the internal control.

shRNA Dropout Screen

shRNA constructs (5-8 individual shRNA constructs per gene) were obtained through the RNAi Consortium and the pool was constructed as previously described [19]. Replication-incompetent lentivirus was produced as described in Venugopal et al., 2015[53].

400 million cells from BT478 BMIC line were transduced with the pooled lentiviral library at an MOI of 0.3 for the shRNA screens, with approximately 80,000-fold representation (cells per construct). Cells were treated for 48 hours with puromycin and then utilized for either the *in vitro* or *in vivo* screen. 10% of cells were collected for use as the baseline for all screens.

a) *In vitro tumorsphere formation shRNA screen*: transduced cells were cultured in T150 flasks, propagated as secondary spheres, and divided into three replicates. Tumorspheres were passaged for four passages. At each passage, genomic DNA was isolated for sequencing.

b) *In vivo* screen: 200,000 cells were injected intracranially into NOD-SCID mice (n=10). At endpoint, brains were harvested, perfused, and genomic DNA isolated for sequencing.

Lentivirus was prepared for individual shRNA constructs similar to the pooled shRNA library. BMIC lines were transduced with lentivirus along with an shGFP control and treated with puromycin for 48 hours prior to in vitro assessment of sphere formation, proliferation, and migration or in vivo injections by all three routes (ICr, IT and ICa) to assess tumor formation and metastasis.

shRNA Dropout Screen Analysis

A list of 150 genes involved in regulation of BM was expertly curated from the literature (Online Resource 1 Table 4). We used Wordle (http://wordle.net) to highlight biological processes associated with the 144 selected shRNAs (select genes in Online Resource 1 Table 5, full list in Online Resource 2). Using Pathway Data Integration Portal ver. 1. (pathDIP, http://ophid.utoronto.ca/pathDIP) we first performed pathway

enrichment analysis across 19 major pathways databases and identified 532 pathways that are significantly enriched by the selected shRNAs ($p < 0.05$). Pathway names were corrected by removing uninformative words (e.g., Homo sapiens) prior to generating the word frequency figure (Fig. 3b).

In vitro analysis

Libraries were sequenced on an Illumina HiSeq 2500. Library preparation and sequencing was carried out as described previously [20]. An average of 3.1M reads were obtained per sample. Reads consisting of 21-22 nucleotides, followed by a XhoI restriction site, allowing a single mismatch, were retained for mapping. Reads were mapped against a library-specific, non-redundant FASTA file using bowtie (v0.12.7) with the following command-line options: -l 21 -m 1 -n 2 --best –strata. On average, 99.5% of properly formatted reads aligned, allowing two mismatches and suppressing multi-mapping reads. Mapped hairpins were enumerated from the resulting SAM file using a bespoke Java program, which also merges together all samples and hairpin annotations. Each sample was normalized by summing the total number of reads assigned to hairpins, dividing the sum by 1,000,000, and then dividing the individual hairpin counts by the normalized sum. The resulting value is "reads per million mapped reads", which is then transformed to log-base2.

Linear regression was performed for each hairpin to model the dropout trend over time. Normalized abundance counts were regressed against the passage number using the lm function in R (v3.1.2). The majority of hairpins, as expected, had zero slope. The 5% of hairpins with the most negative slopes were selected for validation.

In vivo analysis

Sequencing and read mapping were performed as per the in vitro screen. Between 1.1 and 9.5M reads (mean = 4.8M) were processed per sample. Log fold-change values were computed for each hairpin in each in vivo sample by taking the ratio against the matching P0 hairpin abundance and transforming to log2. Only hairpins observed in both the P0 sample, and at least one of the in vivo samples were retained for further analysis. Gene depletion was then ranked by comparing the aggregate fold-change value across all samples to the population of negative control hairpins using the Wilcoxon rank-sum test. P-values were adjusted for multiple testing correction using the method of Benjamini and Hochberg. Finally, dropouts were ranked by the adjusted P-value.

Immunohistochemical staining of patient samples for SPOCK1 and TWIST2

4 µm formalin-fixed paraffin-embedded sections were dewaxed in 5 changes of xylene and brought down to water through graded alcohols. Antigen retrieval was performed by pretreatment with Tris-EDTA (pH 9.0), then primary antibodies for SPOCK1 (Abnova #H00117581-M01; 1/2000) or TWIST2 (Atlas #HPA007450; 1/800) applied. Endogenous peroxidase was blocked with 3% hydrogen peroxide. The detection systems used were MACH 4 universal HRP polymer system (TWIST2, Intermedico Cat# BC- M4U534) and species-specific ImmPRESS polymer system (SPOCK1, Vector Labs). After following kit instructions, color development was performed with freshly prepared DAB (DAKO Cat# K3468). Finally, sections were counterstained lightly with Mayer's Hematoxylin, dehydrated in alcohols, cleared in xylene and mounted with Permount mounting medium (Fisher cat# SP15-500). The optical densities (OD) of each

sample were determined by densitometric analysis using ImageJ software.

Protein-Protein Interaction Mapping of SPOCK1 and TWIST2

Physical protein interactions (PPI) for SPOCK1 and TWIST2 and their interacting partners were identified using Integrated Interaction Database (IID) v.2016-03 (http://ophid.utoronto.ca/iid)[22]. Protein interaction networks were visualized and analyzed using NAViGaTOR version 2.3 (http://ophid.utoronto.ca/navigator)[5]. Corresponding XML file in NAViGaTOR can be downloaded from http://www.cs.utoronto.ca/~juris/data/NCB/BMnetwork.xml. We calculated centrality/betweenness by counting the number of shortest paths through a given node and edge, connecting all possible pairs of nodes in the network, resulting in all pairs shortest path count (APSP). All proteins in the network were selected for pathways enrichment analysis as described above, using Pathway Data Integration Portal (pathDIP) ver. 1 http://ophid.utoronto.ca/pathDIP).

Edge centrality was evaluated by betweenness and nodes participating in the most central interactions were selected for further analysis of prognostic properties (All nodes, edges and betweenness scores are listed in Online Resource 1 Table 8 and connection derivations in Online Resource 3).

Cox Modelling of Prognostic Potential of Top 20 Genes Identified Through PPI Network

To evaluate multivariate prognostic potential of the top 20 genes we developed Cox proportional hazards model (SPOCK1, PLAT, APBB1, CELSR2, PLG, PLAU, PRSS3, PRKCQ, TCF4, INSR, TP53, ATXN1, EP300, JAG2, INHBA, LAMA3, ELAVL1, STMN2, VAV2, ARHGAP26), where the gene expressions served as only

covariates. Model was derived using R's package glmnet[13], applying ridge regression (also known as L2, or Tikhonov regularization) to prevent over-fitting. TCGA's lung adenocarcinoma (ADC) RNA-seq data were standardized by converting to z-scores and along with the corresponding clinical data were used as "training data". Model was validated on the independent, publicly available lung ADC data (GSE31210)[35], and it's prognostic performance was evaluated by concordance index (function survConcordance from R's package survival[50], v2.38.3) and area under receiver operating characteristics (ROC) curve – AUC, measured at the third year after initial time point (function AUC.cd from the R's survAUC package, v 1.0.5). Resulting model then predicted the risk score for each patient in the validation dataset. Patients were grouped into two groups based on the predicted risk score, using the threshold that was obtained prior to validation to maximize the hazard ratio obtained on the training data (for more details see Royston *et al.* 2013)[39]. Validated hazard ratio (HR) between these two groups, as well as associated statistical significance (Log-rank test) were finally calculated (function survdiff from the survival package) and Kaplan-Meier (KM) plot showing time dependent survival probabilities of these two groups was generated.

Generation of Univariate Gene Expression Kaplan-Meier Plots

Kaplan-Meier (KM) curves depicting patient survival by risk group based on SPOCK1 and TWIST2 expression in Fig. 6c, were generated using SurvExpress, a suite for validation of biomarkers and survival analysis[1] using TCGA Lung Adenocacinoma (TCGA-LUAD) dataset (version Sept. 2012)[6]. KM curves were generated from quantile-normalized TCGA lung ADC expression data and matching information about

patient survival.

Prognostic properties of the most central nodes were evaluated using http://kmplot.com (version 2015; data downloaded on March 6, 2016)[17]. Only lung ADC samples were used, and biased samples were removed (n=2,437). Auto select best cutoff and censor at threshold was used, with JetSet probe selection. Obtained hazard ratios and corresponding P-values were plotted in Fig. 7b. Resulting KM plots for overall survival are included in Fig. 7c and Online Resource 1 Fig. 11d; specifying probe sets used.

Statistical Analysis

Replicates from at least three samples were used for each experiment. Respective data represent mean±SD with n values listed in figure legends. Student's *t-test* and *2-way ANOVA* analyses using GraphPad Prism 5. $P<0.05$ was considered significant.

Results

Patient -derived BMICs exhibit stem cell characteristics and enhanced migratory potential *in vitro*

We successfully established several early-passage BM cell lines termed as brain metastasis initiating cells (BMICs) from human patient BM of lung origin (Online Resource 1 Table 1). BMIC lines formed tumorspheres [36] in serum-free media (Fig. 1a) and limiting dilution analysis (LDA) quantified median stem cell frequencies ranging from 1/100-1/350 cells (Fig. 1b, Online Resource 1 Fig. 1). BMIC sphere formation was comparable to that of primary glioblastoma (GBM). Thus, BMIC cultures are highly enriched for BMIC properties but not to homogeneity.

Migratory capacity was variable between individual BMIC lines (Fig. 1c), but overall BMIC lines had enhanced migration compared to invasive GBM lines. Through analysis of each patient's BMICs for known cancer stem cell (CSC) markers, we found differential expression of CSC surface markers CD133, CD15 [46] and CD44 [2,10,25], as well as epithelial cell adhesion marker (EpCAM) [59] (Fig. 1d, Online Resource 1 Fig. 2). Collectively, these data confirm the presence of a migratory CSC-like population *in vitro* and underscore the existence of patient-to-patient heterogeneity between BMIC lines. The variation of CSC expression levels between patients further confirms our previous work, where typical primary tumor CSCs markers are inefficient at identifying BMIC population [34] and emphasizes the necessity of novel BMIC markers.

Patient-derived xeno-transplantation models effectively recapitulate human brain metastases *in vivo*

We have utilized our unique BMICs to establish appropriate patient-derived xeno-transplantation (PDXT) models of BM that allow for serial *in vivo* enrichment and propagation of the functional tumor- initiating cell (TIC) population that initiates BMs. Firstly, BMIC tumor initiation capacity (TIC) was assessed *in vivo* through intracranial injections of two BMIC lines (BT478 and BT530) in NOD-SCID mice. This model was adapted from a PDXT model established by our lab for primary BTIC (Brain tumor initating cell) population[46]. *In vivo* LDA (Online Resource 1 Table 2) showed that BMICs were able to form tumors from as few as 100 cells (Fig. 1e). To evaluate if our BMICs retained original patient tumor marker profile, xeno-transplants were stained with routine marker profiles commonly utilized to diagnose brain metastases from a primary lung cancer, and we found that xenografts recapitulated the original patient tumor histology and cyto-architecture (Online Resource 1 Fig. 3).

Secondly, to assess BMICs ability to complete different stages of the metastatic cycle *in vivo*, we injected two BMIC lines (BT478 and BT530) into NOD-SCID mice through two different injection routes: a) intracardiac injections (ICa) and b) intrathoracic injections (IT) (Online Resource 1 Table 3). Homing potential of BMICs was assessed through ICa injections of 250,000 cells, resulting in preferential micro- and macro-metastasis formation in the brain and none in the lung or heart (Fig. 2, Online Resource 1 Fig. 4a-4b). IT injection of 500,000 cells showed that not only are BMICs capable of re-forming tumors in the lung environment, but they could migrate through the vasculature and seed the brain to form micro-metastases. However, mice succumbed to gross lung tumor burden before full macro-metastases developed (Fig. 2). Primary GBM lines were

injected through our previously developed BTIC-PDX model [46]as well as our novel BMIC PDXT model only achieved tumor formation through ICr injections and not through IT or ICa injections (Online Resource 1 Fig. 4c). Taken together, these data verify the self-renewal and metastatic properties of BMICs *in vivo*, and establishes our PDXT models as appropriate model systems for human BM.

shRNA drop out screen identifies TWIST2 and SPOCK1 as novel genetic regulators of brain metastasis

RNA interference (RNAi) using short-hairpin RNAs (shRNAs) provides a versatile tool allowing for rapid interrogation of gene function in mammalian cells, and has been used to identify genetic regulators of tumorigenesis and metastasis of various solid cancers[48,56,32].

In order to identify key regulators of BMIC migration and self-renewal, we functionally interrogated the 30 Nolte candidates previously identified by our lab[34] as well as an additional 120 key genes known to regulate metastasis [3,52,27] using pooled shRNA screens followed by *in vitro* and *in vivo* validation of chosen hits in our PDXT model systems (Fig. 3a). Pathway enrichment analysis using 19 pathway databases integrated from pathDIP revealed our 150 curated genes to be involved in several key processes and pathways; specifically, gene regulation and cell adhesion (Fig. 3b, Online Resource 1 Fig. 5, Table 5, Online Resource 2). We obtained a corresponding library of shRNAs targeting these 150 genes as well as negative control hairpins (shGFP, shLacZ) and positive control hairpins (shMET, mTOR pathway genes) (Online Resource 1 Table

4), and performed a functional *in vitro* shRNA dropout screen. Our pooled shRNA library included negative control hairpins (shGFP, shLacZ) and positive control hairpins (MET, mTOR pathway genes) (Online Resource 1 Fig. 6a-6c, Online Resource 2). Since tumorsphere culture conditions enrich for self-renewing stem-like populations with metastatic potential to seed the brain, we used these conditions to screen the 150 genes for their role in BMIC self-renewal *in vitro*. We identified several genes that had an influence on self-renewal capacity (Fig. 3d).

Genes from the top 5% of all hits were selected for further validation through our *in vitro* BMIC model based on their rate of dropout of from the shRNA screen (Fig. 3c), as depicted by the negative slope, as well as their novelty and potential role in BM development (Fig. 3d, Online Resource 1 Fig. 6a-6b,7-8). SPOCK1 and TWIST2 showed the most significant results *in vitro* and were validated further with our *in vivo* PDXT model. TWIST2 (or Dermo-1) belongs to the family of basic helix-loop-helix (bHLH) transcription factors and is implicated as an epithelial -mesenchymal transition (EMT) regulator[12], while SPOCK1 (or testican-1) is a seminal plasma proteoglycan and TGF-β target gene[29]. Both genes are overexpressed in several primary cancers[28,57], yet SPOCK1 has no known relevance to BM development. Knockdown of TWIST2 or SPOCK1 with shRNA in three patient-derived BMIC lines showed the most significant reduction of sphere formation, migration, and proliferation (Fig. 4, Online Resource 1 Fig. 9-10). shTWIST2 and shSPOCK1 reduced expression of CD133 as seen by FACS analysis (Online Resource 1 Fig. 11a), further implicating a SPOCK1 and TWIST2 in regulating BMIC stemness. Our functional shRNA screen

was repeated *in vivo* to validate our *in vitro* results. BMICs transduced with the pooled shRNA library were injected ICr into NOD-SCID mice, with tumor formation as the primary outcome measured. BMICs proliferate until tumors are detectable, where the initial homogeneous representation of transduced cells (P0) is skewed towards a set of tumor cells that received shRNAs that do not functionally affect the propagation of cells. SPOCK1 and TWIST2 were found to have high dropout rates as compared to initial representation at P0, confirming both genes as regulators of tumor formation from ICr injections (Fig. 5a, Online Resource 1 Fig. 6d-6e).

Knockdown of SPOCK1 or TWIST2 leads to inhibition of brain metastasis *in vivo*

BMICs were transduced with shGFP, shTWIST2 or shSPOCK1 and injected through the ICr, IT and ICa routes. In ICr injections, which served as controls to validate tumor engraftment, shTWIST2 in BMICs reduced tumor volume when compared to the shGFP transduced control cells, while shSPOCK1 prevented tumor formation altogether (Fig. 5b, n=2, p values not calculated). For IT injections, although BMICs with shTWIST2 did not reduce lung tumor formation, cells failed to metastasize to the brain. shSPOCK1 had both greatly reduced lung tumor formation and no BM (Fig. 5b). Mice receiving shSPOCK1 or shTWIST2 cells had a survival advantage over mice that received control cells through ICa injections. Moreover, knockdown of these genes completely ablated BMIC metastasis to the brain (Fig. 5b-5c). Collectively, these data implicate SPOCK1 as a vital regulator of BMIC self-renewal and the development of brain metastasis, whereas TWIST2 was confirmed to be important to initiation of metastasis of BMICs.

Expression levels of SPOCK1 and TWIST2 in lung cancer patient samples are predictive of brain metastasis

SPOCK1 and TWIST2 expression was profiled by immunohistochemistry (Fig. 6a) in primary NSCLC biopsies in patients who developed BM (n=12) and patients who did not (n=14) to determine if these proteins are predictive of BM formation (Online Resource 1 Table 6). The second cohort (n=14) had a median follow-up time of 36 months and all patients were clearly documented to have no clinical or radiological development BM, in 5 patients who were alive at 5 years and thriving, and in 9 patients who all died of other disease burden (primarily lung disease burden or metastasis to bone). Conversely, the majority of BM patients (n=12) were diagnosed synchronously with the primary lung cancer and thus the short 3-6 month survivorship of these patients was dictated by the BM. Follow up for both sets of patients differed only due to the nature of the disease; the poor survival associated with BM had a much shorter follow up period (19 months follow-up, with all patients dying from brain metastatic burden).

SPOCK1 and TWIST2 expression was only observed in primary lung cancer specimens in patients who ultimately developed BM (Fig. 6b, SPOCK1 $p<0.01$; TWIST2 $p<0.0003$), and was also present in the corresponding patient-matched BM (n=12). Interrogation of The Cancer Genome Database (TCGA) for SPOCK1 and TWIST2 expression in lung cancer patients determined that in a validation cohort of 255 NSCLC patients, high expression of these genes predicted poor patient survival (Fig. 6c, SPOCK1 $p=0.0036$; TWIST2 $p=0.0001$). This data suggests that SPOCK1 and TWIST2

may have clinical utility as predictive biomarkers of BM formation in NSCLC patients.

Protein-Protein interaction mapping between SPOCK1 and TWIST2 identifies novel pathway interactors

We characterized possible interactions between SPOCK1 and TWIST2 that could mediate their role in BM development. Co-expression of SPOCK1 and TWIST2 in BMICs was confirmed in a minority of BMICs though FACS analysis and immunofluorescence (Online Resource 1 Fig. 11b-c). Although co- expression of SPOCK1 and TWIST2 may not be essential to BMIC function, since we showed that each gene regulates functional BMIC properties, we questioned whether their interaction occurring in a small subset of BMICs could further identify novel regulators of brain metastasis. A direct interaction between SPOCK1 and TWIST2 was unlikely, as *in silico* probing of transcription factor binding databases revealed that the SPOCK1 promoter lacked a TWIST2 binding domains[24]. Thus, we derived a physical protein- protein interaction (PPI) network to identify indirect connections between TWIST2 and SPOCK1 (Fig. 7a). In a protein-protein network model, betweenness centrality refers to the number of shortest paths going through a given edge, where higher centrality denotes a very important protein hub. We analyzed centrality/betweenness of the nodes and edges to identify the most central 20 connector proteins (Online Resource 1 Table 8). These genes were then interrogated for prognostic value using transcriptomic data from a NSCLC patient cohort. Individually, nineteen of the twenty genes were found to have significant impact on patient survival (Fig. 7b, Online Resource 1 Fig. 11d and Table 8).

We applied these unique connector genes as a signature to probe the TCGA mRNA-seq dataset of 433 lung adenocarcinoma patients, then validated in an independent dataset of 204 lung adenocarcinoma patients. Strikingly, we found that the signature had significant prognostic value (Fig. 7c). RTPCR screening of select PPI connector genes found expression of only INHBA, the most direct connector between SPOCK1 and TWIST2, to be significantly reduced in BMICs with shTWIST2 or shSPOCK1 (Fig. 7d, Online Resource 1 Fig. 12). INHBA is a ligand of the TGF-β superfamily and was found to be significantly mutated in lung adenocarcinoma[41,9], and further hints at the involvement of the TGFbeta pathway in BM development. Collectively, these data implicate a novel set of connectors between TWIST2 and SPOCK1 involved in BM development that could predict patient prognosis, and provide unique therapeutic targets.

Discussion

The invasive nature of BM and their ability to escape aggressive treatments predicts uniformly poor patient outcome[47]. Advances in screening, detection, and therapeutics for systemic cancers have led to an increase in cancer patient survival, yet leaves cancer survivors vulnerable to an increased prevalence of BM[23,38]. Here we have successfully developed BMIC lines from primary patient BM originating from lung cancer, where these samples represent an enriched source of human cells capable of completing the lung-to-brain metastatic cascade.

Syngeneic mouse models have significantly improved our understanding of molecular factors that govern subclone survival throughout stages of metastasis [16,18,3], though the clinical utility of these models is limited as transgenic murine models may not recapitulate the inter- and intratumoral heterogeneity of lesions in humans. Current models for studying metastasis investigate each stage in isolation, failing to capture the dynamic evolution of tumor subclones during primary tumor growth. Nonetheless these models have contributed to the identification of metastatic drivers, such as ST6GALNAC5[3], L1CAM[7] from breast cancer, and LEF1 and HOXB9[33] (Nguyen 2009) for lung cancer. When paired with RNAi screens, these models have aided the identification novel metastasis suppressor genes[15,32].

Through our BMICs derived from patient samples of BM of lung origin, we have successfully generated an appropriate and feasible model of human BM. We build upon our previous work, where we had confirmed our BMICs to possess typical stem characteristics such as self-renewal and tumor initiation[34]. In our current work, we

show that our BMICs are capable of completing the complexities of metastasizing to the brain. Our unique PDXT model provides a unique opportunity to isolate and characterize BMICs as well as provides a novel platform to screen and validate BM treatments.

Our shRNA dropout screens performed with our *in vitro* BMIC and *in vivo* BMIC PDXT model systems identified SPOCK1 and TWIST2 as regulators of BMICs, with SPOCK1 in particular proving to be critical to BMIC self-renewal, tumor initiation and migration. BMICs with knockdown of SPOCK1 and TWIST2 also displayed reduction in stemness as depicted by downregulation of CSC marker CD133 expression, suggesting a potential relationship between SPOCK1, TWIST2 and stemness. Functional validation of both genes by knockdown in our PDXT model resulted in complete abrogation of brain metastasis through ICa and IT injections. Interestingly, knockdown of SPOCK1 completely inhibited tumor formation in both the primary lung and secondary brain environments, implicating SPOCK1 as an essential regulator of tumor initiation irrespective of the microenvironment. The dramatic reduction in secondary sphere formation seen with shSPOCK1 further corroborated its role in governing BMIC self-renewal. Conversely, knockdown of TWIST2 had no significant effect on primary lung tumor formation but reduced BM, providing further validation for the role of TWIST2 in BMIC initiation of metastasis. Our data implicates SPOCK1 and TWIST2 in metastatic progression, and may prove to be useful as candidate genes in the detection of migrating BMICs or circulating tumor cells (CTCs). Development of anti-metastatic therapies has been limited due to a lack of understanding of the intricacies of the metastatic cycle, with most drugs targeting the end stages[30].

Systemic cancer progression follows two basic models: linear progression, where the metastatic cells develop within the primary tumor prior to dissemination to a secondary site, or parallel progression that is independent of primary tumor formation. Current research favours the parallel progression model, indicating a need to re-evaluate current treatment modalities[21]. Additionally, recent studies have shown that the presence of metastatic CSCs correlates with the overall incidence of metastasis development in patients, and so offers as a novel pre-metastatic therapeutic option in metastasis prevention. However, targeting these cells faces several difficulties. For instance, the limited knowledge of the biology of metastatic CTCs challenges the ability to precisely identify this particular population[11], and conventional therapeutics have a short time in circulation that may result in inefficient exposure and consequently ineffective killing of CTCs[26]. The identification of novel biomarkers of this metastatic population opens up a unique therapeutic avenue for prevention of metastatic development. Early detection and therapeutic targeting of CTCs based on SPOCK1 or TWIST2 expression could terminate the metastatic process at it's initiation, ideally reducing the risk of BM development.

Given that not all lung cancer patients develop BM, the immediate clinical utility of our findings is in the ability to identify those patients who are more likely to develop a BM such that they may receive targeted therapy or an escalation in current treatment protocols of NSCLC. Interestingly, SPOCK1 and TWIST2 immunohistochemistry was only positive in those lung cancer patients who developed BM, whereas lung cancers that did not develop BMs were devoid of SPOCK1 and TWIST2 expression. This data

suggests that SPOCK1 and TWIST2 may have clinical utility as predictive biomarkers of BM formation in newly diagnosed NSCLC patients.

Despite SPOCK1 and TWIST2 being implicated in other primary cancers and metastases[43,58], to date no work has shown any relationship between these two genes. We have shown that although SPOCK1 and TWIST2 are co-expressed in a minority population of BMICs, they have no direct interaction. Through PPI networks analysis we have identified several genes that connect SPOCK1 and TWIST2 indirectly and are specific to lung tissue. Several of these connecting genes have been implicated in neurological development[42] or the progression of neural diseases such as Alzheimer's[60,8] suggesting that these genes may predispose BMICs to home from the lung to the brain. None of these genes have been implicated in co-operating with SPOCK1 or in BM development. Of the top twenty connector genes with the highest centrality in the SPOCK1-TWIST2 PPI network (Fig. 7a), nineteen genes each had significant predictive potential for BMs in a primary lung adenocarcinoma patient cohort. When applied as a signature, these genes had an even greater impact on predicting poor patient survival. Expression of the most significant connector, INHBA, was correlated with SPOCK1 or TWIST2 expression, validating an interaction between these three genes. INHBA is a known TGFbeta ligand, where it's binding to TGFB receptors promotes the downstream activation of the SMADs pathway[51]. Activation of the TGFbeta pathway upregulates expression of several transcription factors known to regulate the epithelial- mesenchymal transition (EMT), such as TWIST2[31]. SPOCK1 has also been shown to be a TGFbeta downstream target gene, where its activity also

promotes EMT[29]. Inhibition of TGFbeta pathway through INHBA has been shown to reduce experimental metastatic development[51]. From this circumstantial evidence, we suggest a possible interactive pathway of INHBA-activated TGFbeta regulation of SPOCK1 and TWIST2, promoting BMIC proliferation and metastasis through EMT.

The known involvement of TGF-β with SPOCK1 and INHBA implicates a role for the TGF-β signalling pathway in BM development[41,29]. Our data presents a novel group of genes interact with TWIST2 and SPOCK1 to influence BMIC metastasis and BM development in lung cancer patients. The multifaceted functional roles of BMIC genes in driving metastasis and the potent ability of BMICs to evade most therapies render BMIC regulatory genes as ideal therapeutic targets.

In conclusion, we have successfully developed a novel BMIC model system of human lung-to- brain metastasis through the establishment of unique patient-derived BMIC lines. Through our clinically relevant BMIC models, we identified SPOCK1 as a novel predictive biomarker of BM and critical regulators of the metastatic process for lung-derived BM. We have also identified a predictive prognostic signature of lung cancer patients and present novel therapeutic targets. Blocking the metastatic process would transform a uniformly fatal systemic disease into a locally controlled and eminently more treatable one.

Authors' Contributions

Conceptualization and Design: M. Singh, C. Venugopal, S. Singh
Methodology: M. Singh, C. Venugopal, N. McFarlane, S. Mahendram, D. Bakhshinyan, P. Vora, M. Qazi, T. Vijaykumar, M. Dhillon, K. Durrer, A. Tong
Data Analysis & Interpretation: M. Singh, C. Venugopal, T. Tokar, K. Brown., R. Hallet, J. Moffat, I. Jurisica, D. Kaplan, S. Singh
Writing, review, and/or revision of the manuscript: M. Singh, C. Venugopal, N. McFarlane, S. Mahendram, D. Bakhshinyan, P. Vora, M. Qazi, B. Manoranjan, J. Moffat,

I. Jurisica, D, S. Singh Supervision, JA. Hassell, J. Moffat, I. Jurisica, S. Singh

Acknowledgements

Financial Support: This work was supported by funds from the Department of Surgery at McMaster University, Ontario Institute for Cancer Research Cancer Stem Cell Program, a Canadian Cancer Society Research Institute Innovation Grant and The Boris Family Fund for Brain Metastasis Research for Dr.
Sheila Singh; Brain Canada PhD Studentship for Mohini Singh; Ontario Research Fund (GL2-01-030), McLaughlin Centre Accelerator grant (#MC-2013-05), Canada Research Chair Program (CRC #225404), and Canada Foundation for Innovation (CFI #12301, #203373, #29272, #225404, #30865) supported Dr. Igor Jurisica.

Disclosure of Potential Conflict of Interest: The authors declare no potential conflict of interest.

References

1. Aguirre-Gamboa R, Gomez-Rueda H, Martinez-Ledesma E, Martinez-Torteya A, Chacolla-Huaringa R, Rodriguez-Barrientos A, Tamez-Pena JG, Trevino V (2013) SurvExpress: an online biomarker validation tool and database for cancer gene expression data using survival analysis. PloS one 8:e74250. doi:10.1371/journal.pone.0074250
2. Al-Hajj M, Wicha MS, Benito-Hernandez A, Morrison SJ, Clarke MF (2003) Prospective identification of tumorigenic breast cancer cells. Proceedings of the National Academy of Sciences of the United States of America 100:3983-3988. doi:10.1073/pnas.0530291100
3. Bos PD, Zhang XH, Nadal C, Shu W, Gomis RR, Nguyen DX, Minn AJ, van de Vijver MJ, Gerald WL, Foekens JA, Massague J (2009) Genes that mediate breast cancer metastasis to the brain. Nature 459:1005-1009. doi:10.1038/nature08021
4. Brastianos PK, Carter SL, Santagata S, Cahill DP, Taylor-Weiner A, Jones RT, Van Allen EM, Lawrence MS, Horowitz PM, Cibulskis K, Ligon KL, Tabernero J, Seoane J, Martinez-Saez E, Curry WT, Dunn IF, Paek SH, Park SH, McKenna A, Chevalier A, Rosenberg M, Barker FG, 2nd, Gill CM, Van Hummelen P, Thorner AR, Johnson BE, Hoang MP, Choueiri TK, Signoretti S, Sougnez C, Rabin MS, Lin NU, Winer EP, Stemmer-Rachamimov A, Meyerson M, Garraway L, Gabriel S, Lander ES, Beroukhim R, Batchelor TT, Baselga J, Louis DN, Getz G, Hahn WC (2015) Genomic Characterization of Brain Metastases Reveals Branched Evolution and Potential Therapeutic Targets. Cancer discovery 5:1164-1177. doi:10.1158/2159-8290.CD-15-0369
5. Brown KR, Otasek D, Ali M, McGuffin MJ, Xie W, Devani B, Toch IL, Jurisica I (2009) NAViGaTOR: Network Analysis, Visualization and Graphing Toronto. Bioinformatics 25:3327-3329. doi:10.1093/bioinformatics/btp595
6. Cancer Genome Atlas Research N (2014) Comprehensive molecular profiling of lung adenocarcinoma. Nature 511:543-550. doi:10.1038/nature13385
7. Chen K, Huang YH, Chen JL (2013) Understanding and targeting cancer stem cells: therapeutic implications and challenges. Acta pharmacologica Sinica 34:732-740. doi:10.1038/aps.2013.27
8. Cousin E, Hannequin D, Ricard S, Mace S, Genin E, Chansac C, Brice A, Dubois B, Frebourg T, Mercken L, Benavides J, Pradier L, Campion D, Deleuze JF (2003) A risk for early-onset Alzheimer's disease associated with the APBB1 gene (FE65) intron 13 polymorphism. Neurosci Lett 342:5-8
9. Ding L, Getz G, Wheeler DA, Mardis ER, McLellan MD, Cibulskis K, Sougnez C, Greulich H, Muzny DM, Morgan MB, Fulton L, Fulton RS, Zhang Q, Wendl MC, Lawrence MS, Larson DE, Chen K, Dooling DJ, Sabo A, Hawes AC, Shen H, Jhangiani SN, Lewis LR, Hall O, Zhu Y, Mathew T, Ren Y, Yao J, Scherer SE, Clerc K, Metcalf GA, Ng B, Milosavljevic A, Gonzalez-Garay ML, Osborne JR, Meyer R, Shi X, Tang Y, Koboldt DC, Lin L, Abbott R, Miner TL, Pohl C, Fewell G, Haipek C, Schmidt H, Dunford-Shore BH, Kraja A, Crosby SD, Sawyer CS, Vickery T,

Sander S, Robinson J, Winckler W, Baldwin J, Chirieac LR, Dutt A, Fennell T, Hanna M, Johnson BE, Onofrio RC, Thomas RK, Tonon G, Weir BA, Zhao X, Ziaugra L, Zody MC, Giordano T, Orringer MB, Roth JA, Spitz MR, Wistuba, II, Ozenberger B, Good PJ, Chang AC, Beer DG, Watson MA, Ladanyi M, Broderick S, Yoshizawa A, Travis WD, Pao W, Province MA, Weinstock GM, Varmus HE, Gabriel SB, Lander ES, Gibbs RA, Meyerson M, Wilson RK (2008) Somatic mutations affect key pathways in lung adenocarcinoma. Nature 455:1069-1075. doi:10.1038/nature07423

10. Du L, Wang H, He L, Zhang J, Ni B, Wang X, Jin H, Cahuzac N, Mehrpour M, Lu Y, Chen Q (2008) CD44 is of functional importance for colorectal cancer stem cells. Clinical cancer research : an official journal of the American Association for Cancer Research 14:6751-6760. doi:10.1158/1078- 0432.CCR-08-1034
11. Faltas B (2012) Cornering metastases: therapeutic targeting of circulating tumor cells and stem cells. Frontiers in oncology 2:68. doi:10.3389/fonc.2012.00068
12. Fang X, Cai Y, Liu J, Wang Z, Wu Q, Zhang Z, Yang CJ, Yuan L, Ouyang G (2011) Twist2 contributes to breast cancer progression by promoting an epithelial-mesenchymal transition and cancer stem- like cell self-renewal. Oncogene 30:4707-4720. doi:10.1038/onc.2011.181
13. Friedman J, Hastie T, Tibshirani R (2010) Regularization Paths for Generalized Linear Models via Coordinate Descent. J Stat Softw 33:1-22
14. Gaspar L, Scott C, Rotman M, Asbell S, Phillips T, Wasserman T, McKenna WG, Byhardt R (1997) Recursive partitioning analysis (RPA) of prognostic factors in three Radiation Therapy Oncology Group (RTOG) brain metastases trials. International journal of radiation oncology, biology, physics 37:745-751
15. Gobeil S, Zhu X, Doillon CJ, Green MR (2008) A genome-wide shRNA screen identifies GAS1 as a novel melanoma metastasis suppressor gene. Genes & development 22:2932-2940. doi:10.1101/gad.1714608
16. Gupta GP, Nguyen DX, Chiang AC, Bos PD, Kim JY, Nadal C, Gomis RR, Manova-Todorova K, Massague J (2007) Mediators of vascular remodelling co-opted for sequential steps in lung metastasis. Nature 446:765-770. doi:10.1038/nature05760
17. Gyorffy B, Surowiak P, Budczies J, Lanczky A (2013) Online survival analysis software to assess the prognostic value of biomarkers using transcriptomic data in non-small-cell lung cancer. PloS one 8:e82241. doi:10.1371/journal.pone.0082241
18. Kang Y, Siegel PM, Shu W, Drobnjak M, Kakonen SM, Cordon-Cardo C, Guise TA, Massague J (2003) A multigenic program mediating breast cancer metastasis to bone. Cancer cell 3:537-549
19. Ketela T, Heisler LE, Brown KR, Ammar R, Kasimer D, Surendra A, Ericson E, Blakely K, Karamboulas D, Smith AM, Durbic T, Arnoldo A, Cheung-Ong K, Koh JL, Gopal S, Cowley GS, Yang X, Grenier JK, Giaever G, Root DE, Moffat J, Nislow C (2011) A comprehensive platform for highly multiplexed mammalian functional genetic screens. BMC Genomics 12:213. doi:10.1186/1471-2164-12-213
20. Kittanakom S, Arnoldo A, Brown KR, Wallace I, Kunavisarut T, Torti D, Heisler LE, Surendra A, Moffat J, Giaever G, Nislow C (2013) Miniature short hairpin RNA screens to characterize antiproliferative drugs. G3 (Bethesda) 3:1375-1387.

doi:10.1534/g3.113.006437
21. Klein CA (2009) Parallel progression of primary tumors and metastases. Nature reviews Cancer 9:302-312. doi:10.1038/nrc2627
22. Kotlyar M, Pastrello C, Sheahan N, Jurisica I (2016) Integrated interactions database: tissue-specific view of the human and model organism interactomes. Nucleic acids research 44:D536-541. doi:10.1093/nar/gkv1115
23. Langley RR, Fidler IJ (2013) The biology of brain metastasis. Clin Chem 59:180-189. doi:10.1373/clinchem.2012.193342
24. Lee YS, Lee HH, Park J, Yoo EJ, Glackin CA, Choi YI, Jeon SH, Seong RH, Park SD, Kim JB (2003) Twist2, a novel ADD1/SREBP1c interacting protein, represses the transcriptional activity of ADD1/SREBP1c. Nucleic acids research 31:7165-7174
25. Leung EL, Fiscus RR, Tung JW, Tin VP, Cheng LC, Sihoe AD, Fink LM, Ma Y, Wong MP (2010) Non-small cell lung cancer cells expressing CD44 are enriched for stem cell-like properties. PloS one 5:e14062. doi:10.1371/journal.pone.0014062
26. Li J, Sharkey CC, Huang D, King MR (2015) Nanobiotechnology for the Therapeutic Targeting of Cancer Cells in Blood. Cellular and molecular bioengineering 8:137-150. doi:10.1007/s12195- 015-0381-z
27. Mani SA, Guo W, Liao MJ, Eaton EN, Ayyanan A, Zhou AY, Brooks M, Reinhard F, Zhang CC, Shipitsin M, Campbell LL, Polyak K, Brisken C, Yang J, Weinberg RA (2008) The epithelial-mesenchymal transition generates cells with properties of stem cells. Cell 133:704-715. doi:10.1016/j.cell.2008.03.027
28. Mao Y, Zhang N, Xu J, Ding Z, Zong R, Liu Z (2012) Significance of heterogeneous Twist2 expression in human breast cancers. PloS one 7:e48178. doi:10.1371/journal.pone.0048178
29. Miao L, Wang Y, Xia H, Yao C, Cai H, Song Y (2013) SPOCK1 is a novel transforming growth factor-beta target gene that regulates lung cancer cell epithelial-mesenchymal transition. Biochem Biophys Res Commun 440:792-797. doi:10.1016/j.bbrc.2013.10.024
30. Mina LA, Sledge GW, Jr. (2011) Rethinking the metastatic cascade as a therapeutic target. Nature reviews Clinical oncology 8:325-332. doi:10.1038/nrclinonc.2011.59
31. Murakami M, Ohkuma M, Nakamura M (2008) Molecular mechanism of transforming growth factor- beta-mediated inhibition of growth arrest and differentiation in a myoblast cell line. Development, growth & differentiation 50:121-130. doi:10.1111/j.1440-169X.2007.00982.x
32. Murugaesu N, Iravani M, van Weverwijk A, Ivetic A, Johnson DA, Antonopoulos A, Fearns A, Jamal- Hanjani M, Sims D, Fenwick K, Mitsopoulos C, Gao Q, Orr N, Zvelebil M, Haslam SM, Dell A, Yarwood H, Lord CJ, Ashworth A, Isacke CM (2014) An in vivo functional screen identifies ST6GalNAc2 sialyltransferase as a breast cancer metastasis suppressor. Cancer discovery 4:304- 317. doi:10.1158/2159-8290.CD-13-0287
33. Nguyen DX, Chiang AC, Zhang XH, Kim JY, Kris MG, Ladanyi M, Gerald WL, Massague J (2009) WNT/TCF signaling through LEF1 and HOXB9 mediates

lung adenocarcinoma metastasis. Cell 138:51-62. doi:10.1016/j.cell.2009.04.030

34. Nolte SM, Venugopal C, McFarlane N, Morozova O, Hallett RM, O'Farrell E, Manoranjan B, Murty NK, Klurfan P, Kachur E, Provias JP, Farrokhyar F, Hassell JA, Marra M, Singh SK (2013) A cancer stem cell model for studying brain metastases from primary lung cancer. J Natl Cancer Inst 105:551- 562. doi:10.1093/jnci/djt022
35. Okayama H, Kohno T, Ishii Y, Shimada Y, Shiraishi K, Iwakawa R, Furuta K, Tsuta K, Shibata T, Yamamoto S, Watanabe S, Sakamoto H, Kumamoto K, Takenoshita S, Gotoh N, Mizuno H, Sarai A, Kawano S, Yamaguchi R, Miyano S, Yokota J (2012) Identification of genes upregulated in ALK- positive and EGFR/KRAS/ALK-negative lung adenocarcinomas. Cancer research 72:100-111. doi:10.1158/0008-5472.CAN-11-1403
36. Pastrana E, Silva-Vargas V, Doetsch F (2011) Eyes wide open: a critical review of sphere-formation as an assay for stem cells. Cell Stem Cell 8:486-498. doi:10.1016/j.stem.2011.04.007
37. Patchell RA (2003) The management of brain metastases. Cancer treatment reviews 29:533-540
38. Rahmathulla G, Toms SA, Weil RJ (2012) The molecular biology of brain metastasis. Journal of oncology 2012:723541. doi:10.1155/2012/723541
39. Royston P, Altman DG (2013) External validation of a Cox prognostic model: principles and methods. BMC Med Res Methodol 13:33. doi:10.1186/1471-2288-13-33
40. Saxena M, Christofori G (2013) Rebuilding cancer metastasis in the mouse. Molecular oncology 7:283-296. doi:10.1016/j.molonc.2013.02.009
41. Seder CW, Hartojo W, Lin L, Silvers AL, Wang Z, Thomas DG, Giordano TJ, Chen G, Chang AC, Orringer MB, Beer DG (2009) Upregulated INHBA expression may promote cell proliferation and is associated with poor survival in lung adenocarcinoma. Neoplasia 11:388-396
42. Shima Y, Kengaku M, Hirano T, Takeichi M, Uemura T (2004) Regulation of dendritic maintenance and growth by a mammalian 7-pass transmembrane cadherin. Developmental cell 7:205-216. doi:10.1016/j.devcel.2004.07.007
43. Shu YJ, Weng H, Ye YY, Hu YP, Bao RF, Cao Y, Wang XA, Zhang F, Xiang SS, Li HF, Wu XS, Li ML, Jiang L, Lu W, Han BS, Jie ZG, Liu YB (2015) SPOCK1 as a potential cancer prognostic marker promotes the proliferation and metastasis of gallbladder cancer cells by activating the PI3K/AKT pathway. Mol Cancer 14:12. doi:10.1186/s12943-014-0276-y
44. Singh M, Manoranjan B, Mahendram S, McFarlane N, Venugopal C, Singh SK (2014) Brain metastasis- initiating cells: survival of the fittest. International journal of molecular sciences 15:9117-9133. doi:10.3390/ijms15059117
45. Singh SK, Clarke ID, Terasaki M, Bonn VE, Hawkins C, Squire J, Dirks PB (2003) Identification of a cancer stem cell in human brain tumors. Cancer research 63:5821-5828
46. Singh SK, Hawkins C, Clarke ID, Squire JA, Bayani J, Hide T, Henkelman RM, Cusimano MD, Dirks PB (2004) Identification of human brain tumor initiating

cells. Nature 432:396-401. doi:10.1038/nature03128
47. Soffietti R, Ruda R, Mutani R (2002) Management of brain metastases. J Neurol 249:1357-1369. doi:10.1007/s00415-002-0870-6
48. Su B, Gao L, Baranowski C, Gillard B, Wang J, Ransom R, Ko HK, Gelman IH (2014) A genome-wide RNAi screen identifies FOXO4 as a metastasis-suppressor through counteracting PI3K/AKT signal pathway in prostate cancer. PloS one 9:e101411. doi:10.1371/journal.pone.0101411
49. Tentler JJ, Tan AC, Weekes CD, Jimeno A, Leong S, Pitts TM, Arcaroli JJ, Messersmith WA, Eckhardt SG (2012) Patient-derived tumor xenografts as models for oncology drug development. Nature reviews Clinical oncology 9:338-350. doi:10.1038/nrclinonc.2012.61
50. Therneau TMG, Patricia M. (2000) Modeling Survival Data: Extending the Cox Model. Statistics for Biology and Health, 1 edn. Springer-Verlag New York. doi:10.1007/978-1-4757-3294-8
51. Tsuchida K, Nakatani M, Uezumi A, Murakami T, Cui X (2008) Signal transduction pathway through activin receptors as a therapeutic target of musculoskeletal diseases and cancer. Endocrine journal 55:11-21
52. Valiente M, Obenauf AC, Jin X, Chen Q, Zhang XH, Lee DJ, Chaft JE, Kris MG, Huse JT, Brogi E, Massague J (2014) Serpins promote cancer cell survival and vascular co-option in brain metastasis. Cell 156:1002-1016. doi:10.1016/j.cell.2014.01.040
53. Venugopal C, Hallett R, Vora P, Manoranjan B, Mahendram S, Qazi MA, McFarlane N, Subapanditha M, Nolte SM, Singh M, Bakhshinyan D, Garg N, Vijayakumar T, Lach B, Provias JP, Reddy K, Murty NK, Doble BW, Bhatia M, Hassell JA, Singh SK (2015) Pyrvinium Targets CD133 in Human Glioblastoma Brain Tumor-Initiating Cells. Clinical cancer research : an official journal of the American Association for Cancer Research 21:5324-5337. doi:10.1158/1078-0432.CCR-14-3147
54. Venugopal C, McFarlane NM, Nolte S, Manoranjan B, Singh SK (2012) Processing of primary brain tumor tissue for stem cell assays and flow sorting. Journal of visualized experiments : JoVE. doi:10.3791/4111
55. Waghorne C, Thomas M, Lagarde A, Kerbel RS, Breitman ML (1988) Genetic evidence for progressive selection and overgrowth of primary tumors by metastatic cell subpopulations. Cancer research 48:6109-6114
56. Wolf J, Muller-Decker K, Flechtenmacher C, Zhang F, Shahmoradgoli M, Mills GB, Hoheisel JD, Boettcher M (2014) An in vivo RNAi screen identifies SALL1 as a tumor suppressor in human breast cancer with a role in CDH1 regulation. Oncogene 33:4273-4278. doi:10.1038/onc.2013.515
57. Yang C, Fischer-Keso R, Schlechter T, Strobel P, Marx A, Hofmann I (2015) Plakophilin 1-deficient cells upregulate SPOCK1: implications for prostate cancer progression. Tumor Biol. doi:10.1007/s13277-015-3628-3
58. Yu F, Li G, Gao J, Sun Y, Liu P, Gao H, Li P, Lei T, Chen Y, Cheng Y, Zhai X, Sayari AJ, Huang H, Mu Q (2016) SPOCK1 is upregulated in recurrent glioblastoma and contributes to metastasis and Temozolomide resistance. Cell

Prolif. doi:10.1111/cpr.12241

59. Zakaria N, Yusoff NM, Zakaria Z, Lim MN, Baharuddin PJ, Fakiruddin KS, Yahaya B (2015) Human non- small cell lung cancer expresses putative cancer stem cell markers and exhibits the transcriptomic profile of multipotent cells. BMC Cancer 15:84. doi:10.1186/s12885-015-1086-3
60. Zhang C, Browne A, Child D, Divito JR, Stevenson JA, Tanzi RE (2010) Loss of function of ATXN1 increases amyloid beta-protein levels by potentiating beta-secretase processing of beta-amyloid precursor protein. The Journal of biological chemistry 285:8515-8526. doi:10.1074/jbc.M109.079079

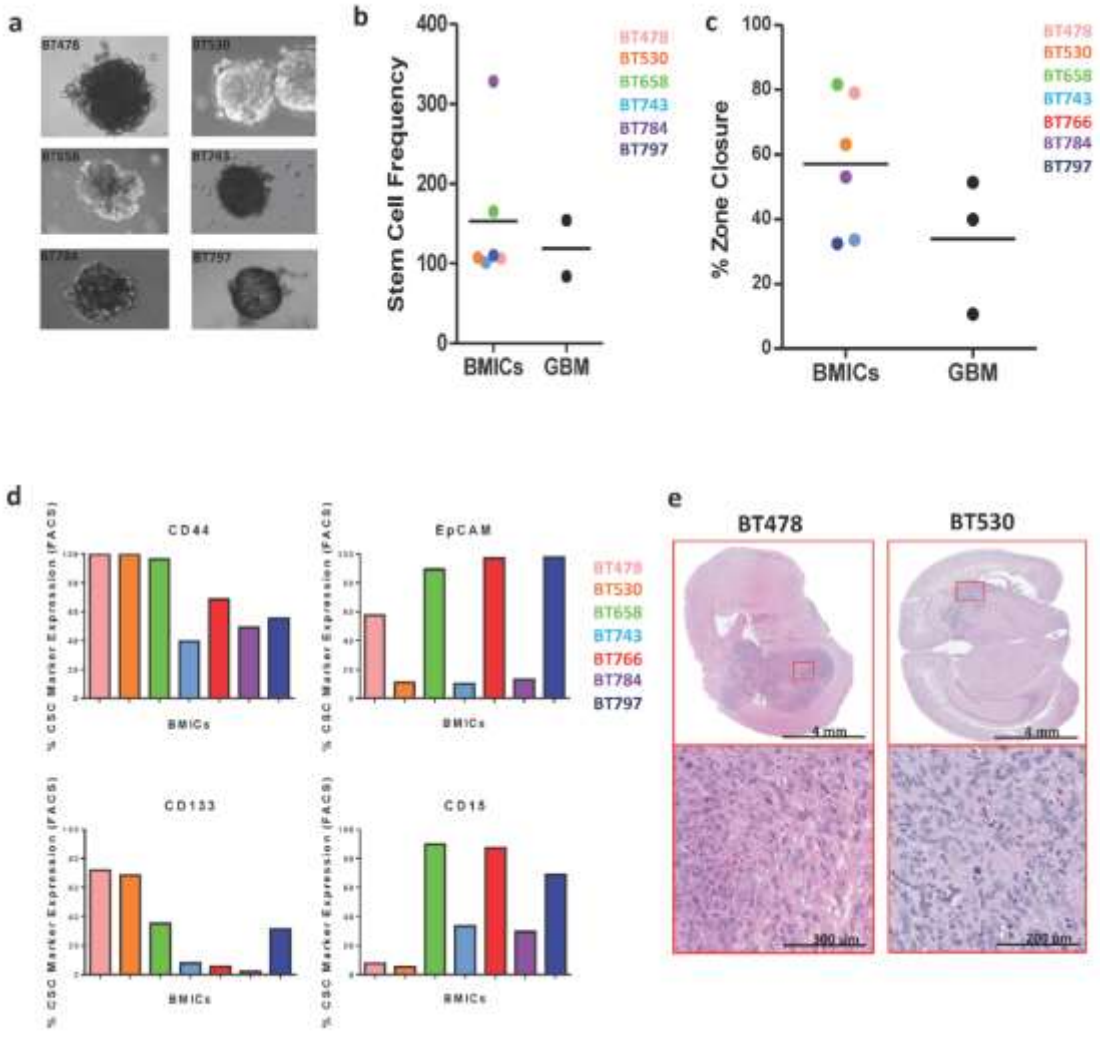

Figure 1. Characterization of BMICs in primary BM from the lung. **a** Representative bright field images of BMIC spheres (20x). **b** Self-renewal of BMICs and primary GBM CSCs determined through secondary sphere formation. **c** Migration capacity of BMICs and

GBMs. **d** Surface expression of CSC markers. Each dot represents a single patient sample, bar indicates mean. **e** BT478 and BT530 reformed tumors with as low as 100 cells after intracranial (IC) injections. Images shown are representative H&E sections. Red scale bar = 4 mm, blue scale bar = 100 μM, n=5.

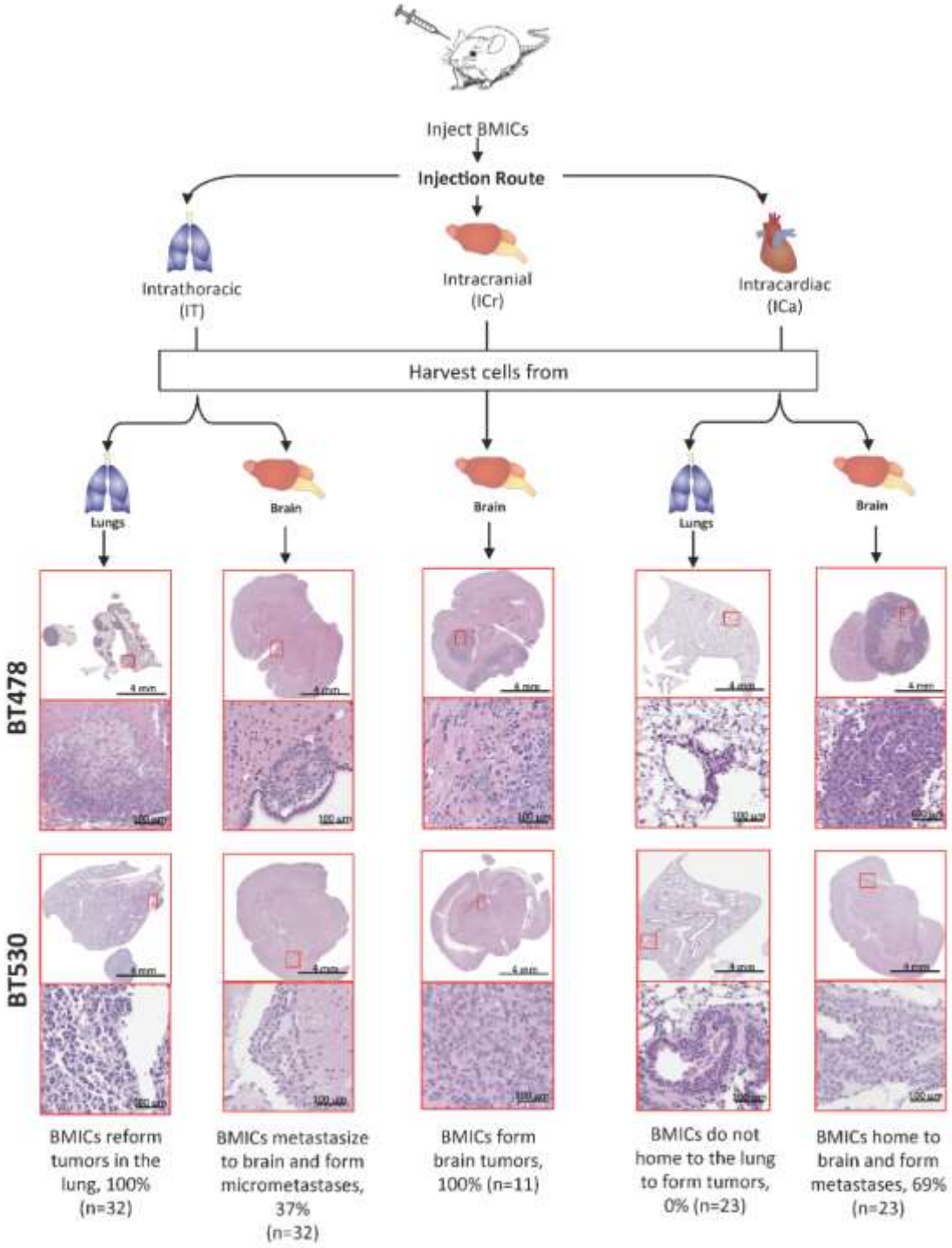

Figure 2. Development of a novel human-mouse xenograft model of lung to brain metastasis**.** Schematic representation of novel in vivo BM model. BMIC capacity is

demonstrated through formation of seeded tumor cell nests and large tumors in the brain after IT and ICa injections, respectively. Images shown are representative H&E sections. Red scale bar = 4 mm, blue scale bar = 100 µM. ICr, n=2; ICa, n=6; IT, n=6).

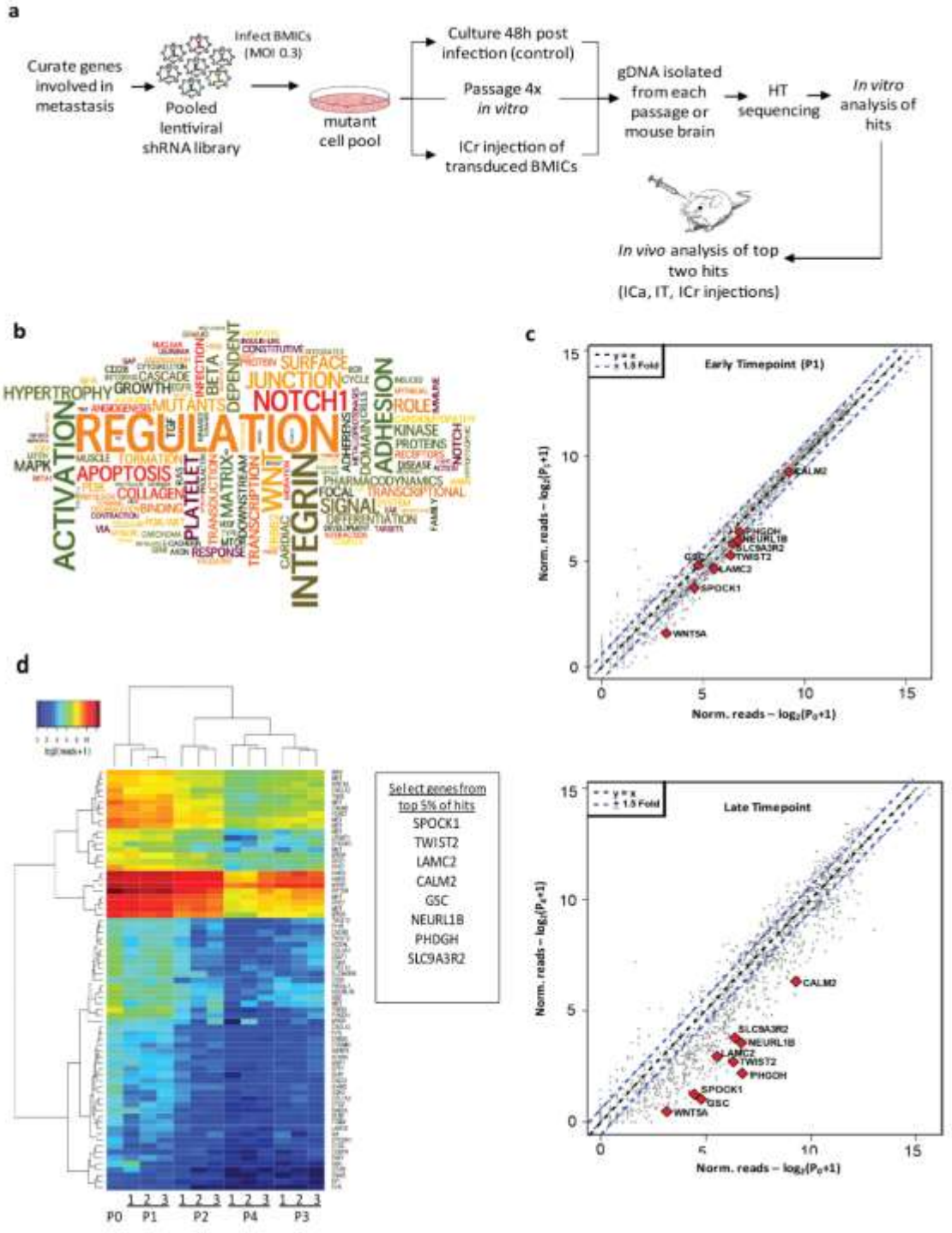

Figure 3. shRNA screen identifies genes involved in BMIC self-renewal. **a** Schematic representation of shRNA screen procedure. **b** Word frequency analysis from significantly enriched pathways using the selected 150 genes. **c** Scatter plots of normalized reads per shRNA between passage 0 (P0) and passage 1 (P1) or passage 4 (P4). Data shown highlights genes whose corresponding shRNAs were specifically depleted in long-term passaging BMICs (red dots). Blue line is diagonal line with ratio of 1.0. Red dashed line shows cut off for 1.7-fold change. **d** Heat map generated from top 5% of hairpins screen hits. Genes selected for further validation and their corresponding slope values are highlighted in the adjoining box.

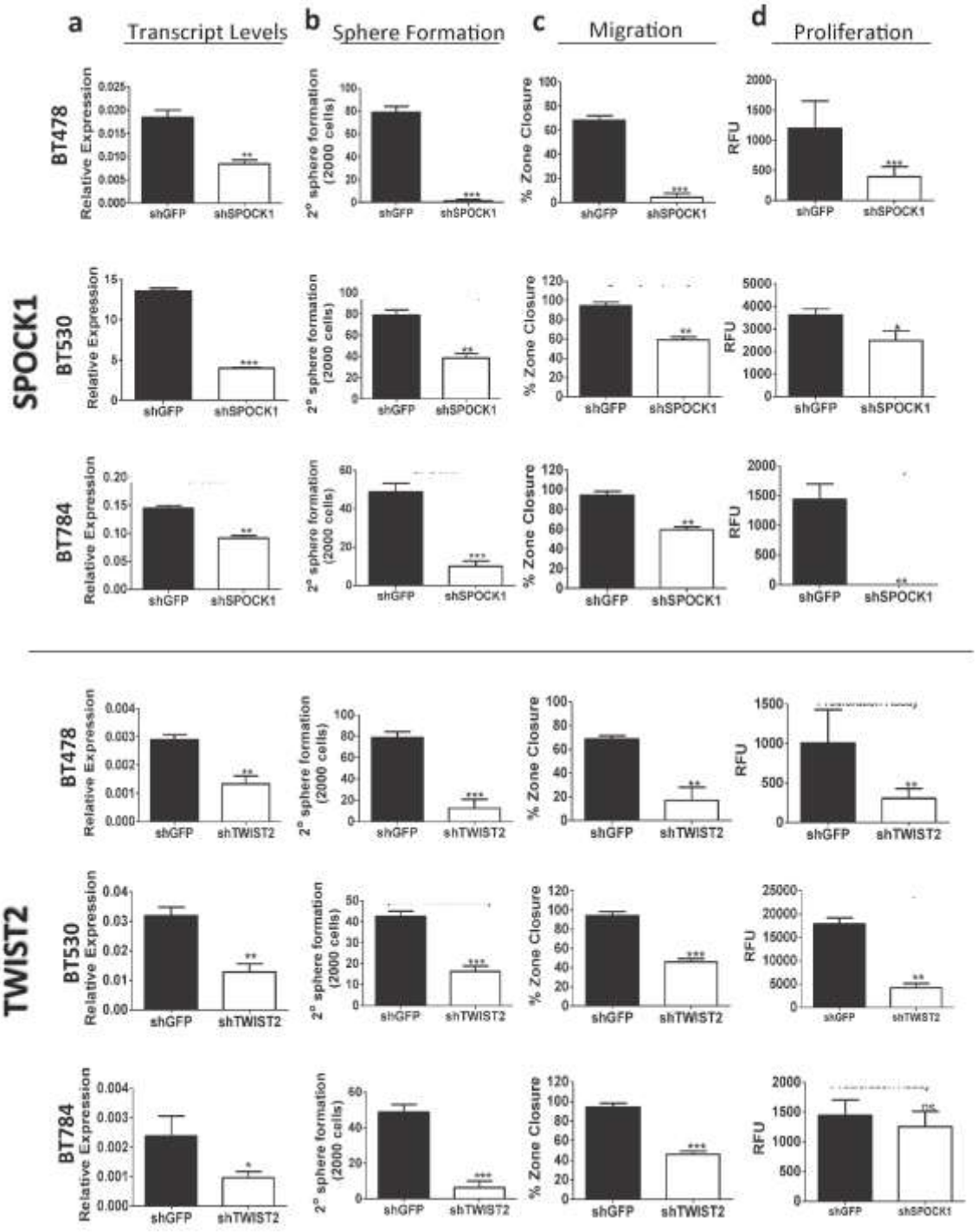

Figure 4. SPOCK1 and TWIST2 identified as novel regulators of BM through shRNA screen. **a** Transcript levels of SPOCK1 and TWIST2 after of lentiviral knockdown. In vitro characterization was carried out through. **b** sphere formation, **c** migration, and **d**

proliferation assays. Data are expressed as mean + SEM of n = 3. ns= not significant, *P<0.05, **P<0.01, ***P<0.001, ****P<0.0001.

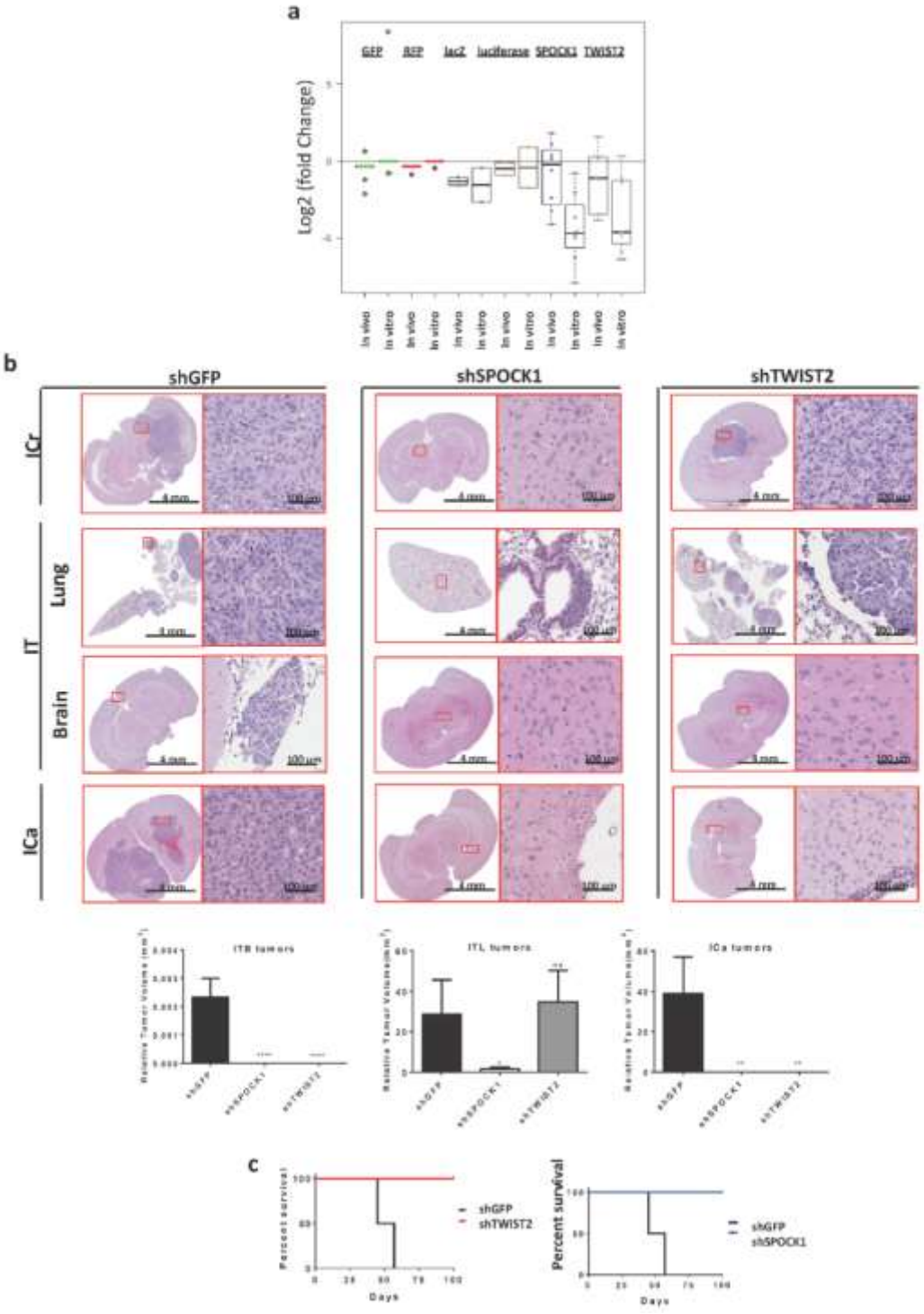

Figure 5. KD of shSPOCK1 and TWIST2 inhibits BM formation in vivo. **a** Evaluation of SPOCK1 and TWIST2 shRNA dropout after in vivo shRNA screen. **b** Representative H&E images of brain and lungs collected at endpoint after ICr (n=2), IT (n=4), and ICa (n=5) injections of BT478 cells were transduced with either shSPOCK1, shTWIST2, or shGFP as control. shSPOCK1 and shTWIST2 both inhibited metastasis to the brain through IT and ICa route. shTWIST had slightly reduced tumor formation from ICr route but no effect on tumor formation in the lung from IT route. shSPOCK1 inhibited tumor formation in both the lung and the brain from IT and ICr routes, respectively. Below are graphs depicting relative tumor volume (mm^2) for ITB and ITL samples. Red scale bar = 4 mm, blue scale bar = 100 µM, ns = not significant, *P<0.05, **P<0.01, ***P<0.001, ****P<0.0001. **c** Kaplan-Meier survival curves for ICr injections of shGFP, shSPOCK1, and shTWIST2, where mice had increased survival for shSPOCK1 and shTWIST2 as compared to the shGFP control.

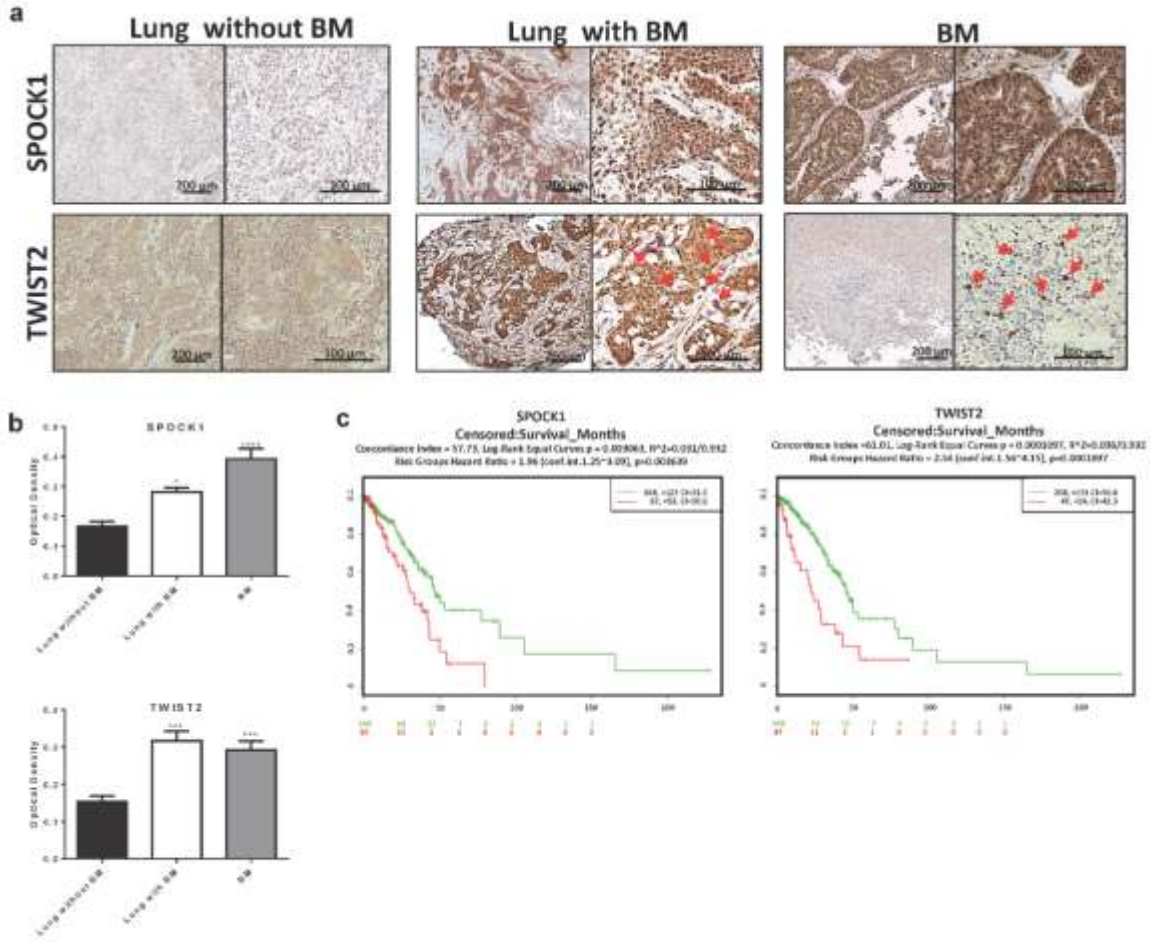

Figure 6. SPOCK1 and TWIST2 are predictive of lung to brain metastasis. a Expression of SPOCK1 and TWIST2 in patient biopsy samples of BM from lung, lung primary adenocarcinomas with known BM, and lung primary adenocarcinomas with no known metastases. b Quantification of optical densities of 6a. Red arrows indicate positively stained cells. Data are expressed as mean + SEM of BM n=10, lung with BM n=6, lung without BM n=6). *P<0.05, **P<0.01, ***P<0.001, ****P<0.0001. c Kaplan-Meier curves depicting gene expression by risk group, as obtained from SurvExpress using in TCGA data from lung adenocarcinoma patients.

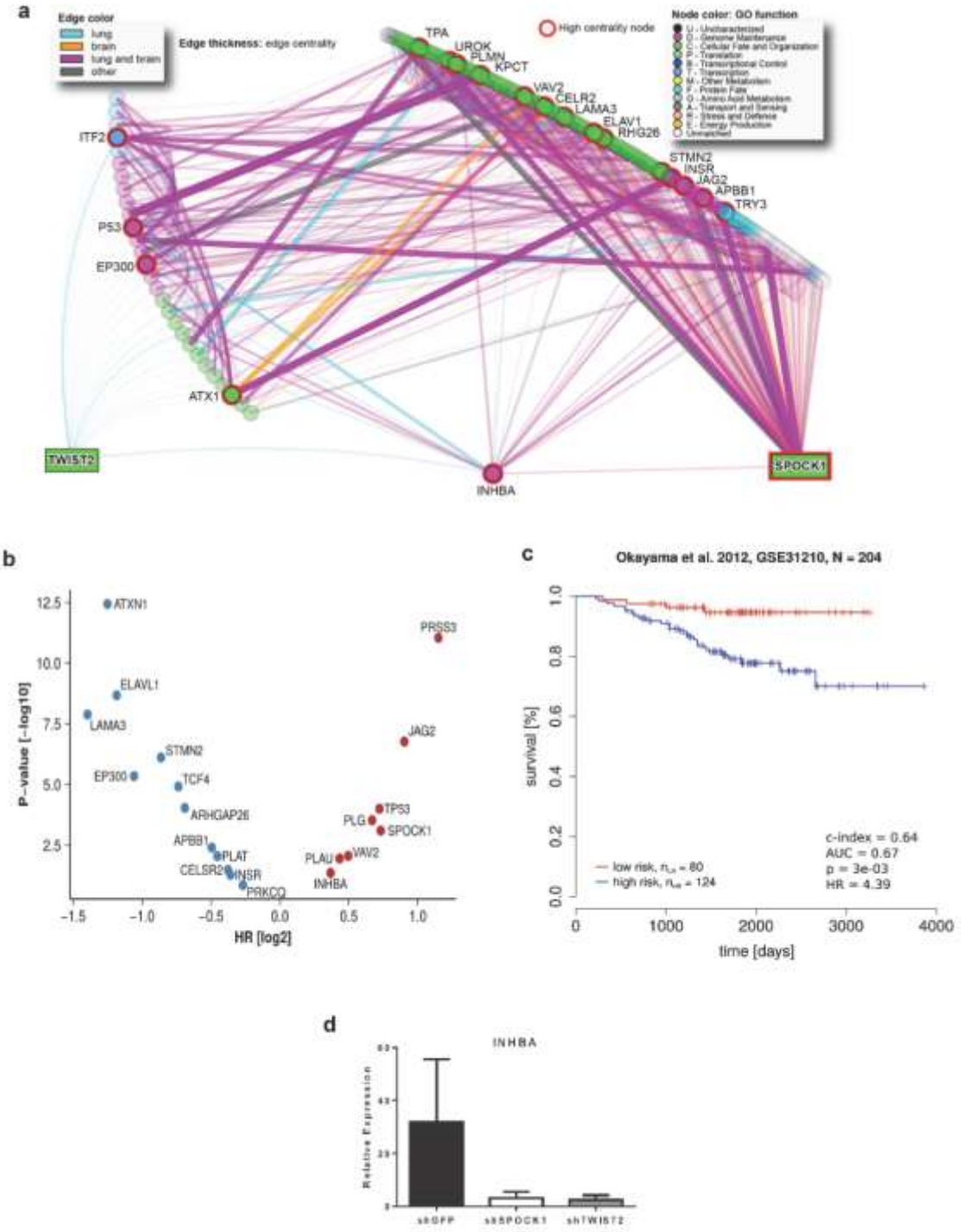
a
Edge color
lung
brain
lung and brain
other
Edge thickness: edge centrality
High centrality node
Node color: GO function
TPA
UROK
PLMN
KPCT
VAV2
CELR2
LAMA3
ELAV1
RHG26
STMN2
INSR
JAG2
APBB1
TRY3
ITF2
PS3
EP300
ATX1
TWIST2
INHBA
SPOCK1
b
P-value [-log10]
HR [log2]
ATXN1
PRSS3
ELAVL1
LAMA3
JAG2
STMN2
EP300
TCF4
ARHGAP26
TPS3
PLG
SPOCK1
APBB1
PLAT
VAV2
PLAU
CELSR2
INSR
INHBA
PRKCQ
c
Okayama et al. 2012, GSE31210, N = 204
survival [%]
time [days]
low risk, n = 80
high risk, n = 124
c-index = 0.64
AUC = 0.67
p = 3e-03
HR = 4.39
d
INHBA
Relative Expression
shGFP
shSPOCK1
shTWIST2

Figure 7. Novel interactors between SPOCK1 and TWIST2 predict BM. **a** Network of physical protein-protein interactions from IID database linking TWIST2 and SPOCK1. Node color corresponds to GeneOntology biological function; Edge color represents tissue evidence for the interaction. Top 20 genes with the highest centrality measure in the network are highlighted with name and red. **b** Volcano plot depicting HRs and corresponding P-values of the 20 genes with the highest centrality in Fig. 7a. Red dots depict harmful genes and blue dots are protective genes. **c** Kaplan-Meier plot showing overall survival rates of low and high risk patients, whose risk score was predicted by the Cox model, where expression of the selected 20 genes served as covariates. Prognostic performance of the model was validated on the independent datasets from [35]. **d** Transcript level of INHBA in BMIC lines (BT478, BT530, BT751) transduced with shGFP (control), shSPOCK1, or shTWIST2.

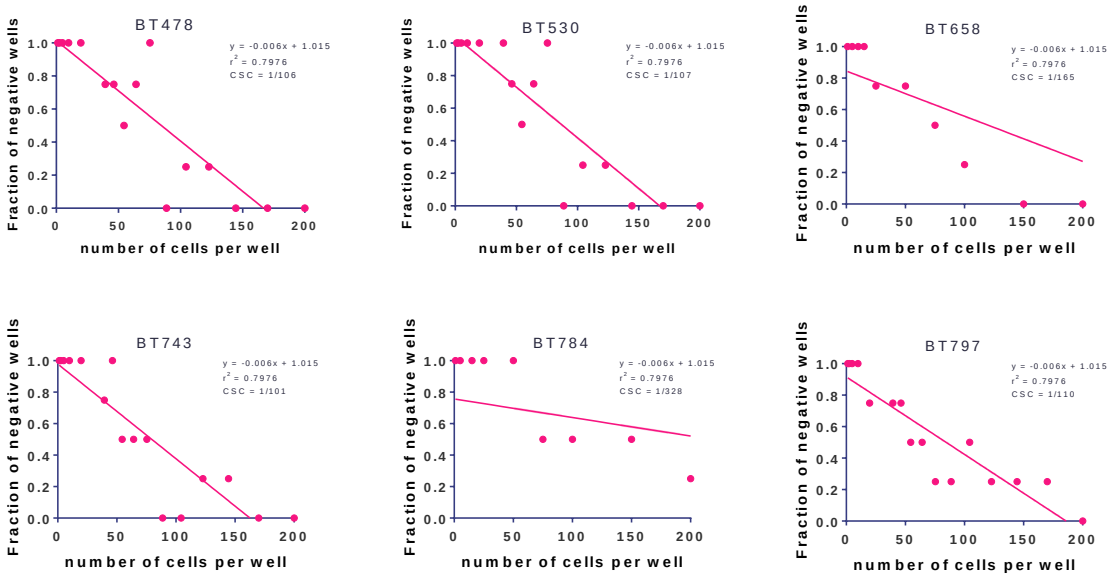

Supplementary Figure 1. Limiting dilution assays of patient-derived BMIC lines, depicting the average stem cell frequency per line.

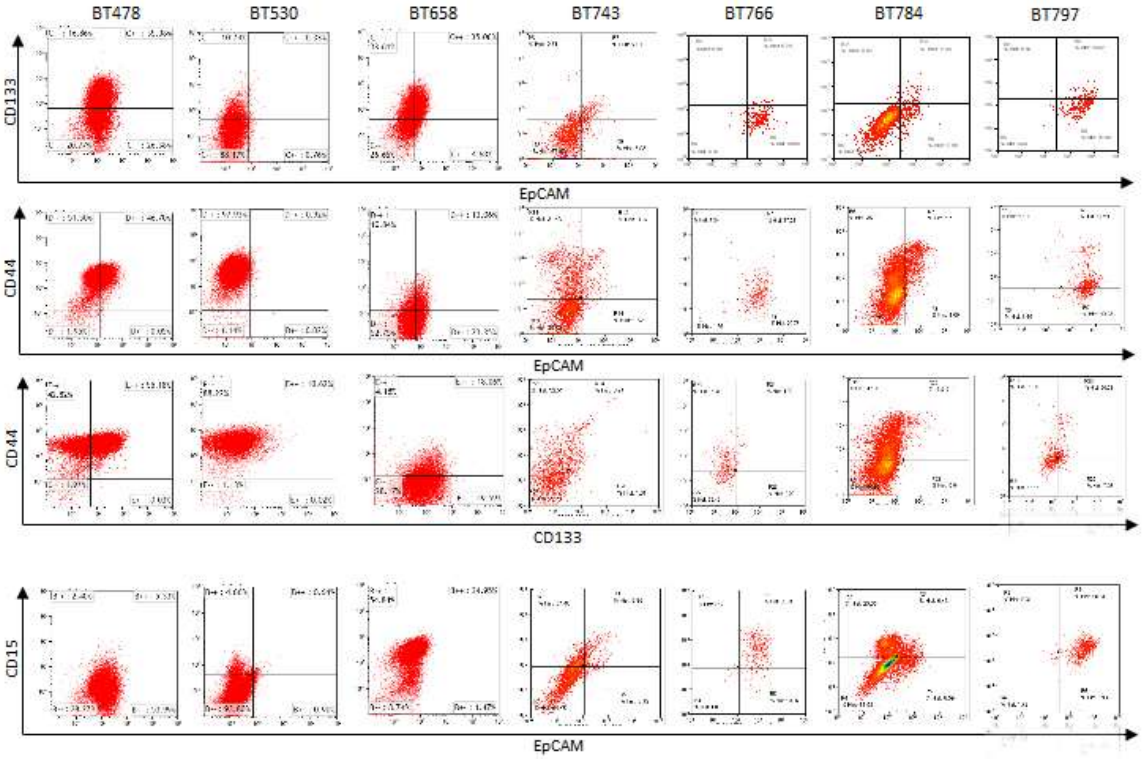

Supplementary Figure 2. FACS analysis determining relative expression of primary brain tumor CSC surface markers (CD133 and CD15) as well as a marker for cells of epithelial lineage (EpCAM) for BMICs.

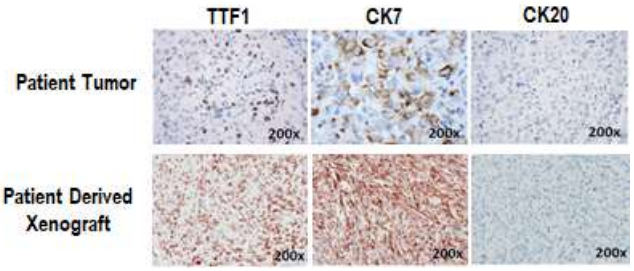

Supplementary Figure 3. Staining profiles of patient and mouse xenograft of BT478, depicting similar staining profiles. CK, cytokeratin (7 and 20); TTF1, thyroid transcription factor 1 to the original patient tunor.

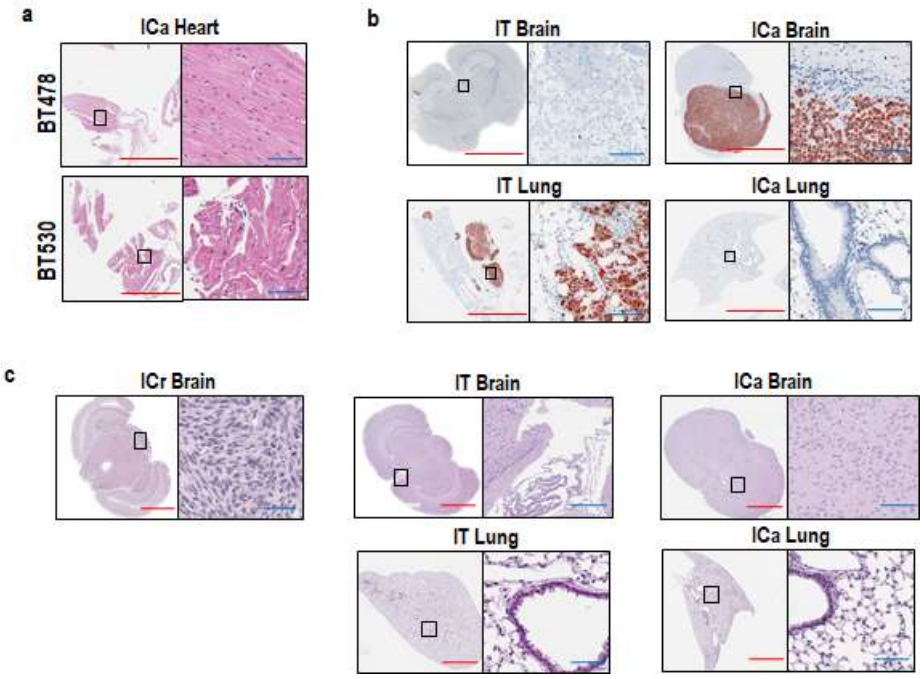

Supplementary Figure 4. a Representative H&E sections of heart from ICa injections of BT478 and BT530, showing no tumors. **b** Representative COXIV stained images of IT and ICa injections of BT478 to identify micro-metastatic tumors. **c** Representative H&E images of ICr, IT, and ICa injections with primary GBM line BT428. Red scale bar = 4 mm, blue scale bar = 100 µM.

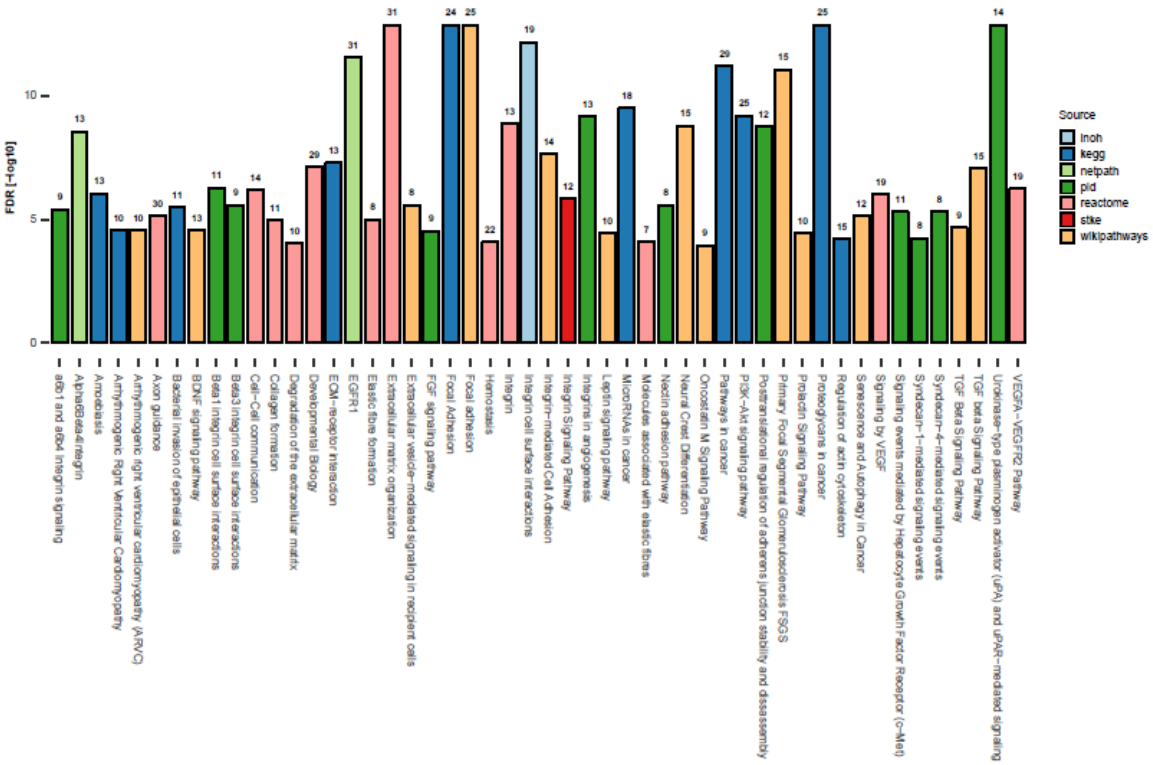

Supplementary Figure. 5. Top 50 most enriched pathways were depicted as a barplot showing significance of the enrichment and number of overlapping genes for each pathway.

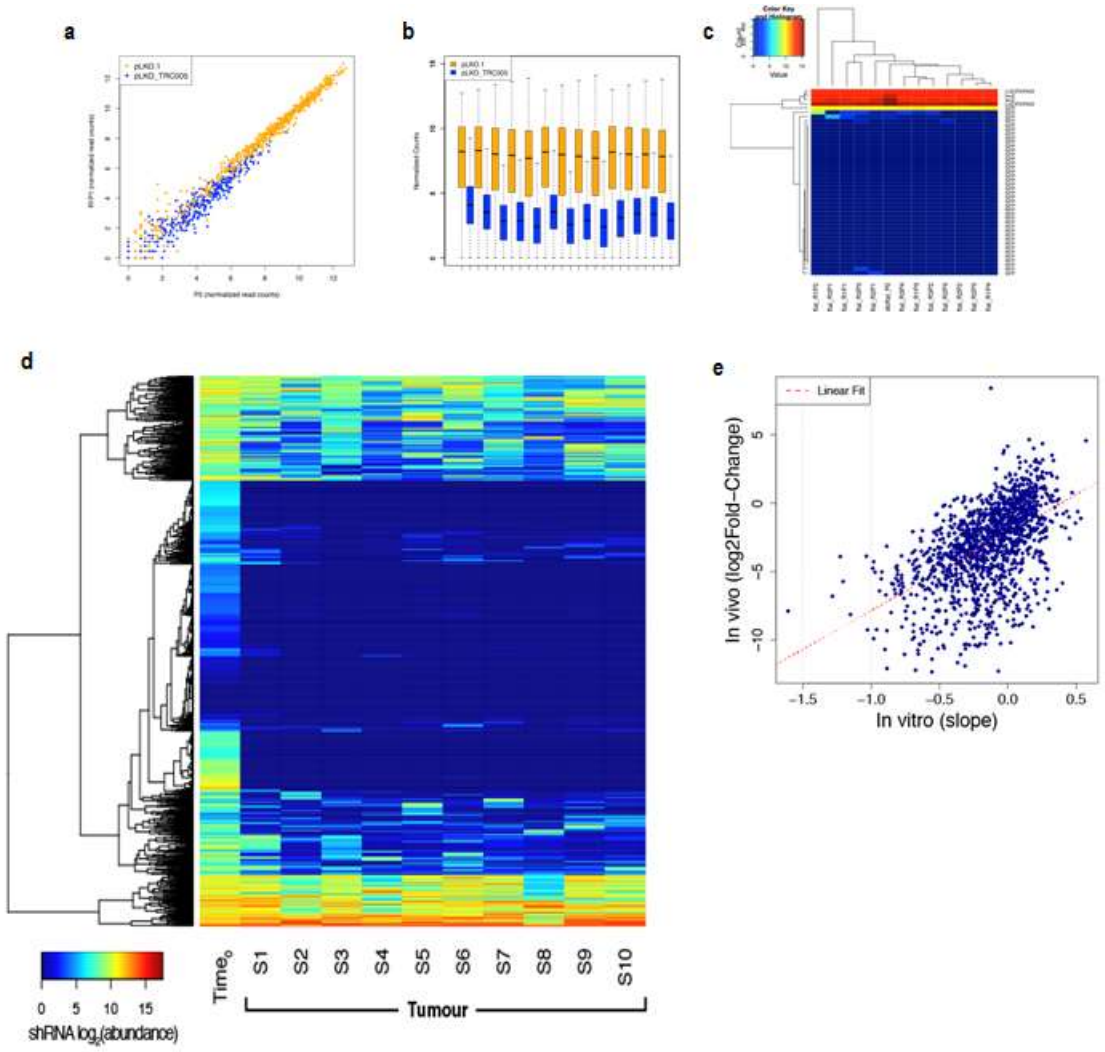

Supplementary Figure 6. Illumina sequencing protocol showing **a** bias against TRC2 hairpins, which are present in the pLKO_TRC005 vector used for the shRNA screens. **b** box and whisker plot showing the desired reproducibility and correlation between samples. **c** heat map generated for negative controls used in the shRNA screen. **d** Heatmap showing changes in hairpin abundance between $Time_0$ and each of the established tumors. **e** comparison between *in vitro* screen and *in vivo* tumors. The slope for *in vitro* hairpins was calculated across all time points using the R package *limma* (v3.26.9), which the *in vivo* fold change is the mean fold change between all tumors and T_0 (Pearson's r = 0.52)

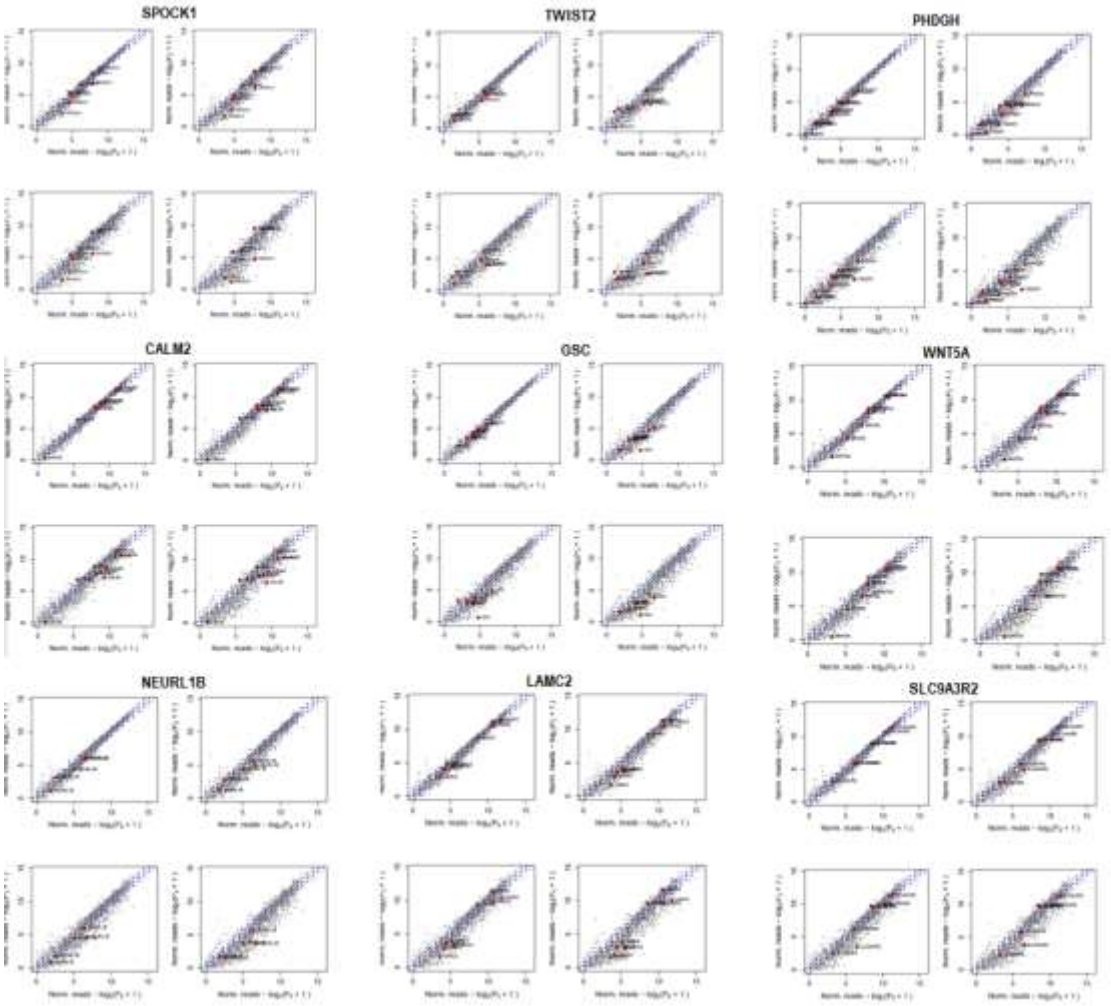

Supplementary Figure 7. Scatter plots of normalized reads per hairpin comparing passage 0 (P_0) to passage 1 (P_1), passage 2 (P_2), passage 3 (P3), or passage 4 (P_4) for select genes from the top 5% hits of the *in vitro* shRNA screen. The data shown highlights each hairpin at each timepoint (red dots). The blue line is the diagonal line with a ratio of 1.0. The red dashed line shows the cut off for 1.7-fold change.

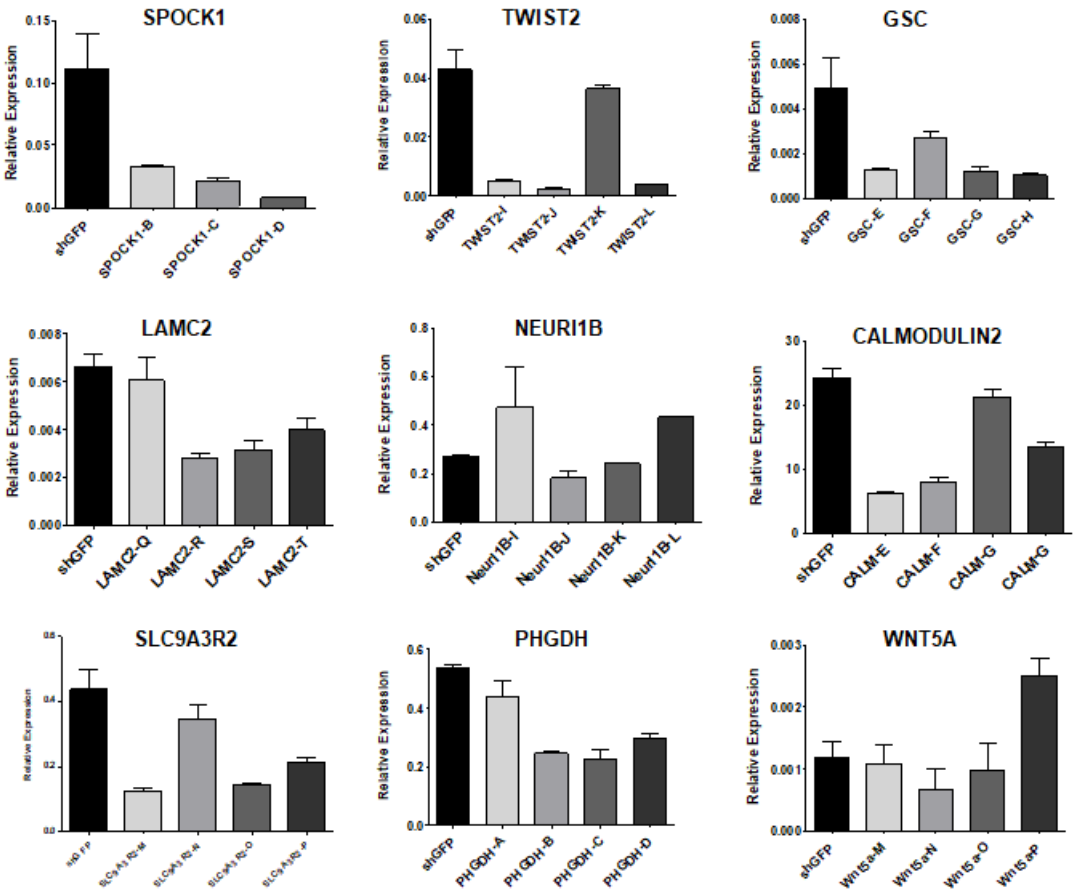

Supplementary Figure 8. Screening of lentiviral vectors for select genes in H1915 cells. 3-4 vectors were chosen for each gene chosen for further validation from the hairpins used in the shRNA screen and transfected into H1915 cells to assess their KD efficiency. The best vector was then packaged into lentivirus for transductions into BMICs.

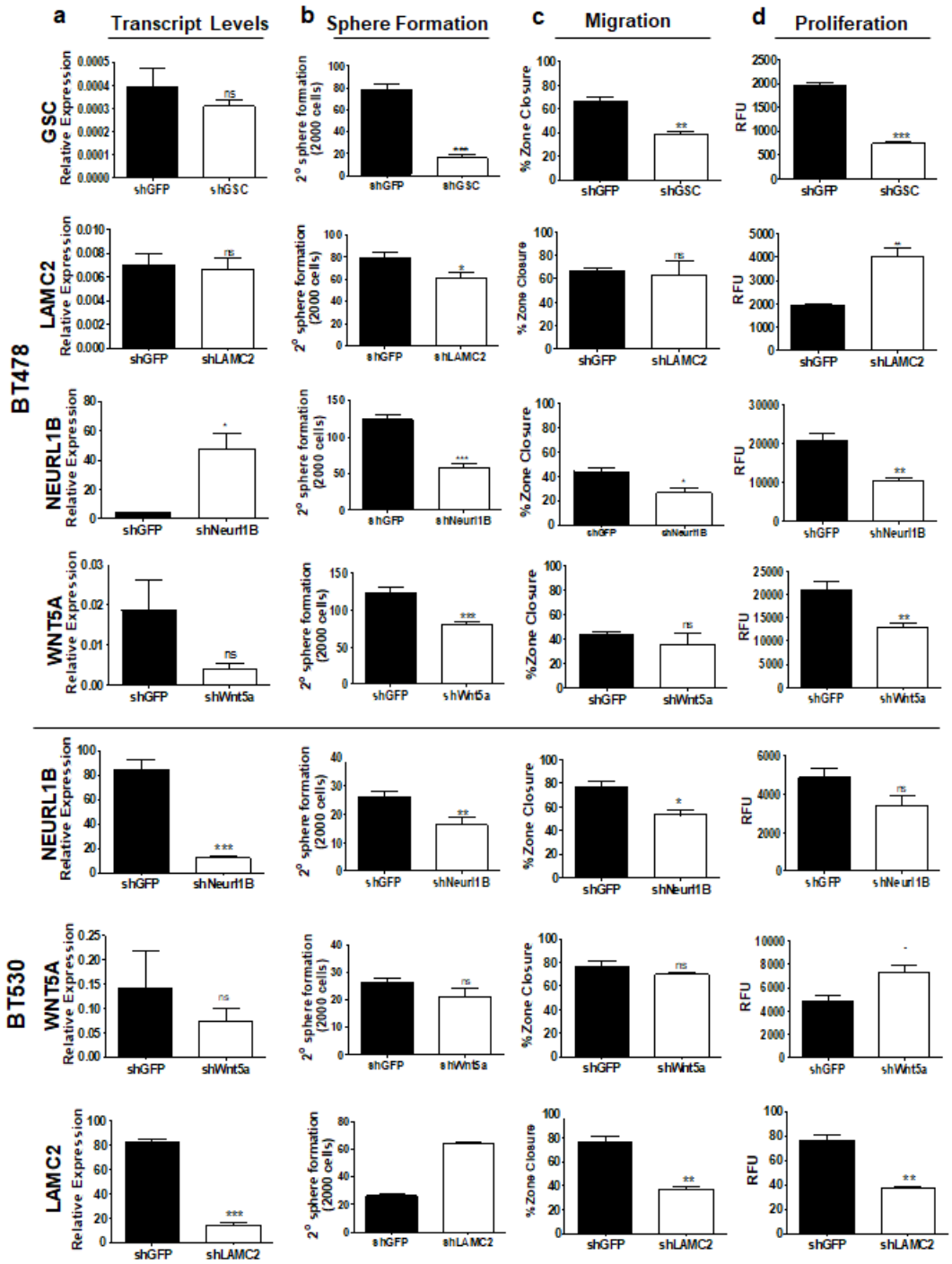

Supplementary Figure 9. Efficiency of lentiviral knockdown for select genes**a** in BT478 and BT530 were confirmed through RTPCR. *In vitro* characterization was carried out for each shRNA in BMIC lines BT478 and BT530 through b sphere formation, c migration, and d proliferation assays. ns = not significant, *P<0.01, **P<0.005,*** P< 0.0001.

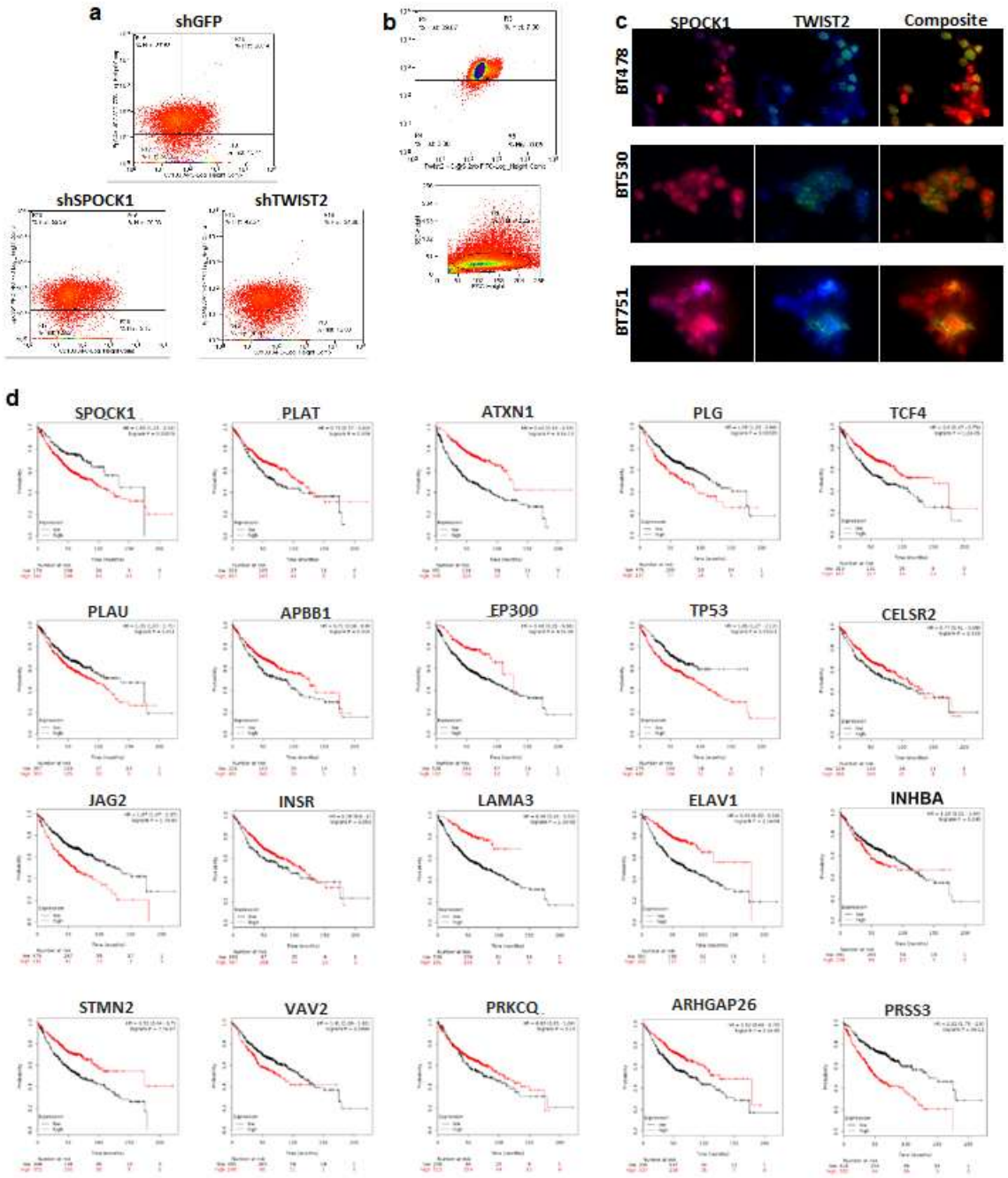

Supplementary Figure 10. a Expression of stem markers CD133 and EpCAM in BMIC line BT478 as confirmed by FACS analysis. **b** Co-expression of TWIST2 and SPOCK1 in BMIC line BT478, as confirmed by FACS analysis. Smaller plot to the right indicate isotype controls. **c** corresponding immunofluorescence of SPOCK1 and TWIST2 expression in BMIC lines BT478, BT530, BT751. Red = SPOCK1, green = TWIST2, blue

= dapi. Immaegs were taken at 20x magnification. **d** Individual KM plots of 20 genes with the highest centrality measure selected from the PPI network in Fig. 7a.

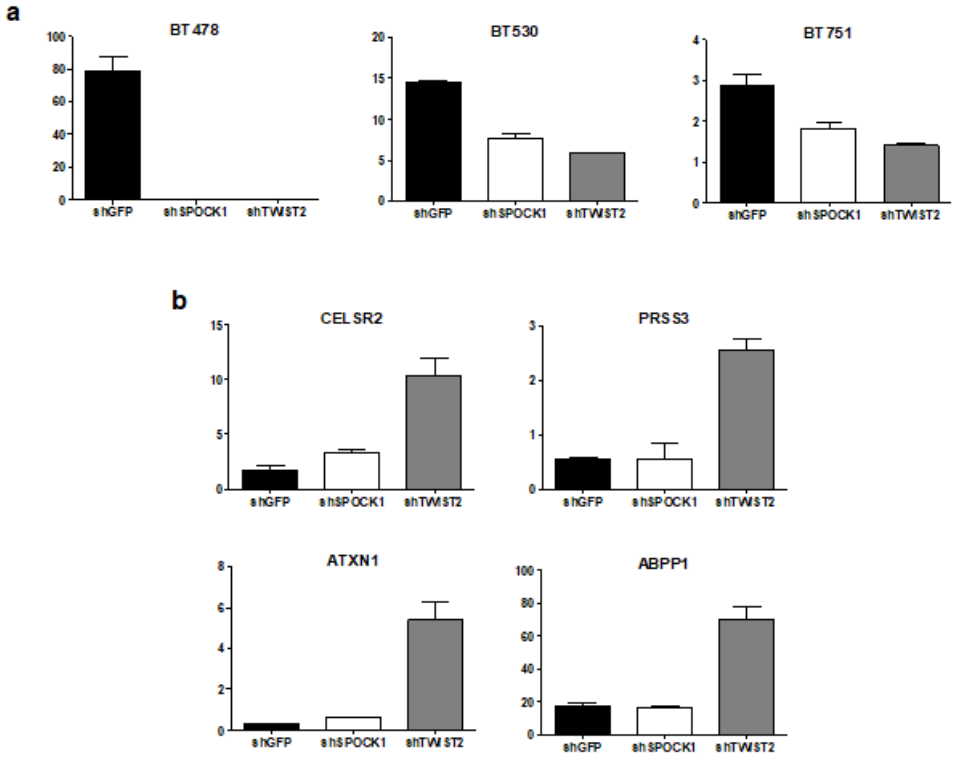

Supplementary Figure 11. a Relative expression of INHBA in BMIC lines BT478, BT530, and BT751 as determined by RTPCR. **b** Relative expression levels of select PPI connector genes in BT478 as determined by RTPCR.

Sample Identifier	Gender	Age	Area of tumor removal	Primary Tumor (NSCLC)	CD44%	CD133%	EpCAM%	CD15%
BT478	Female	75	Left frontal	Metastatic carcinoma, pleiomorphic	99.8	71.9	57.54	7.73
BT530	Male	53	Left cerebellar	Metastatic adenocarcinoma	99.76	68.43	10.94	5.3
BT658	Male	52	Right parietal	Metastatic carcinoma, large cell	96.18	35.18	89.24	89.79
BT743	Male	73	Left frontal	Metastatic adenocarcinoma	39.45	7.9	10.22	33.43
BT766	Male	73	Left frontal	Metastatic adenocarcinoma	68.49	5.63	97.15	87.21
BT784	Male	53	Right parietal	Metastatic adenocarcinoma	49.19	2.15	13.03	29.49
BT797	Male	69	Right parietal	Metastatic adenocarcinoma	55.39	31.34	97.69	68.82

Supplementary Table 1. Patient data for BMIC lines. Related to Fig. 1

BT478

# cells	mice injected	frequency of tumours
100,000	2	2
50,000	3	3
1,000	2	2
100	4	4

BT530

# cells	mice injected	frequency of tumours
100,000	2	2
50,000	3	3
100	2	2

Supplementary Table 2. *In vivo* ICr limiting dilution assays of BT478 and BT530. Related to Fig. 2

BT478

IT	# cells	mice injected	frequency of tumors
	1,000,000	8	0
	500,000	32	12
	250,000	2	0
	100,000	2	0
	50,000	2	0

ICa	# cells	mice injected	frequency of seeding/tumors
	1,000,000	2	2
	250,000	16	11
	200,000	5	0

BT530

IT	# cells	mice injected	frequency of tumours
	500,000	4	4

ICa	# cells	mice injected	frequency of tumours
	250,000	4	2

Supplementary Table 3. In vivo IT and ICa limiting dilution assays of BT478 and BT530.

Unigene	Gene	Ref
Hs.303609	ST6GALNAC5	(Bos PD, Nature 2009)
Hs.196384	COX2	(Bos PD, Nature 2009)
Hs.799	HBEGF	(Bos PD, Nature 2009)
Hs.83169	MMP-1	(Bos PD, Nature 2009)
Hs.9613	ANGPTL4	(Bos PD, Nature 2009)
Hs.118400	FSCN-1	(Bos PD, Nature 2009)
Hs.619315	LTBP1	(Bos PD, Nature 2009)
Hs.115263	EREG	(Bos PD, Nature 2009)
Hs.297413	MMP-9	(Bos PD, Nature 2009)
Hs.621200	4EBP2	
Hs.594084	4EBP3	
Hs.444082	EZH2	(Behrens C, Clin Cancer Res. 2013)
Hs.593413	CXCR4 aka CD184	
Hs.846	CXCR2 aka CD182	Saintigny R, Cancer Res 2013
Hs.132966	c-MET aka HGFR	Lee SJ, Clin Exp Metastasis 2013
Hs.3798	NEDD9	Jin Y Int J Cancer 2013
Hs.596136	SPOCK1	Miao L, Biochem Biophys Res Commun 2013
Hs.163484	FOXA1	Wang H, BMC Genomics 2013
Hs.113577	Neurofibromin 1 aka NF1	Zahrabian VM, Onc Reports 2007
Hs.719906	NPDC1	Zahrabian, Onc Reports 2007
Hs.468442	calmodulin 2	Zahrabian, Onc Reports 2007
Hs.369017	RAB2	Zahrabian, Onc Reports 2007
Hs.502872	MLK3	Zahrabian, Onc Reports 2007
Hs.368921	α1 (XVI) collagen	Zahrabian, Onc Reports 2007
Hs.235368	α3 (V) collagen	Zahrabian, Onc Reports 2007
Hs.375957	Integrin, ß2	Zahrabian, Onc Reports 2007
Hs.632226	Integrin, ß4	Zahrabian, Onc Reports 2007
Hs.470399	Integrin, ß6	Zahrabian, Onc Reports 2007
Hs.28144	FSD1 (fibronectin type III and SPRY domain containing 1)	Zahrabian, Onc Reports 2007
Hs.372031	Peripheral myelin protein 22	Zahrabian, Onc Reports 2007
Hs.100890	Reprimo, TP53-dependent G2 arrest mediator candidate	Zahrabian, Onc Reports 2007
Hs.517106	CCAAT enhancer binding protein (C/EBP), ß	Zahrabian, Onc Reports 2007
Hs.146211	Hect domain and RLD 2 pseudogene 7	Zahrabian, Onc Reports 2007
Hs.518513	Tyrosine kinase, non-receptor, 2	Zahrabian, Onc Reports 2007
Hs.300863	SGK2 (Serum/glucocorticoid regulated kinase 2)	Zahrabian, Onc Reports 2007
Hs.11916	RBKS (ribokinase)	Zahrabian, Onc Reports 2007
Hs.138860	Rho GTPase activating protein 1	Zahrabian, Onc Reports 2007
Hs.118681	ERBB3	Zahrabian, Onc Reports 2007
Hs.62022	Laminin, ß4	Zahrabian, Onc Reports 2007

Unigene	Gene	Ref
Hs.517293	F11R	SA Biosciences
Hs.618430	NFKB1	Zhao, Cancer Res 2013
Hs.1274	BMP1	SA Biosciences
Hs.473163	BMP7	SA Biosciences
Hs.490203	CALD1	SA Biosciences
Hs.731383	CAMK2N1	SA Biosciences
Hs.461086	CDH1	SA Biosciences
Hs.464829	CDH2	SA Biosciences
Hs.489142	COL1A2	SA Biosciences
Hs.443625	COL3A1	SA Biosciences
Hs.235368	COL5A2	SA Biosciences
Hs.203717	FN1	SA Biosciences
Hs.436448	FOXC2	SA Biosciences
Hs.83381	GNG11	SA Biosciences
Hs.462998	IGFBP4	SA Biosciences
Hs.505654	ITGA5	SA Biosciences
Hs.436873	ITGAV	SA Biosciences
Hs.375129	MMP3	SA Biosciences
Hs.87752	MSN	SA Biosciences
Hs.414795	SERPINE1 (PAI1)	SA Biosciences
Hs.48029	SNAI1	SA Biosciences
Hs.360174	SNAI2	SA Biosciences
Hs.673548	SNAI3	SA Biosciences
Hs.111779	SPARC	SA Biosciences
Hs.61635	STEAP1	SA Biosciences
Hs.605153	TCF4	SA Biosciences
Hs.522632	TIMP1	SA Biosciences
Hs.598100	TMEFF1	SA Biosciences
Hs.118552	TMEM132A	SA Biosciences
Hs.66744	TWIST1	SA Biosciences
Hs.422585	TWIST2	SA Biosciences
Hs.643801	VCAN	SA Biosciences
Hs.455493	VIM	SA Biosciences
Hs.459790	VPS13A	SA Biosciences
Hs.643085	WNT5A	SA Biosciences
Hs.306051	WNT5B	SA Biosciences
Hs.212332	CAV2	SA Biosciences
Hs.643813	ITGB1	SA Biosciences
Hs.626544	JAG1	SA Biosciences
Hs.517973	MST1R	SA Biosciences
Hs.460141	NODAL	SA Biosciences
Hs.509067	PDGFRB	SA Biosciences
Hs.413812	RAC1	SA Biosciences
Hs.463059	STAT3	SA Biosciences
Hs.645227	TGFB1	SA Biosciences
Hs.133379	TGFB2	SA Biosciences
Hs.476018	CTNNB1	SA Biosciences
Hs.95612	DSC2	SA Biosciences
Hs.88556	HDAC1	Zhao, Cancer Res 2013
Hs.3352	HDAC2	Zhao, Cancer Res 2013
Hs.479756	KDR	Zhao, Cancer Res 2013
Hs.487296	PHGDH	Zhao, Cancer Res 2013

Unigene	Gene	Ref
Hs.706355	ILK	SA Biosciences
Hs.395482	PTK2	SA Biosciences
Hs.313	SPP1	SA Biosciences
Hs.590970	AXL	SA Biosciences
Hs.504609	ID1	SA Biosciences
Hs.624	IL8	SA Biosciences
Hs.567674	KLF17	SA Biosciences
Hs.491582	PLAT	SA Biosciences
Hs.466871	PLAUR	SA Biosciences
Hs.124503	ZEB1	SA Biosciences
Hs.34871	ZEB2	SA Biosciences
Hs.614734	PROM1	Nolte 2013
Hs.631660	PLEKHG6	Nolte 2013
Hs.502842	CAPN1	Nolte 2013
Hs.412597	DSG2	Nolte 2013
Hs.591484	LAMC2	Nolte 2013
Hs.440896	SLC9A3R2	Nolte 2013
Hs.519873	DSP	Nolte 2013
Hs.252549	CTSZ	Nolte 2013
Hs.467142	MYH14	Nolte 2013
Hs.528693	RASAL1	Nolte 2013
Hs.205163	MRPL3	Nolte 2013
Hs.591415	IRF6	Nolte 2013
Hs.363137	TCP1	Nolte 2013
Hs.744851	LPGAT1	Nolte 2013
Hs.465224	NARS	Nolte 2013
Hs.411501	KRT7	Nolte 2013
Hs.85658	ZNF768	Nolte 2013
Hs.534346	RPS7	Nolte 2013
Hs.289271	CYC1	Nolte 2013
Hs.558536	NOC4L	Nolte 2013
Hs.25313	MCRS1	Nolte 2013
Hs.411641	EIF4EBP1	Nolte 2013
Hs.195659	SRC	Nolte 2013
Hs.166011	CTNND1	Nolte 2013
Hs.440900	BAT3	Nolte 2013
Hs.338207	MTOR	Nolte 2013
Hs.249718	EIF4E	Nolte 2013
Hs.133044	PRTOR	Nolte 2013
Hs.380403	BMI-1	
Hs.390420	CD15 (FUT4)	
Hs.522891	CXCL12	
Hs.474751	MYH9	
Hs.191219	CPNE3	
Hs.473583	YB1	
Hs.369779	SIRT1	
Hs.595333	CELF1	
Hs.589848	PARD6B	Zhao, Cancer Res 2013
Hs.350321	RET	Zhao, Cancer Res 2013
Hs.390567	FYN	Zhao, Cancer Res 2013
Hs.644105	CD24	Lee HJ, J Thorac Oncol

Supplementary Table 4. Candidate List of 150 genes in shRNA screen library.

Gene	Known Path Memberships
WNT5A	KEGG.Basal cell carcinoma - Homo sapiens (human), KEGG.Hedgehog signaling pathway - Homo sapiens (human), KEGG.Hippo signaling pathway - Homo sapiens (human), KEGG.HTLV-I infection - Homo sapiens (human), KEGG.Melanogenesis - Homo sapiens (human), KEGG.Pathways in cancer - Homo sapiens (human), KEGG.Proteoglycans in cancer - Homo sapiens (human), KEGG.Wnt signaling pathway - Homo sapiens (human), NetPath.Wnt, PID.Noncanonical Wnt signaling pathway, PID.Validated targets of C-MYC transcriptional repression, PID.Wnt signaling network, Reactome.Asymmetric localization of PCP proteins, Reactome.beta-catenin independent WNT signaling, Reactome.Ca2+ pathway, Reactome.Class B/2 (Secretin family receptors), Reactome.GPCR ligand binding, Reactome.negative regulation of TCF-dependent signaling by WNT ligand antagonists, Reactome.PCP/CE pathway, Reactome.Signal Transduction, Reactome.Signaling by GPCR, Reactome.Signaling by Wnt, Reactome.TCF dependent signaling in response to WNT, Reactome.WNT ligand biogenesis and trafficking, Reactome.WNT5A-dependent internalization of FZD2, FZD5 and ROR2, Reactome.WNT5A-dependent internalization of FZD4, Signalink.WNT-Core, Wikipathways.DNA Damage Response (only ATM dependent), Wikipathways.MicroRNAs in cardiomyocyte hypertrophy, Wikipathways.miR-targeted genes in epithelium - TarBase, Wikipathways.miR-targeted genes in lymphocytes - TarBase, Wikipathways.miR-targeted genes in muscle cell - TarBase, Wikipathways.Wnt Signaling Pathway, Wikipathways.Wnt Signaling Pathway and Pluripotency, Spike.WNT signaling , IPAVS.non_canonical_Wnt_signaling_pathway_human, IPAVS.Signaling_pathways_controlling_SHF_development, IPAVS.Wnt_signaling_in_cardiomyocyte_hypertrophy, systems-biology.org.beta_cell_v2.3
SPOCK1	Wikipathways.Adipogenesis, NA, Wikipathways.Adipogenesis
TWIST2	KEGG.Proteoglycans in cancer - Homo sapiens (human), NA, KEGG.Proteoglycans in cancer - Homo sapiens (human)
SLC9A3R2	KEGG.Aldosterone-regulated sodium reabsorption - Homo sapiens (human), PharmGKB.Beta-agonist/Beta-blocker Pathway, Pharmacodynamics, PID.LPA receptor mediated events, PID.PDGFR-beta signaling pathway, Wikipathways.miR-targeted genes in lymphocytes - TarBase, Wikipathways.miR-targeted genes in muscle cell - TarBase
NEURL1B	Reactome.Activated NOTCH1 Transmits Signal to the Nucleus, Reactome.Constitutive Signaling by NOTCH1 HD Domain Mutants, Reactome.Constitutive Signaling by NOTCH1 HD+PEST Domain Mutants, Reactome.Constitutive Signaling by NOTCH1 PEST Domain Mutants, Reactome.Disease, Reactome.FBXW7 Mutants and NOTCH1 in Cancer, Reactome.NOTCH2 Activation and Transmission of Signal to the Nucleus, Reactome.Signal Transduction, Reactome.Signaling by NOTCH, Reactome.Signaling by NOTCH1, Reactome.Signaling by NOTCH1 HD Domain Mutants in Cancer, Reactome.Signaling by NOTCH1 HD+PEST Domain Mutants in Cancer, Reactome.Signaling by NOTCH1 in Cancer, Reactome.Signaling by NOTCH1 PEST Domain Mutants in Cancer, Reactome.Signaling by NOTCH1 t(7;9)(NOTCH1:M1580_K2555) Translocation Mutant, Reactome.Signaling by NOTCH2, UniProt.Pathways.protein ubiquitination, UniProt.Pathways.Protein modification
GSC	PID.Regulation of nuclear SMAD2/3 signaling, PID.Regulation of retinoblastoma protein, Reactome.Developmental Biology, Reactome.POU5F1 (OCT4), SOX2, NANOG repress genes related to differentiation, Reactome.Transcriptional regulation of pluripotent stem cells

PHGDH	HumanCyc.serine and glycine biosynthesis, HumanCyc.serine biosynthesis (phosphorylated route), KEGG.Glycine, serine and threonine metabolism - Homo sapiens (human), Reactome.Amino acid synthesis and interconversion (transamination), Reactome.Metabolism, Reactome.Metabolism of amino acids and derivatives, Reactome.Serine biosynthesis, SMPDB.Dihydropyrimidine Dehydrogenase Deficiency (DHPD), SMPDB.Dimethylglycine Dehydrogenase Deficiency, SMPDB.Dimethylglycinuria, SMPDB.Glycine and Serine Metabolism, SMPDB.Hyperglycinemia, non-ketotic, SMPDB.Non Ketotic Hyperglycinemia, SMPDB.Sarcosinemia, Wikipathways.Trans-sulfuration and one carbon metabolism, UniProt.Pathways.L-serine from 3-phospho-D-glycerate: step 1/3, UniProt.Pathways.L-serine biosynthesis, UniProt.Pathways.Amino-acid biosynthesis
LAMC2	BioCarta.agrin in postsynaptic differentiation, BioCarta.prion pathway, INOH.Integrin, KEGG.Amoebiasis - Homo sapiens (human), KEGG.ECM-receptor interaction - Homo sapiens (human), KEGG.Focal adhesion - Homo sapiens (human), KEGG.Pathways in cancer - Homo sapiens (human), KEGG.PI3K-Akt signaling pathway - Homo sapiens (human), KEGG.Small cell lung cancer - Homo sapiens (human), KEGG.Toxoplasmosis - Homo sapiens (human), NetPath.Alpha6Beta4Integrin, PID.a6b1 and a6b4 Integrin signaling, PID.Alpha6 beta4 integrin-ligand interactions, PID.Beta1 integrin cell surface interactions, Reactome.Anchoring fibril formation, Reactome.Assembly of collagen fibrils and other multimeric structures, Reactome.Cell junction organization, Reactome.Cell-Cell communication, Reactome.Collagen formation, Reactome.Degradation of the extracellular matrix, Reactome.Extracellular matrix organization, Reactome.Laminin interactions, Reactome.Non-integrin membrane-ECM interactions, Reactome.Type I hemidesmosome assembly, Wikipathways.Alpha 6 Beta 4 signaling pathway, Wikipathways.Focal Adhesion, Wikipathways.Inflammatory Response Pathway, Wikipathways.miR-targeted genes in lymphocytes - TarBase, Wikipathways.miR-targeted genes in muscle cell - TarBase, systems-biology.org.Toll-Like_receptor_signaling_network

Supplementary Table 5. Main pathways of select genes. Full list provided in Online Resource 2 (see manuscript link).

a

Lung cancer patients with no brain metastasis development

Age	Gender	Lung pathology	Follow up	Metastasis	Status
73	M	LLL well differentiated mucinous adenocarcinoma, EGFR-/ALK-/TTF1-/CK7+, PT3NoMx	13 months	Y - bone	dead
84	M	LUL mixed adenocarcinoma, p63-/TTF1-, PT2bNoMx	9 months	N	dead
69	M	RLL poorly differentiated adenocarcinoma, PT2bNIMx	56 months	local lung metastases	dead
57	F	EGFR, ALK-ROL, RUL, adenocarcinoma (mixed), PT2aNoMx	68 months	Y - multiple lung metastases	dead
51	F	poorly differentiated adenocarcinoma. P63-/EGFR-, p72aNoMx	60 months	N	alive
72	M	RUL moderately differentiated adenocarcinoma, PT2bNoMx	8 months	N	dead
38	M	RUL well differentiated adenocarcinoma, PT2aNoMx	48 months	N	dead
85	m	RLLmucinous adenocarcinoma, EGFR-/ALK-, PT2bNoM1a	4 months	N	dead
79	M	poorly differentiated adenocarcinoma	6 months	Y - local lung metastases	dead
82	F	LUL poorly differentiated adenocarcinoma, EGFR-/ALK-, PT2aN2Mx	3 months	N	dead
70	M	RUL moderately differentiated adenocarcinoma, TTF1+/CK7+/p63-, PT2aNoMo	64 months	N	alive
75	F	RUL poorly differentiated adenocarcinoma, CK7+/TTF1+/p63-, PT2aN1Mx	66 months	N	alive
64	M	LUL differentiated large cell adenocarcinoma, CK7+/TTF1-/p63-, PT3NoMx	54 months	N	alive
81	F	LUL moderately differentiated adenocarcinoma, PT4NoMx	54 months	N	alive

b

Lung cancer patients with brain metastasis development

Age	Gender	Lung pathology	Follow up time	Brain metastasis	Status	Time to death from Dx of brain mets
53	M	adenocarcinoma, stage4	26 months	Yes	Dead	3 months
59	M	moderately differentiated adenocarcinoma, EGFR-/ALK-/TTF1+/CK7+, stage4	15 months	Yes	Dead	2 months
72	F	adenocarcinoma, stage4	18 months	Yes	Dead	18 months
73	M	adenocarcinoma, stage4	3 months	Yes	Dead	3 months
73	M	mucinous adenocarcinoma, stage4	6 months	Yes	Dead	6 months
75	F	pleiomorphic adenocarcinoma, TTF1+/CK7+/CK20+, stage4	6 months	Yes	Dead	6 months
71	M	adenocarcinoma, stage4	50 months	Yes	Dead	7 months
58	F	adenocarcinoma, stage4	28 months	Yes	Dead	10 months
58	F	adenocarcinoma, stage4 (metastatic)	5 months	Yes	Dead	5 months
79	M	adenocarcinoma, stage4 (metastatic)	52 months	Yes	Dead	3 months
63	F	adenocarcinoma, stage4	5 months	Yes	Dead	5 months
74	F	adenocarcinoma, stage4	15 months	Yes	Dead	3 months

Supplementary Table 6. Information of **a** patients with only lung cancer and **b** patients with lung cancer and BM development, identifying tumor pathology, survival, and follow up time.

Gene	Forward Primer	Reverse Primer
28srRNA	AAGCAGGAGGTGTCAGAAA	GTAAAACTAACCTGTCTCACG
SPOCK1	CAACTGCTTGTTCCCAGAGG	GCCAATGACTTCCCTATCCA
TWIST2	GAGCGACGAGATGGACAATAAGA	ATGCGCCACACGGAGAA
LAMC2	TACTATAATCTGGATGGGGGGAACC	ATACAGGTGCCAAAAGGCCCCAGTC
GSC	TCTCAACCAGCTGCACTGTC	GGCGGTTCTTAAACCAGACC
NEURL1B	CTTCAGTGTCAACCAGTCCTC	TCGCCATTCTTGATGCCTG
PHGDH	AACTTCTTCCGCTCCCATTT	GTCATCAACGCAGCTGAGAA
CALM2	GTAATGGCACAATTGACTTCCC	TCACATGGCGAAGTTCTGC
SLC9A3R2	CCCGAGACAGATGAACACTTC	AGGTCACTTCGGGACGAG
WNT5A	CTTCGCCCAGGTTGTAATTGAAGC	CTGCCAAAAACAGAGGTGTTATCC

Supplementary Table 7. Primer sequences for RTPCR. Related to Fig. 4

Symbol	Probe	HR	P.value	Uniprot ID	APSP.Hits	Degree	GO	PubMedID	Long.Name
APBB1	202652_at	0.71	0.004	O00213	479	67	D : Genome Maintenance	14702039	Amyloid beta A4 precursor protein binding family B member 1; Protein Fe65
ARHGAP26	226576_at	0.62	0.000092	Q9UNA1	359	35	C : Cellular Fate and Organization	10908648	Rho GTPase activating protein 26; GTPase regulator associated with focal adhesion kinase; Oligophrenin 1 like protein; Rho type GTPase activating protein 26
ATXN1	203232_s_at	0.42	3.60E-13	P54253	452	15	C : Cellular Fate and Organization	11001934	Ataxin 1; Spinocerebellar ataxia type 1 protein
CELSR2	36499_at	0.77	0.0334	Q9HCU4	681	53	C : Cellular Fate and Organization	10907856	Cadherin EGF LAG seven pass G type receptor 2; Cadherin family member 10; Epidermal growth factor like protein 2; EGF like protein 2; Flamingo homolog 3; Multiple epidermal growth factor like domains protein 3; Multiple EGF like domains protein 3; Precursor
ELAVL1	244660_at	0.44	2.10E-09	Q15717	366	22	C : Cellular Fate and Organization	11729309	ELAV like protein 1; Hu antigen R; HuR
EP300	202221_s_at	0.48	4.5E-06	Q09472	438	41	D : Genome Maintenance	10545121	Histone acetyltransferase p300; p300 HAT; 2.3.1.48 {ECO:0000269
INHBA	204926_at	1.29	0.0445	P08476	407	22	D : Genome Maintenance	12660162	Inhibin beta A chain; Activin beta A chain; Erythroid differentiation protein; EDF; Precursor
INSR	226450_at	0.78	0.053	P06213	460	35	D : Genome Maintenance	10207053	Insulin receptor; IR; 2.7.10.1; CD220; Insulin receptor subunit alpha; Insulin receptor subunit beta; Precursor
JAG2	209784_s_at	1.87	1.7E-07	Q9Y219	409	53	D : Genome Maintenance	10079256	Protein jagged 2; Jagged2; hJ2; Precursor
LAMA3	202202_s_at	0.38	1.3E-08	Q16787	370	31	C : Cellular Fate and Organization	12915477	Laminin subunit alpha 3; Epiligrin 170 kDa subunit; E170; Epiligrin subunit alpha; Kalinin subunit alpha; Laminin 5 subunit alpha; Laminin 6 subunit alpha; Laminin 7 subunit alpha; Nicein subunit alpha; Precursor
PLAT	201860_s_at	0.73	0.009	P00750	787	45	C : Cellular Fate and Organization	10340997	Tissue type plasminogen activator; t PA; t plasminogen activator; tPA; 3.4.21.68; Alteplase; Reteplase; Tissue type plasminogen activator chain A; Tissue type plasminogen activator chain B; Precursor
PLAU	205479_s_at	1.35	0.0113	P00749	595	50	C : Cellular Fate and Organization	10340997	Urokinase type plasminogen activator; U plasminogen activator; uPA; 3.4.21.73; Urokinase type plasminogen activator long chain A; Urokinase type plasminogen activator short chain A; Urokinase type plasminogen activator chain B; Precursor
PLG	230931_at	1.59	0.0003	P00747	456	41	C : Cellular Fate and Organization	10077593	Plasminogen; 3.4.21.7; Plasmin heavy chain A; Activation peptide; Angiostatin; Plasmin heavy chain A
PRKCQ	210038_at	0.83	0.1408	Q04759	556	46	C : Cellular Fate and Organization	10636891	Protein kinase C theta type; 2.7.11.13; nPKC theta
PRSS3	213421_x_at	2.22	9.00E-12	P35030	569	39	F : Protein Fate	11827488	Trypsin 3; 3.4.21.4; Brain trypsinogen; Mesotrypsinogen; Serine protease 3; Serine protease 4; Trypsin III; Trypsin IV; Precursor
SPOCK1	202363_at	1.66	0.0008	Q08629	2086	136	C : Cellular Fate and Organization	1463459	Testican 1; Protein SPOCK; Precursor
STMN2	203000_at	0.55	7.7E-07	Q93045	365	31	C : Cellular Fate and Organization	14702039	Stathmin 2; Superior cervical ganglion 10 protein; Protein SCG10
TCF4	213891_s_at	0.6	0.000012	P15884	538	26	T : Transcription	14702039	Transcription factor 4; TCF 4; Class B basic helix loop helix protein 19; bHLHb19; Immunoglobulin transcription factor 2; ITF 2; SL3 3 enhancer factor 2; SEF 2
TP53	201746_at	1.65	0.0001	P04637	456	33	D : Genome Maintenance	10484981	Cellular tumor antigen p53; Antigen NY CO 13; Phosphoprotein p53; Tumor suppressor p53
VAV2	226063_at	1.41	0.0088	P52735	365	39	C : Cellular Fate and Organization	12454019	Guanine nucleotide exchange factor VAV2; VAV 2

Supplementary Table 8. Top 20 genes and corresponding betweenness scores, HR values and p-values, GO, synonyms, and probesets for KM plots.

Chapter 4: Therapeutic targeting of the pre-metastatic stage in human brain metastasis

Preamble

This chapter is an original manuscript submitted for publication on January 31, 2018 and presented in its original format. (Extended datasets and Supplementary Tables 2-4 will be available upon publication).

Singh M, Venugopal C, Tokar T, Brown KR, McFarlane N, Subapanditha M, Bakhshinyan D, Vora P, Qazi, Murty N, Jurisica I, Moffat J, Singh SK.

Experimental concept and study design was developed by myself C. Venugopal and S. Singh, and the worke supervised by S. Singh. Brain metastases samples were provided by N. Murty. I performed all *in vitro* BMIC line generation, maintenance and characterization. All flow cytometric analyses were performed by N. McFarlane and Subapanditha. Generation of the *in vivo* models was conducted by myself, with surgical assistance (suturing) by D. Bakhshinyan, M. Qazi and P. Vora. Sample collection was performed by myself. Sample preparation and microarray and RNA sequencing experiments were performed by the Farncombe Metagenomics Facility (McMaster University). Analyses of microarray and RNA sequencing results were analyzed by T. Tokar under the supervision of I. Jurisica. *In vitro* drug screening was performed by myself, with advice form C. Venugopal and P .Vora. *In vivo* validation of Apomorphine was performed by myself, with advice from C. Venugopal. *In silico* analyses were performed by T. Tokar under the

supervision of I. Jurisica. The manuscript was prepared myself, with input and edits provided by S. Singh, C. Venugopal, P. Vora, T. Tokar and I. Jurisica.

The main concept of this work was derived from our observation during the generation of our BM models. Where our ICr and ICa models developed large macro-metastases, our IT model developed only tiny, barely visible pockets of cells within the brain. I isolated these BMICs, termed BM^{IT}, and performed trangenomic analyses, where I found these cells to retain a unique genetic phenotype that differed from the primary lung tumors and brain metastases developed in our ICr and ICa routes. I determined these BM^{IT} cells to belong to a "pre-metastatic" state, and upon further *in silico* analysis and *in vivo* validation I identified Apomorphine to be a potential BMIC targeting therapeutic.

Therapeutic targeting of the pre-metastatic stage in human brain metastasis

Mohini Singh[1,2], Chitra Venugopal[1,3], Tomas Tokar[4], Nicole McFarlane[1,3], Minomi Subapanditha[3], Maleeha Qazi[1,2], David Bakhshinyan[1,2], Parvez Vora[1,3], Naresh Murty[3], Igor Jurisica[4,5,6], and Sheila K. Singh[1,2,3]

[1]Stem Cell and Cancer Research Institute, McMaster University, Hamilton, ON, Canada

[2]Department of Biochemistry and Biomedical Sciences, McMaster University, Hamilton, ON, Canada

[3]Department of Surgery, McMaster University, Hamilton, ON, Canada

[4]Krembil Research Institute, University Health Network, Toronto, ON, Canada

[5]Departments of Medical Biophysics and Computer Science, University of Toronto, Toronto, ON, Canada

[6]Institute of Neuroimmunology, Slovak Academy of Sciences, Bratislava, Slovakia

Corresponding Author Contact Information:

Sheila K. Singh MD PhD FRCS(C), MDCL 5027, McMaster University Stem Cell and Cancer Research Institute, 1280 Main Street West, Hamilton, ON, L8S 4K1, CANADA.

T: 905 521 2100 x75237 F: 905 521 9992 Email: ssingh@mcmaster.ca

Abstract

Brain metastases (BM) are a leading cause of adult cancer mortality. Pre-metastasis, where circulating metastatic cells extravasate and seed the secondary organ, is a key stage in metastasis that cannot be captured in humans. Here we have used our established brain metastasis initiating cell (BMIC) models and gene expression analyses to characterize pre-metastasis in human lung-to-brain metastases. Pre-metastatic BMICs engage invasive and epithelial developmental mechanisms while simultaneously impeding proliferation and apoptosis. We identified Apomorphine, a dopamine agonist, to be a potential pre-metastasis targeting drug. *In vivo* treatment with Apomorphine prevented BM formation, potentially through targeting of pre-metastasis-associated genes KIF16B, SEPW1, and TESK2. Furthermore, low expression of these genes was associated with poor survival of lung adenocarcinoma patients. These results illuminate the cellular and molecular dynamics of pre-metastasis, a state currently impossible to identify or interrogate in BM patients, and presents novel therapeutic targets and associated pathways to prevent BM initiation.

Introduction

Metastases to the brain (BM) are the most common neoplasm to affect the adult central nervous system, occurring in up to 40% of cancer patients and at a rate ten times greater than that of primary neural neoplasms(Patchell, 2003). Survival of BM patients is limited to mere weeks, extended to months upon administration of multimodal treatment(Sjobakk *et al.*, 2013). Despite the devastating clinical outcomes, the genetic and molecular events that govern metastatic development remain frustratingly difficult to isolate. The process of metastasis is both complicated and extremely inefficient, where only a minute percentage of disseminated tumor cells are capable of surviving the lympho-vascular system to establish metastatic tumors. Metastatic cells must first adapt to and seed this secondary environment, termed "pre-metastasis"; this tissue colonization stage directly precedes formation of small micro-metastases, and establishment of vasculature will promote larger macro-metastatic growth. Pre-metastasis is the largest barrier to metastatic development and tissue colonization, yet this stage remains poorly characterized(Chambers *et al.*, 2002; Valastyan & Weinberg, 2011). Theoretically, the delay between primary tumor formation and clinical diagnosis of metastatic growth, even with early tumor dissemination, provides a potential window for therapeutic intervention(Vanharanta & Massague, 2013).

Significant investigation into the cancer genome has led to greater understanding of the evolving clonal architecture of tumors(McGranahan & Swanton, 2017), exposing the co-existence of a dominant originating primary tumor clone along with multiple genetically distinct subclones that can give rise to recurrence and metastases(Anderson *et al.*, 2011; Brastianos *et al.*, 2015; Ding *et al.*, 2010; Jamal-Hanjani *et al.*, 2017; Yachida *et*

al., 2010). Further lineage analyses have identified early and initiating conditions that define a "pre-cancerous" stage in the progression of several primary cancers(Hong *et al.*, 2008; Shlush *et al.*, 2014; Wistuba *et al.*, 2002). Initiating events have similarly been explored for metastatic growth, identifying the conditional implementation of various mechanisms such as epithelial-mesenchymal transitions (EMT) and angiogenesis by metastasis initiating cells (MICs)(Celia-Terrassa & Kang, 2016). Unfortunately, there remains a dearth of knowledge of the mechanisms that promote "pre-metastatic" initiation and the tissue-colonization stage(Massague & Obenauf, 2016). The majority of current *in vivo* and clinical studies utilize established macro-metastasis samples, failing to properly capture this temporally-sensitive pre-metastatic stage. Systematic characterization of this pre-metastatic stage could provide more relevant avenues for therapeutic options in BM prevention as opposed to treating existing BM.

Previous work in our lab successfully established patient-derived BM models that mimic various stages of the metastatic process, capturing the separate stages of pre-metastatic initiation and macro-metastatic growth through intrathoracic and intracardiac injections, respectively(M. Singh *et al.*, 2017). In this work, we perform transcriptomic analysis by next-generation sequencing (RNAseq) of brain metastasis initiating cells (BMICs) isolated from various stages of the metastatic cascade. We elucidate the molecular variances that underlie pre-metastatic initiation through focused study of human BMICs injected into immunocompromised mice *via* the intra-thoracic route (BM^{IT}). From our intrathoracic BM model, we found that mice characteristically die of lung tumor burden just as BMICs cross the blood-brain barrier and colonize the brain, giving us a timepoint

to isolate these pre-metastatic BMICs. Importantly, the BM^{IT} phase captures a stage of the metastatic cascade that can never be routinely biopsied or captured in humans, as metastatic cells seeding the brain without yet initiating a secondary tumor would represent subclinical disease that cannot be detected by either clinical symptoms or current surveillance neuro-imaging techniques. We found these pre-metastatic BMICs (termed BM^{IT}) to possess over 7000 dysregulated genes active in invasive but not proliferative mechanisms. Interestingly, these BM^{IT} genes were also enriched in neural neoplasm and neurodegenerative pathways. Through Connectivity Map analysis (CMAP) of these BM^{IT} genes, we generated a list of drugs that could target the BM^{IT} gene signature. We then returned to our BMIC patient-derived xenotransplantation discovery model to demonstrate that the dopamine agonist Apomorphine inhibits BM development *in vivo*, presumably by inhibiting the pre-metastatic state. Further pharmacogenomic interrogation of the BM^{IT} gene list identified 3 genes downregulated genes that are directly targeted by Apomorphine, KIF16B, SEPW1, and TESK2, where administration of Apomorphine restores expression. Lastly, interrogation of lung adenocarcinoma patient databases showed that decreased expression of these genes is associated with poor disease-free survival

With this work we have successfully characterized a novel temporal genetic profile of pre-metastatic growth, and have functionally validated the efficacy of targeting this stage in BM development through administration of Apomorphine. The ability to prevent metastatic progression to the brain can transform an unvaryingly lethal systemic disease into one that is eminently more treatable.

Materials and Methods

Patient Sample Processing and Cell Culture

Brain metastases (BM) originating from non-small cell lung carcinoma (NSCLC) primary samples were obtained from consenting patients, as approved by the Research Ethics Board at Hamilton Health Sciences. BMs were processed and maintained in Tumor Sphere Media (TSM) as previously described(M. Singh *et al.*, 2017; Venugopal *et al.*, 2012). BMICs were grown as tumorspheres that were maintained at 37°C with a humidified atmosphere of 5% CO_2

In vivo Modelling of Metastasis

All experimental procedures involving animals were reviewed and approved by McMaster University Animal Research Ethics Board (AREB). NOD-SCID mice were used for all experiments. Mice were anaesthesized using gas anaesthesia (Isoflurane: 5% induction, 2.5% maintenance) before minimally invasive surgery. Injections were performed as previously described for intracranial (ICr), intrathoracic (IT) and intracardiac (ICr) routes(M. Singh *et al.*, 2017). Mice were monitored weekly, and upon reaching endpoint brains and lungs were harvested and underwent two separate analyses:

a) *Hemotoxylin & Eosin staining (H&E)*: whole brains (and lungs from IT injections) were sectioned, and paraffin-embedded for H&E. Images were scanned using an Aperio Slide Scanner and analyzed by ImageScope v11.1.2.760 software (Aperio).

b) *In vitro culture and expansion*: BMICs were re-isolated from ICr brain tumors (BT), IT lung tumors (LT) and pre-metastatic brain tumors (BM^{IT}), and ICa

brain tumors (BM^{IC}). Whole brains and lungs (IT injections) were dissociated into single cell suspensions (Venugopal 2002) and cultured in DMEM with decreasing concentrations of FBS: the first 2 days in 20% FBS, 10% FBS for 2-3 days, 5% FBS, and finally in TSM with puromycin for a minimum of 1 week prior to any analyses to select out any residual contamination of mouse cells as well as to enrich for the BMICs. Duplicate samples per BT, LT, BM^{IT} and BM^{IC} were collected per BMIC line, RNA isolated, and submitted for microarray analyses (BT478) or RNA sequencing analyses (BT478 and BT530).

For drug treatments, mice were injected through IT and IC route, and cells allowed to engraft for 2 weeks. R-(−)-Apomorphine hydrochloride hemihydrate (Sigma) was resuspended in sterile saline at 0.5mg/mL, and administered by subcutaneous injections (S.C.) to give a final dose of 5mg/kg, 3 times weekly for 1 month. Control mice received only saline. Mice were culled as they succumbed to endpoint (approximately 2.5 months).

IC_{50} curve generation

BMICs were dissociated into a single cell suspension, and 2000 cells/well were plated into a 96 well plate at a volume of 200 mL/well in increasing concentrations (5-25μM) of Apomorphine, GW-8510, Lomustine (Sigma), Acacetin (Sigma), Thioridazine (Sigma), Trifluoroperazine (Sigma), and Prochlorperazine (Sigma). DMSO was used as a control. Cells were incubated for four days. 20 μL of Presto Blue (Invitrogen) was added to each well approximately 2h prior to the readout time point. Fluorescence was measured

using a FLUOstar Omega Fluorescence 556 Microplate reader (BMG LABTECH) at excitation and emission wavelengths of 535 nm and 600 nm, respectively. Readings were analyzed using Omega analysis software. Dose–response curves were fitted to the data.

Reverse transcription and quantitative PCR of mRNA

Total RNA was isolated using Norgen RNA extraction kit (Biotek) and reverse transcribed using qScript cDNA Super Mix (Quanta Biosciences) and a C1000 Thermo Cycler (Bio-Rad). qRT-PCR was performed using the Cfx96 (Bio-Rad) with SsoAdvanced SYBR Green (Bio-Rad) using gene specific primers (Supplementary Table 1) and GAPDH as the internal control.

Flow cytometric characterization

Adherent BMICs were detached through application of TrypleE (Invitrogen) and single cells resuspended in PBS+2mM EDTA. Cell suspensions were stained with human anti-TRA-1-85 (CD147, Miltenyi) and incubated for 30 minutes on ice. Samples were run on a MoFlo XDP Cell Sorter (Beckman Coulter). Dead cells were excluded using the viability dye 7AAD (1:10; Beckman Coulter). Compensation was performed using mouse IgG CompBeads (BD). Surface marker expression was defined as positive or negative based on the analysis regions established using the isotype control.

Microarray data analyses

BT478 samples were prepared, processed and run as per Illumina protocol as previously described(Venugopal *et al.*, 2015). Illumina summary probe profiles along associated control probes profiles were read using a Bioconductor package limma v3.30.13(Ritchie *et al.*, 2015). Data were then background corrected using negative control

probes and subsequently normalized applying quantile normalization using all the available control probes. After normalization, expression of the genes was averaged across the technical replicates obtained from the same biological sample.

To provide qualitative assessment of the dissimilarity of the BM^{IT} against BT, LT, and BM^{IC}, scatterplots were plotted depicting expression of the genes as obtained from individuals samples. The Pearson's coefficient of correlation between the individual samples was calculated and plotted to generate a heatmap of the obtained correlations.

RNA sequencing

Illumina sequencing was performed by the Farncombe Metagenomics Facility (McMaster University). RNA integrity was first verified using the Agilent BioAnalyzer, followed by mRNA enrichment and library prep using the NEBNext Ultra Directional RNA Library Prep Kit along with the NEBNext Poly(A) mRNA Magnetic Isolation Module. Libraries were subject to further BioAnalyzer QC and quantified by qPCR. Sequencing was performed using the HiSeq Rapid v2 chemistry with paired end 2x50 bp read length configurations.

Raw RNA sequencing data were preprocessed and normalized as follows: RNAseq data were aligned against hg38 reference genome, using bowtie2. Reads counts per gene were obtained using R packages GenomicRange and GenomicFeatures and using UCSC hg38 KnowGene database as a reference for genomic locations (TxDb.Hsapiens.UCSC.hg38). Counts were first normalized to counts per million, then additional quantile normalization was applied. Expressions were averaged across pairs of technical replicates. Counts were then log2-transformed and genes whose expression was

< 0 across all the 18 samples were removed. Principal component analysis (PCA) was then conducted and all the samples were depicted in the space defined by the two most principal components. Additionally, a heatmap depicting sample differences, as quantified by euclidean distance of the gene expression, was generated along the dendrogram depicting hierarchical clustering of the samples. Sample 16 was then excluded from further analysis as an outlier.

Differential expression analysis was performed to identify genes whose expression was significantly different when comparing: i) BM^{IT} against BT, LT, and BM^{IC} from BT478 and ii) BM^{IT} against BT, LT, and BM^{IC} of BT530. Using Bioconductor package limma v3.30.13(Ritchie *et al.*, 2015). Log2 fold change of the gene expression was calculated for both comparisons along the associated p-value and false discovery rate (FDR).

Enrichment analysis

Two types of enrichment analysis were conducted, gene set enrichment analysis (GSEA) as described by Subramanian *et al*.(Subramanian *et al.*, 2005), along with over-representation analysis using hypergeometric test to assess significance of overlap between the selected group of genes and given pathway or biol. process. In both cases enrichment against the five major ontologies was assessed, including: KEGG pathways(Kanehisa & Goto, 2000), Gene Onthology (GO) – Biological processes, GO – cellular components, GO – molecular functions(Ashburner *et al.*, 2000), and Disease ontology (DO)(Schriml *et al.*, 2012). All the enrichment analyses were performed using functions implemented within the Bioconductor package ClusterProfiler v3.2.14(G. Yu *et al.*, 2012).

CMAP analysis

Connectivity Map (CMAP) analysis was used to predict effects of the drugs on the expression of the deregulated genes(Lamb, 2007). In this analysis, drugs (comprising 1,289 chemical substances) were assessed with respect to their ability to invert expression changes of the deregulated genes obtained from above described differential gene expression analysis. CMAP analysis was conducted using Bioconductor package PharmacoGx(Smirnov *et al.,* 2016). Drugs were first filtered according to resulting connectivity score (Connectivity score < 0) and associated significance ($P < 0.01$). Finally, drugs were selected for preliminary *in vitro* screening based on the criteria of novelty in metastasis treatment, ability to cross the blood-brain-barrier, and potential to target neural developmental systems or associated disorders.

To further explore effects of Apomorphine on gene expression we constructed a protein-protein interaction (PPI) network using Apomorphine gene targets obtained from DrugBank v5.0.11(Wishart *et al.*, 2018) and The Comparative Toxicogenomics Database (CTD) vJan-2018(Davis *et al.,* 2017). Genes transcriptionally modified by Apomorphine were identified using CMAP ver. 1(Lamb, 2007). Using the three gene lists, we then identified PPIs connecting individual genes in the list using Integrated Interactions Database IID v2017-04(Kotlyar *et al.*, 2016). Resulting PPI network was visualized using NAViGaTOR v3(Brown *et al.,* 2009). As per legend, node color represents GO Molecular Function; edge color corresponds to tissue specificity, specifically highlighting lung and brain tissue, as obtained from IID. The most important BM^{IT} gene targets of Apomorphine were identified by applying PharmacoGx framework for sensitivity modelling (for more details see PharmacoGx user's guide). Genes were filtered according to the drug's

estimated effect on their expression (upregulation of the downregulated genes and downregulation of the upregulated ones) and associated significance ($p < 0.01$).

Kaplan-Meier analysis

Prognostic potential of the genes targeted by the selected drugs was assessed through SurvExpress v2.0 – web resource for validation of cancer gene expression biomarkers(Aguirre-Gamboa *et al.*, 2013). (http://bioinformatica.mty.itesm.mx:8080/Biomatec/SurvivaX.jsp) and lung module of Kaplan-Meier plotter (KMplotter) - tool for meta-analysis based biomarker assessment (http://kmplot.com)(Gyorffy *et al.*, 2013). Prognostic significance of the three target genes (KIF16B, SEPW1 and TESK2), was first tested in SurvExpress using The Cancer Genome Atlas (TCGA) lung adenorcarcinoma gene expression dataset (June 2016) and then validated in KMplotter using all available lung adenocarcinoma datasets. In both cases survival analysis was conducted under default parametrization.

Statistical Analysis

Replicates from at least three samples were used for IC_{50} and RT-PCR experiments. Respective data represent mean±SD with n values listed in figure legends. Student's *t-test* and *2-way ANOVA* analyses using GraphPad Prism 5. $P<0.05$ was considered significant.

Data Availability

The authors declare that all the data supporting the findings of this study are available within the article, its supplementary information files and from the corresponding author upon reasonable request. RNA sequencing files are available as GEO dataset GSE110495 at https://www.ncbi.nlm.nih.gov/geo/query/acc.cgi?acc=GSE110495 upon request.

Results

Capturing the pre- and macro- stages of metastatic growth in BM development

We utilized early passage BM cell lines derived from primary patient samples of lung-to-brain metastases in our work, as these samples are enriched for BMICs that have already successfully completed the metastatic process. Previous work in our lab successfully established preclinical models of lung-to-brain BM(Nolte *et al.*, 2013; M. Singh *et al.*, 2017). Briefly, we injected mice through three different injection routes: a) intracranial (ICr), b) intrathoracic injections (IT), and c) intracardiac injections (ICa), where we were able to replicate the pre-metastatic and macro-metastatic stages from IT and ICa injections respectively(M. Singh *et al.*, 2017). Here, we have further isolated and characterized BMICs at each metastatic stage. BMIC lines transduced with GFP were injected into our BM models and were shown to reform tumors at each stage of the metastatic cascade, from primary lung (LT) and secondary brain (BT) tumor formation to the pre-metastatic (BM^{IT}) and macro-metastasis (BM^{IC}) stages of tumor growth (Fig. 1). BMICs were isolated from BT, BM^{IT}, and BM^{IC} tumors and minimally cultured, and retained the ability to reform secondary spheres, suggesting a preservation of their stem-like and tumor initiation properties (Fig. 1).

To characterize the genetic profiles of each stage of metastatic progression, we performed preliminary microarray analysis of BT478 BMICs from BT, LT, BM^{IT}, and BM^{IC} samples. Intriguingly, we found that genes from BM^{IT} cells clustered separately from BT, LT, and BM^{IC} samples (Supplementary Fig. 1a-b). To corroborate this unique pre-

metastatic BM^{IT} genetic profile we analyzed RNA sequencing data obtained across two separate BMIC lines. Hierarchical clustering along PCA showed that BM^{IT} from both BMIC lines cluster together, irrespective of the cell line origin, whereas established metastatic tumors (BT, LT, BM^{IC}) group into cell line-specific clusters (Fig. 2a-b, Supplementary Fig. 1c). We then performed differential expression analysis comparing expression profiles of BM^{IT} with non-BM^{IT} samples from both cell lines separately. We identified ~7000 differentially expressed genes in the pre-metastatic BM^{IT} stage (Supplementary Table 2). These results indicate temporal evolution of BMICs through metastasis, during which a distinct genetic profile emerges prior to the initiation of the secondary brain metastasis, while established tumors retain a genetically similar profile despite tissue of origin.

Pre-metastatic BMICs retain a unique genetic profile

Using Gene Set Enrichment Analysis (GSEA) we assessed association of BM^{IT} deregulated genes with biological processes (GO), cellular components (GO), molecular functions (GO), biological pathways (KEGG) or diseases (Disease Ontology). We found increased expression of genes regulating cytoskeletal structures and epithelial tumor invasion, as well as decreased expression in processes of cell division and apoptosis (Fig. 3a-b, Extended Dataset 1). These data suggest that pre-metastatic BM^{IT} are not dormant, but have concurrently increased activation of invasive mechanisms while repressing programmed cell death and growth mechanisms. We also found enrichment within several neurodegenerative pathways (Supplementary Fig. 2, Extended Dataset 2) and neural

neoplasm components (Supplementary Fig. 3, Extended Dataset 3). We also performed enrichment analysis (over-representation analysis) of the gene clusters obtained by hierarchical clustering of BT, LT, BM^{IT} and BM^{IT} genes (Fig. 3c). We identified clusters of BM^{IT} deregulated genes to be significantly ($p < 0.01$) enriched in pathways of cancer and neuroactive ligand-receptor interaction. Interestingly, enrichment analysis of the instances of the Disease Ontology revealed enrichment of the Autonomic nervous system neoplasm (Supplementary Table 3).

Therapeutic targeting of pre-metastatic BM^{IT}

Connectivity Map analysis (CMAP) was performed on the dysregulated BM^{IT} gene set to identify potential targeting therapeutics (Fig. 4a, Supplementary Table 4). Drugs were selected for preliminary *in vitro* screening based on the criteria of novelty in metastasis treatment, ability to cross the blood-brain-barrier, and potential targeting of neural developmental systems or associated disorders, from which the DRD2 agonist Apomorphine proved to have a moderately low IC_{50} for both BT478 and BT530 BMIC lines (Fig. 4b). We repeated the drug screening with other dopamine-specific psychological therapeutics, which failed affect BMICs to the same extent as Apomorphine (Fig. 4b).

To assess the efficacy of Apomorphine inhibiting BM^{IT} *in vivo*, we performed ICa injections with BMIC line BT478. BMICs were allowed to engraft for 2 weeks prior to starting a month-long administration of Apomorphine, 3 times weekly along with saline for control mice (Fig. 5a). Mice were culled at endpoint, and their brains minimally cultured to remove the bulk of mouse cellular debris. We then performed FACS for human-

Tra-1-85 to isolate human BMICs. Apomorphine greatly attenuated BM development, as defined by a complete absence of BMICs in Apomorphine-treated brains (Fig. 5b, Supplementary Fig.4). These data together suggest that Apomorphine does target BM^{IT} cells to prevent BM initiation and development, both *in silico* and *in vivo*.

Pre-metastatic BM^{IT} genes are predictive of lung cancer patient survival

We attempted to elucidate the biological context of Apomorphine to determine possible mechanisms of actions. We first generated an interactome to identify overall genes targeted by Apomorphine (Fig. 6a). Application of a targeted PharmacoGx framed CMAP on Apomorphine focusing on the pre-metastatic BM^{IT} genes identified 3 genes downregulated as direct targets, KIF16B, SEPW1 and TESK2 (Fig. 6b). *In vitro* analyses determined transcript levels of these 3 genes to be moderately increased in BMICs treated with Apomorphine (Fig. 6c). These 3 genes were then interrogated for prognostic value using transcriptomic data from a lung adenocarcinoma patient cohort, where a refined collective signature comprised of TESK2, SEPW1, and KI16B was found to have significant impact on patient survival, where low expression of these genes correlated with poor patient survival (Fig. 6c, Supplementary Fig. 4).

Discussion

Our limited mechanistic understanding of metastatic disease greatly hinders therapeutic discovery and improvement of the dismal patient outcome of BM(Steeg, 2016). Despite advancements in preventative and treatment modalities for primary tumors that have resulted in increased patient survival, the inability of these treatments to target residual CSC and BMIC populations leaves cancer patients vulnerable and prone to relapse and metastases(Langley & Fidler, 2013).

Significant study of the genome evolution of cancer has identified pre-cancerous events in several primary cancers(Hong *et al.*, 2008; Sgroi, 2010; Shlush *et al.*, 2014); unfortunately, the molecular mechanisms that drive pre-metastatic cells in the brain remain poorly defined. A significant disadvantage with currently available *in vivo* models is the inability to capture the pre-metastatic stage of brain tissue colonization, instead focusing on the easier to collect macro-metastatic stage. Recent studies with *C. elegans* led by Matus *et al*.(Matus *et al.*, 2015) determined that cellular invasion and proliferation are mutually incompatible stages, where both stages are representative of pre-metastasis and macro-metastasis progression, respectively. This work substantiates the inefficient targeting of invasive cells by current chemotherapies that tend to target rapidly dividing cells, perhaps at the expense of invasive cells(Hurst *et al.*, 2016).

Previous work in our lab successfully established clinically relevant models of BM representing the different stages of metastasis, where we captured both the pre-metastatic and macro-metastatic stages of tumor growth *via* our IT and IC routes, respectively(M. Singh *et al.*, 2017). Through isolation and comparison of BMICs at various stages of

metastatic progression in our established BM models, we identified a genetic pattern unique only to BMICs undergoing pre-metastasis, termed BM^{IT}, whereas established macro-metastatic tumors (BT, LT, BM^{IC}) were genetically similar. These BM^{IT}-BMICs possess ~7000 dysregulated genes, active in mechanisms that promote invasion and repress apoptosis and division, corroborating results by Matus *et al.* in our more relevant patient-related modelling systems(Matus *et al.*, 2015).

The role of neurotransmitters in cancer has drawn varying interest over the years, where they have been found to exert a strong influence over external and internal cellular factors in cancer progression(Jobling *et al.*, 2015). Dopamine receptors (DR) and dopamine have been revealed to exhibit various pleiotropic properties through dependent and independent pathways, and their modulation has enhanced the efficiency of anticancer drugs in preclinical cancer models(Minami *et al.*, 2017; Wang *et al.*, 2015). In particular, DRD2 agonists have recently been shown to suppress proliferation, angiogenesis and invasion in several cancers and tumors(Hoeppner *et al.*, 2015; Huang *et al.*, 2016; Peverelli *et al.*, 2016; Roy *et al.*, 2017). Such studies paired with epidemiological data implicate a relationship between lower rates of cancer development in patients with Parkinson's, intimating a possible link between DR agonists and cancer(Bajaj *et al.*, 2010; Feng *et al.*, 2015).

Through enrichment analyses, we determined that BM^{IT} dysregulated gene sets enrich pathways that regulate autonomic nervous system neoplasms and neural system dysregulation, implying a possible relation between neurodevelopmental pathways and promotion of cancer invasion. CMAP interrogation of the dysregulated BM^{IT} genes

identified a list of targeting therapeutics, of which several of the top hits are currently applied as or are being investigated as antineoplastic agents against various cancers(Fujita *et al.*, 2015; Sumida *et al.*, 2011; Tomoda *et al.*, 2005; Webster & Leibovich, 2005). We selected drugs for preliminary *in vitro* screening based on the ability to pass the BBB, treatment of neurological disorders, and overall novelty as a cancer therapeutic, from which Apomorphine was selected for further validation. Apomorphine is a non-selective dopamine agonist of the morphine derivative, primarily activating dopamine-like receptor 2 (DRD2). Among its multiple uses, Apomorphine administration reduced amyloid β degradation in Alzheimer's patients(Himeno *et al.*, 2011; Stocchi *et al.*, 2016), and recently has shown efficacy in the treatment of Parkinson's(Boyle & Ondo, 2015) as well as a potential targeting of tumor cell invasion(Jung & Lee, 2017). Further screening against other dopamine-specific psychological therapeutics validated the specific efficacy of Apomorphine in targeting pre-metastatic BMICs.

To further validate the ability of Apomorphine to target BM^{IT}, we applied the drug *in vivo* in our BM models. Initial trials administering Apomorphine against our IT model drew inconclusive results, where the relatively low number of BMICs we were able to capture at the pre-metastatic stage made it difficult to confidently determine the efficacy of Apomorphine (data not shown). Thus, we utilized our ICa model to properly interrogate the efficacy of Apomorphine against BM development, collecting samples at early timepoints that follow the micro-metastatic time course of our IT model as well as at survival endpoint to confirm macro-metastatic growth. Apomorphine proved to be successful at inhibiting micro-metastatic growth as well as subsequent macro-metastases.

PharamcoGx directed CMAP analysis determined 3 downregulated BM^{IT} genes specifically targeted by Apomorphine, KIF16B, SEPW1 and TESK2, where *in silico* application of the drug would activate their expression. SEPW1 belongs to a family of selenoproteomes, which have been increasingly implicated in aspects of neurobiology and neurodegenerative disorders(X. Zhang *et al.*, 2016). TESK2 is a serine/threonine protein kinase(Rosok *et al.*, 1999). KIF16B is a kinesin-like motor protein that may be involved in intracellular trafficking(Farkhondeh *et al.*, 2015), where defects in this family of proteins has been associated with neurodegenerative, developmental, and cancer diseases(Hirokawa *et al.*, 2010). *In vitro* analysis of Apomorphine treated BMICs determined transcript levels of these 3 genes to be moderately increased as compared to the control. When theses genes were applied as a predictive signature in a cohort of lung adenocarcinoma patients, they showed significant prognostic value for patient survival.

Conclusion

We present an in-depth genetic characterization of the previously uncaptured stage of pre-metastasis in BM progression. We further identified Apomorphine to be a novel BM^{IT} targeting therapeutic to prevent BM development. Continuing studies will further characterize the role and related mechanisms of DR agonists in BM development. The ability to inhibit BMICs from initiating metastasis would target BM at the ideal stage, preventing the need for more toxic and possibly detrimental treatments. Our identification of this pre-metastatic stage in the development of BM can be mined to provide further

critical therapeutic targets in all cancers that metastasize to the brain, offering a paradigm shift for the current state of BM treatment.

Authors' Contributions

Conceptualization and Design: M. Singh, C. Venugopal, S. Singh
Methodology: M. Singh, C. Venugopal, N. McFarlane, M. Subapanditha, D. Bakhshinyan, P. Vora, M. Qazi
Data Analysis & Interpretation: M. Singh, C. Venugopal, T. Tokar, I. Jurisica, S. Singh
Writing, review, and/or revision of the manuscript: M. Singh, C. Venugopal, P. Vora, I. Jurisica, D, S. Singh
Supervision: I. Jurisica, S. Singh

Acknowledgements

Financial Support: This work was supported by funds from the Department of Surgery at McMaster University, Ontario Institute for Cancer Research Cancer Stem Cell Program, a Canadian Cancer Society Research Institute Innovation Grant and The Boris Family Fund for Brain Metastasis Research for Dr. Sheila Singh; Brain Canada PhD Studentship for Mohini Singh; Ontario Research Fund (GL2-01-030), Canada Research Chair Program (CRC #225404), and Canada Foundation for Innovation (CFI #29272, #225404, #30865) supported Dr. Igor Jurisica.

Disclosure of Potential Conflict of Interest: The authors declare no potential conflict of interest.

References

1 Patchell, R. A. The management of brain metastases. *Cancer treatment reviews* **29**, 533-540 (2003).

2 Sjobakk, T. E. *et al.* Metabolic profiles of brain metastases. *International journal of molecular sciences* **14**, 2104-2118, doi:10.3390/ijms14012104 (2013).

3 Chambers, A. F., Groom, A. C. & MacDonald, I. C. Dissemination and growth of cancer cells in metastatic sites. *Nature reviews. Cancer* **2**, 563-572, doi:10.1038/nrc865 (2002).

4 Valastyan, S. & Weinberg, R. A. Tumor metastasis: molecular insights and evolving paradigms. *Cell* **147**, 275-292, doi:10.1016/j.cell.2011.09.024 (2011).

5 Vanharanta, S. & Massague, J. Origins of metastatic traits. *Cancer cell* **24**, 410-421, doi:10.1016/j.ccr.2013.09.007 (2013).

6 McGranahan, N. & Swanton, C. Clonal Heterogeneity and Tumor Evolution: Past, Present, and the Future. *Cell* **168**, 613-628, doi:10.1016/j.cell.2017.01.018 (2017).

7 Yachida, S. *et al.* Distant metastasis occurs late during the genetic evolution of pancreatic cancer. *Nature* **467**, 1114-1117, doi:10.1038/nature09515 (2010).

8 Ding, L. *et al.* Genome remodelling in a basal-like breast cancer metastasis and xenograft. *Nature* **464**, 999-1005, doi:10.1038/nature08989 (2010).

9 Anderson, K. *et al.* Genetic variegation of clonal architecture and propagating cells in leukaemia. *Nature* **469**, 356-361, doi:10.1038/nature09650 (2011).

10 Brastianos, P. K. *et al.* Genomic Characterization of Brain Metastases Reveals Branched Evolution and Potential Therapeutic Targets. *Cancer discovery* **5**, 1164-1177, doi:10.1158/2159-8290.CD-15-0369 (2015).

11 Jamal-Hanjani, M. *et al.* Tracking the Evolution of Non-Small-Cell Lung Cancer. *The New England journal of medicine* **376**, 2109-2121, doi:10.1056/NEJMoa1616288 (2017).

12 Hong, D. *et al.* Initiating and cancer-propagating cells in TEL-AML1-associated childhood leukemia. *Science* **319**, 336-339, doi:10.1126/science.1150648 (2008).

13 Shlush, L. I. *et al.* Identification of pre-leukaemic haematopoietic stem cells in acute leukaemia. *Nature* **506**, 328-333, doi:10.1038/nature13038 (2014).

14 Wistuba, II, Mao, L. & Gazdar, A. F. Smoking molecular damage in bronchial epithelium. *Oncogene* **21**, 7298-7306, doi:10.1038/sj.onc.1205806 (2002).

15 Celia-Terrassa, T. & Kang, Y. Distinctive properties of metastasis-initiating cells. *Genes & development* **30**, 892-908, doi:10.1101/gad.277681.116 (2016).

16 Massague, J. & Obenauf, A. C. Metastatic colonization by circulating tumor cells. *Nature* **529**, 298-306, doi:10.1038/nature17038 (2016).

17 Singh, M. *et al.* RNAi screen identifies essential regulators of human brain metastasis-initiating cells. *Acta Neuropathol*, doi:10.1007/s00401-017-1757-z (2017).

18 Venugopal, C., McFarlane, N. M., Nolte, S., Manoranjan, B. & Singh, S. K. Processing of primary brain tumor tissue for stem cell assays and flow sorting. *Journal of visualized experiments : JoVE*, doi:10.3791/4111 (2012).

19 Venugopal, C. *et al.* Pyrvinium Targets CD133 in Human Glioblastoma Brain Tumor-Initiating Cells. *Clinical cancer research : an official journal of the American Association for Cancer Research* **21**, 5324-5337, doi:10.1158/1078-0432.CCR-14-3147 (2015).

20 Ritchie, M. E. *et al.* limma powers differential expression analyses for RNA-sequencing and microarray studies. *Nucleic acids research* **43**, e47, doi:10.1093/nar/gkv007 (2015).

21 Subramanian, A. *et al.* Gene set enrichment analysis: a knowledge-based approach for interpreting genome-wide expression profiles. *Proceedings of the National Academy of Sciences of the United States of America* **102**, 15545-15550, doi:10.1073/pnas.0506580102 (2005).

22 Kanehisa, M. & Goto, S. KEGG: kyoto encyclopedia of genes and genomes. *Nucleic acids research* **28**, 27-30 (2000).

23 Ashburner, M. *et al.* Gene ontology: tool for the unification of biology. The Gene Ontology Consortium. *Nature genetics* **25**, 25-29, doi:10.1038/75556 (2000).

24 Schriml, L. M. *et al.* Disease Ontology: a backbone for disease semantic integration. *Nucleic acids research* **40**, D940-946, doi:10.1093/nar/gkr972 (2012).

25 Yu, G., Wang, L. G., Han, Y. & He, Q. Y. clusterProfiler: an R package for comparing biological themes among gene clusters. *Omics : a journal of integrative biology* **16**, 284-287, doi:10.1089/omi.2011.0118 (2012).

26 Lamb, J. The Connectivity Map: a new tool for biomedical research. *Nature reviews. Cancer* **7**, 54-60, doi:10.1038/nrc2044 (2007).

27 Smirnov, P. *et al.* PharmacoGx: an R package for analysis of large pharmacogenomic datasets. *Bioinformatics* **32**, 1244-1246, doi:10.1093/bioinformatics/btv723 (2016).

28 Wishart, D. S. *et al.* DrugBank 5.0: a major update to the DrugBank database for 2018. *Nucleic acids research* **46**, D1074-D1082, doi:10.1093/nar/gkx1037 (2018).

29 Davis, A. P. *et al.* The Comparative Toxicogenomics Database: update 2017. *Nucleic acids research* **45**, D972-D978, doi:10.1093/nar/gkw838 (2017).

30 Kotlyar, M., Pastrello, C., Sheahan, N. & Jurisica, I. Integrated interactions database: tissue-specific view of the human and model organism interactomes. *Nucleic acids research* **44**, D536-541, doi:10.1093/nar/gkv1115 (2016).

31 Brown, K. R. *et al.* NAViGaTOR: Network Analysis, Visualization and Graphing Toronto. *Bioinformatics* **25**, 3327-3329, doi:10.1093/bioinformatics/btp595 (2009).

32 Aguirre-Gamboa, R. *et al.* SurvExpress: an online biomarker validation tool and database for cancer gene expression data using survival analysis. *PloS one* **8**, e74250, doi:10.1371/journal.pone.0074250 (2013).

33 Gyorffy, B., Surowiak, P., Budczies, J. & Lanczky, A. Online survival analysis software to assess the prognostic value of biomarkers using transcriptomic data in non-small-cell lung cancer. *PloS one* **8**, e82241, doi:10.1371/journal.pone.0082241 (2013).

34 Nolte, S. M. *et al.* A cancer stem cell model for studying brain metastases from primary lung cancer. *J Natl Cancer Inst* **105**, 551-562, doi:10.1093/jnci/djt022 (2013).

35 Steeg, P. S. Targeting metastasis. *Nature reviews. Cancer* **16**, 201-218, doi:10.1038/nrc.2016.25 (2016).

36 Langley, R. R. & Fidler, I. J. The biology of brain metastasis. *Clin Chem* **59**, 180-189, doi:10.1373/clinchem.2012.193342 (2013).

37 Sgroi, D. C. Preinvasive breast cancer. *Annual review of pathology* **5**, 193-221, doi:10.1146/annurev.pathol.4.110807.092306 (2010).

38 Matus, D. Q. *et al.* Invasive Cell Fate Requires G1 Cell-Cycle Arrest and Histone Deacetylase-Mediated Changes in Gene Expression. *Developmental cell* **35**, 162-174, doi:10.1016/j.devcel.2015.10.002 (2015).

39 Hurst, R. E., Bastian, A., Bailey-Downs, L. & Ihnat, M. A. Targeting dormant micrometastases: rationale, evidence to date and clinical implications. *Therapeutic advances in medical oncology* **8**, 126-137, doi:10.1177/1758834015624277 (2016).

40 Jobling, P. *et al.* Nerve-Cancer Cell Cross-talk: A Novel Promoter of Tumor Progression. *Cancer research* **75**, 1777-1781, doi:10.1158/0008-5472.CAN-14-3180 (2015).

41 Minami, K. *et al.* Inhibitory Effects of Dopamine Receptor D1 Agonist on Mammary Tumor and Bone Metastasis. *Scientific reports* **7**, 45686, doi:10.1038/srep45686 (2017).

42 Wang, S. *et al.* Dopamine enhances the response of sunitinib in the treatment of drug-resistant breast cancer: Involvement of eradicating cancer stem-like cells. *Biochemical pharmacology* **95**, 98-109, doi:10.1016/j.bcp.2015.03.013 (2015).

43 Peverelli, E. *et al.* Dopamine receptor type 2 (DRD2) inhibits migration and invasion of human tumorous pituitary cells through ROCK-mediated cofilin inactivation. *Cancer letters* **381**, 279-286, doi:10.1016/j.canlet.2016.08.005 (2016).

44 Hoeppner, L. H. *et al.* Dopamine D2 receptor agonists inhibit lung cancer progression by reducing angiogenesis and tumor infiltrating myeloid derived suppressor cells. *Molecular oncology* **9**, 270-281, doi:10.1016/j.molonc.2014.08.008 (2015).

45 Roy, S. *et al.* Activation of D2 Dopamine Receptors in CD133+ve Cancer Stem Cells in Non-small Cell Lung Carcinoma Inhibits Proliferation, Clonogenic Ability, and Invasiveness of These Cells. *The Journal of biological chemistry* **292**, 435-445, doi:10.1074/jbc.M116.748970 (2017).

46 Huang, H. *et al.* Dopamine D2 receptor suppresses gastric cancer cell invasion and migration via inhibition of EGFR/AKT/MMP-13 pathway. *International immunopharmacology* **39**, 113-120, doi:10.1016/j.intimp.2016.07.002 (2016).

47 Feng, D. D., Cai, W. & Chen, X. The associations between Parkinson's disease and cancer: the plot thickens. *Translational neurodegeneration* **4**, 20, doi:10.1186/s40035-015-0043-z (2015).

48 Bajaj, A., Driver, J. A. & Schernhammer, E. S. Parkinson's disease and cancer risk: a systematic review and meta-analysis. *Cancer causes & control : CCC* **21**, 697-707, doi:10.1007/s10552-009-9497-6 (2010).

49 Webster, W. S. & Leibovich, B. C. Exisulind in the treatment of prostate cancer. *Expert review of anticancer therapy* **5**, 957-962, doi:10.1586/14737140.5.6.957 (2005).

50 Sumida, T. *et al.* Anti-stromal therapy with imatinib inhibits growth and metastasis of gastric carcinoma in an orthotopic nude mouse model. *International journal of cancer* **128**, 2050-2062, doi:10.1002/ijc.25812 (2011).

51 Fujita, K., Kubota, Y., Ishida, H. & Sasaki, Y. Irinotecan, a key chemotherapeutic drug for metastatic colorectal cancer. *World journal of gastroenterology* **21**, 12234-12248, doi:10.3748/wjg.v21.i43.12234 (2015).

52 Tomoda, R. *et al.* Low-dose methotrexate inhibits lung metastasis and lengthens survival in rat osteosarcoma. *Clinical & experimental metastasis* **22**, 559-564, doi:10.1007/s10585-005-5377-y (2005).

53 Himeno, E. *et al.* Apomorphine treatment in Alzheimer mice promoting amyloid-beta degradation. *Annals of neurology* **69**, 248-256, doi:10.1002/ana.22319 (2011).

54 Stocchi, F., Torti, M. & Fossati, C. Advances in dopamine receptor agonists for the treatment of Parkinson's disease. *Expert opinion on pharmacotherapy* **17**, 1889-1902, doi:10.1080/14656566.2016.1219337 (2016).

55 Boyle, A. & Ondo, W. Role of apomorphine in the treatment of Parkinson's disease. *CNS drugs* **29**, 83-89, doi:10.1007/s40263-014-0221-z (2015).

56 Jung, Y. S. & Lee, S. O. Apomorphine suppresses TNF-alpha-induced MMP-9 expression and cell invasion through inhibition of ERK/AP-1 signaling pathway in MCF-7 cells. *Biochemical and biophysical research communications* **487**, 903-909, doi:10.1016/j.bbrc.2017.04.151 (2017).

57 Zhang, X. *et al.* Selenotranscriptomic Analyses Identify Signature Selenoproteins in Brain Regions in a Mouse Model of Parkinson's Disease. *PloS one* **11**, e0163372, doi:10.1371/journal.pone.0163372 (2016).

58 Rosok, O., Pedeutour, F., Ree, A. H. & Aasheim, H. C. Identification and characterization of TESK2, a novel member of the LIMK/TESK family of protein kinases, predominantly expressed in testis. *Genomics* **61**, 44-54, doi:10.1006/geno.1999.5922 (1999).

59 Farkhondeh, A., Niwa, S., Takei, Y. & Hirokawa, N. Characterizing KIF16B in neurons reveals a novel intramolecular "stalk inhibition" mechanism that regulates its capacity to potentiate the selective somatodendritic localization of early endosomes. *The Journal of neuroscience : the official journal of the Society for Neuroscience* **35**, 5067-5086, doi:10.1523/JNEUROSCI.4240-14.2015 (2015).

60 Hirokawa, N., Niwa, S. & Tanaka, Y. Molecular motors in neurons: transport mechanisms and roles in brain function, development, and disease. *Neuron* **68**, 610-638, doi:10.1016/j.neuron.2010.09.039 (2010).

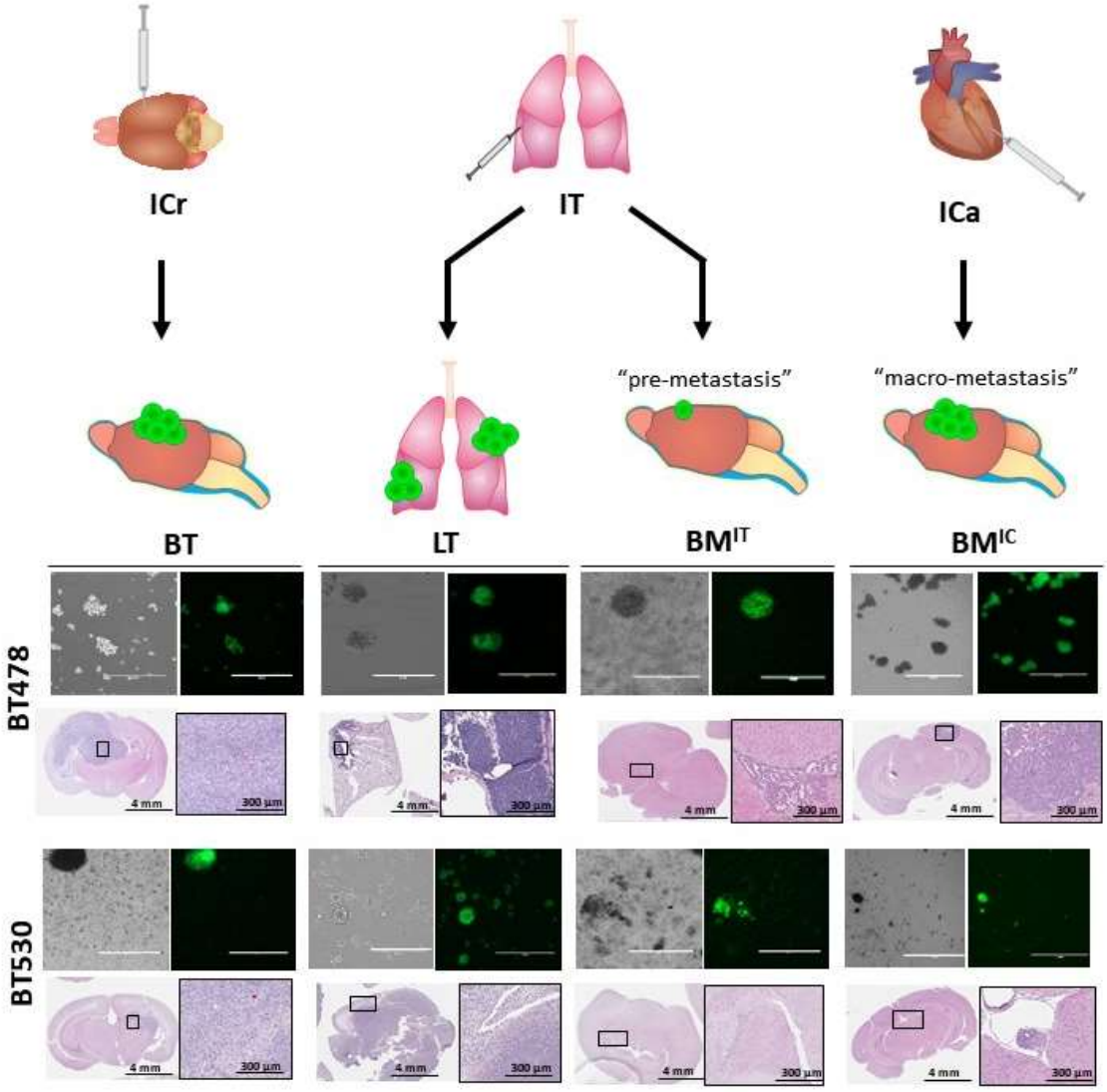

Figure 1 Isolation and characterization of in vivo BMICS, BT, LT, BM^{IT} and BM^{IC}. Upper panels: BT478 and BT530 BMICs were tagged with a GFP-expressing vector containing a puromycin-resistant cassette. GFP+ BMICs were injected via ICr, ICa, and IT routes and characterized via hematoxylin and eosin (H&E) staining. BMICs are able to recapitulate metastatic stages of primary lung (LT) and secondary orthotopic brain (BT) tumors, micro-metastases (BMIT) and macro-metastases (BMIC). Lower panels: Whole organs (brain or lung) were isolated from each metastatic stage and cultured under TSM

conditions with puromycin to select for only GFP+ BMICs, where recovered BMICs were able to reform spheres. (Scale bar = 400 µM).

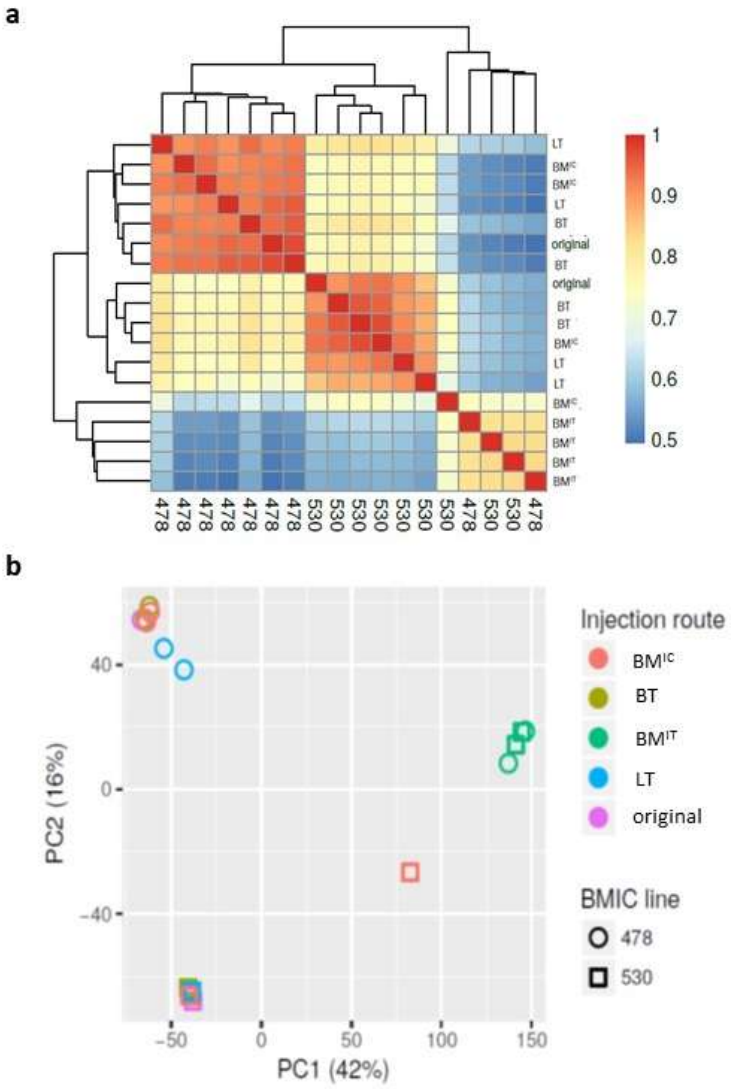

Figure 2. Characterization of the individual stages of brain metastasis progression. **a** Heatmaps depicting Pearson's correlation coefficient of genes expression across the samples as measured initially by RNAseq, along associated hierarchical clustering of the samples using Euclidean distance between samples expression profiles. **b** PCA plot

depicting samples in the planed defined by two main components (% indicates variance explained) (”original” denotes BMIC samples collected prior to injection).

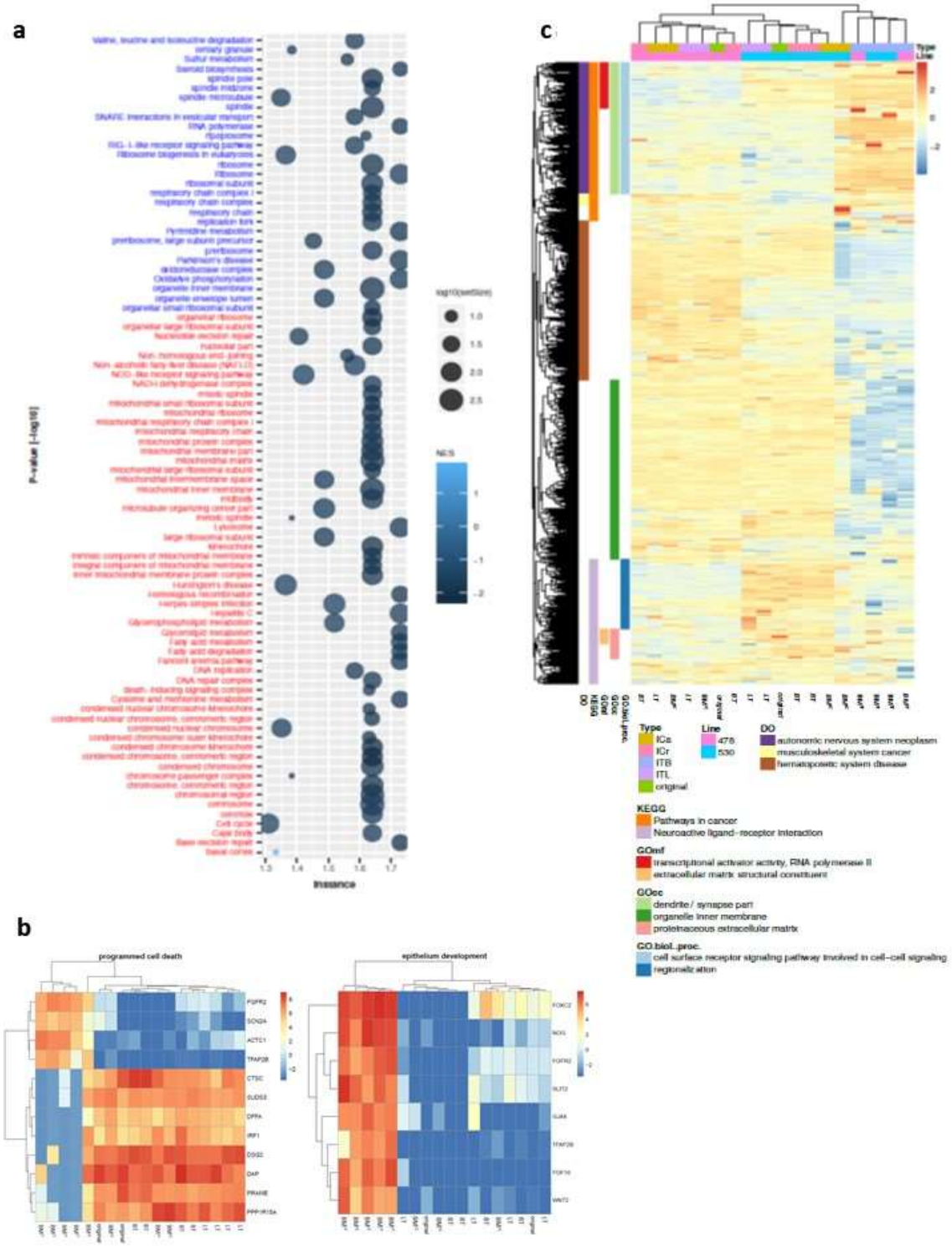

Figure 3. Cellular processes and biological pathways associated with BMIT. **a** Visualisation of the gene set enrichment analysis across GO cellular components ontology

and KEGG pathways database, using BMIT deregulated genes ordered according to their expression fold change (y-axis = statistical significance, point size = size of the gene set (cellular component / pathway), color = normalised enrichment score (NES)). **b** Heatmaps depicting Pearson's correlation coefficient of genes expression in select cellular processes across the samples as measured initially by RNA sequencing. **c** Heatmap depicting expression of the BMIT deregulated genes across all the samples, along the dendrogram obtained by hierarchical clustering of these genes. Enrichment (over-representation) analysis of BMIT genes across individual branches of the dendrogram revealed enrichment of several KEGG pathways, as well as Disease Ontology (DO) instances, Gene Ontology (GO) biological processes, cellular compartments and molecular functions. (”original” denotes BMIC samples collected prior to injection).

a

ID	Connectivity.score	P.value
Exisulind	-0.75624	0.004053962
STOCK1N-35696	-0.70678	0.287153571
TTNPB	-0.59715	0.363244572
Imatinib	-0.5883	0.001831414
AH-6809	-0.51576	0.240747991
Irinotecan	-0.38382	6.88236E-05
GW-8510	**-0.34521**	**5.76645E-05**
Phenoxybenzamine	-0.30583	5.35389E-05
mycophenolic acid	-0.28866	6.28462E-05
Methotrexate	-0.28	6.02111E-05
HC toxin	-0.27469	0.000223636
Mebendazole	-0.27214	0.000110503
0173570-0000	-0.26159	5.78433E-05
Kaempferol	-0.25736	6.32117E-05
Lomustine	**-0.2512**	**0.001424542**
Fenbufen	-0.24856	0.000479702
Apomorphine	**-0.24818**	**7.24423E-05**
betulinic acid	-0.24815	0.001312346
Semustine	-0.24761	0.000236301
CP-645525-01	-0.24662	0.43769451
Vinblastine	-0.24533	0.022654335
Harmol	-0.24475	0.001959415
Etynodiol	-0.2423	0.003504644
PHA-00851261E	-0.24017	0.000152595
Acacetin	**-0.23993**	**0.000212983**

b

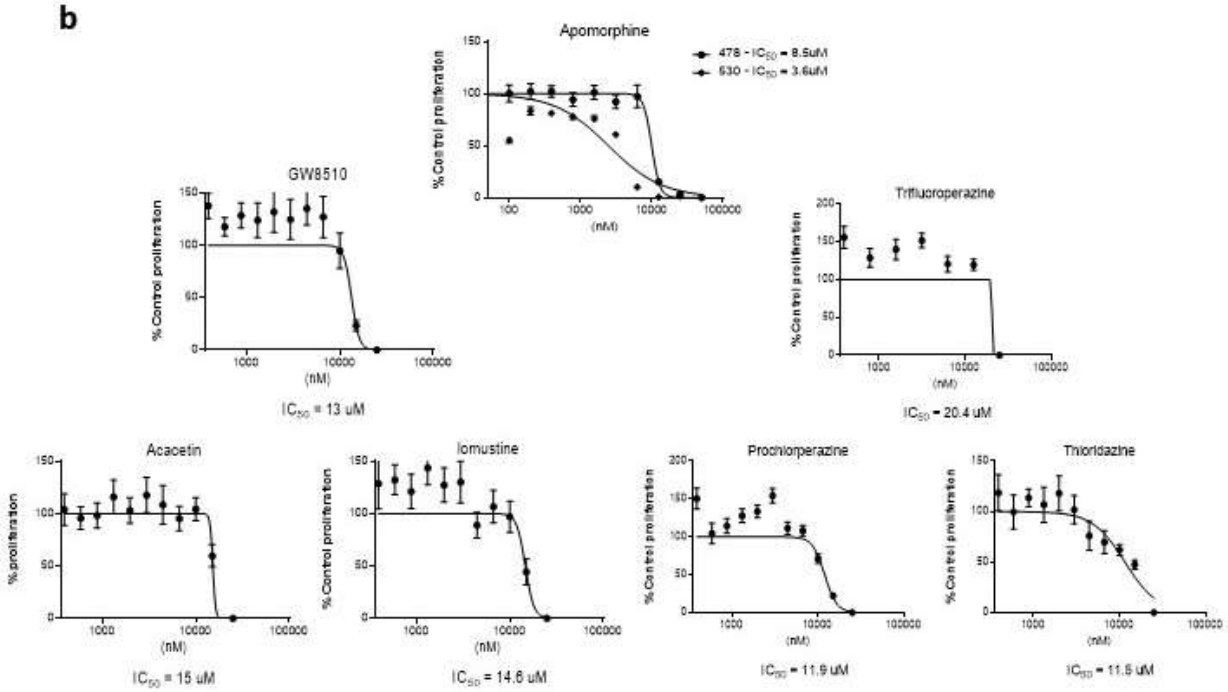

Figure 4. In vitro IC50 screening of potential brain metastasis targeting drugs. **a** List of potential BMIT targeting therapeutics identified through CMAP analysis (bolded items indicate what drugs were carried into tested in vitro). **b** IC50 curves of selected BMIT targeted drugs. (n=3; ns = not significant, *P<0.05, **P<0.01, ***P<0.001, ****P<0.0001).

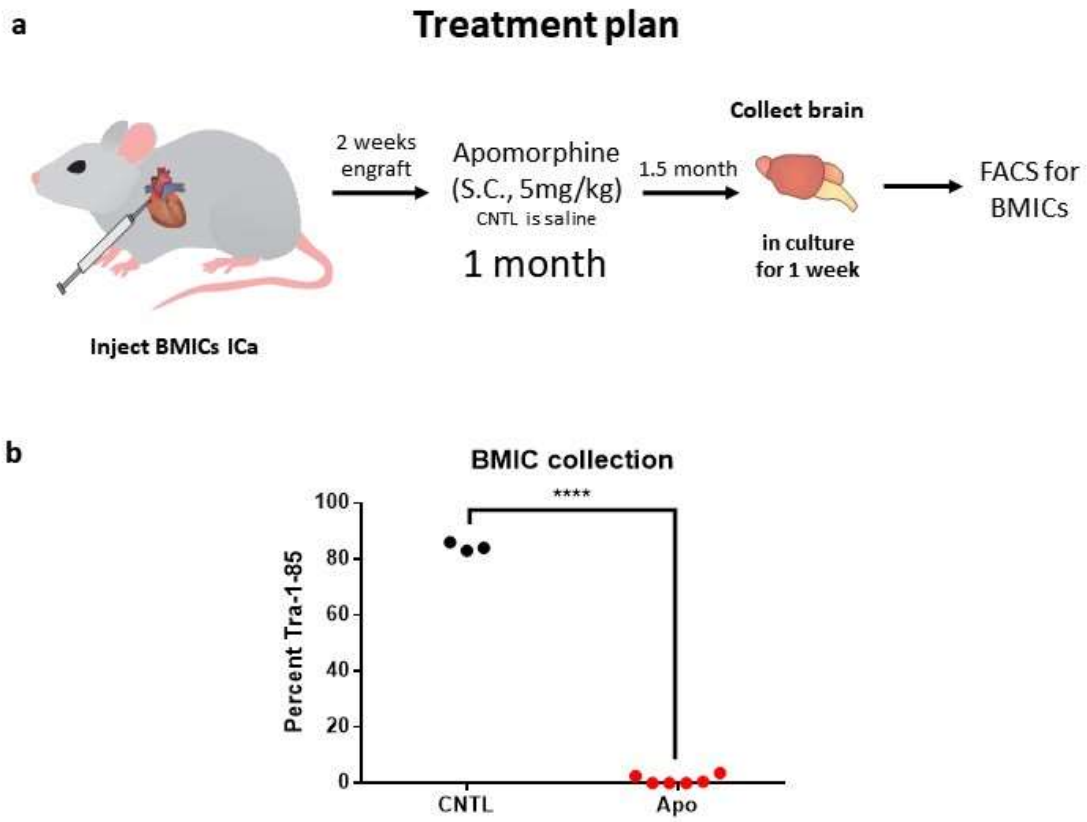

Figure 5. Preclinical testing of Apomorphine to prevent brain metastasis. **a** schematic representation of dosing regimen for Apomorphine. **b** Scatter plot graph depicting percentage of Human-Tra-1-85 positive GFP tagged BMIC cells re-isolated from Apomorphine (Apo) treatment and control (CNTL) BM model (control, n=3, treatment, n=6, ****P<0.0001).

a

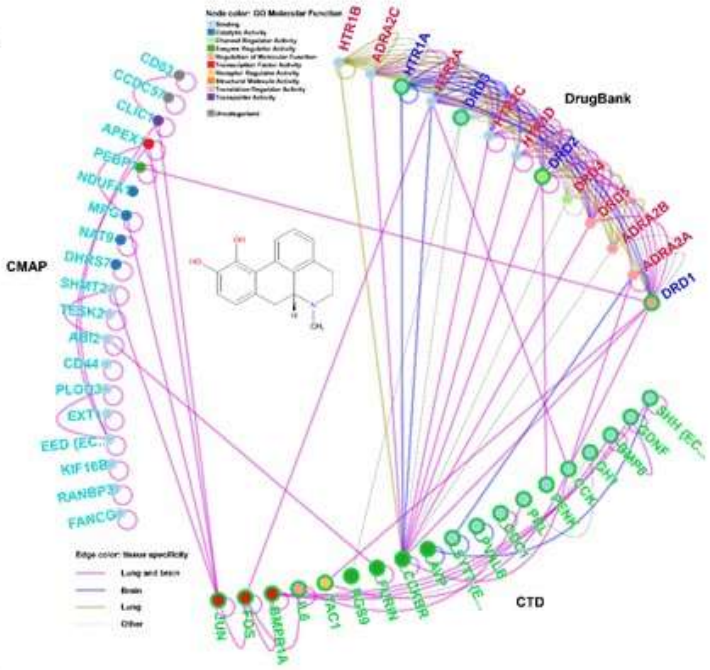

b

Apomorphine	direction	pvalue
KIF16B	-1	0.007951877
SEPW1	-1	0.007708172
TESK2	-1	0.008827382

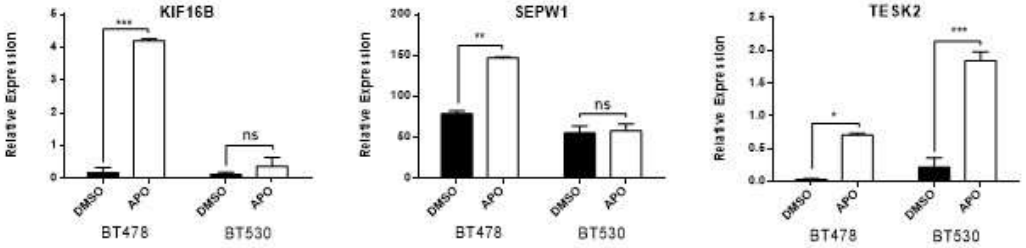

c

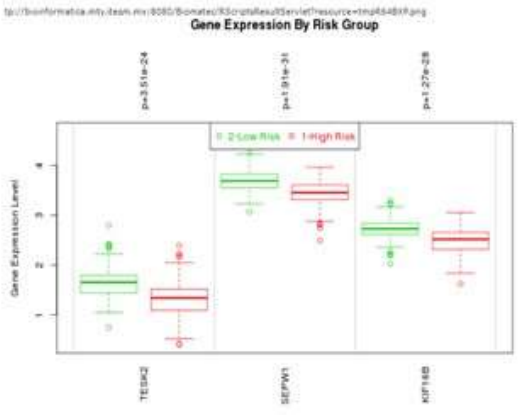

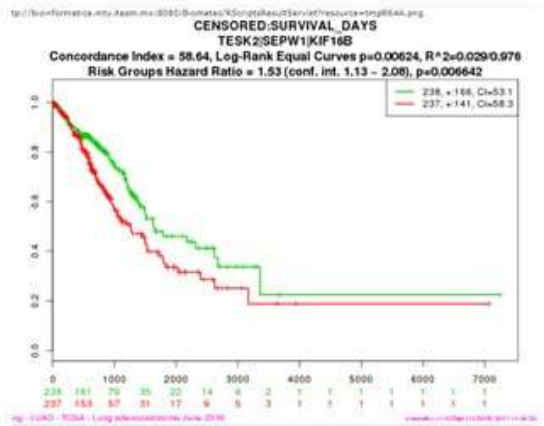

Figure 6. Novel gene targets of Apomorphine. a Protein-protein interaction (PPI) network identifying common gene targets of Apomorphine. **b** BMIT genes directly targeted by Apomorphine, as determined by CMAP analysis. Relative transcript levels of KIF16B, SEPW1 and TESK2 in BMICs treated with Apomorphine. (n=3; ns = not significant, *P<0.05, **P<0.01, ***P<0.001, ****P<0.0001). **c** Kaplan-Meier curves depicting gene expression by risk group, as obtained from SurvExpress using in TCGA data from lung adenocarcinoma patients.

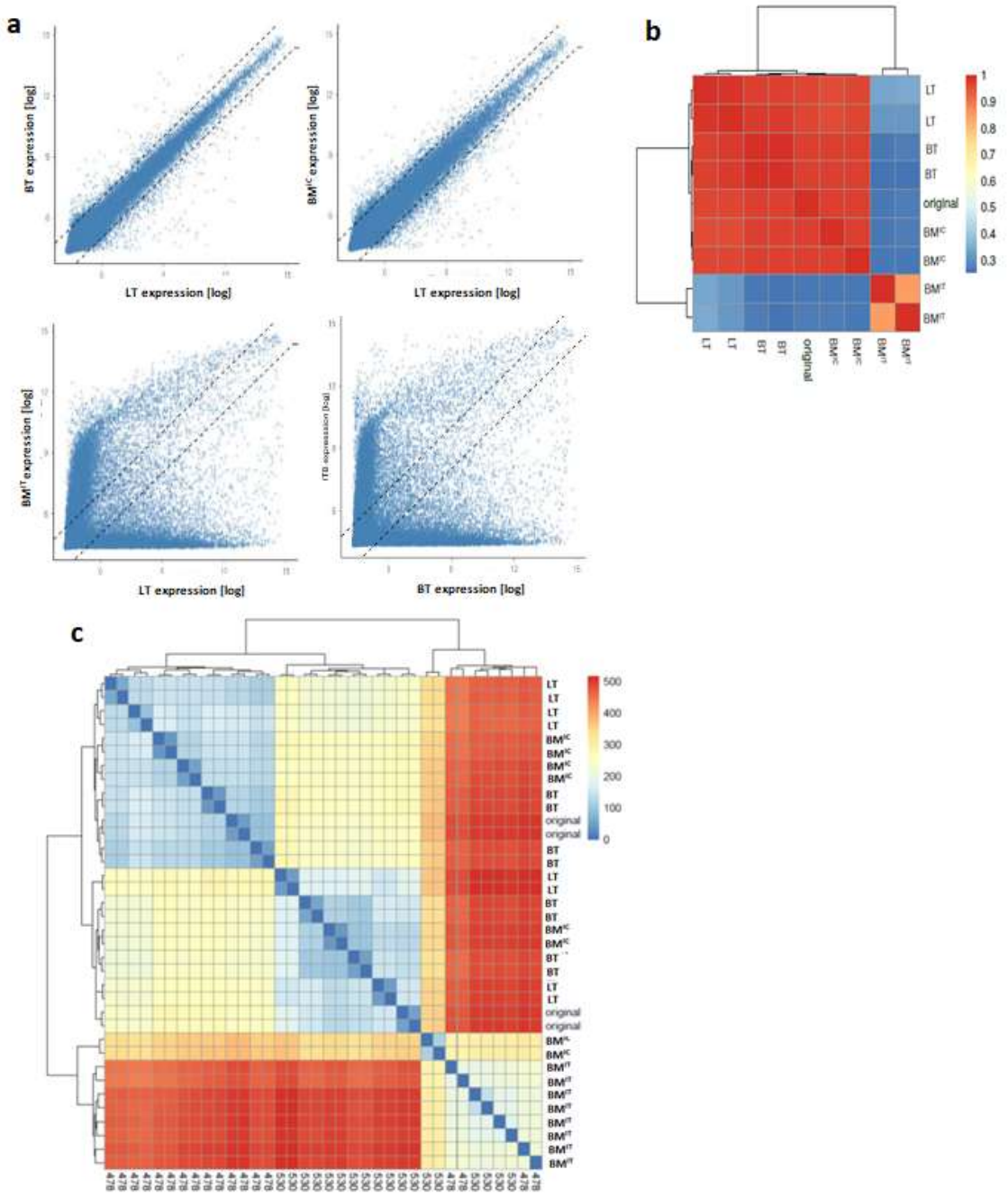

Supplementary Figure 1. a Graphical representation and **b** corresponding heatmap depicting Pearson's correlation coefficient of gene expression profiles as measured across all sample cohorts, where profile of BM^{IT} shows substantial difference when compared to BT, LT, BM^{IC} profiles. **c** Heatmap derived from RNA sequencing analysis depicting gene expression variations of BT, LT, BM^{IT} and BM^{IC} samples across BMIC lines BT478 and BT530 (n=2 per sample for each BMIC line. "original" denotes BMIC samples collected prior to injection).

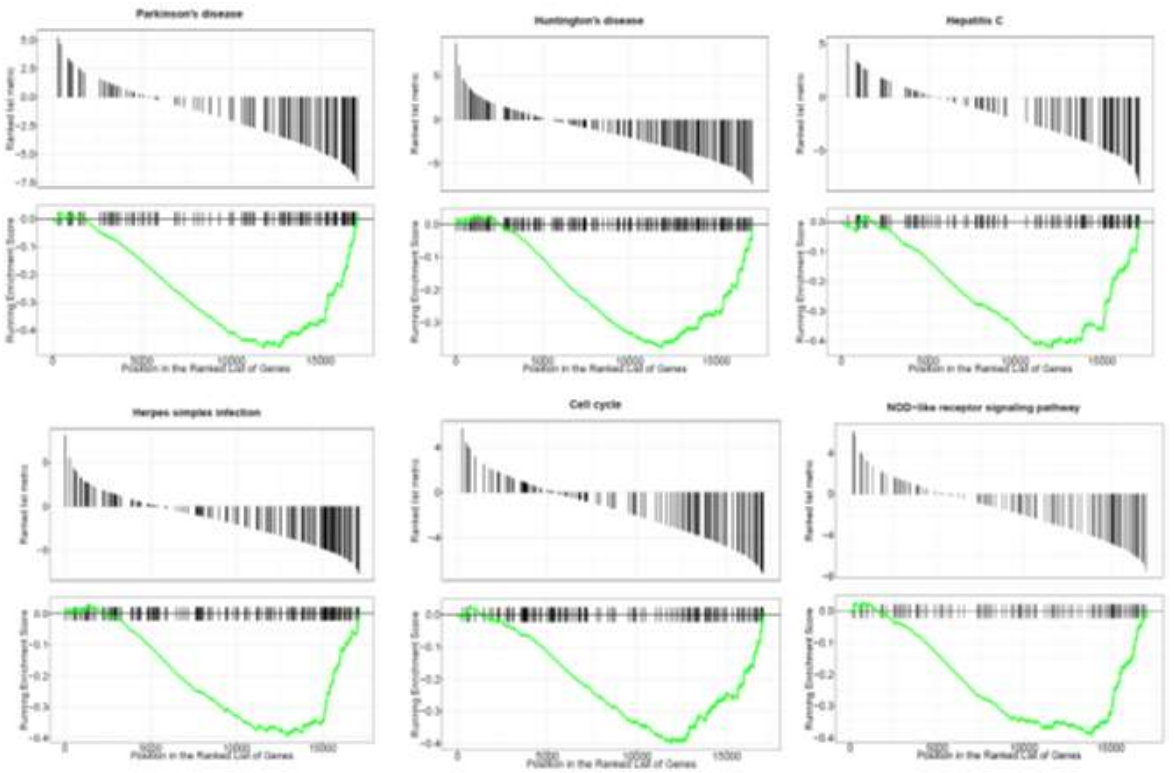

ID	Description	setSize	enrichmentScore	NES	pvalue	p.adjust	qvalues	rank
Hsa03010	Ribosome	129	-0.426418006	-1.57186852	0.001009082	0.02447358	0.018652113	5183
Hsa04142	Lysosome	118	-0.485044145	-1.780092875	0.001011122	0.02447358	0.018652113	5790
Hsa05012	Parkinson's disease	118	-0.463273209	-1.700194399	0.001011122	0.02447358	0.018652113	5300
Hsa00190	Oxidative phosphorylation	113	-0.446405921	-1.631125353	0.001017294	0.02447358	0.018652113	6849
Hsa05160	Hepatitis C	110	-0.425209594	-1.545872836	0.001022495	0.02447358	0.018652113	5073
Hsa00240	Pyrimidine metabolism	95	-0.522053556	-1.874220248	0.001027749	0.02447358	0.018652113	4884
Hsa03460	Fanconi anemia pathway	51	-0.560471204	-1.863145992	0.001072961	0.02447358	0.018652113	6384
Hsa00561	Glycerolipid metabolism	49	-0.51621257	-1.701966004	0.001081081	0.02447358	0.018652113	4009
Hsa00270	Cysteine and methionine metabolism	40	-0.579470211	-1.865773049	0.001089325	0.02447358	0.018652113	5289
Hsa01212	Fatty acid metabolism	47	-0.542046765	-1.773560277	0.001089325	0.02447358	0.018652113	5198
Hsa03440	Homologous recombination	39	-0.573581618	-1.837489694	0.001092896	0.02447358	0.018652113	6373
Hsa00071	Fatty acid degradation	38	-0.542593846	-1.731373722	0.001096491	0.02447358	0.018652113	5198
Hsa03410	Base excision repair	33	-0.627020863	-1.964830765	0.001111111	0.02447358	0.018652113	4882
Hsa03020	RNA polymerase	31	-0.572512977	-1.765887156	0.001129944	0.02447358	0.018652113	3573
Hsa00100	Steroid biosynthesis	19	-0.629565044	-1.762260123	0.001191895	0.02447358	0.018652113	5310
Hsa04932	Non-alcoholic fatty liver disease (NAFLD)	135	-0.423989633	-1.566785134	0.002020202	0.034222222	0.026081871	5300
Hsa04622	RIG-I-like receptor signaling pathway	53	-0.484409904	-1.615117509	0.002143623	0.034222222	0.026081871	3252
Hsa00280	Valine, leucine and isoleucine degradation	47	-0.499643143	-1.634816935	0.002178649	0.034222222	0.026081871	3902
Hsa03030	DNA replication	35	-0.543543651	-1.718583177	0.00220022	0.034222222	0.026081871	4843
hsa04130	SNARE interactions in vesicular transport	33	-0.536329341	-1.680640075	0.002222222	0.034222222	0.026081871	4798
hsa03450	Non-homologous end-joining	12	-0.713146865	-1.792400783	0.002506266	0.036129032	0.027535113	4553

Supplementary Figure. 2. Select plots showing BM^{IT} gene set enrichment across GO biological processes

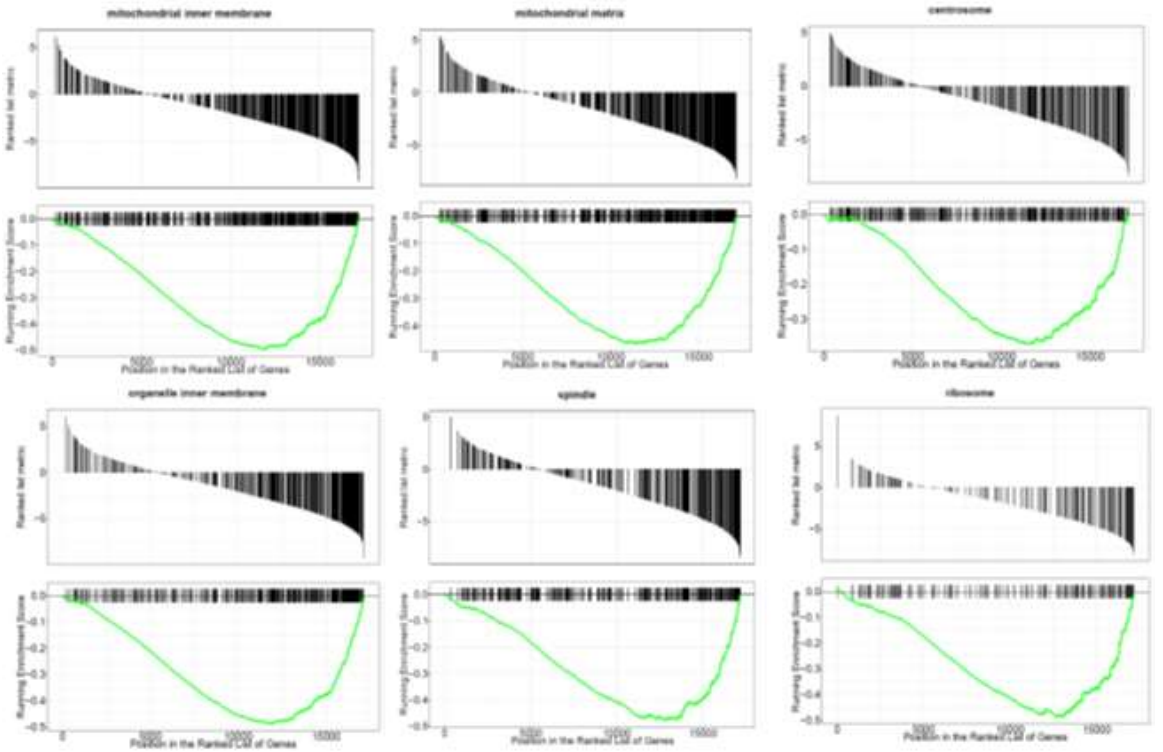

ID	Description	setSize	enrichmentScore	NES	pvalue	p.adjust	qvalues	rank
GO:0005743	mitochondrial inner membrane	444	-0.495151185	-1.913807714	0.000999001	0.027182771	0.022915263	5193
GO:0005759	mitochondrial matrix	391	-0.465611167	-1.79212627	0.000999001	0.027182771	0.022915263	5760
GO:0005813	centrosome	467	-0.370569854	-1.433999311	0.000999001	0.027182771	0.022915263	5730
GO:0019866	organelle inner membrane	492	-0.487591731	-1.890228058	0.000999001	0.027182771	0.022915263	5193
GO:0098687	chromosomal region	318	-0.423636114	-1.619709547	0.000999001	0.027182771	0.022915263	5298
GO:0005819	spindle	276	-0.479274452	-1.82316369	0.001	0.027182771	0.022915263	4346
GO:0005840	ribosome	213	-0.489017848	-1.843231256	0.001	0.027182771	0.022915263	4420
GO:0000793	condensed chromosome	186	-0.496482368	-1.865115854	0.001002004	0.027182771	0.022915263	4887
GO:0044455	mitochondrial membrane part	172	-0.492079677	-1.840974719	0.001002004	0.027182771	0.022915263	4877
GO:0000775	chromosome, centromeric region	177	-0.504561498	-1.892118714	0.001003009	0.027182771	0.022915263	5298
GO:0030496	midbody	129	-0.471954388	-1.735860166	0.001006036	0.027182771	0.022915263	3458
GO:0044391	ribosomal subunit	151	-0.455072995	-1.686283148	0.001006036	0.027182771	0.022915263	4420
GO:0098798	mitochondrial protein complex	140	-0.478378972	-1.765064915	0.001006036	0.027182771	0.022915263	5390
GO:0000776	kinetochore	126	-0.54612767	-2.005510998	0.001007049	0.027182771	0.022915263	5404
GO:0000922	spindle pole	119	-0.542230383	-1.986335329	0.001008065	0.027182771	0.022915263	4346
GO:0005814	centriole	101	-0.457961315	-1.664585489	0.001010101	0.027182771	0.022915263	4679
GO:0000779	condensed chromosome, centromeric region	106	-0.596908423	-2.173219283	0.001011122	0.027182771	0.022915263	4844
GO:0098800	inner mitochondrial membrane protein complex	109	-0.489653269	-1.784855083	0.001011122	0.027182771	0.022915263	5300
GO:0000777	condensed chromosome kinetochore	97	-0.60294241	-2.180115938	0.001014199	0.027182771	0.022915263	4844
GO:0070469	respiratory chain	78	-0.52324886	-1.858201784	0.001031992	0.027182771	0.022915263	6148

Supplementary Figure 3. Select plots showing BM^{IT} gene set enrichment across GO cellular compartment.

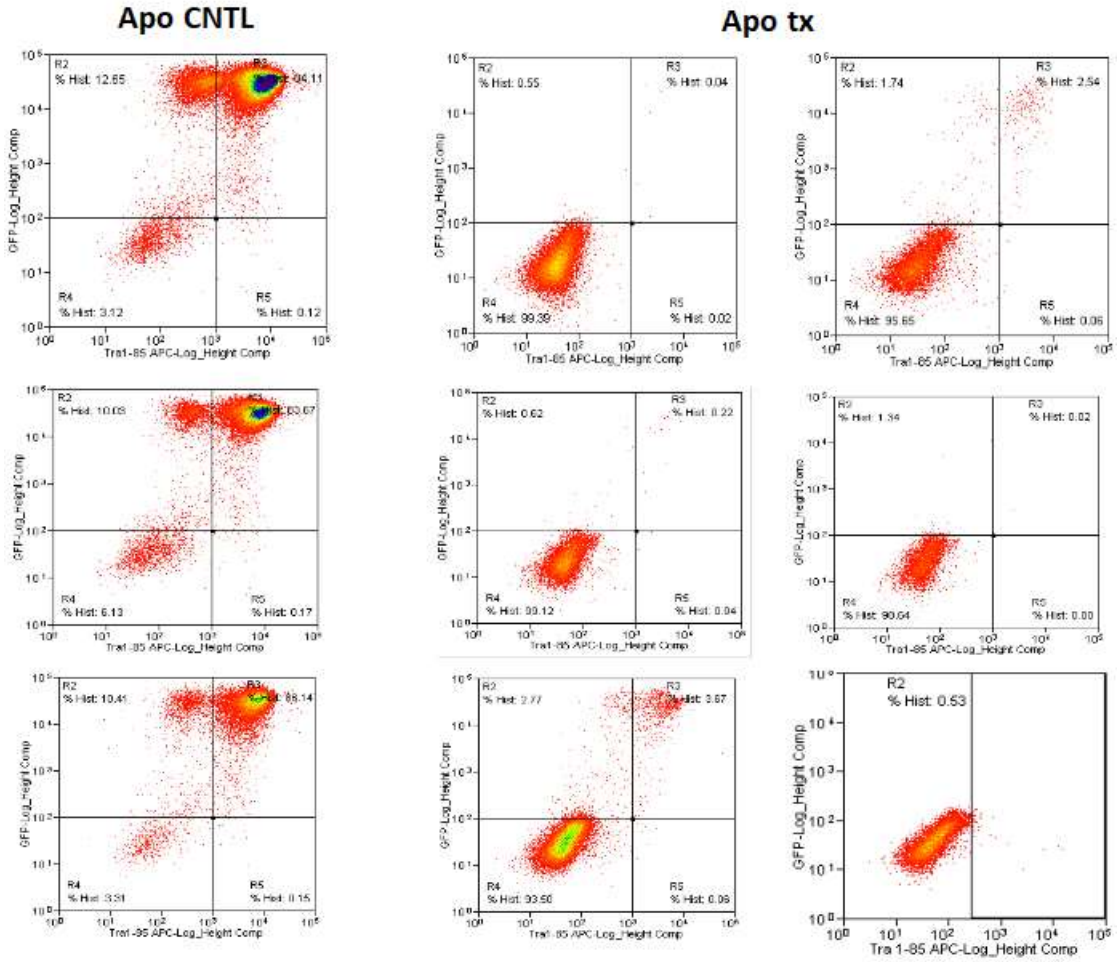

Supplementary Figure 4. Individual FACS profiles of BT478 BMICs isolated from the brains of IC injected mouse, (n=3 for controls, n=6 for Apomorphine treated).

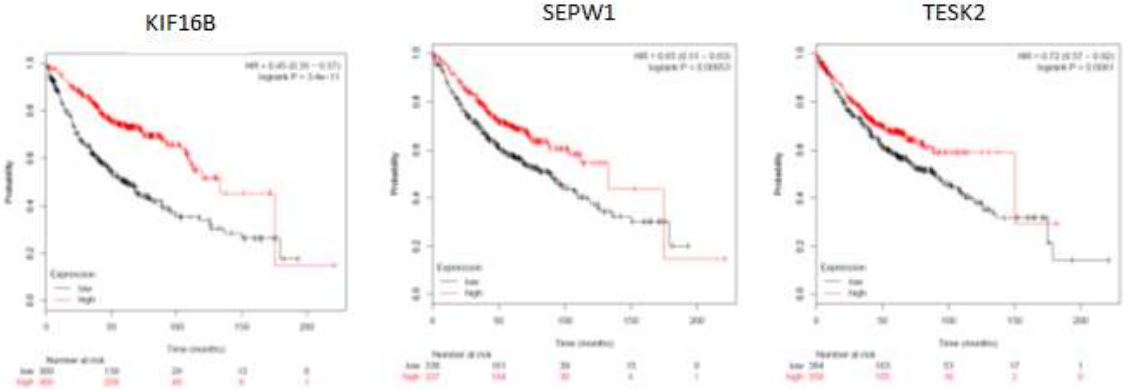

Supplementary Figure 5. Individual KM plots of Apomorphine targeted BM^{IT} genes.

	Forward	Reverse
GAPDH	TGCACCACCAACTGCTTAGC	GGCATGGACTGTGGTCATGAG
B-actin	TATCCCTGTACGCCTCT	AGGTCTTTGCGGATGT
cofilin1	CTCCTCTGGCGTTGAAGACT	GTGCCCTCTCCTTTTCGTTT
C19orf66	CTCCATCGTGTACGGGGTAAA	GGTCCTGCTTCATATCCTCTGGT
DENND3	TCATGGGAGCATCACCTACTC	GAGCTGGAGGCTCTGCAC
KIF16B	GGCACGGAGATTGAAGAGCA	CTGACTGGCAAGCTGGAAGA
SEPW1	GAGGCTACAAGTCCAAGTATCTTCA	CATCAGGGAAAGACCAGGTG
TESK2	CTGAGGCCCACTGCTATGTC	TCCCATCCCAACATCCTTAG

Supplementary Table 1. RT-PCR primer sequences.

Chapter 5: Discussion

5.1 Generation of patient-derived BMIC lines

A key component of any model development is the source of cells. Commercially available cell lines are a commonly utilized cell source, providing an unlimited number of cells for cost-effective use, and are utilized in ~80% of mouse model development (Gengenbacher *et al.*, 2017). Unfortunately, these lines have undergone significant selective pressures from years of culturing that they rarely represent the genotypic or phenotypic profile of the original patient sample, and are sometimes even misidentified or cross-contaminated (Hughes, Marshall, Reid, Parkes, & Gelber, 2007). Conversely, patient-derived cell lines provide a much more accurate representation of clonal heterogeneity existing within the original patient tumor, as the length of culture remains minimal, though these lines also face difficulties due to poor growth and engraftment, and a limited life span (Hughes, et al., 2007). A significant concern with patient-derived cell lines is that the majority of patients have already received some form of therapy, thus there are very few samples that have not faced a selection pressure from exposure to a chemotherapeutic (Francia, Cruz-Munoz, Man, Xu, & Kerbel, 2011).

Several factors indicate that MICs may arise from subpopulations of CSC clones, and within the primary tumor may reside various metastatic clones the possess different organotropism and seeding capacities. As such, MIC populations have been confirmed in prostate (van den Hoogen *et al.*, 2010), oral (Pascual *et al.*, 2017) and renal (Khan *et al.*, 2014) cancers. In this thesis I generated several patient-derived cell lines from samples of

BM of lung origin (**Chapter 4, Figure 1**). I utilized BMs as opposed to the primary lung tumors since these samples already possess cells that have successfully undergone and survived metastasis. These lines were cultured in media tailored for enrichment of a BTIC/CSC population, and underwent CSC-specific assays to validate their CSC-like properties. Flow assisted cytometry (FACs) analyses was performed as each line was developed to establish a base-line of sorts, assessing expression of CD133, CD44, and EpCAM. CD133 and CD15 are known BTIC markers for primary brain tumors (Mao *et al.*, 2009; S. K. Singh *et al.*, 2003), CD44 is a known CSC marker in several cancers and has been implicated in the progression of metastasis (Marhaba *et al.*, 2008) (Marangoni *et al.*, 2009; Patrawala *et al.*, 2006), and EpCAM is a marker of cells of epithelial origin as well has been implicated in tumorigenesis and metastasis(Hiraga *et al.*, 2016; Ni *et al.*, 2012; van der Gun *et al.*, 2010). The variation in expression of these markers between each line is representative of inter-patient differences. When in culture, these BMIC lines were capable of forming spheres (**Chapter 4**, **Figure 1**), indicative of the presence of a CSC population and further affirming the results that were previously determined in our lab (Nolte *et al.*, 2013). Tumor initiation capacity (TIC) was assessed by *in vivo* limiting dilution analysis (LDA), where increasing numbers of BMICs were injected intracranially (ICr) to assess tumor reformation in the secondary neural site. BMICs were found to reproduce large brain tumors with as low as 100 cells injected (Data not shown). With this work I confirmed the presence of a CSC-like population within BMs, and generated patient-derived cell lines enriched with BMICs, providing us with proper starting material to develop BM models.

5.2 *In Vivo* Modelling of BM

It has been made clear in recent years that there is a detrimental lack of understanding towards the metastatic process, resulting in a significant hindrance to the development of targeted therapeutics and subsequently a depressing lack of progress towards extending patient survival (Steeg *et al.*, 2009). The investigation of the biology of metastasis requires the use of proper tools that can emulate the clinical progression of the disease. Several groups have proven successful in developing preclinical models of BM, providing significant information of MIC survival within the circulation and in part some of the mechanisms underlying metastasis. However, these studies typically employ intravenous injection methods to develop systemic metastases or multiple rounds of injection to generate cells that "home" to the brain (Bos *et al.*, 2009; Fidler, 1973); it is indistinct as to whether the garnered information is relevant to what is observed in patients (Daphu *et al.*, 2013). If these models that are utilized to understand metastasis do not accurately represent the phenomenon, then it is not unsurprising as to the lack of progress towards managing such a fatal disease. Furthemore, recent data is validating the adaption of inoculated human cells to the mouse host environment and undergo mouse-specific tumor evolution (Ben-David *et al.*, 2017).

I utilized the established BMIC lines to generate models of BM that model different stages of metastasis. My ICr model tested the ability of BMICs to reform tumors within a neural environment, and my IT and ICa models tested the ability of BMICs to successfully

complete the early and later stages of metastasis to produce BMs. I found with the ICa model, an injection route typically used in studies of BM, BMICs had a propensity to migrate to the brain, resulting in formation of macro-metastatic growths without the need for several rounds of injections. With the IT model I was able to show that not only were BMICs capable of reforming primary tumors within the lung, suggesting that these cells still retain the capacity to survive in their original microenvironment, BMICs were able to successfully enter the circulation and arrest at and seed the brain prior to the mice succumbing to gross lung tumor burden. Where the development of BMIC lines through rounds of serial injections would theoretically enhance the expression of metastatic genes required for homing to the brain, this is not a process that occurs in BM patients, and so our declination to use that method allowed us to retain a genetic profile more similar to what our patient-derived BM samples exhibit. Taken together, this data shows that I was able to generate clinically relevant models of BM, capable being used as platforms to interrogate the biological processes of metastasis.

5.3 Regulators of BM

Various PDX models have been established over the years to study BM, resulting in the identification of numerous genes implicated in the metastatic process. Unfortunately, there has been very little overlap between BM genes identified from PDX models and direct patient studies, implicating a significant discrepancy in the translation of preclinical results to the clinic(Daphu *et al.*, 2013). As such, there is an urgent need for more thorough

validation of genes identified from preclinical models in order to make proper in-depth comparisons to patients.

5.3.1. STAT3 pathway

Several pathways have been shown to support self renewal and metastatic potential of BMICs (Rahmathulla *et al.*, 2012). Amongst these is the STAT3 pathway, where interest of this gene in the regulation of cancer has increased in recent years. The normal STAT3 pathway can be activated by numerous molecules, not limited to cytokines and growth factors, and has a broad spectrum of biological functions (Levy & Darnell, 2002). Within cancer, this pathway has been shown to be constitutively phosphorylated, and several downstream STAT3 target genes have been implicated in the activation of the fundamental process of metastasis such as invasion and angiogenesis (Kamran *et al.*, 2013). Therapeutic intervention has shown to be effective in inhibiting metastatic progression of a wide variety of primary cancers (Cao *et al.*, 2016; Cao *et al.*, 2014; Saini *et al.*, 2017; Ye *et al.*, 2017). Despite the elevated activity of STAT3 in cancer progression, there remains limited knowledge on the precise mechanisms employed to stimulate metastatic functions.

Through protein-protein interaction networking of previously identified BMIC genes (Nolte *et al.*, 2013), STAT3 was identified as a possible regulator for BM. I showed that knockdown of and therapeutic inhibition using a novel STAT3 inhibitor reduced tumor generation by BMICs through ICr injections. Furthermore, for the first time, miR-21 was shown to be a possible downstream target and effector of STAT3 activity. Together this

works augments the current data pointing to STAT3 as a possible universal instigator of metastasis and significant therapeutic target.

5.3.2. SPOCK1 and TWIST2

Despite advances in technology that have led to genomic and proteomic characterization of regulatory molecules of BM, there remains a lack of further functional validation of these potential hits that hinders better comprehension of the biology of the disease. RNA interference (RNAi) screens, otherwise known as short hairpin RNA (shRNA) dropout screens, are powerful and versatile tools employed to provide causal associations between specific genes and a phenotype of interest through loss of function (LOF) in mammalian cells. Various shRNA expression libraries have been created and are commercially available that allow targeted knockdown of thousands of different genes at one time in "pooled" screens (Hu & Luo, 2012). These screens are based on the principle of incorporating only one shRNA expression construct per cell to ensure only one gene is targeted in each resulting clone, and so requires optimization of viral titres, multiplicity of infection (MOI) and antibiotic selection (Boettcher & Hoheisel, 2010). However, there remains a fraction of cells that receive multiple constructs and so necessitates further functional validation of identified "hits". To date, numerous screens, ranging from small scale to whole genome interrogation, have provided significant functional validation of metastasis-associated genes (Duquet *et al.*, 2014; Gobeil *et al.*, 2008; Sasaki *et al.*, 2017; Schonherr *et al.*, 2014; Su *et al.*, 2014).

Here I performed an in-depth RNA interference screen on our BMICs with a library of select genes implicated in metastatic progression, and through subsequent *in vitro* and *in vivo* validation I present for the first time SPOCK1 and TWIST2 as BMIC regulators and potential BMIC markers. SPOCK1 regulation of metastasis has been observed in glioblastoma (F. Yu *et al.*, 2016), prostate (Q. Chen *et al.*, 2016), gallbladder (Y. J. Shu *et al.*, 2015) and lung primary cancers (Miao *et al.*, 2013), appearing to activate EMT and subsequent metastatic properties. TWIST2 has been associated with promotion of EMT and stem-like properties in breast (Fang *et al.*, 2011), hepatocellular (A. Y. Liu *et al.*, 2014), and cervical cancers (Y. Liu *et al.*, 2015). In this work I found SPOCK1 to regulate both tumor formation and metastasis to the brain, completely abrogating primary lung tumor or secondary BM formation, whereas TWIST2 was found to primarily regulate metastasis to the brain but had no significant impact on tumor formation. Taken together, this data further corroborates the roles for SPOCK1 and TWIST2 in brain metastasis, where overexpression of these genes may contribute to cancer progression, potentially through induction of EMT.

Though there is yet no evidence to substantiate a direct relationship between SPOCK1 and STAT3, both genes are induced by TGF-β to activate EMT (R. Y. Liu *et al.*, 2014; Miao *et al.*, 2013). The TGF-β pathway is an ultimate regulator of several cellular processes, from cell growth and death to angiogenesis, and is a vital suppressor of epithelial tumors. However, dysregulation of this process or compensation by tumor cells can result in a tumor cell response that favors migration and invasion and stimulate tumor growth.

Additionally, TGF-β signalling can influence the microenvironment and PMN to be more accommodating for tumor growth (Derynck & Zhang, 2003).

Direct targeting of TGF-β faces many difficulties. Most cancer cells display altered or non-functional TGF-β signalling. As such TGF-β inhibitors have shown better anti-tumoral efficacy by affecting microenvironmental cells that respond to TGF-β, where TGF-β inhibition can "normalize" the tissue, and the subsequent reduction of TGF-β levels expressed by the stromal cells would indirectly impact tumor cells. Moreover, there lies a potential hazard of inducing synchronous occult tumor growth by inhibiting the tumor suppressing nature of TGF-β (Neuzillet *et al.*, 2015). Thus, targeting downstream executors of TGF-β activity may prove to have better sensitivity and specificity in preventing tumor growth, especially if these factors denote a TIC or MIC population. As seen with the work presented in this thesis, we show preliminary results of such efficacy in tumor prevention by targeting STAT3.

5.4 Pre-metastasis: a novel alternative therapeutic window to prevent BM development

The process of metastasis is both complicated and extremely inefficient, where only a minute percentage of disseminated tumor cells are capable of surviving the lympho-vascular system to establish growths in secondary organs; the largest barrier to metastatic development is tissue colonization (Luzzi 1998, chambers 2002 nat rev cancer, Valastyan and Weinberg 2013(Fidler, 1973)). Characteristically, this creates a delay between primary

tumor formation and clinical diagnosis of metastatic growth, even with early tumor dissemination, and provides an ideal potential window for therapeutic intervention (Husemann Cancer Cell. 2008, Rhim Cell. 2012, Yachida Nature. 2010). Several studies have investigated the niche of BM, providing much insight into the interactions between BMICs and secondary microenvironment (Q. Chen *et al.*, 2017; Malanchi *et al.*, 2011; Oskarsson *et al.*, 2011; Psaila *et al.*, 2006), however less known about the mechanisms required by the BMICs to initiate these interactions

5.4.1. Characterization of the pre-metastatic stage

Pre-cancerous states have been identified in several primary cancers, determining the requirements and conditions for cancer initiation (Fidler, 1973; Hong *et al.*, 2008; Sgroi, 2010; Shlush *et al.*, 2014; Wistuba *et al.*, 2002). However, a similar "pre-metastatic" state has yet to be tracked within a clinical setting, remaining elusive to current diagnostic technologies; as opposed to established macro-metastasis, the constantly shifting nature of cells undergoing metastasis make it difficult to detect when pre-metastasis is underway. Thus far, pre-metastasis has been identified in metastasis in *C. elegans* (Matus *et al.*, 2015), where the MIC undergoes extravasation and adaption to the secondary environment prior to proliferating and colonizing the tissue, and both seeding and colonization stages are distinctly separate. In mammalian cells, the conditional implementation of certain processes have been associated with metastatic progression, such as the epithelial-mesenchymal transition (EMT) and angiogenesis (Celia-Terrassa & Kang, 2016).

Unfortunately, more in-depth characterization is required of pre-metastatic MICs to better understand the biology behind this stage in metastatic initiation.

Here I developed a model of BM through the intrathoracic injection of BMICs, where I recapitulated the metastatic progression from primary lung tumor formation to seeding growth. In this model, mice would succumb to gross lung tumor burden, leaving cells that had escaped and metastasized to the brain but were unable to complete BM initiation. I isolated these pre-metastatic BMICs, termed BM^{IT}, and through transgenomic analysis showed dysregulation of over ~7000 genes as compared to BMICs isolated from larger, established lung and BM tumors from the BM models. Intriguingly, contrary to the other samples, BM^{IT} cells were active in mechanisms regulating cytoskeletal arrangement and epithelial development, but repressed mechanisms of apoptosis and cell division. This work corroborates the initial data presented by Matus *et al*. (Matus *et al.*, 2015), confirming in mammalian cells that the stages of invasion and seeding require different mechanisms than tissue colonization (Celia-Terrassa & Kang, 2016). I present a list of ~7000 genes dysregulated in metastasis that could provide novel therapeutic targets, several of which appeared to be associated with pathways of neural neoplasm and neural system developmental pathways.

A relationship between cancer and neurodegenerative disorders has undergone much interrogation in the field of cancer research. Emerging evidence hints to shared abnormal genetic and molecular mechanisms, where genes that are up-regulated in cancer are found

to be down-regulated in neurodegenerative disorders and *vice versa* (Ibanez *et al.*, 2014). Several studies imply a reverse correlation between the risk of developing a neurodegenerative disease and certain cancers. For instance, a study of Parkinson's disease suggests reports a reduced risk of most cancers, with an exception of malignant melanoma (Bajaj *et al.*, 2010; Inzelberg & Jankovic, 2007). Similar reduced risks were found with Alzheimer's disease (Bennett & Leurgans, 2010) and Huntington's disease (Sorensen *et al.*, 1999). The summation of our presented data provides additional insight into a possible relationship between BM and neurodegenerative disorders and neurodevelopmental pathways.

5.4.2. Therapeutic inhibition of Pre-metastatic BMICs

Metastases often received the same treatment regimes as the originating primary tumor, with the assumption that the secondary metastases are of the same nature of the originating primary tumor and will elicit the same response. However, there are several characteristics apparent in MICs and metastases that are not seen in the primary tumor, indicating a separate treatment protocol may be required for metastases. Additionally, there are increasing numbers of examples that shown that some treatments can increase the proclivity for metastatic development. For instance, anti-angiogenic therapies, while showing great efficacy at controlling primary tumor burden in preclinical studies did not significantly improve patient survival (Escudier *et al.*, 2007; Hurwitz, 2004; Miller *et al.*, 2007; Sandler *et al.*, 2006). Moreover recent studies imply these treatments to promote experimental metastasis through induction of hypoxic conditions (Lu *et al.*, 2012; Paez-

Ribes *et al.*, 2009). Adjuvant radiotherapy is used to treat local tumor growth, and can promote metastasis through an alleged tumor-bed effect, where the recurrent tumor within the irradiated area is associated with higher metastatic progression and poorer prognosis (Suit, 1992). These off-target effects necessitate further preclinical testing of novel therapeutics on possible metastases or development of novel therapeutics specifically on metastases (Steeg *et al.*, 2009).

Through connectivity map analysis of our BM^{IT} genes, a list of potential targeting therapeutics was identified, several of which are in current testing or use as chemotherapies. Further *in vitro* screening led us to Apomorphine, a dopamine receptor D2 (DRD2) agonist, as a potential BM^{IT} inhibitor. Originally prescribed for treatment for Parkinson's disease (Boyle & Ondo, 2015), Apomorphine has been reported as a potential Alzheimer's treatment due to its ability to inhibit amyloid beta fibre formation (Himeno *et al.*, 2011).

I found that after a month-long administration of Apomorphine in mice previously injected ICa with BMICs, I was unable to isolate any BMICs within the brain, suggesting Apomorphine inhibits BM. DRD2 agonists have shown potential efficacy in cancer inhibition and as an anti-angiogenic (Chauvet *et al.*, 2017; Hoeppner *et al.*, 2015; Pornour *et al.*, 2015). This data implicates the dopamine pathway as a novel active pathway in the development of BM.

Further *in silico* analysis determined Apomorphine to directly influence 3 BM^{IT} genes, KIF16B, SEPW1 and TESK2. Of the three genes, SEPW1 and KIF16B have associations with neurodegenerative disorders (Hirokawa *et al.*, 2010; X. Zhang *et al.*, 2016), whereas TESK2 is associated with cytoskeletal rearrangement (Rosok *et al.*, 1999). While these three genes were shown to have downregulated expression in our BM^{IT} dysregulated gene list, upon *in vitro* administration of Apomorphine to BMICs I saw an increase in transcript levels of these 3 genes. Futher preliminary data suggests that Apomorphine may exhibit its BM inhibitory activty through reduction of cofilin expression and subsequent dysregulation of the actin cytoskeleton, possibly resulting in BMICs that are too large to extravasate (data not shown). Lastly, interrogation of a cohort of lung adenocarcinoma patients found low expression of these genes to be associated with poor survival. The culmination of our data suggests a possible novel therapeutic avenue with dopamine agonists (DA) in BM inhibition or prevention. Repurposing such drugs would avoid the hindrance of overcoming the BBB, as several DA are BBB permeable and are FDA approved.

5.5 Future Directions

While this thesis has provided novel insight into the dynamics and potential therapeutic targeting of human BM, there are several avenues available for this work to be improved upon. Primarily, further tailoring of the *in vivo* models may offer different outlooks to lung cancer progression.

Our ongoing collaboration with Dr. Charles Swanton (London Research Institute, UK) (de Bruin *et al.*, 2014; Gerlinger *et al.*, 2012; Swanton, 2012) will provide an opportunity to apply primary patient-derived lung cancer samples to our *in vivo* models, to prospectively define the BMIC frequency *de novo* in primary NSCLC. We will receive clinically and genomically annotated patient specimens from his TRAcking Non-small Cell Lung Cancer Evolution Through Therapy (TRACERx) trial(Jamal-Hanjani *et al.*, 2014), to interrogate the ability of these cells to form BM in my animal model. Furthermore, we can then apply a chemotherapy-radiation treatment strategy adapted from patient protocols, as previously established in our lab to treat glioblastoma (Qazi *et al.*, 2016). Administration of this protocol should lead to shrinkage the primary lung tumors and prolong mouse survival to generate BM, producing a more thorough representation of the clinical progression of BM as seen in patients.

Recent work by Semenkow *et al*. established a model of glioblastoma (GBM) in an immune competent mouse, utilizing Abatacept (CTLA-4-Ig) to transiently block T-Cell co-stimulation. The resulting tumors more closely resemble the clinical pathophysiology of human patient GBM as compared to transplants generated in immunodeficient models (Semenkow *et al.*, 2017). Application of a similar method to refine my current BM models would have great utility in studying the biology of metastasis in relation to the immune system, potentially progressing into more in depth study of the PMN and effective screening of novel immunotherapies.

Current work is in progress to determine if my identified BM^{IT} signature is universal or tissue-specific. I have generated additional mouse models of melanoma-to-brain (MBM) and breast-to-brain (BBM) metastasis, *via* subcutaneous and secondary fatpad injection respectively, of enriched BMIC samples derived from corresponding primary patient samples of BM (Figure 7). I then isolated BMICs that had metastasized to the brain but had not yet formed tumors, considered the "pre-metastatic" stage of each model, dubbed BM^{MB} and BM^{BB}, and submitted isolated RNA for transgenomic analysis, similarly to our lung-to-brain model samples. Preliminary data shows that our BM^{IT} signature is tissue-specific, whereas our BM^{MB} and BM^{BB} signatures are more similar to each other than with BM^{IT} (Figure 8).

Another avenue of research could expand on the efficacy of neurotransmitters and dopamine-targeting therapeutics on BM inhibition. Our data suggests more insight into the possible relationship between neurodegenerative and cancer pathways. DRD2 receptors are overexpressed in several cancers and is correlated with metastatic progression (Li *et al.*, 2006; Mu *et al.*, 2017), where recent preclinical studies have shown DRD2 inhibition to be effective in reducing cancer (Mu *et al.*, 2017; Peverelli *et al.*, 2016).

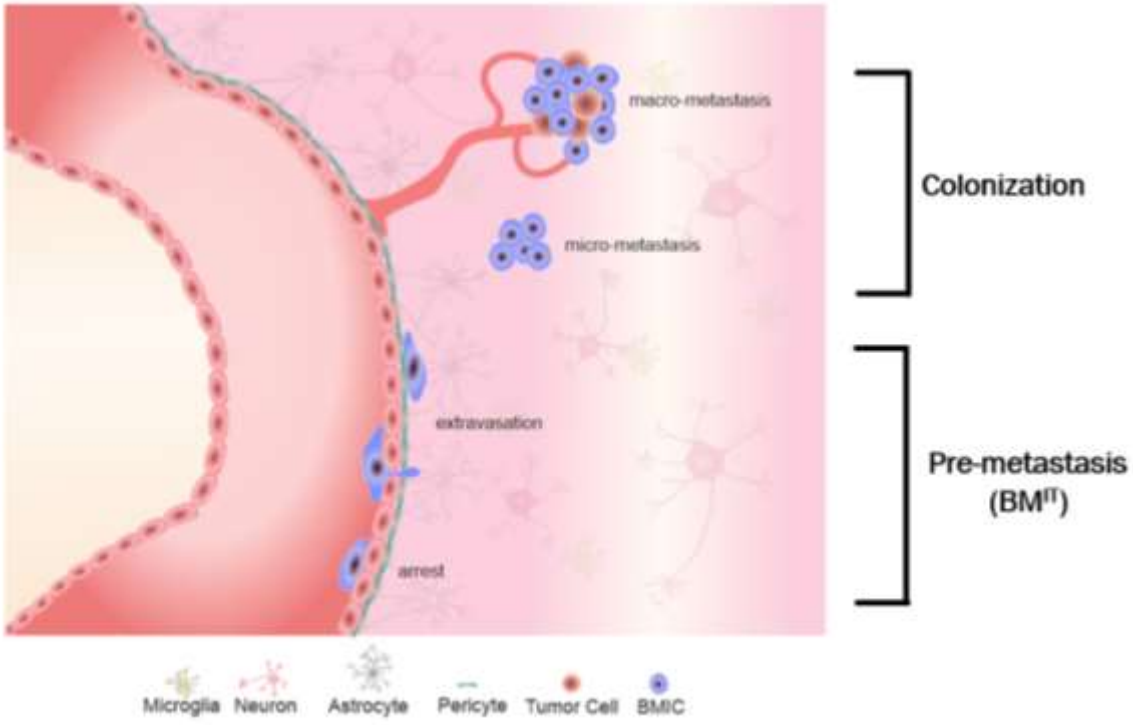

Figure 6. Schematic representation of stages of pre-metastasis and colonization. Pre-metastasis encopasses the stages of arrest, estravasation and initial seeding of the secondary tissue, whereas colonization is the formation of micro- and macro-metastatic growths.

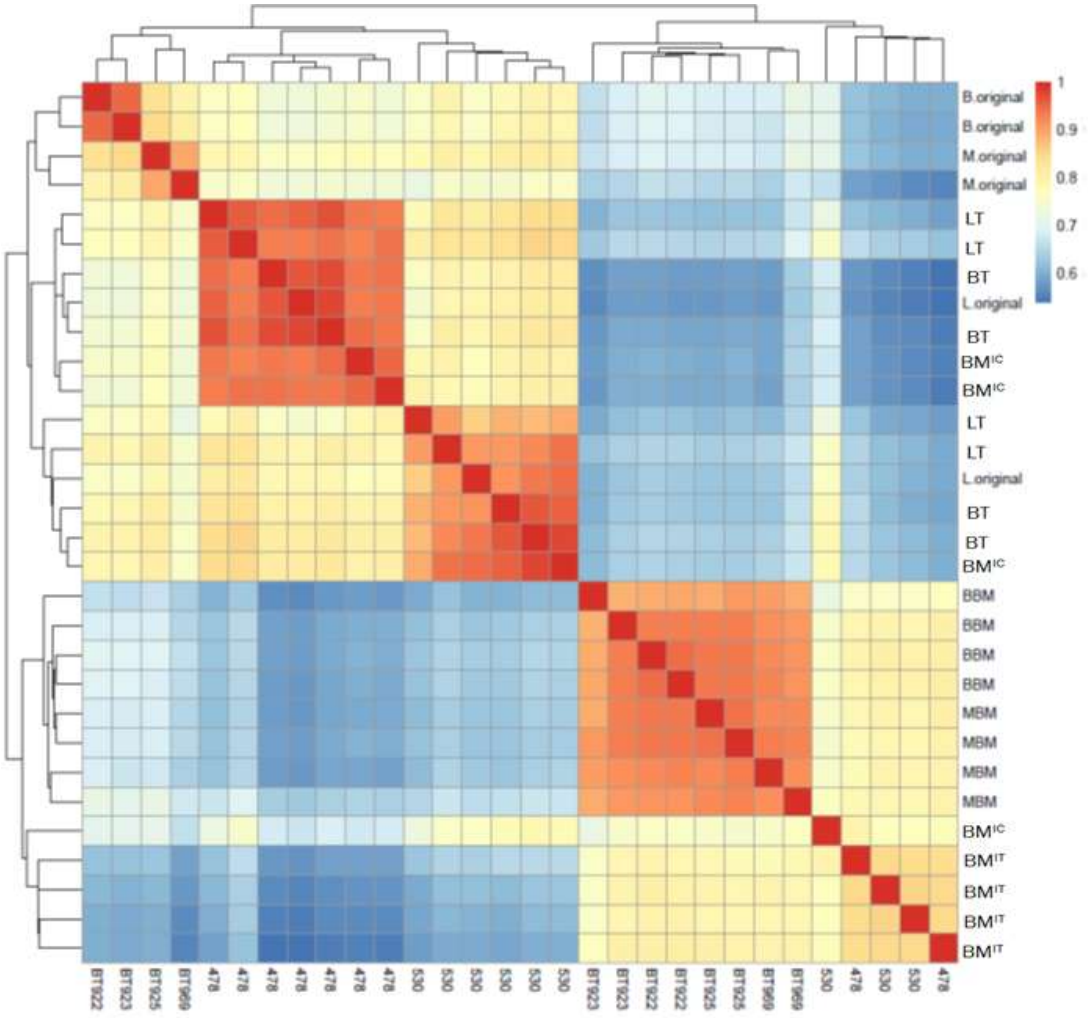

Figure 7. Generation of breast-to-brain and melanoma-to-brain metastasis in vivo models of BM. Patient-derived BMIC lines from samples of breast-to-brain (BBM) and melanoma-to-brain (MBM) BM were tagged green fluorescent protein (GFP) and injected in vivo to generate models of BM. For the BBM model, approximately 500,000 cells (BT922 and BT923) were injected in a 1:1 ratio with Matrigel (Biosciences) into the secondary fatpad (Primary tumor indicated by the blue arrow). For the MBM model, 100,000-250,000 cells (BT925 and BT969) were injected in a 1:1 ratio with Matrigel S.C. into the right flank. Upon endpoint, tumors from the initial site of injection and brains were collected and cultured in TSM under puromycin to select out contaminating mouse cells.

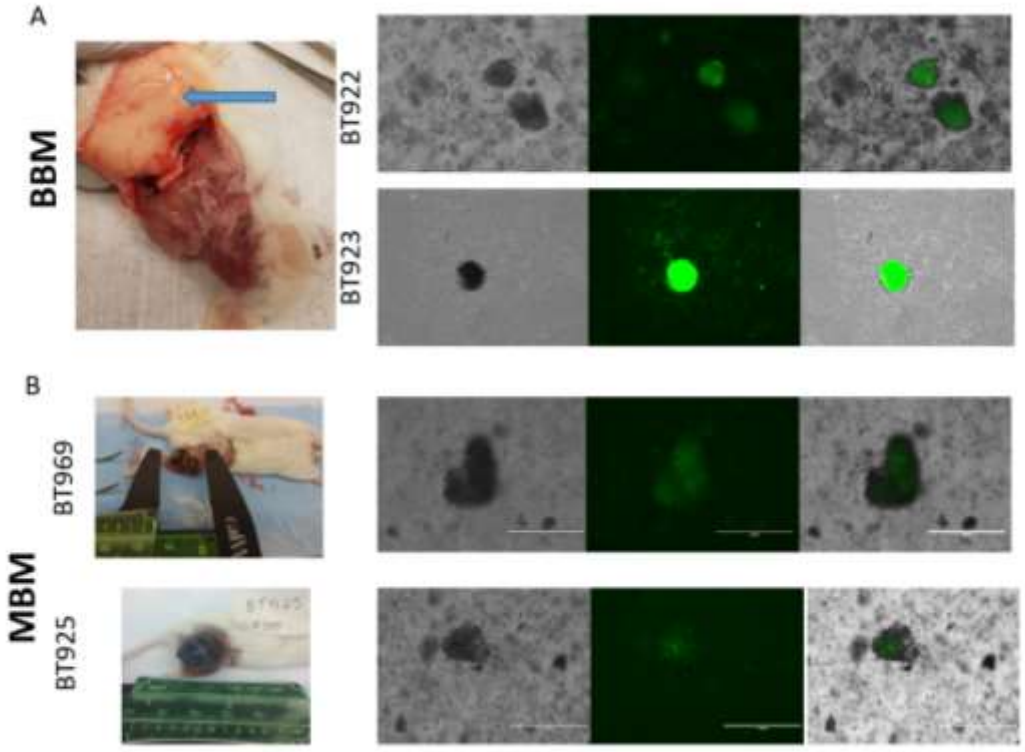

Figure 8. Heat maps of BMIC isolated from models of lung, breast and melanoma BM. RNA was isolated from BBM and MBM BMICs prior to inject as well as cells that metastasized to the brain within the models and submitted for sequencing similarly to lung models of BM. Featured is the resulting heatmap, depicting a similar gene expression profile between MBM and BBM but that differs from ITB. ("original" denotes BMIC samples prior to injection, with L=lung, B=breast, M=melanoma; MBM=BMICs that metastasized from the S.C. tumor to the brain; BBM = BMICs that metastasized from the secondary fatpad to the brain).

5.6 Concluding Remarks

Little attention has been paid to the study of metastasis and is instead focused on tumorigenesis of primary cancers(Steeg *et al.*, 2009), and while this has led to significant advancements made to the treatment and increased survival of these primary cancers it leaves patients susceptible to relapse and metastatic progression. The identification of

genes, pathways, and markers vital to the function of BMICs and the formation of BMs may prove to be ideal therapeutic targets. Successful development of targeted therapies would lead to the arrest of metastasis to the brain, keeping the primary cancer in a localized state, and ultimately increasing patient survival. However, several challenges exist in selectively targeting the BMICs. The first of which is that BMICs account for a rare subgroup of cells within the bulk tumor and therefore only present at low frequencies (Nolte *et al.*, 2013). Another significant drawback when studying BMICs is the lack of appropriate markers. Even if a dependable marker is found, the ability of BMICs to undergo asymmetric division suggests that a population enriched to homogeneity will eventually dilute itself out. This also leads to a third challenge of the depth of intratumoral heterogeneity; clonal evolution within the solid tumor could result in the brain metastasis having little or no resemblance to the primary tumor (Brastianos *et al.*, 2015). The development of novel therapeutics is further complicated by the hurdles encountered throughout delivery of anticancer drugs to the brain(Groves 2010). The findings presented in this thesis shed much needed light into the process of BM development. I developed clinically relevant PDX models of BM through the application of BMICs, our enriched BM stem cell population. I identified STAT3, SPOCK1 and TWIST2 all to be putative regulators of BM. I also utilized our IT model to characterize a unique pre-metastatic stage, determining several vital regulatory mechanisms that promote this intriguing process of seeding the brain. Lastly, I show that BM formation can be inhibited by application of the repurposed Parkinson's drug Apomorphine, identifying 3 pre-metastatic genes, KIF16B, SEPW1 and TESK2, that may promote pre-metastasis and are associated with poor survival

in lung cancer patients. While there is still much progress to be made in the field of BM, our observations open novel therapeutic avenues to BM prevention as opposed to current BM treatment.

Bibliography.

Abdullah, L. N., & Chow, E. K. (2013). Mechanisms of chemoresistance in cancer stem cells. *Clin Transl Med, 2*(1), 3. doi: 10.1186/2001-1326-2-3

Aceto, N., Bardia, A., Miyamoto, D. T., Donaldson, M. C., Wittner, B. S., Spencer, J. A., . . . Maheswaran, S. (2014). Circulating tumor cell clusters are oligoclonal precursors of breast cancer metastasis. *Cell, 158*(5), 1110-1122. doi: 10.1016/j.cell.2014.07.013

Agarwala, S. S., Kirkwood, J. M., Gore, M., Dreno, B., Thatcher, N., Czarnetski, B., . . . Rankin, E. M. (2004). Temozolomide for the treatment of brain metastases associated with metastatic melanoma: a phase II study. *J Clin Oncol, 22*(11), 2101-2107. doi: 10.1200/JCO.2004.11.044

Aguirre-Gamboa, R., Gomez-Rueda, H., Martinez-Ledesma, E., Martinez-Torteya, A., Chacolla-Huaringa, R., Rodriguez-Barrientos, A., . . . Trevino, V. (2013). SurvExpress: an online biomarker validation tool and database for cancer gene expression data using survival analysis. *PLoS One, 8*(9), e74250. doi: 10.1371/journal.pone.0074250

Aguirre Ghiso, J. A., Kovalski, K., & Ossowski, L. (1999). Tumor dormancy induced by downregulation of urokinase receptor in human carcinoma involves integrin and MAPK signaling. *J Cell Biol, 147*(1), 89-104.

Ahluwalia, M. S., Vogelbaum, M. V., Chao, S. T., & Mehta, M. M. (2014). Brain metastasis and treatment. *F1000Prime Rep, 6*, 114. doi: 10.12703/P6-114

Al-Hajj, M., Wicha, M. S., Benito-Hernandez, A., Morrison, S. J., & Clarke, M. F. (2003). Prospective identification of tumorigenic breast cancer cells. *Proc Natl Acad Sci U S A, 100*(7), 3983-3988. doi: 10.1073/pnas.0530291100

Anderson, K., Lutz, C., van Delft, F. W., Bateman, C. M., Guo, Y., Colman, S. M., . . . Greaves, M. (2011). Genetic variegation of clonal architecture and propagating cells in leukaemia. *Nature, 469*(7330), 356-361. doi: 10.1038/nature09650

Antonadou, D., Paraskevaidis, M., Sarris, G., Coliarakis, N., Economou, I., Karageorgis, P., & Throuvalas, N. (2002). Phase II randomized trial of temozolomide and concurrent radiotherapy in patients with brain metastases. *J Clin Oncol, 20*(17), 3644-3650. doi: 10.1200/JCO.2002.04.140

Asangani, I. A., Rasheed, S. A., Nikolova, D. A., Leupold, J. H., Colburn, N. H., Post, S., & Allgayer, H. (2008). MicroRNA-21 (miR-21) post-transcriptionally downregulates tumor suppressor Pdcd4 and stimulates invasion, intravasation and metastasis in colorectal cancer. *Oncogene, 27*(15), 2128-2136. doi: 10.1038/sj.onc.1210856

Ashburner, M., Ball, C. A., Blake, J. A., Botstein, D., Butler, H., Cherry, J. M., . . . Sherlock, G. (2000). Gene ontology: tool for the unification of biology. The Gene Ontology Consortium. *Nat Genet, 25*(1), 25-29. doi: 10.1038/75556

Bajaj, A., Driver, J. A., & Schernhammer, E. S. (2010). Parkinson's disease and cancer risk: a systematic review and meta-analysis. *Cancer Causes Control, 21*(5), 697-707. doi: 10.1007/s10552-009-9497-6

Banks, W. A. (2009). Characteristics of compounds that cross the blood-brain barrier. *BMC Neurol, 9 Suppl 1*, S3. doi: 10.1186/1471-2377-9-S1-S3

Barnholtz-Sloan, J. S., Sloan, A. E., Davis, F. G., Vigneau, F. D., Lai, P., & Sawaya, R. E. (2004). Incidence proportions of brain metastases in patients diagnosed (1973 to 2001) in the Metropolitan Detroit Cancer Surveillance System. *J Clin Oncol, 22*(14), 2865-2872. doi: 10.1200/JCO.2004.12.149

Bartel, D. P. (2004). MicroRNAs: genomics, biogenesis, mechanism, and function. *Cell, 116*(2), 281-297.

Bartel, D. P. (2009). MicroRNAs: target recognition and regulatory functions. *Cell, 136*(2), 215-233. doi: 10.1016/j.cell.2009.01.002

Ben-David, U., Ha, G., Tseng, Y. Y., Greenwald, N. F., Oh, C., Shih, J., . . . Golub, T. R. (2017). Patient-derived xenografts undergo mouse-specific tumor evolution. *Nat Genet, 49*(11), 1567-1575. doi: 10.1038/ng.3967

Bennett, D. A., & Leurgans, S. (2010). Is there a link between cancer and Alzheimer disease? *Neurology, 74*(2), 100-101. doi: 10.1212/WNL.0b013e3181cbb89a

Boettcher, M., & Hoheisel, J. D. (2010). Pooled RNAi Screens - Technical and Biological Aspects. *Curr Genomics, 11*(3), 162-167. doi: 10.2174/138920210791110988

Bos, P. D., Zhang, X. H., Nadal, C., Shu, W., Gomis, R. R., Nguyen, D. X., . . . Massague, J. (2009). Genes that mediate breast cancer metastasis to the brain. *Nature, 459*(7249), 1005-1009. doi: 10.1038/nature08021

Boyle, A., & Ondo, W. (2015). Role of apomorphine in the treatment of Parkinson's disease. *CNS Drugs, 29*(2), 83-89. doi: 10.1007/s40263-014-0221-z

Brastianos, P. K., Carter, S. L., Santagata, S., Cahill, D. P., Taylor-Weiner, A., Jones, R. T., . . . Hahn, W. C. (2015). Genomic Characterization of Brain Metastases Reveals Branched Evolution and Potential Therapeutic Targets. *Cancer Discov, 5*(11), 1164-1177. doi: 10.1158/2159-8290.CD-15-0369

Brennecke, J., Stark, A., Russell, R. B., & Cohen, S. M. (2005). Principles of microRNA-target recognition. *PLoS Biol, 3*(3), e85. doi: 10.1371/journal.pbio.0030085

Brown, D., Smeets, D., Szekely, B., Larsimont, D., Szasz, A. M., Adnet, P. Y., . . . Desmedt, C. (2017). Phylogenetic analysis of metastatic progression in breast cancer using somatic mutations and copy number aberrations. *Nat Commun, 8*, 14944. doi: 10.1038/ncomms14944

Brown, H. K., Schiavone, K., Tazzyman, S., Heymann, D., & Chico, T. J. (2017). Zebrafish xenograft models of cancer and metastasis for drug discovery. *Expert Opin Drug Discov, 12*(4), 379-389. doi: 10.1080/17460441.2017.1297416

Brown, K. R., & Jurisica, I. (2005). Online predicted human interaction database. *Bioinformatics, 21*(9), 2076-2082. doi: 10.1093/bioinformatics/bti273

Brown, K. R., & Jurisica, I. (2007). Unequal evolutionary conservation of human protein interactions in interologous networks. *Genome Biol, 8*(5), R95. doi: 10.1186/gb-2007-8-5-r95

Brown, K. R., Otasek, D., Ali, M., McGuffin, M. J., Xie, W., Devani, B., . . . Jurisica, I. (2009). NAViGaTOR: Network Analysis, Visualization and Graphing Toronto. *Bioinformatics, 25*(24), 3327-3329. doi: 10.1093/bioinformatics/btp595

Budczies, J., von Winterfeld, M., Klauschen, F., Bockmayr, M., Lennerz, J. K., Denkert, C., . . . Stenzinger, A. (2015). The landscape of metastatic progression patterns

across major human cancers. *Oncotarget, 6*(1), 570-583. doi: 10.18632/oncotarget.2677

Buscaglia, L. E., & Li, Y. (2011). Apoptosis and the target genes of microRNA-21. *Chin J Cancer, 30*(6), 371-380.

Cao, H. H., Chu, J. H., Kwan, H. Y., Su, T., Yu, H., Cheng, C. Y., . . . Yu, Z. L. (2016). Inhibition of the STAT3 signaling pathway contributes to apigenin-mediated anti-metastatic effect in melanoma. *Sci Rep, 6*, 21731. doi: 10.1038/srep21731

Cao, H. H., Tse, A. K., Kwan, H. Y., Yu, H., Cheng, C. Y., Su, T., . . . Yu, Z. L. (2014). Quercetin exerts anti-melanoma activities and inhibits STAT3 signaling. *Biochem Pharmacol, 87*(3), 424-434. doi: 10.1016/j.bcp.2013.11.008

Cavallaro, S. (2013). CXCR4/CXCL12 in Non-Small-Cell Lung Cancer Metastasis to the Brain. *Int J Mol Sci, 14*(1), 1713-1727. doi: 10.3390/ijms14011713

Celia-Terrassa, T., & Kang, Y. (2016). Distinctive properties of metastasis-initiating cells. *Genes Dev, 30*(8), 892-908. doi: 10.1101/gad.277681.116

Celia-Terrassa, T., Meca-Cortes, O., Mateo, F., de Paz, A. M., Rubio, N., Arnal-Estape, A., . . . Thomson, T. M. (2012). Epithelial-mesenchymal transition can suppress major attributes of human epithelial tumor-initiating cells. *J Clin Invest, 122*(5), 1849-1868. doi: 10.1172/JCI59218

Chambers, A. F., Groom, A. C., & MacDonald, I. C. (2002). Dissemination and growth of cancer cells in metastatic sites. *Nat Rev Cancer, 2*(8), 563-572. doi: 10.1038/nrc865

Chauvet, N., Romano, N., Lafont, C., Guillou, A., Galibert, E., Bonnefont, X., . . . Coutry, N. (2017). Complementary actions of dopamine D2 receptor agonist and anti-vegf therapy on tumoral vessel normalization in a transgenic mouse model. *Int J Cancer, 140*(9), 2150-2161. doi: 10.1002/ijc.30628

Chen, K., Huang, Y. H., & Chen, J. L. (2013). Understanding and targeting cancer stem cells: therapeutic implications and challenges. *Acta Pharmacol Sin, 34*(6), 732-740. doi: 10.1038/aps.2013.27

Chen, Q., Boire, A., Jin, X., Valiente, M., Emrah Er, E., Lopez-Soto, A., . . . Massague, J. (2017). Corrigendum: Carcinoma-astrocyte gap junctions promote brain metastasis by cGAMP transfer. *Nature, 544*(7648), 124. doi: 10.1038/nature21730

Chen, Q., Yao, Y. T., Xu, H., Chen, Y. B., Gu, M., Cai, Z. K., & Wang, Z. (2016). SPOCK1 promotes tumor growth and metastasis in human prostate cancer. *Drug Des Devel Ther, 10*, 2311-2321. doi: 10.2147/DDDT.S91321

Chiu, W. T., Lee, H. T., Huang, F. J., Aldape, K. D., Yao, J., Steeg, P. S., . . . Huang, S. (2011). Caveolin-1 upregulation mediates suppression of primary breast tumor growth and brain metastases by stat3 inhibition. *Cancer Res, 71*(14), 4932-4943. doi: 10.1158/0008-5472.CAN-10-4249

Clark, A. G., & Vignjevic, D. M. (2015). Modes of cancer cell invasion and the role of the microenvironment. *Curr Opin Cell Biol, 36*, 13-22. doi: 10.1016/j.ceb.2015.06.004

Collins, A. T., Berry, P. A., Hyde, C., Stower, M. J., & Maitland, N. J. (2005). Prospective identification of tumorigenic prostate cancer stem cells. *Cancer Res, 65*(23), 10946-10951. doi: 10.1158/0008-5472.CAN-05-2018

Cruz-Munoz, W., Man, S., Xu, P., & Kerbel, R. S. (2008). Development of a preclinical model of spontaneous human melanoma central nervous system metastasis. *Cancer Res, 68*(12), 4500-4505. doi: 10.1158/0008-5472.CAN-08-0041

Daphu, I., Sundstrom, T., Horn, S., Huszthy, P. C., Niclou, S. P., Sakariassen, P. O., . . . Thorsen, F. (2013). In vivo animal models for studying brain metastasis: value and limitations. *Clin Exp Metastasis, 30*(5), 695-710. doi: 10.1007/s10585-013-9566-9

Darnell, J. E., Jr. (1997). STATs and gene regulation. *Science, 277*(5332), 1630-1635.

Davis, A. P., Grondin, C. J., Johnson, R. J., Sciaky, D., King, B. L., McMorran, R., . . . Mattingly, C. J. (2017). The Comparative Toxicogenomics Database: update 2017. *Nucleic Acids Res, 45*(D1), D972-D978. doi: 10.1093/nar/gkw838

de Bruin, E. C., McGranahan, N., Mitter, R., Salm, M., Wedge, D. C., Yates, L., . . . Swanton, C. (2014). Spatial and temporal diversity in genomic instability processes defines lung cancer evolution. *Science, 346*(6206), 251-256. doi: 10.1126/science.1253462

de Lucas, B., Bernal, A., Perez, L. M., San Martin, N., & Galvez, B. G. (2016). Membrane Blebbing Is Required for Mesenchymal Precursor Migration. *PLoS One, 11*(3), e0150004. doi: 10.1371/journal.pone.0150004

DeAngelis, L. M., & Boutros, D. (2005). Leptomeningeal metastasis. *Cancer Invest, 23*(2), 145-154.

DeBerardinis, R. J., Lum, J. J., Hatzivassiliou, G., & Thompson, C. B. (2008). The biology of cancer: metabolic reprogramming fuels cell growth and proliferation. *Cell Metab, 7*(1), 11-20. doi: 10.1016/j.cmet.2007.10.002

DeCicco-Skinner, K. L., Henry, G. H., Cataisson, C., Tabib, T., Gwilliam, J. C., Watson, N. J., . . . Wiest, J. S. (2014). Endothelial cell tube formation assay for the in vitro study of angiogenesis. *J Vis Exp*(91), e51312. doi: 10.3791/51312

Derynck, R., & Zhang, Y. E. (2003). Smad-dependent and Smad-independent pathways in TGF-beta family signalling. *Nature, 425*(6958), 577-584. doi: 10.1038/nature02006

Ding, L., Ellis, M. J., Li, S., Larson, D. E., Chen, K., Wallis, J. W., . . . Mardis, E. R. (2010). Genome remodelling in a basal-like breast cancer metastasis and xenograft. *Nature, 464*(7291), 999-1005. doi: 10.1038/nature08989

Duquet, A., Melotti, A., Mishra, S., Malerba, M., Seth, C., Conod, A., & Ruiz i Altaba, A. (2014). A novel genome-wide in vivo screen for metastatic suppressors in human colon cancer identifies the positive WNT-TCF pathway modulators TMED3 and SOX12. *EMBO Mol Med, 6*(7), 882-901. doi: 10.15252/emmm.201303799

Eichler, A. F., & Loeffler, J. S. (2007). Multidisciplinary management of brain metastases. *Oncologist, 12*(7), 884-898. doi: 10.1634/theoncologist.12-7-884

Eiring, A. M., Page, B. D., Kraft, I. L., Mason, C. C., Vellore, N. A., Resetca, D., . . . Deininger, M. W. (2014). Combined STAT3 and BCR-ABL1 inhibition induces

synthetic lethality in therapy-resistant chronic myeloid leukemia. *Leukemia*. doi: 10.1038/leu.2014.245

Ekenel, M., Hormigo, A. M., Peak, S., Deangelis, L. M., & Abrey, L. E. (2007). Capecitabine therapy of central nervous system metastases from breast cancer. *J Neurooncol, 85*(2), 223-227. doi: 10.1007/s11060-007-9409-0

Escudier, B., Pluzanska, A., Koralewski, P., Ravaud, A., Bracarda, S., Szczylik, C., . . . investigators, A. T. (2007). Bevacizumab plus interferon alfa-2a for treatment of metastatic renal cell carcinoma: a randomised, double-blind phase III trial. *Lancet, 370*(9605), 2103-2111. doi: 10.1016/S0140-6736(07)61904-7

Ewing, J. (1928). Neoplastic Diseases: A Treatise on Tumours. By James Ewing, A.M., M.D., Sc.D., Professor of Pathology at Cornell University Medical College, N.Y.; Pathologist to the Memorial Hospital. Third edition. Royal 8vo. Pp. 1127, with 546 illustrations. 1928. Philadelphia and London: W. B. Saunders Co. Ltd. 63s. net. *British Journal of Surgery, 16*(61), 174-175. doi: 10.1002/bjs.1800166126

Fang, X., Cai, Y., Liu, J., Wang, Z., Wu, Q., Zhang, Z., . . . Ouyang, G. (2011). Twist2 contributes to breast cancer progression by promoting an epithelial-mesenchymal transition and cancer stem-like cell self-renewal. *Oncogene, 30*(47), 4707-4720. doi: 10.1038/onc.2011.181

Farber, S. H., Tsvankin, V., Narloch, J. L., Kim, G. J., Salama, A. K., Vlahovic, G., . . . Fecci, P. E. (2016). Embracing rejection: Immunologic trends in brain metastasis. *Oncoimmunology, 5*(7), e1172153. doi: 10.1080/2162402X.2016.1172153

Farkhondeh, A., Niwa, S., Takei, Y., & Hirokawa, N. (2015). Characterizing KIF16B in neurons reveals a novel intramolecular "stalk inhibition" mechanism that regulates its capacity to potentiate the selective somatodendritic localization of early endosomes. *J Neurosci, 35*(12), 5067-5086. doi: 10.1523/JNEUROSCI.4240-14.2015

Faure, J., Lachenal, G., Court, M., Hirrlinger, J., Chatellard-Causse, C., Blot, B., . . . Sadoul, R. (2006). Exosomes are released by cultured cortical neurones. *Mol Cell Neurosci, 31*(4), 642-648. doi: 10.1016/j.mcn.2005.12.003

Feng, D. D., Cai, W., & Chen, X. (2015). The associations between Parkinson's disease and cancer: the plot thickens. *Transl Neurodegener, 4*, 20. doi: 10.1186/s40035-015-0043-z

Ferrara, N., & Kerbel, R. S. (2005). Angiogenesis as a therapeutic target. *Nature, 438*(7070), 967-974. doi: 10.1038/nature04483

Fidler, I. J. (1970). Metastasis: guantitative analysis of distribution and fate of tumor embolilabeled with 125 I-5-iodo-2'-deoxyuridine. *J Natl Cancer Inst, 45*(4), 773-782.

Fidler, I. J. (1973). Selection of successive tumour lines for metastasis. *Nat New Biol, 242*(118), 148-149.

Fidler, I. J. (2003). The pathogenesis of cancer metastasis: the 'seed and soil' hypothesis revisited. *Nat Rev Cancer, 3*(6), 453-458. doi: 10.1038/nrc1098

Fischer, K. R., Durrans, A., Lee, S., Sheng, J., Li, F., Wong, S. T., . . . Gao, D. (2015). Epithelial-to-mesenchymal transition is not required for lung metastasis but

contributes to chemoresistance. *Nature, 527*(7579), 472-476. doi: 10.1038/nature15748

Fodde, R., & Tomlinson, I. (2010). Nuclear beta-catenin expression and Wnt signalling: in defence of the dogma. *J Pathol, 221*(3), 239-241. doi: 10.1002/path.2718

Francia, G., Cruz-Munoz, W., Man, S., Xu, P., & Kerbel, R. S. (2011). Mouse models of advanced spontaneous metastasis for experimental therapeutics. *Nat Rev Cancer, 11*(2), 135-141. doi: 10.1038/nrc3001

Friedl, P., & Alexander, S. (2011). Cancer invasion and the microenvironment: plasticity and reciprocity. *Cell, 147*(5), 992-1009. doi: 10.1016/j.cell.2011.11.016

Friedl, P., & Wolf, K. (2003). Tumour-cell invasion and migration: diversity and escape mechanisms. *Nat Rev Cancer, 3*(5), 362-374. doi: 10.1038/nrc1075

Friedrich, J., Seidel, C., Ebner, R., & Kunz-Schughart, L. A. (2009). Spheroid-based drug screen: considerations and practical approach. *Nat Protoc, 4*(3), 309-324. doi: 10.1038/nprot.2008.226

Fujita, K., Kubota, Y., Ishida, H., & Sasaki, Y. (2015). Irinotecan, a key chemotherapeutic drug for metastatic colorectal cancer. *World J Gastroenterol, 21*(43), 12234-12248. doi: 10.3748/wjg.v21.i43.12234

Garcia-Olmo, D., Garcia-Olmo, D. C., Ontanon, J., Martinez, E., & Vallejo, M. (1999). Tumor DNA circulating in the plasma might play a role in metastasis. The hypothesis of the genometastasis. *Histol Histopathol, 14*(4), 1159-1164.

Garg, N., Po, A., Miele, E., Campese, A. F., Begalli, F., Silvano, M., . . . Gulino, A. (2013). microRNA-17-92 cluster is a direct Nanog target and controls neural stem cell through Trp53inp1. *EMBO J, 32*(21), 2819-2832. doi: 10.1038/emboj.2013.214

Gavrilovic, I. T., & Posner, J. B. (2005). Brain metastases: epidemiology and pathophysiology. *J Neurooncol, 75*(1), 5-14. doi: 10.1007/s11060-004-8093-6

Gengenbacher, N., Singhal, M., & Augustin, H. G. (2017). Preclinical mouse solid tumour models: status quo, challenges and perspectives. *Nat Rev Cancer, 17*(12), 751-765. doi: 10.1038/nrc.2017.92

Gerlinger, M., Rowan, A. J., Horswell, S., Larkin, J., Endesfelder, D., Gronroos, E., . . . Swanton, C. (2012). Intratumor heterogeneity and branched evolution revealed by multiregion sequencing. *N Engl J Med, 366*(10), 883-892. doi: 10.1056/NEJMoa1113205

GK, S. (2005). Limma: linear models for microarray data. In C. V. Gentleman R, Huber W, Irizarry R, Dudoit S (Ed.), *Bioinformatics and Computational Biology Solutions Using R and Bioconductor* (pp. 397-420). Mew York: Springer.

Gobeil, S., Zhu, X., Doillon, C. J., & Green, M. R. (2008). A genome-wide shRNA screen identifies GAS1 as a novel melanoma metastasis suppressor gene. *Genes Dev, 22*(21), 2932-2940. doi: 10.1101/gad.1714608

Gomis, R. R., & Gawrzak, S. (2016). Tumor cell dormancy. *Mol Oncol*. doi: 10.1016/j.molonc.2016.09.009

Gottesman, M. M., Fojo, T., & Bates, S. E. (2002). Multidrug resistance in cancer: role of ATP-dependent transporters. *Nat Rev Cancer, 2*(1), 48-58. doi: 10.1038/nrc706

Grossmann, J. (2002). Molecular mechanisms of "detachment-induced apoptosis--Anoikis". *Apoptosis, 7*(3), 247-260.

Groves, M. D. (2010). New strategies in the management of leptomeningeal metastases. *Arch Neurol, 67*(3), 305-312. doi: 10.1001/archneurol.2010.18

Gyorffy, B., Surowiak, P., Budczies, J., & Lanczky, A. (2013). Online survival analysis software to assess the prognostic value of biomarkers using transcriptomic data in non-small-cell lung cancer. *PLoS One, 8*(12), e82241. doi: 10.1371/journal.pone.0082241

Haftchenary, S., Luchman, H. A., Jouk, A. O., Veloso, A. J., Page, B. D., Cheng, X. R., . . . Gunning, P. T. (2013). Potent Targeting of the STAT3 Protein in Brain Cancer Stem Cells: A Promising Route for Treating Glioblastoma. *ACS Med Chem Lett, 4*(11), 1102-1107. doi: 10.1021/ml4003138

Hardesty, D. A., & Nakaji, P. (2016). The Current and Future Treatment of Brain Metastases. *Front Surg, 3*, 30. doi: 10.3389/fsurg.2016.00030

Hart, I. R., & Fidler, I. J. (1980). Role of organ selectivity in the determination of metastatic patterns of B16 melanoma. *Cancer Res, 40*(7), 2281-2287.

Hay, E. D. (2005). The mesenchymal cell, its role in the embryo, and the remarkable signaling mechanisms that create it. *Dev Dyn, 233*(3), 706-720. doi: 10.1002/dvdy.20345

Heasman, S. J., & Ridley, A. J. (2008). Mammalian Rho GTPases: new insights into their functions from in vivo studies. *Nat Rev Mol Cell Biol, 9*(9), 690-701. doi: 10.1038/nrm2476

Heerboth, S., Housman, G., Leary, M., Longacre, M., Byler, S., Lapinska, K., . . . Sarkar, S. (2015). EMT and tumor metastasis. *Clin Transl Med, 4*, 6. doi: 10.1186/s40169-015-0048-3

Herlyn, M., Thurin, J., Balaban, G., Bennicelli, J. L., Herlyn, D., Elder, D. E., . . . et al. (1985). Characteristics of cultured human melanocytes isolated from different stages of tumor progression. *Cancer Res, 45*(11 Pt 2), 5670-5676.

Hermann, P. C., Huber, S. L., Herrler, T., Aicher, A., Ellwart, J. W., Guba, M., . . . Heeschen, C. (2007). Distinct populations of cancer stem cells determine tumor growth and metastatic activity in human pancreatic cancer. *Cell Stem Cell, 1*(3), 313-323. doi: 10.1016/j.stem.2007.06.002

Himeno, E., Ohyagi, Y., Ma, L., Nakamura, N., Miyoshi, K., Sakae, N., . . . Kira, J. (2011). Apomorphine treatment in Alzheimer mice promoting amyloid-beta degradation. *Ann Neurol, 69*(2), 248-256. doi: 10.1002/ana.22319

Hiraga, T., Ito, S., & Nakamura, H. (2016). EpCAM expression in breast cancer cells is associated with enhanced bone metastasis formation. *Int J Cancer, 138*(7), 1698-1708. doi: 10.1002/ijc.29921

Hirokawa, N., Niwa, S., & Tanaka, Y. (2010). Molecular motors in neurons: transport mechanisms and roles in brain function, development, and disease. *Neuron, 68*(4), 610-638. doi: 10.1016/j.neuron.2010.09.039

Hodge, D. R., Hurt, E. M., & Farrar, W. L. (2005). The role of IL-6 and STAT3 in inflammation and cancer. *Eur J Cancer, 41*(16), 2502-2512. doi: 10.1016/j.ejca.2005.08.016

Hoeppner, L. H., Wang, Y., Sharma, A., Javeed, N., Van Keulen, V. P., Wang, E., . . . Mukhopadhyay, D. (2015). Dopamine D2 receptor agonists inhibit lung cancer progression by reducing angiogenesis and tumor infiltrating myeloid derived suppressor cells. *Mol Oncol, 9*(1), 270-281. doi: 10.1016/j.molonc.2014.08.008

Hoffman, R. M. (2015). Patient-derived orthotopic xenografts: better mimic of metastasis than subcutaneous xenografts. *Nat Rev Cancer, 15*(8), 451-452. doi: 10.1038/nrc3972

Hong, D., Gupta, R., Ancliff, P., Atzberger, A., Brown, J., Soneji, S., . . . Enver, T. (2008). Initiating and cancer-propagating cells in TEL-AML1-associated childhood leukemia. *Science, 319*(5861), 336-339. doi: 10.1126/science.1150648

Hu, G., & Luo, J. (2012). A primer on using pooled shRNA libraries for functional genomic screens. *Acta Biochim Biophys Sin (Shanghai), 44*(2), 103-112. doi: 10.1093/abbs/gmr116

Huang, H., Wu, K., Ma, J., Du, Y., Cao, C., & Nie, Y. (2016). Dopamine D2 receptor suppresses gastric cancer cell invasion and migration via inhibition of EGFR/AKT/MMP-13 pathway. *Int Immunopharmacol, 39*, 113-120. doi: 10.1016/j.intimp.2016.07.002

Hurst, R. E., Bastian, A., Bailey-Downs, L., & Ihnat, M. A. (2016). Targeting dormant micrometastases: rationale, evidence to date and clinical implications. *Ther Adv Med Oncol, 8*(2), 126-137. doi: 10.1177/1758834015624277

Hurwitz, H. (2004). Integrating the anti-VEGF-A humanized monoclonal antibody bevacizumab with chemotherapy in advanced colorectal cancer. *Clin Colorectal Cancer, 4 Suppl 2*, S62-68.

Hynynen, K., McDannold, N., Vykhodtseva, N., & Jolesz, F. A. (2001). Noninvasive MR imaging-guided focal opening of the blood-brain barrier in rabbits. *Radiology, 220*(3), 640-646. doi: 10.1148/radiol.2202001804

Ibanez, K., Boullosa, C., Tabares-Seisdedos, R., Baudot, A., & Valencia, A. (2014). Molecular evidence for the inverse comorbidity between central nervous system disorders and cancers detected by transcriptomic meta-analyses. *PLoS Genet, 10*(2), e1004173. doi: 10.1371/journal.pgen.1004173

Iliopoulos, D., Jaeger, S. A., Hirsch, H. A., Bulyk, M. L., & Struhl, K. (2010). STAT3 activation of miR-21 and miR-181b-1 via PTEN and CYLD are part of the epigenetic switch linking inflammation to cancer. *Mol Cell, 39*(4), 493-506. doi: 10.1016/j.molcel.2010.07.023

Inzelberg, R., & Jankovic, J. (2007). Are Parkinson disease patients protected from some but not all cancers? *Neurology, 69*(15), 1542-1550. doi: 10.1212/01.wnl.0000277638.63767.b8

Jamal-Hanjani, M., Hackshaw, A., Ngai, Y., Shaw, J., Dive, C., Quezada, S., . . . Swanton, C. (2014). Tracking genomic cancer evolution for precision medicine: the lung TRACERx study. *PLoS Biol, 12*(7), e1001906. doi: 10.1371/journal.pbio.1001906

Jamal-Hanjani, M., Wilson, G. A., McGranahan, N., Birkbak, N. J., Watkins, T. B. K., Veeriah, S., . . . Consortium, T. R. (2017). Tracking the Evolution of Non-Small-

Cell Lung Cancer. *N Engl J Med, 376*(22), 2109-2121. doi: 10.1056/NEJMoa1616288

Jiang, C., Xuan, Z., Zhao, F., & Zhang, M. Q. (2007). TRED: a transcriptional regulatory element database, new entries and other development. *Nucleic Acids Res, 35*(Database issue), D137-140. doi: 10.1093/nar/gkl1041

Jobling, P., Pundavela, J., Oliveira, S. M., Roselli, S., Walker, M. M., & Hondermarck, H. (2015). Nerve-Cancer Cell Cross-talk: A Novel Promoter of Tumor Progression. *Cancer Res, 75*(9), 1777-1781. doi: 10.1158/0008-5472.CAN-14-3180

Joo, K. M., Kim, J., Jin, J., Kim, M., Seol, H. J., Muradov, J., . . . Nam, D. H. (2013). Patient-specific orthotopic glioblastoma xenograft models recapitulate the histopathology and biology of human glioblastomas in situ. *Cell Rep, 3*(1), 260-273. doi: 10.1016/j.celrep.2012.12.013

Jung, Y. S., & Lee, S. O. (2017). Apomorphine suppresses TNF-alpha-induced MMP-9 expression and cell invasion through inhibition of ERK/AP-1 signaling pathway in MCF-7 cells. *Biochem Biophys Res Commun, 487*(4), 903-909. doi: 10.1016/j.bbrc.2017.04.151

Kamran, M. Z., Patil, P., & Gude, R. P. (2013). Role of STAT3 in cancer metastasis and translational advances. *Biomed Res Int, 2013*, 421821. doi: 10.1155/2013/421821

Kanehisa, M., & Goto, S. (2000). KEGG: kyoto encyclopedia of genes and genomes. *Nucleic Acids Res, 28*(1), 27-30.

Kaplan, R. N., Riba, R. D., Zacharoulis, S., Bramley, A. H., Vincent, L., Costa, C., . . . Lyden, D. (2005). VEGFR1-positive haematopoietic bone marrow progenitors initiate the pre-metastatic niche. *Nature, 438*(7069), 820-827. doi: 10.1038/nature04186

Katt, M. E., Placone, A. L., Wong, A. D., Xu, Z. S., & Searson, P. C. (2016). In Vitro Tumor Models: Advantages, Disadvantages, Variables, and Selecting the Right Platform. *Front Bioeng Biotechnol, 4*, 12. doi: 10.3389/fbioe.2016.00012

Khan, M. I., Czarnecka, A. M., Duchnowska, R., Kukwa, W., & Szczylik, C. (2014). Metastasis-Initiating Cells in Renal Cancer. *Curr Signal Transduct Ther, 8*(3), 240-246. doi: 10.2174/1574362409666140206222431

Kikuchi, T., Daigo, Y., Ishikawa, N., Katagiri, T., Tsunoda, T., Yoshida, S., & Nakamura, Y. (2006). Expression profiles of metastatic brain tumor from lung adenocarcinomas on cDNA microarray. *Int J Oncol, 28*(4), 799-805.

Kircher, D. A., Silvis, M. R., Cho, J. H., & Holmen, S. L. (2016). Melanoma Brain Metastasis: Mechanisms, Models, and Medicine. *Int J Mol Sci, 17*(9). doi: 10.3390/ijms17091468

Klampfer, L. (2006). Signal transducers and activators of transcription (STATs): Novel targets of chemopreventive and chemotherapeutic drugs. *Curr Cancer Drug Targets, 6*(2), 107-121.

Klein, C. A. (2009). Parallel progression of primary tumours and metastases. *Nat Rev Cancer, 9*(4), 302-312. doi: 10.1038/nrc2627

Klein, C. A., & Holzel, D. (2006). Systemic cancer progression and tumor dormancy: mathematical models meet single cell genomics. *Cell Cycle, 5*(16), 1788-1798. doi: 10.4161/cc.5.16.3097

Kolde, R., Laur, S., Adler, P., & Vilo, J. (2012). Robust rank aggregation for gene list integration and meta-analysis. *Bioinformatics, 28*(4), 573-580. doi: 10.1093/bioinformatics/btr709

Kotlyar, M., Pastrello, C., Pivetta, F., Lo Sardo, A., Cumbaa, C., Li, H., . . . Jurisica, I. (2014). In silico prediction of physical protein interactions and characterization of interactome orphans. *Nat Methods*. doi: 10.1038/nmeth.3178

Kotlyar, M., Pastrello, C., Sheahan, N., & Jurisica, I. (2016). Integrated interactions database: tissue-specific view of the human and model organism interactomes. *Nucleic Acids Res, 44*(D1), D536-541. doi: 10.1093/nar/gkv1115

Kramer, N., Walzl, A., Unger, C., Rosner, M., Krupitza, G., Hengstschlager, M., & Dolznig, H. (2013). In vitro cell migration and invasion assays. *Mutat Res, 752*(1), 10-24. doi: 10.1016/j.mrrev.2012.08.001

Kroigard, A. B., Larsen, M. J., Brasch-Andersen, C., Laenkholm, A. V., Knoop, A. S., Jensen, J. D., . . . Kruse, T. A. (2017). Genomic Analyses of Breast Cancer Progression Reveal Distinct Routes of Metastasis Emergence. *Sci Rep, 7*, 43813. doi: 10.1038/srep43813

Lachmann, A., Xu, H., Krishnan, J., Berger, S. I., Mazloom, A. R., & Ma'ayan, A. (2010). ChEA: transcription factor regulation inferred from integrating genome-wide ChIP-X experiments. *Bioinformatics, 26*(19), 2438-2444. doi: 10.1093/bioinformatics/btq466

Lagerwaard, F. J., Levendag, P. C., Nowak, P. J., Eijkenboom, W. M., Hanssens, P. E., & Schmitz, P. I. (1999). Identification of prognostic factors in patients with brain metastases: a review of 1292 patients. *Int J Radiat Oncol Biol Phys, 43*(4), 795-803.

Lamb, J. (2007). The Connectivity Map: a new tool for biomedical research. *Nat Rev Cancer, 7*(1), 54-60. doi: 10.1038/nrc2044

Lambert, A. W., Pattabiraman, D. R., & Weinberg, R. A. (2017). Emerging Biological Principles of Metastasis. *Cell, 168*(4), 670-691. doi: 10.1016/j.cell.2016.11.037

Langley, R. R., & Fidler, I. J. (2011). The seed and soil hypothesis revisited--the role of tumor-stroma interactions in metastasis to different organs. *Int J Cancer, 128*(11), 2527-2535. doi: 10.1002/ijc.26031

Langley, R. R., & Fidler, I. J. (2013). The biology of brain metastasis. *Clin Chem, 59*(1), 180-189. doi: 10.1373/clinchem.2012.193342

Lawson, D. A., Bhakta, N. R., Kessenbrock, K., Prummel, K. D., Yu, Y., Takai, K., . . . Werb, Z. (2015). Single-cell analysis reveals a stem-cell program in human metastatic breast cancer cells. *Nature, 526*(7571), 131-135. doi: 10.1038/nature15260

Leal, T., Chang, J. E., Mehta, M., & Robins, H. I. (2011). Leptomeningeal Metastasis: Challenges in Diagnosis and Treatment. *Curr Cancer Ther Rev, 7*(4), 319-327. doi: 10.2174/157339411797642597

Levy, D. E., & Darnell, J. E., Jr. (2002). Stats: transcriptional control and biological impact. *Nat Rev Mol Cell Biol, 3*(9), 651-662. doi: 10.1038/nrm909

Li, L., Miyamoto, M., Ebihara, Y., Mega, S., Takahashi, R., Hase, R., . . . Kondo, S. (2006). DRD2/DARPP-32 expression correlates with lymph node metastasis and tumor progression in patients with esophageal squamous cell carcinoma. *World J Surg, 30*(9), 1672-1679; discussion 1680-1671. doi: 10.1007/s00268-006-0035-3

Liotta, L. A., Saidel, G. M., & Kleinerman, J. (1976a). Stochastic model of metastases formation. *Biometrics, 32*(3), 535-550.

Liotta, L. A., Saidel, M. G., & Kleinerman, J. (1976b). The significance of hematogenous tumor cell clumps in the metastatic process. *Cancer Res, 36*(3), 889-894.

Liu, A. Y., Cai, Y., Mao, Y., Lin, Y., Zheng, H., Wu, T., . . . Ouyang, G. (2014). Twist2 promotes self-renewal of liver cancer stem-like cells by regulating CD24. *Carcinogenesis, 35*(3), 537-545. doi: 10.1093/carcin/bgt364

Liu, C. F., Zhang, Y., Lim, S., Hosaka, K., Yang, Y., Pavlova, T., . . . Cao, Y. (2017). A zebrafish model discovers a novel mechanism of stromal fibroblast-mediated cancer metastasis. *Clin Cancer Res*. doi: 10.1158/1078-0432.CCR-17-0101

Liu, H., Patel, M. R., Prescher, J. A., Patsialou, A., Qian, D., Lin, J., . . . Clarke, M. F. (2010). Cancer stem cells from human breast tumors are involved in spontaneous metastases in orthotopic mouse models. *Proc Natl Acad Sci U S A, 107*(42), 18115-18120. doi: 10.1073/pnas.1006732107

Liu, R. Y., Zeng, Y., Lei, Z., Wang, L., Yang, H., Liu, Z., . . . Zhang, H. T. (2014). JAK/STAT3 signaling is required for TGF-beta-induced epithelial-mesenchymal transition in lung cancer cells. *Int J Oncol, 44*(5), 1643-1651. doi: 10.3892/ijo.2014.2310

Liu, Y., & Cao, X. (2016). Characteristics and Significance of the Pre-metastatic Niche. *Cancer Cell, 30*(5), 668-681. doi: 10.1016/j.ccell.2016.09.011

Liu, Y., Qian, W., Zhang, J., Dong, Y., Shi, C., Liu, Z., & Wu, S. (2015). The indicative function of Twist2 and E-cadherin in HPV oncogene-induced epithelial-mesenchymal transition of cervical cancer cells. *Oncol Rep, 33*(2), 639-650. doi: 10.3892/or.2014.3620

Loffler, D., Brocke-Heidrich, K., Pfeifer, G., Stocsits, C., Hackermuller, J., Kretzschmar, A. K., . . . Horn, F. (2007). Interleukin-6 dependent survival of multiple myeloma cells involves the Stat3-mediated induction of microRNA-21 through a highly conserved enhancer. *Blood, 110*(4), 1330-1333. doi: 10.1182/blood-2007-03-081133

Lokman, N. A., Elder, A. S., Ricciardelli, C., & Oehler, M. K. (2012). Chick chorioallantoic membrane (CAM) assay as an in vivo model to study the effect of newly identified molecules on ovarian cancer invasion and metastasis. *Int J Mol Sci, 13*(8), 9959-9970. doi: 10.3390/ijms13089959

Lorger, M., Krueger, J. S., O'Neal, M., Staflin, K., & Felding-Habermann, B. (2009). Activation of tumor cell integrin alphavbeta3 controls angiogenesis and metastatic growth in the brain. *Proc Natl Acad Sci U S A, 106*(26), 10666-10671. doi: 10.1073/pnas.0903035106

Lu-Emerson, C., & Eichler, A. F. (2012). Brain metastases. *Continuum (Minneap Minn), 18*(2), 295-311. doi: 10.1212/01.CON.0000413659.12304.a6

Lu, K. V., Chang, J. P., Parachoniak, C. A., Pandika, M. M., Aghi, M. K., Meyronet, D., . . . Bergers, G. (2012). VEGF inhibits tumor cell invasion and mesenchymal transition through a MET/VEGFR2 complex. *Cancer Cell, 22*(1), 21-35. doi: 10.1016/j.ccr.2012.05.037

Luzzi, K. J., MacDonald, I. C., Schmidt, E. E., Kerkvliet, N., Morris, V. L., Chambers, A. F., & Groom, A. C. (1998). Multistep nature of metastatic inefficiency: dormancy of solitary cells after successful extravasation and limited survival of early micrometastases. *Am J Pathol, 153*(3), 865-873. doi: 10.1016/S0002-9440(10)65628-3

Malanchi, I., Santamaria-Martinez, A., Susanto, E., Peng, H., Lehr, H. A., Delaloye, J. F., & Huelsken, J. (2011). Interactions between cancer stem cells and their niche govern metastatic colonization. *Nature, 481*(7379), 85-89. doi: 10.1038/nature10694

Mani, S. A., Guo, W., Liao, M. J., Eaton, E. N., Ayyanan, A., Zhou, A. Y., . . . Weinberg, R. A. (2008). The epithelial-mesenchymal transition generates cells with properties of stem cells. *Cell, 133*(4), 704-715. doi: 10.1016/j.cell.2008.03.027

Mao, X. G., Zhang, X., Xue, X. Y., Guo, G., Wang, P., Zhang, W., . . . Yang, H. (2009). Brain Tumor Stem-Like Cells Identified by Neural Stem Cell Marker CD15. *Transl Oncol, 2*(4), 247-257.

Marangoni, E., Lecomte, N., Durand, L., de Pinieux, G., Decaudin, D., Chomienne, C., . . . Poupon, M. F. (2009). CD44 targeting reduces tumour growth and prevents post-chemotherapy relapse of human breast cancers xenografts. *Br J Cancer, 100*(6), 918-922. doi: 10.1038/sj.bjc.6604953

Marhaba, R., Klingbeil, P., Nuebel, T., Nazarenko, I., Buechler, M. W., & Zoeller, M. (2008). CD44 and EpCAM: cancer-initiating cell markers. *Curr Mol Med, 8*(8), 784-804.

Marsden, C. G., Wright, M. J., Carrier, L., Moroz, K., Pochampally, R., & Rowan, B. G. (2012). "A novel in vivo model for the study of human breast cancer metastasis using primary breast tumor-initiating cells from patient biopsies". *BMC Cancer, 12*, 10. doi: 10.1186/1471-2407-12-10

Martinez-Aranda, A., Hernandez, V., Picon, C., Modolell, I., & Sierra, A. (2013). Development of a preclinical therapeutic model of human brain metastasis with chemoradiotherapy. *Int J Mol Sci, 14*(4), 8306-8327. doi: 10.3390/ijms14048306

Mashimo, T., Pichumani, K., Vemireddy, V., Hatanpaa, K. J., Singh, D. K., Sirasanagandla, S., . . . Bachoo, R. M. (2014). Acetate is a bioenergetic substrate for human glioblastoma and brain metastases. *Cell, 159*(7), 1603-1614. doi: 10.1016/j.cell.2014.11.025

Massague, J., & Obenauf, A. C. (2016). Metastatic colonization by circulating tumour cells. *Nature, 529*(7586), 298-306. doi: 10.1038/nature17038

Matus, D. Q., Lohmer, L. L., Kelley, L. C., Schindler, A. J., Kohrman, A. Q., Barkoulas, M., . . . Sherwood, D. R. (2015). Invasive Cell Fate Requires G1 Cell-Cycle

Arrest and Histone Deacetylase-Mediated Changes in Gene Expression. *Dev Cell, 35*(2), 162-174. doi: 10.1016/j.devcel.2015.10.002

McGranahan, N., & Swanton, C. (2017). Clonal Heterogeneity and Tumor Evolution: Past, Present, and the Future. *Cell, 168*(4), 613-628. doi: 10.1016/j.cell.2017.01.018

Meairs, S. (2015). Facilitation of Drug Transport across the Blood-Brain Barrier with Ultrasound and Microbubbles. *Pharmaceutics, 7*(3), 275-293. doi: 10.3390/pharmaceutics7030275

Miao, L., Wang, Y., Xia, H., Yao, C., Cai, H., & Song, Y. (2013). SPOCK1 is a novel transforming growth factor-beta target gene that regulates lung cancer cell epithelial-mesenchymal transition. *Biochem Biophys Res Commun, 440*(4), 792-797. doi: 10.1016/j.bbrc.2013.10.024

Miller, K., Wang, M., Gralow, J., Dickler, M., Cobleigh, M., Perez, E. A., . . . Davidson, N. E. (2007). Paclitaxel plus bevacizumab versus paclitaxel alone for metastatic breast cancer. *N Engl J Med, 357*(26), 2666-2676. doi: 10.1056/NEJMoa072113

Minami, K., Liu, S., Liu, Y., Chen, A., Wan, Q., Na, S., . . . Yokota, H. (2017). Inhibitory Effects of Dopamine Receptor D1 Agonist on Mammary Tumor and Bone Metastasis. *Sci Rep, 7*, 45686. doi: 10.1038/srep45686

Morley, S., Hager, M. H., Pollan, S. G., Knudsen, B., Di Vizio, D., & Freeman, M. R. (2014). Trading in your spindles for blebs: the amoeboid tumor cell phenotype in prostate cancer. *Asian J Androl, 16*(4), 530-535. doi: 10.4103/1008-682X.122877

Mu, J., Huang, W., Tan, Z., Li, M., Zhang, L., Ding, Q., . . . Xu, H. (2017). Dopamine receptor D2 is correlated with gastric cancer prognosis. *Oncol Lett, 13*(3), 1223-1227. doi: 10.3892/ol.2017.5573

Nan, X., Xie, C., Yu, X., & Liu, J. (2017). EGFR TKI as first-line treatment for patients with advanced EGFR mutation-positive non-small-cell lung cancer. *Oncotarget, 8*(43), 75712-75726. doi: 10.18632/oncotarget.20095

Nathoo, N., Chahlavi, A., Barnett, G. H., & Toms, S. A. (2005). Pathobiology of brain metastases. *J Clin Pathol, 58*(3), 237-242. doi: 10.1136/jcp.2003.013623

Nayak, L., Lee, E. Q., & Wen, P. Y. (2012). Epidemiology of brain metastases. *Curr Oncol Rep, 14*(1), 48-54. doi: 10.1007/s11912-011-0203-y

Neph, S., Stergachis, A. B., Reynolds, A., Sandstrom, R., Borenstein, E., & Stamatoyannopoulos, J. A. (2012). Circuitry and dynamics of human transcription factor regulatory networks. *Cell, 150*(6), 1274-1286. doi: 10.1016/j.cell.2012.04.040

Neuzillet, C., Tijeras-Raballand, A., Cohen, R., Cros, J., Faivre, S., Raymond, E., & de Gramont, A. (2015). Targeting the TGFbeta pathway for cancer therapy. *Pharmacol Ther, 147*, 22-31. doi: 10.1016/j.pharmthera.2014.11.001

Ni, J., Cozzi, P. J., Duan, W., Shigdar, S., Graham, P. H., John, K. H., & Li, Y. (2012). Role of the EpCAM (CD326) in prostate cancer metastasis and progression. *Cancer Metastasis Rev, 31*(3-4), 779-791. doi: 10.1007/s10555-012-9389-1

Nieswandt, B., Hafner, M., Echtenacher, B., & Mannel, D. N. (1999). Lysis of tumor cells by natural killer cells in mice is impeded by platelets. *Cancer Res, 59*(6), 1295-1300.

Nolte, S. M., Venugopal, C., McFarlane, N., Morozova, O., Hallett, R. M., O'Farrell, E., . . . Singh, S. K. (2013). A cancer stem cell model for studying brain metastases from primary lung cancer. *J Natl Cancer Inst, 105*(8), 551-562. doi: 10.1093/jnci/djt022

Nurnberg, A., Kitzing, T., & Grosse, R. (2011). Nucleating actin for invasion. *Nat Rev Cancer, 11*(3), 177-187. doi: 10.1038/nrc3003

Nussbaum, E. S., Djalilian, H. R., Cho, K. H., & Hall, W. A. (1996). Brain metastases. Histology, multiplicity, surgery, and survival. *Cancer, 78*(8), 1781-1788.

O'Brien, C. A., Pollett, A., Gallinger, S., & Dick, J. E. (2007). A human colon cancer cell capable of initiating tumour growth in immunodeficient mice. *Nature, 445*(7123), 106-110. doi: 10.1038/nature05372

Ocana, O. H., Corcoles, R., Fabra, A., Moreno-Bueno, G., Acloque, H., Vega, S., . . . Nieto, M. A. (2012). Metastatic colonization requires the repression of the epithelial-mesenchymal transition inducer Prrx1. *Cancer Cell, 22*(6), 709-724. doi: 10.1016/j.ccr.2012.10.012

Okuda, H., Xing, F., Pandey, P. R., Sharma, S., Watabe, M., Pai, S. K., . . . Watabe, K. (2013). miR-7 suppresses brain metastasis of breast cancer stem-like cells by modulating KLF4. *Cancer Res, 73*(4), 1434-1444. doi: 10.1158/0008-5472.CAN-12-2037

Oldendorf, W. H. (1974). Lipid solubility and drug penetration of the blood brain barrier. *Proc Soc Exp Biol Med, 147*(3), 813-815.

Orvis, T., Hepperla, A., Walter, V., Song, S., Simon, J., Parker, J., . . . Weissman, B. (2014). BRG1/SMARCA4 Inactivation Promotes Non-Small Cell Lung Cancer Aggressiveness by Altering Chromatin Organization. *Cancer Res, 74*(22), 6486-6498. doi: 10.1158/0008-5472.CAN-14-0061

Oskarsson, T., Acharyya, S., Zhang, X. H., Vanharanta, S., Tavazoie, S. F., Morris, P. G., . . . Massague, J. (2011). Breast cancer cells produce tenascin C as a metastatic niche component to colonize the lungs. *Nat Med, 17*(7), 867-874. doi: 10.1038/nm.2379

Paez-Ribes, M., Allen, E., Hudock, J., Takeda, T., Okuyama, H., Vinals, F., . . . Casanovas, O. (2009). Antiangiogenic therapy elicits malignant progression of tumors to increased local invasion and distant metastasis. *Cancer Cell, 15*(3), 220-231. doi: 10.1016/j.ccr.2009.01.027

Page, B. D., Fletcher, S., Yue, P., Li, Z., Zhang, X., Sharmeen, S., . . . Gunning, P. T. (2011). Identification of a non-phosphorylated, cell permeable, small molecule ligand for the Stat3 SH2 domain. *Bioorg Med Chem Lett, 21*(18), 5605-5609. doi: 10.1016/j.bmcl.2011.06.056

Palmer, T. D., Lewis, J., & Zijlstra, A. (2011). Quantitative analysis of cancer metastasis using an avian embryo model. *J Vis Exp*(51). doi: 10.3791/2815

Palmieri, C., Monteverde, M., Lattanzio, L., Gojis, O., Rudraraju, B., Fortunato, M., . . . Crook, T. (2012). Site-specific CpG methylation in the CCAAT/enhancer binding protein delta (CEBPdelta) CpG island in breast cancer is associated with metastatic relapse. *Br J Cancer, 107*(4), 732-738. doi: 10.1038/bjc.2012.308

Palmieri, D. (2012). An Introduction to Brain Metastasis. In D. Palmieri (Ed.), *Central Nervous System Metastasis, the Biological Basis and Clinical Considerations* (Vol. 18, pp. 1-13): Springer Netherlands.

Palumbo, J. S., Talmage, K. E., Massari, J. V., La Jeunesse, C. M., Flick, M. J., Kombrinck, K. W., . . . Degen, J. L. (2007). Tumor cell-associated tissue factor and circulating hemostatic factors cooperate to increase metastatic potential through natural killer cell-dependent and-independent mechanisms. *Blood, 110*(1), 133-141. doi: 10.1182/blood-2007-01-065995

Pang, R., Law, W. L., Chu, A. C., Poon, J. T., Lam, C. S., Chow, A. K., . . . Wong, B. C. (2010). A subpopulation of CD26+ cancer stem cells with metastatic capacity in human colorectal cancer. *Cell Stem Cell, 6*(6), 603-615. doi: 10.1016/j.stem.2010.04.001

Pardridge, W. M. (2005). The blood-brain barrier: bottleneck in brain drug development. *NeuroRx, 2*(1), 3-14. doi: 10.1602/neurorx.2.1.3

Pascual, G., Avgustinova, A., Mejetta, S., Martin, M., Castellanos, A., Attolini, C. S., . . . Benitah, S. A. (2017). Targeting metastasis-initiating cells through the fatty acid receptor CD36. *Nature, 541*(7635), 41-45. doi: 10.1038/nature20791

Pastrello, C., Otasek, D., Fortney, K., Agapito, G., Cannataro, M., Shirdel, E., & Jurisica, I. (2013). Visual data mining of biological networks: one size does not fit all. *PLoS Comput Biol, 9*(1), e1002833. doi: 10.1371/journal.pcbi.1002833

Patchell, R. A. (2003). The management of brain metastases. *Cancer Treat Rev, 29*(6), 533-540.

Patrawala, L., Calhoun, T., Schneider-Broussard, R., Li, H., Bhatia, B., Tang, S., . . . Tang, D. G. (2006). Highly purified CD44+ prostate cancer cells from xenograft human tumors are enriched in tumorigenic and metastatic progenitor cells. *Oncogene, 25*(12), 1696-1708. doi: 10.1038/sj.onc.1209327

Pekmezci, M., & Perry, A. (2013). Neuropathology of brain metastases. *Surg Neurol Int, 4*(Suppl 4), S245-255. doi: 10.4103/2152-7806.111302

Peverelli, E., Giardino, E., Treppiedi, D., Locatelli, M., Vaira, V., Ferrero, S., . . . Mantovani, G. (2016). Dopamine receptor type 2 (DRD2) inhibits migration and invasion of human tumorous pituitary cells through ROCK-mediated cofilin inactivation. *Cancer Lett, 381*(2), 279-286. doi: 10.1016/j.canlet.2016.08.005

Pires, A., Fortuna, A., Alves, G., & Falcao, A. (2009). Intranasal drug delivery: how, why and what for? *J Pharm Pharm Sci, 12*(3), 288-311.

Pornour, M., Ahangari, G., Hejazi, S. H., & Deezagi, A. (2015). New perspective therapy of breast cancer based on selective dopamine receptor D2 agonist and antagonist effects on MCF-7 cell line. *Recent Pat Anticancer Drug Discov, 10*(2), 214-223.

Portales-Casamar, E., Arenillas, D., Lim, J., Swanson, M. I., Jiang, S., McCallum, A., . . . Wasserman, W. W. (2009). The PAZAR database of gene regulatory information coupled to the ORCA toolkit for the study of regulatory sequences. *Nucleic Acids Res, 37*(Database issue), D54-60. doi: 10.1093/nar/gkn783

Psaila, B., Kaplan, R. N., Port, E. R., & Lyden, D. (2006). Priming the 'soil' for breast cancer metastasis: the pre-metastatic niche. *Breast Dis, 26*, 65-74.

Psaila, B., & Lyden, D. (2009). The metastatic niche: adapting the foreign soil. *Nat Rev Cancer, 9*(4), 285-293. doi: 10.1038/nrc2621

Qazi, M. A., Vora, P., Venugopal, C., McFarlane, N., Subapanditha, M. K., Murty, N. K., . . . Singh, S. K. (2016). A novel stem cell culture model of recurrent glioblastoma. *J Neurooncol, 126*(1), 57-67. doi: 10.1007/s11060-015-1951-6

Rahmathulla, G., Toms, S. A., & Weil, R. J. (2012). The molecular biology of brain metastasis. *J Oncol, 2012*, 723541. doi: 10.1155/2012/723541

Ramakrishna, R., & Rostomily, R. (2013). Seed, soil, and beyond: The basic biology of brain metastasis. *Surg Neurol Int, 4*(Suppl 4), S256-264. doi: 10.4103/2152-7806.111303

Ramaswamy, S., Ross, K. N., Lander, E. S., & Golub, T. R. (2003). A molecular signature of metastasis in primary solid tumors. *Nat Genet, 33*(1), 49-54. doi: 10.1038/ng1060

Redzic, Z. (2011). Molecular biology of the blood-brain and the blood-cerebrospinal fluid barriers: similarities and differences. *Fluids Barriers CNS, 8*(1), 3. doi: 10.1186/2045-8118-8-3

Resemann, H. K., Watson, C. J., & Lloyd-Lewis, B. (2014). The Stat3 paradox: a killer and an oncogene. *Mol Cell Endocrinol, 382*(1), 603-611. doi: 10.1016/j.mce.2013.06.029

Reymond, N., d'Agua, B. B., & Ridley, A. J. (2013). Crossing the endothelial barrier during metastasis. *Nat Rev Cancer, 13*(12), 858-870. doi: 10.1038/nrc3628

Ribas, J., Ni, X., Castanares, M., Liu, M. M., Esopi, D., Yegnasubramanian, S., . . . Lupold, S. E. (2012). A novel source for miR-21 expression through the alternative polyadenylation of VMP1 gene transcripts. *Nucleic Acids Res, 40*(14), 6821-6833. doi: 10.1093/nar/gks308

Ritchie, M. E., Phipson, B., Wu, D., Hu, Y., Law, C. W., Shi, W., & Smyth, G. K. (2015). limma powers differential expression analyses for RNA-sequencing and microarray studies. *Nucleic Acids Res, 43*(7), e47. doi: 10.1093/nar/gkv007

Rodriguez-Hernandez, I., Cantelli, G., Bruce, F., & Sanz-Moreno, V. (2016). Rho, ROCK and actomyosin contractility in metastasis as drug targets. *F1000Res, 5*. doi: 10.12688/f1000research.7909.1

Rosok, O., Pedeutour, F., Ree, A. H., & Aasheim, H. C. (1999). Identification and characterization of TESK2, a novel member of the LIMK/TESK family of protein kinases, predominantly expressed in testis. *Genomics, 61*(1), 44-54. doi: 10.1006/geno.1999.5922

Roy, S., Lu, K., Nayak, M. K., Bhuniya, A., Ghosh, T., Kundu, S., . . . Basu, S. (2017). Activation of D2 Dopamine Receptors in CD133+ve Cancer Stem Cells in Non-small Cell Lung Carcinoma Inhibits Proliferation, Clonogenic Ability, and Invasiveness of These Cells. *J Biol Chem, 292*(2), 435-445. doi: 10.1074/jbc.M116.748970

Rozovski, U., Calin, G. A., Setoyama, T., D'Abundo, L., Harris, D. M., Li, P., . . . Estrov, Z. (2013). Signal transducer and activator of transcription (STAT)-3 regulates microRNA gene expression in chronic lymphocytic leukemia cells. *Mol Cancer, 12*, 50. doi: 10.1186/1476-4598-12-50

Sahai, E. (2007). Illuminating the metastatic process. *Nat Rev Cancer, 7*(10), 737-749. doi: 10.1038/nrc2229

Saini, U., Naidu, S., ElNaggar, A. C., Bid, H. K., Wallbillich, J. J., Bixel, K., . . . Selvendiran, K. (2017). Elevated STAT3 expression in ovarian cancer ascites promotes invasion and metastasis: a potential therapeutic target. *Oncogene, 36*(2), 168-181. doi: 10.1038/onc.2016.197

Sakamoto, S., Inoue, H., Ohba, S., Kohda, Y., Usami, I., Masuda, T., . . . Nomoto, A. (2015). New metastatic model of human small-cell lung cancer by orthotopic transplantation in mice. *Cancer Sci, 106*(4), 367-374. doi: 10.1111/cas.12624

Sanborn, J. Z., Chung, J., Purdom, E., Wang, N. J., Kakavand, H., Wilmott, J. S., . . . Cho, R. J. (2015). Phylogenetic analyses of melanoma reveal complex patterns of metastatic dissemination. *Proc Natl Acad Sci U S A, 112*(35), 10995-11000. doi: 10.1073/pnas.1508074112

Sanden, E., Dyberg, C., Krona, C., Gallo-Oller, G., Olsen, T. K., Enriquez Perez, J., . . . Darabi, A. (2017). Establishment and characterization of an orthotopic patient-derived Group 3 medulloblastoma model for preclinical drug evaluation. *Sci Rep, 7*, 46366. doi: 10.1038/srep46366

Sandler, A., Gray, R., Perry, M. C., Brahmer, J., Schiller, J. H., Dowlati, A., . . . Johnson, D. H. (2006). Paclitaxel-carboplatin alone or with bevacizumab for non-small-cell lung cancer. *N Engl J Med, 355*(24), 2542-2550. doi: 10.1056/NEJMoa061884

Sasaki, K., Kurahara, H., Young, E. D., Natsugoe, S., Ijichi, A., Iwakuma, T., & Welch, D. R. (2017). Genome-wide in vivo RNAi screen identifies ITIH5 as a metastasis suppressor in pancreatic cancer. *Clin Exp Metastasis, 34*(3-4), 229-239. doi: 10.1007/s10585-017-9840-3

Sasser, A. K., Mundy, B. L., Smith, K. M., Studebaker, A. W., Axel, A. E., Haidet, A. M., . . . Hall, B. M. (2007). Human bone marrow stromal cells enhance breast cancer cell growth rates in a cell line-dependent manner when evaluated in 3D tumor environments. *Cancer Lett, 254*(2), 255-264. doi: 10.1016/j.canlet.2007.03.012

Schabet, M., & Herrlinger, U. (1998). Animal models of leptomeningeal metastasis. *J Neurooncol, 38*(2-3), 199-205.

Schonherr, M., Bhattacharya, A., Kottek, T., Szymczak, S., Koberle, M., Wickenhauser, C., . . . Kunz, M. (2014). Genomewide RNAi screen identifies protein kinase Cb and new members of mitogen-activated protein kinase pathway as regulators of melanoma cell growth and metastasis. *Pigment Cell Melanoma Res, 27*(3), 418-430. doi: 10.1111/pcmr.12216

Schouten, L. J., Rutten, J., Huveneers, H. A., & Twijnstra, A. (2002). Incidence of brain metastases in a cohort of patients with carcinoma of the breast, colon, kidney, and lung and melanoma. *Cancer, 94*(10), 2698-2705.

Schramedei, K., Morbt, N., Pfeifer, G., Lauter, J., Rosolowski, M., Tomm, J. M., . . . Brocke-Heidrich, K. (2011). MicroRNA-21 targets tumor suppressor genes ANP32A and SMARCA4. *Oncogene, 30*(26), 2975-2985. doi: 10.1038/onc.2011.15

Schriml, L. M., Arze, C., Nadendla, S., Chang, Y. W., Mazaitis, M., Felix, V., . . . Kibbe, W. A. (2012). Disease Ontology: a backbone for disease semantic integration. *Nucleic Acids Res, 40*(Database issue), D940-946. doi: 10.1093/nar/gkr972

Semenkow, S., Li, S., Kahlert, U. D., Raabe, E. H., Xu, J., Arnold, A., . . . Walczak, P. (2017). An immunocompetent mouse model of human glioblastoma. *Oncotarget, 8*(37), 61072-61082. doi: 10.18632/oncotarget.17851

Sgroi, D. C. (2010). Preinvasive breast cancer. *Annu Rev Pathol, 5*, 193-221. doi: 10.1146/annurev.pathol.4.110807.092306

Sherry, M. M., Reeves, A., Wu, J. K., & Cochran, B. H. (2009). STAT3 is required for proliferation and maintenance of multipotency in glioblastoma stem cells. *Stem Cells, 27*(10), 2383-2392. doi: 10.1002/stem.185

Shirdel, E. A., Xie, W., Mak, T. W., & Jurisica, I. (2011). NAViGaTing the micronome--using multiple microRNA prediction databases to identify signalling pathway-associated microRNAs. *PLoS One, 6*(2), e17429. doi: 10.1371/journal.pone.0017429

Shlush, L. I., Zandi, S., Mitchell, A., Chen, W. C., Brandwein, J. M., Gupta, V., . . . Dick, J. E. (2014). Identification of pre-leukaemic haematopoietic stem cells in acute leukaemia. *Nature, 506*(7488), 328-333. doi: 10.1038/nature13038

Shu, Q., Wong, K. K., Su, J. M., Adesina, A. M., Yu, L. T., Tsang, Y. T., . . . Li, X. N. (2008). Direct orthotopic transplantation of fresh surgical specimen preserves CD133+ tumor cells in clinically relevant mouse models of medulloblastoma and glioma. *Stem Cells, 26*(6), 1414-1424. doi: 10.1634/stemcells.2007-1009

Shu, Y. J., Weng, H., Ye, Y. Y., Hu, Y. P., Bao, R. F., Cao, Y., . . . Liu, Y. B. (2015). SPOCK1 as a potential cancer prognostic marker promotes the proliferation and metastasis of gallbladder cancer cells by activating the PI3K/AKT pathway. *Mol Cancer, 14*(1), 12. doi: 10.1186/s12943-014-0276-y

Shultz, L. D., Ishikawa, F., & Greiner, D. L. (2007). Humanized mice in translational biomedical research. *Nat Rev Immunol, 7*(2), 118-130. doi: 10.1038/nri2017

Sieh, S., Lubik, A. A., Clements, J. A., Nelson, C. C., & Hutmacher, D. W. (2010). Interactions between human osteoblasts and prostate cancer cells in a novel 3D in vitro model. *Organogenesis, 6*(3), 181-188.

Singh, M., Manoranjan, B., Mahendram, S., McFarlane, N., Venugopal, C., & Singh, S. K. (2014). Brain metastasis-initiating cells: survival of the fittest. *Int J Mol Sci, 15*(5), 9117-9133. doi: 10.3390/ijms15059117

Singh, M., Venugopal, C., Tokar, T., Brown, K. R., McFarlane, N., Bakhshinyan, D., . . . Singh, S. K. (2017). RNAi screen identifies essential regulators of human brain metastasis-initiating cells. *Acta Neuropathol*. doi: 10.1007/s00401-017-1757-z

Singh, M., Yelle, N., Venugopal, C., & Singh, S. K. (2018). EMT: Mechanisms and therapeutic implications. *Pharmacol Ther, 182*, 80-94. doi: 10.1016/j.pharmthera.2017.08.009

Singh, S. K., Clarke, I. D., Terasaki, M., Bonn, V. E., Hawkins, C., Squire, J., & Dirks, P. B. (2003). Identification of a cancer stem cell in human brain tumors. *Cancer Res, 63*(18), 5821-5828.

Singh, S. K., Hawkins, C., Clarke, I. D., Squire, J. A., Bayani, J., Hide, T., . . . Dirks, P. B. (2004). Identification of human brain tumour initiating cells. *Nature, 432*(7015), 396-401. doi: 10.1038/nature03128

Sjobakk, T. E., Vettukattil, R., Gulati, M., Gulati, S., Lundgren, S., Gribbestad, I. S., . . . Bathen, T. F. (2013). Metabolic profiles of brain metastases. *Int J Mol Sci, 14*(1), 2104-2118. doi: 10.3390/ijms14012104

Sleeman, J., & Steeg, P. S. (2010). Cancer metastasis as a therapeutic target. *Eur J Cancer, 46*(7), 1177-1180. doi: 10.1016/j.ejca.2010.02.039

Smirnov, P., Safikhani, Z., El-Hachem, N., Wang, D., She, A., Olsen, C., . . . Haibe-Kains, B. (2016). PharmacoGx: an R package for analysis of large pharmacogenomic datasets. *Bioinformatics, 32*(8), 1244-1246. doi: 10.1093/bioinformatics/btv723

Soffietti, R., Ruda, R., & Mutani, R. (2002). Management of brain metastases. *J Neurol, 249*(10), 1357-1369. doi: 10.1007/s00415-002-0870-6

Song, H. T., Jordan, E. K., Lewis, B. K., Liu, W., Ganjei, J., Klaunberg, B., . . . Frank, J. A. (2009). Rat model of metastatic breast cancer monitored by MRI at 3 tesla and bioluminescence imaging with histological correlation. *J Transl Med, 7*, 88. doi: 10.1186/1479-5876-7-88

Sorensen, S. A., Fenger, K., & Olsen, J. H. (1999). Significantly lower incidence of cancer among patients with Huntington disease: An apoptotic effect of an expanded polyglutamine tract? *Cancer, 86*(7), 1342-1346.

Steeg, P. S. (2006). Tumor metastasis: mechanistic insights and clinical challenges. *Nat Med, 12*(8), 895-904. doi: 10.1038/nm1469

Steeg, P. S. (2016). Targeting metastasis. *Nat Rev Cancer, 16*(4), 201-218. doi: 10.1038/nrc.2016.25

Steeg, P. S., Anderson, R. L., Bar-Eli, M., Chambers, A. F., Eccles, S. A., Hunter, K., . . . Welch, D. R. (2009). An open letter to the FDA and other regulatory agencies: Preclinical drug development must consider the impact on metastasis. *Clin Cancer Res, 15*, 4529. doi: 10.1158/1078-0432.CCR-09-1363

Stelzer, K. J. (2013). Epidemiology and prognosis of brain metastases. *Surg Neurol Int, 4*(Suppl 4), S192-202. doi: 10.4103/2152-7806.111296

Stocchi, F., Torti, M., & Fossati, C. (2016). Advances in dopamine receptor agonists for the treatment of Parkinson's disease. *Expert Opin Pharmacother, 17*(14), 1889-1902. doi: 10.1080/14656566.2016.1219337

Su, B., Gao, L., Baranowski, C., Gillard, B., Wang, J., Ransom, R., . . . Gelman, I. H. (2014). A genome-wide RNAi screen identifies FOXO4 as a metastasis-suppressor through counteracting PI3K/AKT signal pathway in prostate cancer. *PLoS One, 9*(7), e101411. doi: 10.1371/journal.pone.0101411

Subramanian, A., Tamayo, P., Mootha, V. K., Mukherjee, S., Ebert, B. L., Gillette, M. A., . . . Mesirov, J. P. (2005). Gene set enrichment analysis: a knowledge-based approach for interpreting genome-wide expression profiles. *Proc Natl Acad Sci U S A, 102*(43), 15545-15550. doi: 10.1073/pnas.0506580102

Sugarbaker, E. V. (1979). Cancer metastasis: a product of tumor-host interactions. *Curr Probl Cancer, 3*(7), 1-59.

Suit, H. D. (1992). Local control and patient survival. *Int J Radiat Oncol Biol Phys, 23*(3), 653-660.

Sumida, T., Kitadai, Y., Shinagawa, K., Tanaka, M., Kodama, M., Ohnishi, M., . . . Chayama, K. (2011). Anti-stromal therapy with imatinib inhibits growth and metastasis of gastric carcinoma in an orthotopic nude mouse model. *Int J Cancer, 128*(9), 2050-2062. doi: 10.1002/ijc.25812

Swanton, C. (2012). Intratumor heterogeneity: evolution through space and time. *Cancer Res, 72*(19), 4875-4882. doi: 10.1158/0008-5472.CAN-12-2217

Talmadge, J. E., Singh, R. K., Fidler, I. J., & Raz, A. (2007). Murine models to evaluate novel and conventional therapeutic strategies for cancer. *Am J Pathol, 170*(3), 793-804. doi: 10.2353/ajpath.2007.060929

Thiery, J. P., Acloque, H., Huang, R. Y., & Nieto, M. A. (2009). Epithelial-mesenchymal transitions in development and disease. *Cell, 139*(5), 871-890. doi: 10.1016/j.cell.2009.11.007

Tirino, V., Camerlingo, R., Franco, R., Malanga, D., La Rocca, A., Viglietto, G., . . . Pirozzi, G. (2009). The role of CD133 in the identification and characterisation of tumour-initiating cells in non-small-cell lung cancer. *Eur J Cardiothorac Surg, 36*(3), 446-453. doi: 10.1016/j.ejcts.2009.03.063

Tomoda, R., Seto, M., Hioki, Y., Sonoda, J., Matsumine, A., Kusuzaki, K., & Uchida, A. (2005). Low-dose methotrexate inhibits lung metastasis and lengthens survival in rat osteosarcoma. *Clin Exp Metastasis, 22*(7), 559-564. doi: 10.1007/s10585-005-5377-y

Tsai, J. H., Donaher, J. L., Murphy, D. A., Chau, S., & Yang, J. (2012). Spatiotemporal regulation of epithelial-mesenchymal transition is essential for squamous cell carcinoma metastasis. *Cancer Cell, 22*(6), 725-736. doi: 10.1016/j.ccr.2012.09.022

Valastyan, S., & Weinberg, R. A. (2011). Tumor metastasis: molecular insights and evolving paradigms. *Cell, 147*(2), 275-292. doi: 10.1016/j.cell.2011.09.024

Valiente, M., Obenauf, A. C., Jin, X., Chen, Q., Zhang, X. H., Lee, D. J., . . . Massague, J. (2014). Serpins promote cancer cell survival and vascular co-option in brain metastasis. *Cell, 156*(5), 1002-1016. doi: 10.1016/j.cell.2014.01.040

van den Hoogen, C., van der Horst, G., Cheung, H., Buijs, J. T., Lippitt, J. M., Guzman-Ramirez, N., . . . van der Pluijm, G. (2010). High aldehyde dehydrogenase activity identifies tumor-initiating and metastasis-initiating cells in human prostate cancer. *Cancer Res, 70*(12), 5163-5173. doi: 10.1158/0008-5472.CAN-09-3806

van der Gun, B. T., Melchers, L. J., Ruiters, M. H., de Leij, L. F., McLaughlin, P. M., & Rots, M. G. (2010). EpCAM in carcinogenesis: the good, the bad or the ugly. *Carcinogenesis, 31*(11), 1913-1921. doi: 10.1093/carcin/bgq187

Vanharanta, S., & Massague, J. (2013). Origins of metastatic traits. *Cancer Cell, 24*(4), 410-421. doi: 10.1016/j.ccr.2013.09.007

Venugopal, C., Hallett, R., Vora, P., Manoranjan, B., Mahendram, S., Qazi, M. A., . . . Singh, S. K. (2015). Pyrvinium Targets CD133 in Human Glioblastoma Brain Tumor-Initiating Cells. *Clin Cancer Res, 21*(23), 5324-5337. doi: 10.1158/1078-0432.CCR-14-3147

Venugopal, C., McFarlane, N. M., Nolte, S., Manoranjan, B., & Singh, S. K. (2012). Processing of primary brain tumor tissue for stem cell assays and flow sorting. *J Vis Exp*(67). doi: 10.3791/4111

Voulgari, A., & Pintzas, A. (2009). Epithelial-mesenchymal transition in cancer metastasis: mechanisms, markers and strategies to overcome drug resistance in the clinic. *Biochim Biophys Acta, 1796*(2), 75-90. doi: 10.1016/j.bbcan.2009.03.002

Wakimoto, H., Mohapatra, G., Kanai, R., Curry, W. T., Jr., Yip, S., Nitta, M., . . . Rabkin, S. D. (2012). Maintenance of primary tumor phenotype and genotype in glioblastoma stem cells. *Neuro Oncol, 14*(2), 132-144. doi: 10.1093/neuonc/nor195

Wang, S., Mou, Z., Ma, Y., Li, J., Li, J., Ji, X., . . . Zhou, T. (2015). Dopamine enhances the response of sunitinib in the treatment of drug-resistant breast cancer: Involvement of eradicating cancer stem-like cells. *Biochem Pharmacol, 95*(2), 98-109. doi: 10.1016/j.bcp.2015.03.013

Webster, W. S., & Leibovich, B. C. (2005). Exisulind in the treatment of prostate cancer. *Expert Rev Anticancer Ther, 5*(6), 957-962. doi: 10.1586/14737140.5.6.957

Weiss, L. (1992). Comments on hematogenous metastatic patterns in humans as revealed by autopsy. *Clin Exp Metastasis, 10*(3), 191-199.

Weiss, L. (2000). Metastasis of cancer: a conceptual history from antiquity to the 1990s. *Cancer Metastasis Rev, 19*(3-4), I-XI, 193-383.

Went, P. T. H., Lugli, A., Meier, S., Bundi, M., Mirlacher, M., Sauter, G., & Dirnhofer, S. (2004). Frequent EpCam protein expression in human carcinomas. *Human Pathology, 35*(1), 122-128. doi: http://dx.doi.org/10.1016/j.humpath.2003.08.026

Wilhelm, I., Fazakas, C., Molnar, J., Hasko, J., Vegh, A. G., Cervenak, L., . . . Krizbai, I. A. (2014). Role of Rho/ROCK signaling in the interaction of melanoma cells with the blood-brain barrier. *Pigment Cell Melanoma Res, 27*(1), 113-123. doi: 10.1111/pcmr.12169

Wilson, S. M., & Chambers, A. F. (2004). Experimental metastasis assays in the chick embryo. *Curr Protoc Cell Biol, Chapter 19*, Unit 19 16. doi: 10.1002/0471143030.cb1906s21

Wishart, D. S., Feunang, Y. D., Guo, A. C., Lo, E. J., Marcu, A., Grant, J. R., . . . Wilson, M. (2018). DrugBank 5.0: a major update to the DrugBank database for 2018. *Nucleic Acids Res, 46*(D1), D1074-D1082. doi: 10.1093/nar/gkx1037

Wistuba, II, Mao, L., & Gazdar, A. F. (2002). Smoking molecular damage in bronchial epithelium. *Oncogene, 21*(48), 7298-7306. doi: 10.1038/sj.onc.1205806

Wolf, K., Mazo, I., Leung, H., Engelke, K., von Andrian, U. H., Deryugina, E. I., . . . Friedl, P. (2003). Compensation mechanism in tumor cell migration: mesenchymal-amoeboid transition after blocking of pericellular proteolysis. *J Cell Biol, 160*(2), 267-277. doi: 10.1083/jcb.200209006

Wu, K., Fukuda, K., Xing, F., Zhang, Y., Sharma, S., Liu, Y., . . . Watabe, K. (2015). Roles of the cyclooxygenase 2 matrix metalloproteinase 1 pathway in brain metastasis of breast cancer. *J Biol Chem, 290*(15), 9842-9854. doi: 10.1074/jbc.M114.602185

Wu, Z., & Irizarry, R. A. (2004). Preprocessing of oligonucleotide array data. *Nat Biotechnol, 22*(6), 656-658; author reply 658. doi: 10.1038/nbt0604-656b

Xie, T. X., Huang, F. J., Aldape, K. D., Kang, S. H., Liu, M., Gershenwald, J. E., . . . Huang, S. (2006). Activation of stat3 in human melanoma promotes brain metastasis. *Cancer Res, 66*(6), 3188-3196. doi: 10.1158/0008-5472.CAN-05-2674

Yachida, S., Jones, S., Bozic, I., Antal, T., Leary, R., Fu, B., . . . Iacobuzio-Donahue, C. A. (2010). Distant metastasis occurs late during the genetic evolution of pancreatic cancer. *Nature, 467*(7319), 1114-1117. doi: 10.1038/nature09515

Yan, L. X., Huang, X. F., Shao, Q., Huang, M. Y., Deng, L., Wu, Q. L., . . . Shao, J. Y. (2008). MicroRNA miR-21 overexpression in human breast cancer is associated with advanced clinical stage, lymph node metastasis and patient poor prognosis. *RNA, 14*(11), 2348-2360. doi: 10.1261/rna.1034808

Yang, C. H., Yue, J., Pfeffer, S. R., Handorf, C. R., & Pfeffer, L. M. (2011). MicroRNA miR-21 regulates the metastatic behavior of B16 melanoma cells. *J Biol Chem, 286*(45), 39172-39178. doi: 10.1074/jbc.M111.285098

Ye, T. H., Yang, F. F., Zhu, Y. X., Li, Y. L., Lei, Q., Song, X. J., . . . Wei, Y. Q. (2017). Inhibition of Stat3 signaling pathway by nifuroxazide improves antitumor immunity and impairs colorectal carcinoma metastasis. *Cell Death Dis, 8*(1), e2534. doi: 10.1038/cddis.2016.452

Yilmaz, M., Christofori, G., & Lehembre, F. (2007). Distinct mechanisms of tumor invasion and metastasis. *Trends Mol Med, 13*(12), 535-541. doi: 10.1016/j.molmed.2007.10.004

Yu, F., Li, G., Gao, J., Sun, Y., Liu, P., Gao, H., . . . Mu, Q. (2016). SPOCK1 is upregulated in recurrent glioblastoma and contributes to metastasis and Temozolomide resistance. *Cell Prolif*. doi: 10.1111/cpr.12241

Yu, G., Wang, L. G., Han, Y., & He, Q. Y. (2012). clusterProfiler: an R package for comparing biological themes among gene clusters. *OMICS, 16*(5), 284-287. doi: 10.1089/omi.2011.0118

Yu, H., Kortylewski, M., & Pardoll, D. (2007). Crosstalk between cancer and immune cells: role of STAT3 in the tumour microenvironment. *Nat Rev Immunol, 7*(1), 41-51. doi: 10.1038/nri1995

Yu, L., Baxter, P. A., Voicu, H., Gurusiddappa, S., Zhao, Y., Adesina, A., . . . Li, X. N. (2010). A clinically relevant orthotopic xenograft model of ependymoma that maintains the genomic signature of the primary tumor and preserves cancer stem cells in vivo. *Neuro Oncol, 12*(6), 580-594. doi: 10.1093/neuonc/nop056

Zhang, K., & Waxman, D. J. (2010). PC3 prostate tumor-initiating cells with molecular profile FAM65Bhigh/MFI2low/LEF1low increase tumor angiogenesis. *Mol Cancer, 9*, 319. doi: 10.1186/1476-4598-9-319

Zhang, X., Ye, Y. L., Zhu, H., Sun, S. N., Zheng, J., Fan, H. H., . . . Zhu, J. H. (2016). Selenotranscriptomic Analyses Identify Signature Selenoproteins in Brain Regions in a Mouse Model of Parkinson's Disease. *PLoS One, 11*(9), e0163372. doi: 10.1371/journal.pone.0163372

Zhang, Z., Hatori, T., & Nonaka, H. (2008). An experimental model of brain metastasis of lung carcinoma. *Neuropathology, 28*(1), 24-28. doi: 10.1111/j.1440-1789.2007.00826.x

Zhao, X., Liu, Z., Yu, L., Zhang, Y., Baxter, P., Voicu, H., . . . Li, X. N. (2012). Global gene expression profiling confirms the molecular fidelity of primary tumor-based orthotopic xenograft mouse models of medulloblastoma. *Neuro Oncol, 14*(5), 574-583. doi: 10.1093/neuonc/nos061

Zheng, G., Tu, K., Yang, Q., Xiong, Y., Wei, C., Xie, L., . . . Li, Y. (2008). ITFP: an integrated platform of mammalian transcription factors. *Bioinformatics, 24*(20), 2416-2417. doi: 10.1093/bioinformatics/btn439

Zheng, X., Carstens, J. L., Kim, J., Scheible, M., Kaye, J., Sugimoto, H., . . . Kalluri, R. (2015). Epithelial-to-mesenchymal transition is dispensable for metastasis but induces chemoresistance in pancreatic cancer. *Nature, 527*(7579), 525-530. doi: 10.1038/nature16064

Zhu, S., Wu, H., Wu, F., Nie, D., Sheng, S., & Mo, Y. Y. (2008). MicroRNA-21 targets tumor suppressor genes in invasion and metastasis. *Cell Res, 18*(3), 350-359. doi: 10.1038/cr.2008.24

Zohrabian, V. M., Nandu, H., Gulati, N., Khitrov, G., Zhao, C., Mohan, A., . . . Jhanwar-Uniyal, M. (2007). Gene expression profiling of metastatic brain cancer. *Oncol Rep, 18*(2), 321-328.

Appendix I: Copyright Statements

Chapters 1 and 5 License Agreements

*Chapters 1 and 5 contain exceprts from the following review papers:

- **Singh M**, *et al*. *Brain metastasis-initiating cells: survival of the fittest.* Int J Mol Sci. 2014;15(5):9117-33. doi: 10.3390/ijms15059117. © <2014>. This manuscript version is made available under the CC-BY 3.0 license https://creativecommons.org/licenses/by/3.0/

  This material was published under the following Attribution 3.0 unported license which allows for the free use of this material under the following conditions: http://creativecommons.org/licenses/by/3.0/legalcode Creative Commons Attributions 3.0 Unported License.
  The work is provided under the terms of this creative commons public license)"CCPL" or "License"). The work is protected by copyright and/or other applicable law. Any use of the work other than was authorized under this license or copyright laws is prohibited. By exercising any rights to the work provided here, You accept and agree to be bound by the terms of this license. To the extent this license may be considered to be a contract, the licensor grants you the rights contained here in consideration of your acceptance of such terms and conditions.

- **Singh M**, Bakhshinyan D, Venugopal C, Singh SK. *Mechanisms and Therapy for Cancer Metastasis to the Central Nervous System*. Front Oncol. 2017;19(7)220. doi: 10.3389/fonc.2017.00220.

  This material was published under the following Attribution 4.0 International license which allows for the free use of this material under the following conditions: http://creativecommons.org/licenses/by/4.0/legalcode Creative Commons Attributions 4.0 International Public License.
  By exercising the Licensed Rights, You accept and agree to be bound by the terms and conditions of this Creative Commons Attribution 4.0 International Public License ("Public License"). To the extent this Public License may be interpreted as a contract, You are granted the Licensed Rights in consideration of Your acceptance of these terms and conditions, and the Licensor grants You such rights in consideration of benefits the Licensor receives from making the Licensed Material available under these terms and conditions.

- **Singh M**, Yelle N, Venugopal C, Singh SK. *EMT: mechanisms and therapeutic implications*. (2017) Pharmacol Ther. 2017 Aug 20. pii: S0163-7258(17)30219-X. doi: 10.1016/j.pharmthera.2017.08.009.

  This material was published under the following Attribution-Non-Commercial-No-

Chapter 2 License Agreement

Singh M, *et al. STAT3 pathway regulates lung-derived brain metastasis initiating cell capacity through miR-21 activation.* Oncotarget 2015; 6(29):27461-77

Editorial Office <editorialoffice@oncotarget.com>

Sat 2017-12-16, 11:06 PM

Dear Dr. Singh,

You may use the paper as needed, as long as Oncotarget is cited as the source, in accordance with the license I use for all our
papers: http://creativecommons.org/licenses/by/3.0/

Sun 2017-12-10, 1:58 PM

s.naveen@diacritech.com

Dear Mr. Shanmugam,

I am completing a Ph.D thesis at McMaster University . I would like your permission to reprint in full the following journal article in my thesis:

STAT3 pathway regulates lung-derived brain metastasis initiating cell capacity through miR-21 activation. Oncotarget. 2015; 6:27461-27477. https://doi.org/10.18632/oncotarget.4742

Please note that I, Mohini Singh, am the primary author of this work, performed under the supervision of Dr. Sheila Singh.

I am also requesting that you grant irrevocable, nonexclusive license to McMaster University [and to the National Library of Canada] to reproduce this material as a part of the thesis. Proper acknowledgement of your copyright of the reprinted material will be given in the thesis. Thank you very much.

Sincerely,

Mohini Singh

Chapter 3 License Agreement

Singh M, *et al*. *RNAi screen identifies essential regulators of human brain metastasis initiating cells*. (2017) Acta Neuropathologica (epub ahead of print http://link.springer.com/article/10.1007/s00401-017-1757-z)

This Agreement between McMaster University -- Mohini Singh ("You") and Springer Nature ("Springer Nature") consists of your license details and the terms and conditions provided by Springer Nature and Copyright Clearance Center.

License Number	4279040703056
License date	Jan 30, 2018
Licensed Content Publisher	Springer Nature
Licensed Content Publication	Acta Neuropathologica

Licensed Content Title	RNAi screen identifies essential regulators of human brain metastasis-initiating cells
Licensed Content Author	Mohini Singh, Chitra Venugopal, Tomas Tokar et al
Licensed Content Date	Jan 1, 2017
Licensed Content Volume	134
Licensed Content Issue	6
Type of Use	Thesis/Dissertation
Requestor type	academic/university or research institute
Format	print and electronic
Portion	full article/chapter
Will you be translating?	no
Circulation/distribution	<501
Author of this Springer Nature content	yes
Title	RNAi screen identifies essential regulators of human brain metastasis initiating cells
Instructor name	Sheila Singh
Institution name	McMaster University
Expected presentation date	Mar 2018
Portions	entire article
Requestor Location	McMaster University 1280 Main Street West

Terms and Conditions

Springer Nature Terms and Conditions for RightsLink Permissions

Springer Customer Service Centre GmbH (the Licensor) hereby grants you a non-exclusive, world-wide licence to reproduce the material and for the purpose and requirements specified in the attached copy of your order form, and for no other use, subject to the conditions below:

Where **'reuse in a dissertation/thesis'** has been selected the following terms apply: Print rights for up to 100 copies, electronic rights for use only on a personal website or institutional repository as defined by the Sherpa guideline (www.sherpa.ac.uk/romeo/).

Appendix II: Accomplishments

Work conducted not featured in this thesis

- I've been responsible for training several incoming members of the lab for intracranial injections.
- Brain Metastasis: I've begun testing specificity of Epcam IgGs, a precursor to BiTES, for the targeting of brain metastasis. It is anticipated that more pre-metastatic targets will be identified and developed into BiTES. I've also screened and optimizezd several variations of migration and invasion assays. I've screened several libraries of therapeutic compounds to identify potential hits against brain metastases (STAT3, mTOR, natural products). I've established several patient-derived cell lines of brain metastasis from different primary sites (lung, melanoma, breast, small cell lung cancers).
- Glioblastoma: I've conducted the significant *in vivo* work concerning BTIC engraftments, preclinical testing for CD133 BiTES and Car-Ts. I've aided other members with their *in vivo* surgeries, and occasional collection of samples. I've aided in preliminary optimization of humanized mouse models to test immunotherapies.
- Medulloblastoma: I've performed and assisted with *in vivo* surgeries, sample collection, BMI inhibitor testing.

Publications arising from this work:

- **Singh M**, *et al*. *Characterization of Initiating Cells Human Brain Metastasis of Different Origins*. (in prep).
- **Singh M**, *et al*. *Therapeutic targeting of the pre-metastatic stage in human brain metastasis.* (submitted to Nature Communications).
- **Singh M**, *et al*. *RNAi screen identifies essential regulators of human brain metastasis initiating cells*. Acta Neuropathol. 2017 Dec;134(6):923-940. doi: 10.1007/s00401-017-1757-z.
- **Singh M**, Bakhshinyan D, Venugopal C, Singh SK. *Mechanisms and Therapy for Cancer Metastasis to the Central Nervous System*. Front Oncol. 2017;19(7)220. doi: 10.3389/fonc.2017.00220
- **Singh M**, Yelle N, Venugopal C, Singh SK. *EMT: mechanisms and therapeutic implications*. Pharmacol Ther. 2018 Feb;182:80-94. doi: 10.1016/j.pharmthera.2017.08.009.
- **Singh M**, *et al. STAT3 pathway regulates lung-derived brain metastasis initiating cell capacity through miR-21 activation.* Oncotarget 2015; 6(29):27461-77.
- **Singh M**, *et al*. *Brain metastasis-initiating cells: survival of the fittest.* Int J Mol Sci. 2014;15(5):9117-33.

Publications not included in this work:

*The following publications and book chapters included work performed by me during my PhD, however are not presented in this thesis:

- Sheila Singh, David Bakhshinyan, Chitra Venugopal, Ashley Adile, Neha Garg, Branavan Manoranjan, Robin Hallet, Xin Wang, Sujeivan Mahendram, Parvez Vora,

Thusyanth Vijayakumar, Minomi Subapanditha, **Mohini Singh**, Michelle Kameda-Smith, Maleeha Qazi, Nicole McFarlane, Aneet Mann, Olufemi Ajani, Blake Yarascavitch, Vijay Ramaswamy, Hamza Farooq, Sorana Morrissy, Liangxian Cao, Nadiya Sydorenko, Ramil Baiazitov, Wu Du, Josephine Sheedy, Marla Weetall, Young-Choon Moon, Chang-Sun Lee, Jacek Kwiecien, Kathleen Delaney, Bradley Doble, Yoon-Jae Cho, Siddhartha Mitra, David Kaplan, Michael Taylor, and Thomas Davis. *Bmi1 is a therapeutic target in recurrent medulloblastoma.* (Under review at Clin Canc Res).

- Maleeha Qazi, Parvez Vora, Chitra Venugopal, Jarrett Adams, **Mohini Singh**, Amy Hu, Maryna Gorelik, Jiahe Yang, Minomi Subapanditha, Neil Savage, Chirayu Chokshi, Max London, Alexander Gont, David Bobrowski, Natalie Grinshtein, Kevin Brown, Naresh Murty, Johan Nilvebrant, David Kaplan, Jason Moffat, Sachdev Sidhu, and Sheila Singh. *Identification and co-targeting of EphA2+/EphA3+ cancer stem cells in recurrent glioblastoma.* (Submitted to Clin Canc Res).
- Bakhshinyan D, Adile AA, Qazi MA, **Singh M**, Kameda-Smith MM, Yelle N, Chokshi C, Venugopal C, Singh SK. *Introduction to Cancer Stem Cells: Past, Present, and Future*. Methods Mol Biol. 2018;1692:1-16. doi: 10.1007/978-1-4939-7401-6_1.
- **Singh M**, Savage N, Venugopal C, Singh SK. In vivo murine models of brain metastasis. Brain tumor stem cells: methods and protocols. 2017
- Venugopal C, Hallett R, Vora P, Manoranjan B, Mahendram S, Qazi MA, McFarlane N, Subapanditha M, Nolte SM, **Singh M**, Bakhshinyan D, Garg N, Vijayakumar T, Lach B, Provias JP, Reddy K, Murty NK, Doble BW, Bhatia M, Hassell JA, Singh SK. *Pyrvinium Targets CD133 in Human Glioblastoma Brain Tumor-Initiating Cells.* Clin Cancer Res. 2015 Dec 1;21(23):5324-37. doi: 10.1158/1078-0432.CCR-14-3147. Epub 2015 Jul 7.

Poster and Oral Presentations:

- **M Singh** *et al*. *Characterization and targeting of a temporal micro-metastatic signature in human brain metastases.* (2018) Poster presented at the American Association of Cancer Research (AACR, Chicago).
- **M Singh,** Singh SK*, *et al*. *Development and Application of a Novel Model of Human Lung-To-Brain Metastasis: The Identification of TWIST2 and SPOCK1 as Unique Regulators of Brain Metastases*. (2016) Oral presentation given at the Canadian Neuro-Oncology Meeting (CNO, Toronto), the American Association of Cancer Research (AACR, New Orleans)*, and the Society of Neuro-oncology (SNO, Phoenix).
- **M Singh**, *et al*. *Development and Application of a Novel Model of Lung-to-Brain Metastasis to Identify Unique Metastatic Gene Signatures*. (2015) Oral presentation given at the 5th Annual Brain Metastasis Research and Emerging Therapy Conference (Marseille), poster presented at the Stem Cell Network Conference (SCN, Toronto) and Society of Neuro-Oncology (SNO, San Diego).

- **M Singh**, C Venugopal, S Nolte, N McFarlane, SK Singh. *Novel In Vivo Modelling of Lung-to-Brain Metastases To Target Brain Metastasis Initiating Cells*. (2014) Poster presented at the Stem Cell Network Conference (SCN, Ottawa).

Scholarships and Awards

- Brain Canada CIBC Brain Cancer Training Award, held Sept 2013-Aug 2016 $30000 for 3 years, plus additional $15000 stipend
- Till and McCulloch Travel Award, received each year of 2013-2015
- Canadian Cancer Research Conference Travel Award, received 2013
- McMaster University Graduate Entrance Scholarship ($2500), received 2012

Media Relations

- McMaster Daily News, EurekAlert! AAAS, AANS: 8 Aug 2017, "New genes discovered regulating brain metastases in lung cancer"
  - http://dailynews.mcmaster.ca/article/new-genes-discovered-regulating-brain-metastases-in-lung-cancer-patients/
  - https://www.eurekalert.org/pub_releases/2017-08/mu-ngd080817.php
  - https://news.oicr.on.ca/2017/08/new-genes-discovered-regulating-brain-metastases-in-lung-cancer/
  - http://aansneurosurgeon.org/new-genes-discovered-regulating-brain-metastases-lung-cancer-patients/
  - https://medicalxpress.com/news/2017-08-genes-brain-metastases-lung-cancer.html
  - https://www.mdlinx.com/oncology/article/1029
- Canadian Cancer Society "Mission Day" and tours: 26 Jan 2017, 14 Aug 2017, 19 Jan 2018
- The Hamilton Spectator, The Bay Observer: 1 May 2013: "CIBC-Brain Canada brain cancer studentship recipient"